2019

Interaction Phenomena of Nonlinear Waves in Unmagnetized Plasmas

Alam, Mohammad Shah

University of Rajshahi, Rajshahi

INTERACTION PHENOMENA OF NONLINEAR WAVES IN UNMAGNETIZED PLASMAS

MOHAMMAD SHAH ALAM

UNIQUE ID: 1713028502

SESSION: 2016-2017

UNIVERSITY OF RAJSHAHI, RAJSHAHI-6205,

BANGLADESH

2019

INTERACTION PHENOMENA OF NONLINEAR WAVES IN UNMAGNETIZED PLASMAS

DISSERTATION SUBMITTED IN PARTIAL FULFILLMENTS FOR THE DEGREE OF DOCTOR OF PHILOSOPHY

MOHAMMAD SHAH ALAM

UNIQUE ID: 1713028502

SESSION: 2016-2017

DEPARTMENT OF APPLIED MATHEMATICS

FACULTY OF SCIENCE, UNIVERSITY OF RAJSHAHI,

RAJSHAHI-6205, BANGLADESH

2019

DECLARATION

It is hereby declared that the dissertation entitled **"Interaction Phenomena of Nonlinear Waves in Unmagnetized Plasmas"** has been carried out by fellow **(Unique ID: 1713028502, Session: 2016-2017)**. This work is original and has not been submitted in part or in full for any other degree or diploma to this University or elsewhere. He has already published 16 highly prestigious international journal papers (abstracted and peer reviewed).

Mohammad Shah Alam
PhD Fellow
Department of Applied Mathematics, University of Rajshahi
Rajshahi-6205, Bangladesh.

Principal supervisor
Professor Dr. Mamunur Rashid Talukder
Department of Electrical & Electronic Engineering
University of Rajshahi, Rajshahi,
Bangladesh.

Co-supervisor
Professor Dr. M. Hossain Ali
Department of Applied Mathematics
University of Rajshahi, Rajshahi
Bangladesh.

Acknowledgement

I would like to take this opportunity to express my deep gratitude to my principal supervisor **Professor Dr. Mamunur Rashid Talukder**, Department of Electrical & Electronic Engineering and Co-supervisor **Professor Dr. M. Hssain Ali**, Department of Applied Mathematics, University of Rajshahi, Rajshahi, Bangladesh for their willingness to accept me as a Ph. D. student. I express a special debt of gratitude and a heartfelt thanks to reverent **Professor Dr. Mamunur Rashid Talukder** and **Professor Dr. M. Hssain Ali** for their constant guidance, invaluable instruction, endless encouragement, unstinted help and constant good cheer preparing this dissertation. I am grateful to Professor Dr. Syed Mustafizur Rahman, Department of Electrical & Electronic Engineering, University of Rajshahi, Rajshahi, Bangladesh for providing me with excellent advice and endless encouragement on making this dissertation. I express my deep sense of gratitude to my Lab members Dr. N.C. Roy and Dr. M.G. Hafez for their invaluable suggestion and knowingly or unknowingly helped or influenced in the making of this dissertation. I wish to express my great indebtedness to the Chairman, Department of Applied Mathematics, University of Rajshahi, Rajshahi, Bangladesh for his help in matter concerning academic affairs. I also like to thank all staffs of Plasma Science and Technology Lab, Department of Electrical & Electronic Engineering, and Department of Applied Mathematics, University of Rajshahi, Rajshahi, Bangladesh for their efforts during my Ph.D. works in University of Rajshahi. I want to express my heartfelt love and appreciation to my mother, brothers, wife and only daughter Samia Alam Tonny for their constant support. My sincere thanks go to last but not least, to the Almighty Allah, who has been the main driving force and has given me the patience and understanding to rise to this level of sophistication.

JUNE, 2019 **THE AUTHOR**

Abstract

This dissertation is concerned with the study of interaction phenomena of nonlinear waves in unmagnetized plasmas. The plasma system considered is fully ionized, collisionless and homogeneous and/or inhomogeneous that contains multi-component plasma species under different situations. To investigate the physical issues of the interaction phenomena of nonlinear waves the nonlinear evolution equations are derived. The extended Poincaré-Lighthill-kue (ePLK) method is used to derive the nonlinear evolution equations. The interaction phenomena pertaining to plasma parameters on the production of ion-acoustic solitary waves, ion-acoustic shock waves and rogue waves and their consequences on phase shifts and amplitudes are investigated in different plasma situation. The interaction processes among the waves (such as ion-acoustic solitary waves, ion-acoustic shock waves) for single and multi-soliton plasmas are also studied considering the analytical solutions to the nonlinear evolution equations under some assumptions to discuss the characteristic of the waves in the plasmas that are observed in astrophysical, space and laboratory plasmas. In **chapter one**, some important physical terms that are relevant to the plasma phenomena are briefly discussed.

Chapter two discusses the interaction phenomena of ion-acoustic multi-solition and the production of rogue waves in an unmagnetized plasmas composing non-relativistic as well as relativistic degenerate electrons and positrons, and inertial non-relativistic helium ions. The interaction phenomena are investigated by deriving two-sided Korteweg-de Vries (KdV) equations with their corresponding phase shifts employing extended Poicaré-Lighthill-Kuo (ePLK) method and to study the properties of rogue waves the nonlinear Schrödinger equation (NLSE) is obtained from the modified KdV (mKdV) equation.

Chapter three presents a comparative study of the interactions between nonlinear ion acoustic solitary waves propagating toward each other, and the electrostatic nonlinear propagation of ion-acoustic solitary waves, both for the weakly and highly relativistic regimes. The considered plasma system is consisted of relativistic warm ions, nonthermal electrons, and positrons.

On the other hand, the propagation characteristics and interaction phenomena among the dust acoustic solitons in unmagnetized dusty plasmas are studied in **chapter four**. To do

so, the solutions of the KdV equations are constructed using the Hirota bilinear method both for single- and multi-solitons and the phase shifts are determined for the interactions among the two-, four-, and six-dust acoustic solitons.

Chapter five incorporates the head-on collision of ion acoustic shock waves and the consequences after collision are investigated in the plasma system to be consisting of relativistic warm ions and nonextensive electrons and positrons. In this regard two-sided KdV-Burger equations are derived employing the ePLK method. The effects of plasma parameters on the formation of shock, phase shift after collision, and amplitude of the solitons are also studied.

In **Chapter six** the head-on collisions between positron acoustic solitary waves as well as the production of rogue waves in homogeneous and positron acoustic solitary waves inhomogeneous unmagnetized plasma systems are investigated deriving the nonlinear evolution equations. Besides, to investigate the basic feature of positron acoustic solitary waves due to head-on collision in homogeneous unmagnetized plasma the KdV and mKdV equations are derived using ePLK method along with generic case. To study the characteristic of rogue waves, the nonlinear Schrödinger equation from mKdV equation is derived. Furthermore, to investigate the effect of inhomogeneity on the propagation of positron acoustic solitary waves the KdV and mKdV equations with variable coefficients are derived using stretched coordinates applicable for spatially inhomogeneous plasmas.

Finally, the important results found in this work are summarized with future plan in **chapter seven**.

Table of Contents

Chapter 1

General Introduction

1.1 Plasma description

Plasma is the fourth state of matter; the remaining three are solid, liquid and gaseous. It is either partially or fully ionized state depending on the properties of plasma. Plasma is a quasi-neutral gas of charged and neutral particles, that is, the plasma is almost neutral, but not neutral enough to remove all the electromagnetic forces; which exhibits collective behavior. The collective behavior means that the dynamics of plasma are not controlled by the interactions between individual particles (e.g., binary collision) and are determined by the particle system as a whole. As the temperature of a material is raised, its state changes from solid to liquid and then to gas. If the temperature is raised further, a significant number of gas particles are ionized and then become the high temperature gaseous state in which the numbers of ions and electrons are almost the same and the charge neutrality condition is satisfied macroscopically. Typically plasma consists of electrons, ions in conjunction with energetic metastables and neutrals. When the ions and electrons move collectively, these charged particles interact with Coulomb force which is a long range force and decays only in inverse-square of the distance between the charged particles. The resultant current flows due to the motion of charged particles and consequently Lorentz interactions take place. Therefore, many charged particles interact with each other by long range forces and various collective movements occur in the gaseous state. The typical cases show different types of instabilities and wave phenomena. However, modern life-style is vastly depending on plasma technologies [1-3] for manufacturing semiconductor devices and components. The applications of plasma technologies include in manufacturing computer processors, storage devices, plasma display panel, solar cells, light sources, protective coatings, processing of exotic new materials, rocket thrusters and so on. Very recently, plasma technologies are applied in agriculture [4-7], wastewater treatment [8-11] and medicine. Based on the relative temperatures of the species, plasmas are classified as thermal and nonthermal. Plasma is said to be thermal, if the plasma species temperatures are in thermodynamic equilibrium, i.e.,$T_e \approx T_h$, where T_e and T_h are the electron and heavy species or neutral temperatures, respectively.

On the other hand, plasma is said to be nonthermal, if plasma species are not in thermodynamic equilibrium, i.e., $T_e \gg T_h$ [12]. Under this situation, the velocity distribution functions are different for different species present in plasma [12]. Plasmas can also be magnetized or unmagnetized. The plasma is said to be magnetized, if the magnetic field is strong enough to influence the motion of charged particles. Due to the high conductivity of plasma, the electric field is usually small, then the electric field associated with plasma moving in magnetic field is defined by $\mathbf{E} = \mathbf{v} \times \mathbf{B}$, where $\mathbf{E}$ is the electric field, $\mathbf{v}$ is the velocity, and $\mathbf{B}$ is the magnetic field, and is not affected by Debye shielding [13]. On the other hand, the unmagnetized plasma is one in which neither ambient magnetic field nor self-consistent magnetic field is present due to the plasma current, that is $\mathbf{B} \to 0$. In particular, unmagnetized plasma is assumed isotropic. Plasmas are ubiquitous in astrophysical, space and laboratory environments. The nearest natural region dominated by plasmas is Earth's ionosphere and magnetosphere. 99% of observable universe is in plasma state, such as in the ionosphere, solar corona and solar wind, magnetospheres of the earth and other planets, tails of comets, interstellar and inter-galactic spaces, and in the accretion disks, Van Allen radiation belts etc. are the names of a few. Besides, the space plasma is very prosperous environment in terms of different physical phenomena that demonstrates over a wide range of parameters, which makes it thrilling as well as challenging field to investigate.

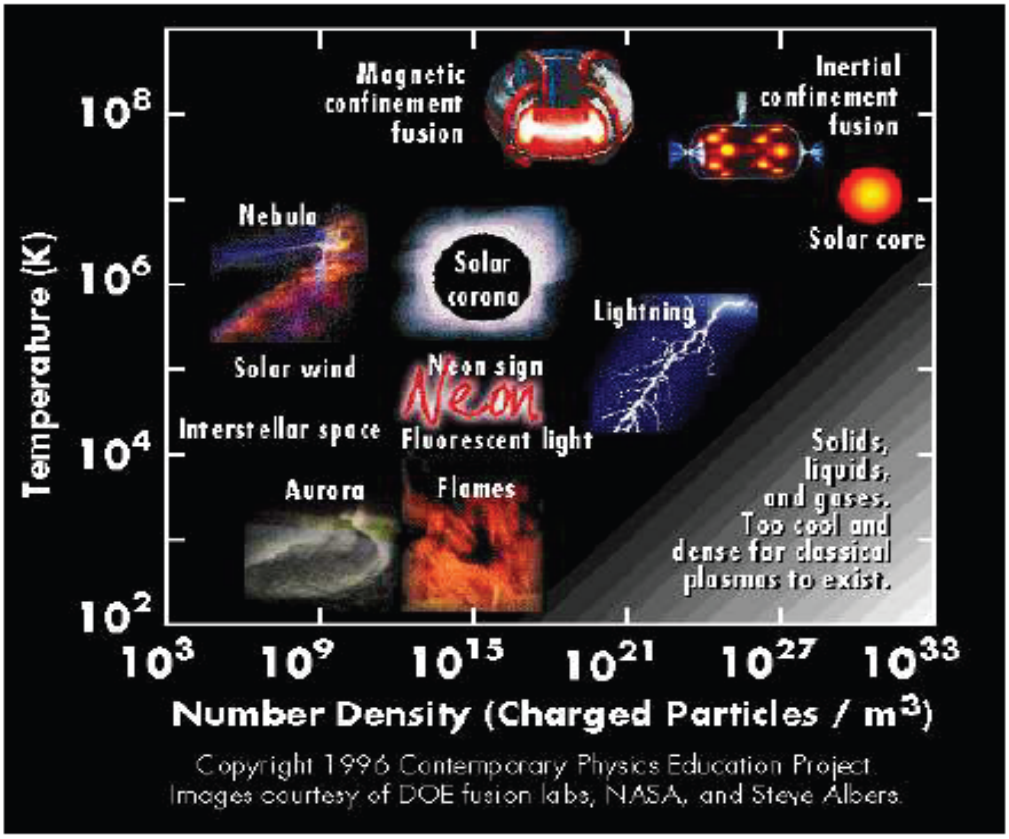

Figure 1.1 Plasmas in terms of temperature (T) and number densities (n) [14].

Plasmas are found in many contexts: both in nature, industry and laboratory. Fig.1.1 represents some of those and their general properties in terms of temperature and number densities. The plasmas can also be collisional and collisionless. The collisionless plasma is one in which the mean free path (λ_{mfp}) for binary Coulomb collision is usually much larger than the typical size of the system and the collision frequency is much smaller than the typical frequency at which the plasma quantities vary. Time scale for observing the phenomenon is much smaller than the time of collision between the two particles. Tokamak, solar wind, planetary magnetospheres are a few names of collisionless plasma. In space physics, the magnetopause phenomena are apparently collisionless [15] because of typical distance ($d \approx 10^3$ km) much less than $\lambda_{mfp} \approx 10^7$ km. Besides, the collisional plasma is one in which mean free path for binary Coulomb collision is usually much less than the typical size of the system. The collision between particles does not play a role in the dynamics of the plasma in collisionless case.

1.1.1 Properties of Plasmas

A number of natural frequencies are associated with the motions of particles in plasmas. The angular plasma frequency for the particle of species α is defined by [16]

$$\omega_{p\alpha} = \left(\frac{n_\alpha q_\alpha^2}{m_\alpha \epsilon_0}\right)^{1/2}, \tag{1.1}$$

where, n_α, q_α, and m_α are the number density, charge and mass of the particles of species α, respectively, and ϵ_0 is the permittivity of free space. Plasmas have various characteristic length scales. The Debye length $\lambda_{D\alpha}$ is, the scale over which mobile charge carriers screen out the electric fields in the plasmas, given by [16]

$$\lambda_{D\alpha} = \frac{v_\alpha}{\omega_{p\alpha}}, \tag{1.2}$$

where $v_\alpha = \sqrt{k_B T_\alpha / m_\alpha}$ is the thermal speed, T_α is the particle temperature and k_B is the Boltzmann constant. The plasma frequency and Debye length are related with the velocity of the particle α by the formula

$$v_\alpha = \omega_{p\alpha} \lambda_{D\alpha}. \tag{1.3}$$

It is required that $\lambda_{D\alpha}$ to be very small compared to the physical dimension (L) of the system, that is $\lambda_{D\alpha} \ll L$, so as to fulfill the condition of collective shielding. For the validation of ideal plasma, the necessary conditions can be expressed mathematically as: (i) $L \gg \lambda_{D\alpha}$ (ii) $N_D \gg 1$, and (iii) $\omega\tau > 1$, where $N_D = \frac{4}{3}\pi n \lambda_{D\alpha}^3$ is the number of charged particles in the Debye sphere, τ is the mean free time, ω is the angular frequency of typical plasma oscillation. The sum of energies of interactions of the test charge with each of the surrounding charged particles represents the interaction energy of the test charge with all the charged particles in the plasma. The interaction energy of two charged particles in plasma is determined [17] by

$$U(r) = \frac{eq}{4\pi r \epsilon_0} \exp\left(-\frac{r}{\lambda_{D\alpha}}\right), \tag{1.4}$$

where $q = \pm e$ and r is the distance between the particles. Due to plasma quasi-neutrality, the average interaction energy of the test charge would be vanished when the influence of test charge on the space charge distribution is neglected. The solution for the potential distribution is obtained [17] as

$$\phi(r) = \frac{e}{4\pi r \epsilon_0} \exp\left(-\frac{r}{\lambda_{D\alpha}}\right). \tag{1.5}$$

The potential will interact with the Coulomb potential in free space for $r \ll \lambda_{D\alpha}$, but it is much less for $r \gg \lambda_{D\alpha}$ because of the plasma shielding effect. Therefore, the characteristic scale of the plasma shielding region is determined by the Debye radius.

1.1.2 Electron-positron-ion (epi) plasma

The electron-positron-ion (epi) plasma is a special case of ambiplasma, the term was introduced by H. Alfven in 1965 [18], means the existence of matter and antimatter in plasmas. It is a quasi-neutral space plasma, containing electrons, positrons, and ions with neutrals as background. The formation [19] of ambistars (i.e. stars consisting of ambiplasma) can be described by several models due to star-antistar collisions. The epi plasmas occur in a wide variety in the universe, such as in inner region of accretion discs in the vicinity of black holes [20-21], magnetosphere of neutron stars [22-23], active galactic cores [24] and even in solar flare plasma [25] are the names of a few. A number of authors [26-34] have studied the characteristics of plasma waves in different situations due to their potentiality concerning the epi plasma. Most of them are focused in nonrelativistic plasmas. But when the streaming velocity of the plasma particle is comparable to the velocity of light, then the relativistic effect cannot be neglected. The relativistic energy is considered in the range 0.1-100 MeV [35-36]. The e-p-i relativistic plasmas are the well established phenomena in pulsar magnetosphere [37] and laser-plasma interaction [38-39]. Recently, in the vicinity of blazers and micro-quasars the narrow-collimated extended relativistic jets of epi plasma were observed [24, 40-42]. A significant number of researchers have carried out works [43-53] concerning the velocities of astrophysical particles comparable to the speed of light at different plasma situations. Thus, the studies of nonlinear phenomena of ion-acoustic and ion-acoustic shock waves in epi nonrelativistic and relativistic plasmas have drawn attention to understand the physical issues involved in astrophysical, space and laboratory plasmas.

1.1.3 Dusty plasma

Dusty plasmas are composed of electrons, ions and micron or submicron size massively charged dusts with masses in the range $10^6 - 10^{12}$ of proton masses [54]. The plasma is said to be “dusty plasma”, if $R_d \ll A < \lambda_D$ is fulfilled, where R_d and A are the dust grain radius and average integration, respectively. These plasmas are considered for understanding several types of collective processes that are existed in the lower and upper mesosphere, cometary tails, planetary rings, interstellar media, planetary magnetosphere, interplanetary spaces [54-57], as well as in laboratory dusty plasmas [58-60]. Research on dusty plasma have drawn interest after the discovery of dust acoustic wave [58], dust ion acoustic wave [61], dusty plasma crystal [62-64] and dust lattice wave [65]. The dust ion acoustic solitary waves appear on a time scale larger than the ion plasma period in dusty plasma, as a result the charged dust particles remain stationary and they provide only the back-ground charge-neutrality [66]. Rao

et al. [58] have investigated the characteristics of low phase speed dust acoustic waves in dusty plasmas that are observed in space and laboratory. They have found that the inertia is provided by the mass of the dust particles, while the pressure of the inertialess electrons and ions provides restoring force due to the production of dust acoustic waves in plasmas. Many researchers [67-70] have investigated the propagation characteristics of dust acoustic waves in dusty plasmas considering different plasma assumptions. On the other hand, the effect of dust charge fluctuation plays a significant role only for the wave whose time period (T_ω) is comparable to the dust charging time period ($T_{c\omega}$) [71]. Bandyopadhyay et al. [72] have studied the nonlinear dust acoustic solitary waves experimentally with constant dust charge fluctuation in dusty plasmas and determined ion density $n_i = 7 \times 10^{-3} m^{-3}$, dust density $n_d = 1 \times 10^{10} m^{-3}$, ion temperature $T_i = 0.3$ eV, dust charge number $Z_d = 3 \times 10^3$, and dust mass $m_d = 1 \times 10^{-3}$ kg.

1.2 Nonlinearity of plasma

Nonlinearity is a charming element of nature. The importance of nonlinearity has appreciated for many years when large amplitude wave motions are observed [73] in various fields, such as in fluids and plasmas, astrophysics, particle physics etc. are the names of a few. Innumerable instabilities are present in plasmas while the amplitude of rising perturbations is small. If the amplitude becomes suitably large, the linearization process breaks down. Thus, the nonlinearity cannot be ignored and the plasma is then effectively a nonlinear medium. The nonlinearities occur due to harmonic generation involving fluid, Lorenz force, trapping of particles in the wave potentials, and ponderomotive force etc. The localized large amplitude waves called solitons propagate with particle-like properties in a medium without spreading; it is one of the most outstanding aspects of nonlinear phenomena. The nonlinearities in the plasmas contribute to the localization of waves, leading to different types of interesting articulate of nonlinear wave structures such as: solitary structures (solitons), shock waves, vortices and double layers etc. The studies of nonlinear waves have gained momentum in various configurations of plasma dynamics, laboratory, astrophysical, and space plasmas [74]. Nonlinear wave dynamics (referred to as nonlinear science or chaos theory) is a rapidly growing topic in many fields. Besides, due to enormous applications of nonlinear dynamics, the study of nonlinear wave propagation in astrophysical, space and laboratory plasmas in the form of soliton and sheath dynamics has drawn considerable interest.

1.3 Plasma waves

Plasma waves are produced due to the production and annihilation of interconnecting set of particles and fields. These include instabilities, fluctuations, wave-induced transport and so on. Waves can deliver energy to the particles in plasmas by heating, current drive, particle acceleration, mode stabilization and so on. Plasma waves are observed in almost all objects of the solar system [75-76] such as in planets and their satellites, comets, interplanetary medium and sun. Plasma has many degrees of freedom, so it supports many waves, e.g. Langmuir wave, ion acoustic solitary wave, electrostatic ion cyclotron wave, ion acoustic shock wave, Rouge wave, Alfven wave, and magneto sonic wave, and so on. This dissertation is confined into the ion acoustic solitary waves, ion acoustic shock waves, positron acoustic waves and rouge waves.

1.3.1 Solitary waves and soliton

The solitary wave is a permanent form of finite amplitude wave. This type of wave arises from the balance of nonlinearity and dispersive effects of the medium. The solitary water wave was first observed and documented by Scottish scientist and engineer Russell [77]. The solitary waves can be described by certain nonlinear wave equations (which either integrable, or close to integrable). Solitary waves are bell-shaped and travel with maintaining their original shapes and velocities. They can cross each other without any change in structure and phase. The resulting nonlinear solitary waves are known as solitons. Solitons are found through the solutions of model equations together with the Korteweg-de Vries (KdV) and the nonlinear Schödinger equations. These model equations are approximations which grasp under a prevailing set of conditions. To obtain the soliton solutions for nonlinear waves, the necessary ingredients are nonlinearity and dispersion. These soliton solutions deliver the information about solitary waves. The name “solitons” of the solitary wave, due to exhibiting the properties of particles, was first proposed Zabusky and Kruskal [78]. The phenomena, regarding excitation, propagation, and interaction, of solitons play a vital role in plasma physics. The phase of the solitons changes without changing their amplitudes due to interactions.

1.3.2 Ion acoustic waves

Acoustic wave is a type of longitudinal wave that propagates by adiabatic compression and decompression. Sound pressure, particle velocity, particle displacement and sound intensity

etc. are the quantities for describing the acoustic waves. The acoustic waves propagate with the speed of sound which depends on the properties of medium. The ion acoustic waves are the acoustic-type waves, which commonly occurs due to pressure gradients, with time scale longer than the frequency corresponding to the relevant length scale. In the ion acoustic waves, the restoring force is provided by the pressure of lighter species such as electrons, positrons etc., and inertia is provided by the massive ionic species. As the ions interact with electrostatic or electromagnetic fields at long distance, therefore the ion acoustic waves may propagate in collisionless medium. The motion of massive ions are occupied in the ion acoustic waves, this will result in low frequency oscillations. Under these conditions, the dispersion relation can be defined as

$$\omega^2 = k^2 \left(\frac{\kappa_B T_e}{M} + \frac{\gamma_i \kappa_B T_i}{M}\right), \qquad (1.6)$$

where, M is the mass of ions, γ_i is the ratio of specific heat at constant pressure to constant volume, ω is the angular wave frequency and k is the wave number.

1.3.3 Positron acoustic solitary waves

Positron acoustic waves are acoustic-type of waves. The Positron acoustic waves are the low frequency electrostatic waves in plasma system. In Positron acoustic waves, the restoring force is provided by the thermal pressure of hot positrons and electrons, and the inertia comes from the mass of cold positron. The propagation of the positron acoustic solitary wave is very important for the understanding of electrostatic disturbances as observed in space and laboratory plasmas.

1.3.4 Shock waves

Much interest has grown to the research community in the study of shock waves due to their (shock waves) significant importance in plasmas. It carries energy and can propagate through the medium (solid, liquid, gas or plasma). shock waves are a special class of nonlinear waves in the form of propagating discontinuous disturbances that are characterized [79] by abrupt nearly-discontinuous change in the characteristic of the medium. The properties of shock include rapid rise in velocity, pressure, temperature and density. shock wave occurs in a variety of neutral media such as in gas [80], liquid [81] and solid [82]. They are also observed in space during the early stages of star formation and the interaction between the magnetic fields of the Earth and the solar wind. In plasma, shock wave can be excited when a large amplitude mode propagates in the presence of strong dissipation such as due to collisions with neutrals, viscosity or Landau damping [83-84]. In collision dominated media like the Earth's

atmosphere, energy dissipation is accomplished through binary collision of particles. The shock waves are found in air and water which are produced when the flow velocity of air molecule relative to the water is greater than the speed of sound. Shock waves are the final stage of nonlinearity steeping wave that balance between nonlinearity and energy dissipation (i.e. irreversible energy transformation) [85-87]. Thus, one can conclude that the shock is produced due to the balance between the nonlinearity and dissipation. Depending on the modes of small-amplitude waves, shock wave can be of three types: the fast, slow, and intermediate as can be observed in magneto hydrodynamics. shock waves are also found in a wide variety of plasmas in the universe. These plasmas are generally collisionless, which means that the energy is dissipated with wave-particle interaction instead of particle-particle interaction. The collisionless shock waves are known to be the efficient mechanisms by which charged particles can be heated and/or accelerated. There are four possible mechanisms by which a collisionless shock could transfer energy: wave dispersion [88-90], wave-particle interactions [91-92], particle reflection [93-95] and macroscopic quasi-static field effects [96-98]. The Earth's bow shocks, the interplanetary shocks and the supernova remnant are some examples of the collisionless shocks.

1.3.5 Rogue wave

Rogue waves are large, unexpected and suddenly appearing surface waves. Rogue waves are also known as freak waves, monster waves, episodic waves, killer waves, extreme waves, and abnormal waves. For the first time in 1995, the Rogue waves were recorded by [99] during a winter storm in the North Sea, when the "New Years Wave" hit the Draupner platform with a wave height of 27 m and 2.25 times the average wave height. The formations of rogue waves are now being investigated in various physical contexts, such as in nonlinear optics [100-102], plasma physics [103], and superfluids [104]. Therefore, the studies on rogue waves will enrich the concept and bring a full understanding of the mysterious phenomenon.

1.3.6 Bohm potential

The quantum potential is the concept of de Brogle-Bohm formulation of quantum mechanics, was first introduced by David Bohm in 1952[105]. It is also known as Bohm potential, quantum Bohm potential or Bohm quantum potential and which could be taken as the source of quantum novelties. Lee and Jung [106] have found that the Bohm potential term generates the propagation mode in quantum plasmas. There exists a parameter in the study of ion acoustic waves in degenerate plasmas, called quantum parameter, due to the Bohm potential, which is solely responsible for the tunneling effect of the corresponding plasma

components. The tunneling effect is sometimes exhibited by moving particles that succeed in passing from one side of a potential barrier to the other having insufficient energy to pass over the top.

1.4 Basic hydrodynamic equation in plasma

As the plasma consists of electrons, ions and neutral particles, thus the system of fluid transport equation, which describes the plasma properties, can be derived separately for each type of particle.

Continuity equation: If v and n are the velocity and number density, then the continuity equations [107] can be written as

$$\frac{\partial n_0}{\partial t} + \boldsymbol{\nabla}.(n_0 v_0) = R_0^{rec} - R_i^{ion}\ , \tag{1.7}$$

$$\frac{\partial n_i}{\partial t} + \boldsymbol{\nabla}.(n_i v_i) = R_i^{ion} - R_0^{rec} \tag{1.8}$$

$$\frac{\partial n_e}{\partial t} + \boldsymbol{\nabla}.(n_e v_e) = R_i^{ion} - R_0^{rec} \tag{1.9}$$

The function $R_j^{rec}\left(n_{0,} n_i, n_{e,} \cdots, p, T\right)$ and $R_j^{ion}\left(n_{0,} n_i, n_{e,} \cdots, p, T\right)$ are the recombination and ionization rate of j (= i for ion and 0 for neutral) species, respectively and p is the pressure. The mass conservation equations can be obtained by multiplying each of the above continuity equations with the corresponding mass per molecule. The total mass density of the plasma fluid defined as

$$\rho = n_0 m_0 + n_i m_i + n_e e, \tag{1.10}$$

and the plasma fluid mass averaged velocity denoted and defined by

$$v_a = \frac{1}{\rho}(n_0 m_0 \boldsymbol{v_0} + n_i m_i \boldsymbol{v_i} + n_e m_e \boldsymbol{v_e}). \tag{1.11}$$

Therefore,

$$\frac{\partial \rho}{\partial t} + \boldsymbol{\nabla}.(\rho \boldsymbol{v_a}) = 0\ . \tag{1.12}$$

This is known as the equation of continuity describing the conservation of mass. The first term represents the time rate of change of density of a particular species in a volume and the second term represents the difference of outflow and inflow fluxes of particles inside a small volume.

Momentum equation:

Let us consider the plasma flows through a fixed element in space. Therefore, the electromagnetic (EM) force on the element per unit volume is defined as

$$\boldsymbol{F}_{em} = nq(\boldsymbol{E} + \boldsymbol{v} \times \boldsymbol{B}). \tag{1.13}$$

Where, nq is the charge density. The momentum flow across the boundary per unit volume is

$$\nabla \cdot \left[\int m(\boldsymbol{v}+\boldsymbol{v_q})(\boldsymbol{v}+\boldsymbol{v_q})f(\boldsymbol{v_q})d^3\boldsymbol{v_q}\right]$$

$$= \nabla \cdot \left[\int m(\boldsymbol{vv}+(\boldsymbol{vv_q}+\boldsymbol{v_qv})+\boldsymbol{v_qv_q})f(\boldsymbol{v_q})d^3\boldsymbol{v_q}\right]$$

$$= \nabla \cdot [mn\boldsymbol{vv}+p]$$

$$= mn(\boldsymbol{v}\cdot\nabla)+m\boldsymbol{v}\{\nabla\cdot(n\boldsymbol{v})\}+\nabla p \text{ [as, } \int(\boldsymbol{vv_q}+\boldsymbol{v_qv})f(\boldsymbol{v_q})d^3\boldsymbol{v_q}=0]. \quad (1.14)$$

$\boldsymbol{v_q}$ is the peculiar velocity[107-108]**.** As the momentum density of the element is $mn\boldsymbol{v}$**,** thus the rate of change of momentum within the element per unit volume is $\partial(mn\boldsymbol{v})/\partial t$. Therefore, the total momentum balance equation becomes

$$\frac{\partial}{\partial t}(mn\boldsymbol{v})+mn(\boldsymbol{v}\cdot\nabla)+m\boldsymbol{v}\{\nabla\cdot(n\boldsymbol{v})\}+\nabla p=\boldsymbol{F}_{em},$$

$$\Longrightarrow m\boldsymbol{v}\left\{\frac{\partial n}{\partial t}+\boldsymbol{\nabla}\cdot(n\boldsymbol{v})\right\}+mn(\boldsymbol{v}\cdot\nabla)\boldsymbol{v}+mn\frac{\partial \boldsymbol{v}}{\partial t}+\nabla p=nq(\boldsymbol{E}+\boldsymbol{v}\times\boldsymbol{B}). \quad (1.15)$$

From Eq. (1.12) and Eq. (1.15) one can determine the momentum equation

$$mn\left(\frac{\partial \boldsymbol{v}}{\partial t}+(\boldsymbol{v}\cdot\nabla)\boldsymbol{v}\right)=nq(\boldsymbol{E}+\boldsymbol{v}\times\boldsymbol{B})-\nabla p. \quad (1.16)$$

Poisson's equation:

The Maxwell's equations are

$$\left.\begin{array}{c}\nabla\cdot\boldsymbol{E}=\rho/\varepsilon_0\\ \nabla\cdot\boldsymbol{B}=0\\ \nabla\times\boldsymbol{E}=\boldsymbol{0}\\ \nabla\times\boldsymbol{B}=\mu_o\boldsymbol{J}\end{array}\right\}. \quad (1.17)$$

Where ρ and $\boldsymbol{J}$ are the densities of electric charges and current, respectively and ε_0 is the electric permittivity in vacuum. Since $\nabla\times\boldsymbol{E}=\boldsymbol{0}$**,** there exits an electric potential ϕ such that $E=-\nabla\phi$, thus $\nabla\cdot\boldsymbol{E}=\rho/\varepsilon_0$ gives Poisson's equation

$$\nabla^2\phi=-\frac{\rho}{\varepsilon_0}. \quad (1.18)$$

1.5 Distribution functions in plasma system

The distribution functions $f(x,v,t)$ are the basic elements in the plasma system that describes how particles are distributed in both physical space and velocity space. In this section it is important to discuss some important distribution functions that are relevant to this dissertation.

1.5.1 Maxwell distribution

The Maxwell-Boltzmann distribution illustrates speeds of particle in gases, where the particles move freely between short collisions, but do not interact with each other. The normalized distribution function [109] for molecular velocities can be defined as:

$$f(v)d^3vd^3x = n(m/2\pi\kappa_B T)^{3/2}\exp(-mv^2/2\kappa_B T)\, d^3xd^3v. \quad (1.19)$$

After the name of James Clark Maxwell the distribution represents by Eq. (1.19) is known as the Maxwell velocity distribution. For the inertialess and isothermal electron the Boltzmann distributed electron can be taken into account as

$$n_e = n_o \exp(e\phi/\kappa_B T_e). \quad (1.20)$$

Where, e is the electronic charge and n_o is the initial density of the electron.

1.5.2 Non-thermal distribution

To understand the nonlinear electrostatic disturbances in space plasma environments such as in the aurora acceleration region [110-111], upper ionosphere [112], lower part of the magnetosphere [113-114], around the Earth's bow shock [115], etc. the population of non-thermal particles, and their distribution have received a great deal of interest. To represent the population of the nonthermal particles Cairns et al [116] have introduced a distribution function known as "Cairns distribution", which is able to explain some special features of the ion acoustic solitary structures (e.g. the existence of rarefactive ion-acoustic solitons or density cavitons that are observed by the Freja Satellite [114] and Viking spacecraft [113]). Theoretical discussion of Cairns et al. [116] provided a model describing the velocity distribution function is written as

$$f(v) = n_0\{1 + (m^2v^4/4)\alpha\}\exp\{-mv^2/2(1+3\alpha)\}. \quad (1.21)$$

α is the nonthermal parameter determines the number of energetic electrons or ions. Subsequently, the electron number density appearing in the Eq. (1.22) can be obtained as

$$n_e = (1 - \beta\phi + \beta\phi^2)\exp(-\phi), \quad (1.22)$$

where $\beta = 4\alpha/(1+3\alpha)$ represents the nonthermality of electron distribution. In the limit $\beta = 0$ the Eq. (1.22) expresses the isothermally distributed electrons. The electron distribution given by Eq. (1.22) is common to many space and laboratory plasmas [110-116].

1.5.3 Superthermal distribution

When the plasmas are not in thermal equilibrium, as observed in space plasmas such as in the magnetosphere environment, solar wind, the corona [117-118] and so on, the particle distribution functions are characterized by non-Maxwellian power-law [119-121]. Such particle velocity distributions function known as the generalized Lorenzian or the kappa distribution [122-123]. In the one-dimensional case, the kappa distribution is given by [121]

$$f(v) = \frac{n\Gamma(\kappa+1)}{\theta\sqrt{\pi}\kappa^{3/2}\Gamma(\kappa-1/2)}\{1 + v^2/(\kappa\theta^2)\}^{-\kappa}, \quad (1.23)$$

and in the three dimensional case, the kappa distribution is given [124] by

$$f(v) = \frac{n\Gamma(\kappa+1)}{\theta^3\pi^{3/2}\kappa^{3/2}\Gamma(\kappa-1/2)}\{1 + v^2/(\kappa\theta^2)\}^{-(\kappa+1)}, \quad (1.24)$$

where $f(v)$ is the distribution function, κ, the spectral index, is a measure of the slope of the energy spectrum of the superthermal electrons forming the tail of the velocity distribution function, θ is the thermal speed, and Γ is the gamma function. The kappa distribution has a power-law tail for finite values of the spectral index κ at velocities larger than θ, and in the limit $\kappa \to \infty$, it becomes Maxwellian distribution.

1.5.4 Nonextensive distribution

In fact, the Maxwell distribution is valid for the macroscopic ergodic equilibrium state [125-127]. However, the Maxwell distribution is not enough to describe the systems in thermally non-equilibrium state with long range interactions. The plasmas in space and laboratory [128-129] undoubtedly designate the presence of particle population distribution functions that may be different from the Maxwellian distributions but behave like the power-law. For instance, the spacecraft measurements indicated that "suprathermal" power-law tail at the high energies [130], which can be modeled more effectively by generalized Lorentzian κ-distribution [131]. Such a κ-distribution is known to be equal to the q-distribution in nonextensive statistics [132-133]. In 1988, Tsallis proposed the nonextensive entropy or the q-entropy [134] and it is called nonextensive statistics. The nonextensive distribution function for species α can be defined [135] as

$$f_\alpha(v) = C_{q\alpha}\left[1 - (q_\alpha - 1)\left(\frac{m_\alpha v^2}{2k_B T_\alpha} + \frac{e_\alpha \Phi}{k_B T_\alpha}\right)\right]^{\frac{1}{q_\alpha - 1}}, \quad (1.25)$$

with $$C_{q\alpha} = n_{\alpha 0}\frac{\Gamma\left(\frac{1}{1-q_\alpha}\right)}{\Gamma\left(\frac{1}{1-q_\alpha}-\frac{1}{2}\right)}\sqrt{\frac{m_\alpha(1-q_\alpha)}{2\pi k_B T_\alpha}}, \text{ for } 1 < q_\alpha < 1,$$

and $$C_{q\alpha} = n_{\alpha 0}\left(\frac{1+q_\alpha}{2}\right)\frac{\Gamma\left(\frac{1}{1-q_\alpha}+\frac{1}{2}\right)}{\Gamma\left(\frac{1}{1-q_\alpha}\right)}\sqrt{\frac{m_\alpha(1-q_\alpha)}{2\pi k_B T_\alpha}}, \text{ for } q_\alpha > 1,$$

where $C_{q\alpha}$ and Γ are the normalization constant and Gamma function, respectively. The nonextensive densities of electrons and positrons can be obtained [136] in the form $n_e = n_{e0}\left[1 + (q_e - 1)\frac{\Phi}{k_B T_e}\right]^{\frac{q_e+1}{2(q_e-1)}}$ and $n_p = \left[1 + (q_p - 1)\frac{\Phi}{k_B T_p}\right]^{\frac{q_p+1}{2(q_p-1)}}$, respectively. q_e and q_p indicate nonextensive parameters which characterizing the degree of nonextensivity. For

superthermality $-1 < q_{e,p} < 1$ and for subthermality $q_{e,p} > 1$ and in the limit $q_{e,p} \to 1$ the nonextensive distribution becomes the Maxwell- Boltzmann distribution function.

1.6 Nonlinear methodology

Different methods are used to study the structures and properties of nonlinear solitary waves. The reductive perturbation method is one, which was first proposed by Washima and Taniuti [137]. It is used to solve a set of nonlinear differential equations in almost all branches of physics such as, in plasma physics [137], fluid dynamics [138-139], nonlinear lattice [140-141], etc. The RP method is only valid for small amplitude and long wave length nonlinear waves [142]. On the other hand, the quasi-potential (Sagdeev potential) method [143] is typically used for the case of large amplitude waves. The quasi-potential method is valid only for the special case in which the waveform remains unchanged. For the head-on collision between two counter propagating solitary waves, neither the reductive perturbation method nor the quasi-potential method can solve such type of problem. To solve such type of problem, asymptotic expansion method is employed like the extended Poincar*e*´-Lighthill-Kuo (ePLK) method [144-147]. This method is comprehensively used in many branches of physics, for instance, in plasma physics [148-149], in Boes-Einstein condensates [147,150], and in nonlinear lattice dynamics [151-152], etc. In fact, the ePLK method can be considered as an extension of the reductive perturbation method. The ePLK is only valid when the amplitudes of both the colliding solitary waves are small enough [153].

1.6.1 Poincar*e*´-Lighthill-Kuo (ePLK) method

In 1880, Poincar*e*´ introduced a technique of strained parameters in the study of celestial mechanics [154], which is later on generalized by Lighthill in 1949 and applied to some complicated problem in aerodynamics [155]. In 1953, Kuo realized a perfect combination of Lighthill technique with the boundary layer method which is summarized and reviewed by Tsien in 1956 [156-157]. Thus the method was named as the extended ePLK method.

The dependent variables are expanded as:

$$\left.\begin{aligned} n_i &= 1 + \varepsilon^2 n_i^{(1)} + \varepsilon^3 n_i^{(2)} + \varepsilon^4 n_i^{(3)} + \cdots \\ u_i &= u_0 + \varepsilon^2 u_i^{(1)} + \varepsilon^3 u_i^{(2)} + \varepsilon^4 u_i^{(3)} + \cdots \\ \phi &= 0 + \varepsilon^2 \phi^{(1)} + \varepsilon^3 \phi^{(2)} + \varepsilon^4 \phi^{(3)} + \cdots \end{aligned}\right\}. \tag{1.26}$$

The stretched variables are expanded as:

$$\left.\begin{array}{c}\xi = \varepsilon(x - c_1 t) + \varepsilon^2 P_0(\zeta,\tau) + \varepsilon^3 P_1(\zeta,\xi,\tau) + \cdots \\ \zeta = \varepsilon(x + c_2 t) + \varepsilon^2 Q_0(\xi,\tau) + \varepsilon^3 Q_1(\zeta,\xi,\tau) + \cdots \\ \tau = \varepsilon^3 t\end{array}\right\}. \quad (1.27)$$

Where ξ and ζ denote the trajectories of two solitons traveling toward each other, and c_1 and c_2 are the unknown phase velocities.

1.7 Outline of the dissertation

In this dissertation, the interaction phenomena of nonlinear waves in unmagnetized plasmas in different plasma conditions are investigated. Such plasmas are homogeneous or inhomogeneous, collisionless, and relativistic or nonrelativistic comprising multi-species. The purpose of this study is to investigate the production of nonlinear solitary, shock and rogue waves as well as the phase shifts and amplitudes due to collision for the effects of plasma parameters arising in this dissertation to better understanding the physics concerned. The dissertation is organized as follows:

Chapter one includes the brief discussion on some basic physical terms that are relevant to the works presented in this dissertation.

Chapter two: The interactions among solitons and their consequences in the production of rogue waves in an unmagnetized plasmas, composing non-relativistic as well as relativistic degenerate electrons and positrons, and inertial non-relativistic helium ions, are investigated. The extended Poincaré–Lighthill–Kuo (ePLK) method is employed to derive the two-sided Korteweg–de Vries (KdV) equations with their corresponding phase shifts. The NLSE is obtained from the modified KdV (mKdV) equation, which allows one to study the properties of rogue waves. It is found that the Fermi temperature and quantum mechanical effects become pronounced due to the quantum diffraction of electrons and positrons in the plasmas. The densities and temperatures of the helium ions, degenerate electrons and positrons, and quantum parameters strongly modify the electrostatic ion acoustic resonances and their corresponding phase shifts due to the interactions among solitons and produce rogue waves in the plasma.

Chapter three: A comparative study of the interactions between nonlinear ion acoustic solitary waves propagating toward each other, and the electrostatic nonlinear propagation of ion acoustic solitary waves, both for the weakly and highly relativistic regimes consisting of relativistic warm ions, nonthermal electrons, and positrons, is carried out. Two-sided KdV equations are derived using the ePLK method to reveal the physical issues concerned. The effects of positron concentration, ion-electron temperature ratio, electron-positron temperature ratio, relativistic streaming factor, the population of electron, and positron nonthermality on

the electrostatic resonances and their phase shifts are investigated for both regimes. It is found that the plasma parameters significantly modify the phase shifts, electrostatic resonances, hump-shaped electrostatic potential profiles, and the electric fields on the nonlinear propagation characteristics of ion acoustic solitary waves. The results obtained may be useful for clarifications of interaction between ion acoustic solitary waves in astrophysical and laboratory plasmas, especially in pulsar magnetosphere, laser-produced inertial confinement plasmas, and pulsar relativistic winds with supernova ejecta that produce nonthermal electrons, positrons and relativistic ions.

Chapter four: Propagation characteristics and interaction phenomena among the dust acoustic solitons in unmagnetized dusty plasmas are studied. The plasma is composed of negatively charged mobile dust, Boltzmann distributed electrons, and nonthermally distributed cold and hot ions. The extended ePLK method is employed to derive the two-sided KdV-equations. The solutions of the KdV equations are constructed using the Hirota bilinear method both for single- and multi-solitons. The phase shifts are determined for the interactions among the two-, four-, and six- dust acoustic solitons. The effects of plasma parameters on the head-on collisions of the dust acoustic single- and multi-solitons and their corresponding phase shifts are investigated.

Chapter five: Head-on collision between ion acoustic shock waves and the consequences after collision are investigated considering the plasma system to be consisting of relativistic warm ions and nonextensive electrons and positrons, taking into account the effects of nonlinearity and dispersion. Two-sided KdV-Burger equations are derived employing the ePLK method. The results reveal that the plasma parameters are responsible for the modification of the structures along with phase shifts of the shock waves. The nonlinearity effects on ion acoustic shock waves in a highly relativistic regime (HRR) become pronounced rather than the weakly relativistic regime (WRR). The phase shifts of ion acoustic shock waves are enhanced by the relativistic streaming factor and superthermality. The electrostatic ion acoustic shock waves become rarefactive depending on temperatures, kinematic viscosity, and superthermality in both WRR and HRR. The amplitudes of ion acoustic shock waves are increasing for WRR but decreasing for HRR due to increasing ion thermal velocities. Besides, the amplitudes of the solitons are detaining due to the increase in the positron concentration for the depopulation of ions.

Chapter six: The head-on collision between positron acoustic solitary waves as well as the production of rogue waves in homogeneous and positron acoustic solitary waves in

inhomogeneous unmagnetized plasma systems are investigated deriving the nonlinear evolution equations. The plasmas are composed of immobile positive ions, mobile cold and hot positrons, and hot electrons, where the hot positrons and hot electrons are assumed to follow the Kappa distributions. The evolution equations are derived using the appropriate coordinate transformation and the reductive perturbation technique. The effects of concentrations, kappa parameters of hot electrons and positrons, and temperature ratios on the characteristics of positron acoustic solitary waves and rogue waves are examined. It is found that the kappa parameters and temperature ratios significantly modify phase shifts after head-on collisions and rogue waves in homogeneous as well as positron acoustic solitary waves in inhomogeneous plasmas. The amplitudes of the positron acoustic solitary waves in inhomogeneous plasmas are diminished with increasing kappa parameters, concentration and temperature ratios. Further, the amplitudes of rogue waves are reduced with increasing concentrations of charged particles, while it enhances with increasing kappa- and temperature parameters. Besides, the compressive and rarefactive solitons are produced at critical densities from KdV equation for hot and cold positrons, while the compressive solitons are only produced from mKdV equation for both in homogeneous and inhomogeneous plasmas.

Chapter seven: The important results obtained and conclusions are summarized in this chapter. Prospects for the future works are also presented therein.

References

1. W. Crookes, Lecture on british association for the advancement of science, Sheiffield (1879).
2. J. J. Thomson, Lecture to the royal institution, Philosophical Magazine (1897).
3. I. Langmuir, Oscillations in ionized gases, Proc. Nat. Acad. Sci. U.S. **14,** 8 (1928).
4. N. C. Roy, M. M. Hasan, A. H. Kabir, M.A Reza, M. R. Talukder and A. N Chowdhury, Plasma Sci. Technol. **20,** 115501 (2018).
5. A. H Kabir, M. M Rahman, U. Das, U. Sarkar, N. C Roy, M. A Reza, et al. PLoS ONE, **14,** e0214509 (2019).
6. N. C. Roy, M. M. Hasan, M. R. Talukder, M. D. Hossain, A. N. Chowdhury, Plasma Chem. Plasma Process **38,** 13–28 (2018).
7. S. Islam, F. B. Omar, S. A. Sajib, N. C. Roy, A. Reza, M. Hasan, M. R. Talukder and A. H. Kabir, Gesunde Pflanzen, https//dio.org/10.1007/s10343-109-00463-9 (2019).
8. Y. Bashaar , African J. Biotech. **3,** 236-238 (2004).
9. S. J. Bury, C. K. Groot, C. Huth, and N. Hardt, Water Sci. & Tech.**45,** 355-363 (2002).
10. D. Carini, Ph.D. thesis, Swiss Federal Institute of Technology, Zurich, Switzerland (1999).
11. A. Mahdi, I. Azni, A. Aofah, J . Engg. Sci. and Tech. **2,** 55-69 (2007).
12. A.V. Engel, and J.R. Cozens, "Flame Plasma" in Advances in electronics and electron physics (1976), (L. L. Marton ed.), Academic Press, ISBN 978-0-12-014520-1, p. 99 Archived (2016).
13. R. Fitzpatrick, Introduction to Plasma Physics, Magnetized plasmas Archived (2006).
14. V. L. Rekaa, Ph.D. thesis, Faculty of Mathematics and Natural Sciences, University of Oslo No. 1496 (2014).
15. G. Belmont, R. Grappin, F. Mottez, F. Pantellini and G. Pelletier, Collisionless Plasma in Astrophysics, Wiley-VCH; 1 edi. (2013).
16. F. F. Chen, Introduction to Plasma Physics and Controlled Fusion, Volume 1: Plasma Physics, 2nd edition, (1984), Plenum Press, New York.
17. J. D. Callen, Fundamentals of Plasma Physics**,** University of Wisconsin, Madison (2006).
18. H. Alfven, Rev. Mod. Phys. **37,** 652 (1965).
19. H. Alfven, Cosmic Plasma (Reidel, Dordrecht, 1981; Mir, Moscow, 1983).

20. S. Beskin and E. E. Nokhrina, The effective acceleration of plasma outflow in the paraboloidal magnetic field, Monthly Notices of the Royal Astronomical Society, **367,** 375–86 (2006).
21. W. H. Lee, E. Ramirez-Ruiz and D. Page, Opaque or transparent? a link between neutrino optical depths and the characteristic duration of short gamma-ray bursts, The Astrophys. J. Lett. **608,** L5-L8 (2004).
22. M. Lipunov, The ecology of rotators, Astrophys. and space sci. **132,** 1-51 (1987).
23. F. C. Michel, Theory of pulsar magnetospheres, Rev. Modern Phys. **54,** 1 (1982).
24. M. C. Begelman, R. D. Blandford and M. J. Rees, Theory of extragalactic radio sources, Rev. Modern Phys. **56,** 255 (1984).
25. B. Kozlovsky, R. J. Murphy and G. H. Share, Positron-emitter production in solar flares from 3he reactions, The Astrophys. J. **604,** 892–99 (2004).
26. S.I. Popel, S.V. Vladimirov, and P.K. Shukla, Phys. Plasmas **2,**716 (1995).
27. R.S. Tiwari, A. Kaushik, and M. K. Mishra, Phys. Lett. A **365,** 335 (2007).
28. Y.N. Nejoh, Phys. Plasmas **3,** 1447 (1996).
29. S. Ali, W.M. Moslem, P.K. Shukla, and R. Schlickeiser, Phys. Plasma14 (2007) 082307.
30. T.S. Gill, A. Singh, H. Kaur, et al., Phys. Lett. A **361,** 364 (2007).
31. E.I. El-wady, S.A. El-Tantawy, W.M. Moslem, and P.K. Shukla, Phys. Lett.A**374,** 3216-3219 (2010).
32. M. A. Moghanjoughi, Phys. Plasmas **17,** 082315 (2010).
33. G.C. Das and S.G. Tagare, Plasma Phys. **17,** 1025-1032 (1975).
34. T.K. baluku, Plasmas Phys. Cont. Fusion **53,** 095007 (2011).
35. W. Droge, P. Mayer, P. Evension and D. Moses, Solar Phys. **121,** 95-103 (1989)
36. F. Aharonian and S.Casanov, MultipleMesengers and Challenges in Astroparticle Physics,Springer (R. Aloisio, E. Coccica and F. Vissani, Eds.), (2018).
37. M. C. Michel, Rev. Mod. Phys. **54**, 1 (1982).
38. B. Shen and J. Meyer-ter-Vehn, Phys. Rev. E **65**, 016405 (2001).
39. E. P. Liang, S. C. Wilks and M. Tabak, Phys. Rev. Lett. **81,** 4887 (1998)
40. V.V. Zheleznyakov and S.A. Koryagin, Astron. Lett. **28,** 277 (2002).
41. V.V. Zheleznyakov and S.A. Koryagin, Astron. Lett.**31,** 713 (2005).
42. E. V. Derishev, V.V. Kocharovshii, VI.V. Kocharovshii, and V. Yu.Mart'yanov, Nonlinear Waves (IPF, RAN, Nizhni Novgorod, 2007) 268 [in Ruussian].

43. F.L. Scraf, F.V. Coroniti, C.F. Kennel, E.J. Smith, J.A. Slavin, B.T. Tsuuruutani, S.J. Bame, and W.C. Feldman, Geophys. Ress. Lett. **11,**1050 (1984).
44. F.L. Scraf, F.V. Coroniti, C.F. Kennel, R. W. Fredicks, D.A. Curnett, and E.J. Smith, Geophys. Ress. Lett.**11,** 335 (1984).
45. H. Alfen and P. Cariqvist, Solar Phys. **1,** 220 (1967).
46. J. Arons, Space Sci. Rev. **24,** 24 (1979).
47. T. Jajima and T. Taniuti, Phys. Rev. A **42,** 3587 (1990).
48. G.C. Das and S.N. Paul, Phys. Fluids **28,** 823 (1985).
49. H.H. Kuehl and C.Y. Zhang, Phys. Fluids B **3,** 26 (1991).
50. H.H. Kuehl and C.Y. Zhang, Phys. Fluids B **3,** 555 (1991).
51. S. K. El-Labany, H.O. Nafie, and a. El-sheikh, J. Plasma Phys. **56,** 13 (1996).
52. Y. Nejoh, J. Plasma Phys.**37,** 487 (1987).
53. Y. Nejoh, Phys. Fluids B **4**, 2830 (1992).
54. P. K. Shukla and A. A. Mamun, Introduction to Dusty Plasma Physics (IOP, Bristol, 2002).
55. P. K. Shukla, Phys. Plasmas **8,** 1791 (2001).
56. D. A. Mendis and M. Rosenberg, Annu. Rev. Astron. Astrophys. **32,** 418 (1994).
57. F. Verheest, Waves in Dusty Plasmas (Kluwer, Dordrecht, 2000).
58. N. N. Rao, P. K. Shukla, and M. Y. Yu, Planet. Space Sci. **38,** 543 (1990).
59. A. Barkan, R. L. Merlino, and N. D'Angelo, Phys. Plasmas **2,** 3563 (1995).
60. J. T. Mendonça, N. N. Rao, and A. Guerreiro, Euro-phys. Lett. **54,** 741 (2001).
61. P.K. Shukla and V.P. Silin, Phys. Scr. **45,** 508 (1992).
62. H. Thomas, G.E. Morfill, V. Demell et al. Phys. Rev. Lett.**73,** 652 (1994).
63. Y. Hayashi and K. Tachibana, Jpn. J. Appl. Phys. Part2 **33,** L804 (1994).
64. Y. Hyashi, Phys. Rev. Lett. **83,** 4764 (1999).
65. F. Melandso, Phys. Plasmas **3,** 3890 (1996).
66. P.K. Shukla, Phys. Plasmas **10,** 1619 (2003).
67. Y. Nakamura, H. Bailung, and P. K. Shukla, Phys. Rev. Lett. **83**, 1602 (1999).
68. A. A. Mamun, R. A. Cairns, and P. K. Shukla, Phys. Plasmas **3**, 702 (1996).
69. A. A. Mamun, Astrophys. Space Sci. **260**, 507 (1998).
70. A. A. Mamun, S. M. Russel, C. A. M. Briceno, M. N. Alan, T. K. Datta, and A. K. Das, Planet. Space Sci. **48**, 599 (2000).
71. I. Tasnim , M. M. Masud, and A. A. Mamun, Plasma Phys. Reports **40**, 723(2014).

72. P. Bandyopadhyay , G. Prasad, A. Sen, and P. K. Kaw, PRL **101**, 065006 (2008).
73. M. Remoissenet, Waves Called Solitons (Concepts and Experiments), Springer-Verlag Berlin Heidelberg New York (1994).
74. Washimi and Tanniuti, Phys. Rev. Lett.**17,** 996 (1966).
75. V.K. Yadav and A. Bhardwaj, Conference on Planetary Space and Exploration, Ahamedabad, India, (2011) pp.160-161.
76. V.K. Yadab, R.S. Thempi and A. Bhardwaj, 27th national symposium on plasma science and technology, Pondicherry University, Pundicherry, India (2012) pp.454-458.
77. J.S. Russell, *Report on waves*. Report of the fourteenth meeting of the British Association for the Advancement of Science, York (1844) pp.311-390.
78. N.J. Zabusky and M.D. Kruskal, Phys. Rev. Lett. **15,** 240 (1965).
79. J. D. Jr. Anderson, Fundamentals of Aerodynamics (3rd ed.), McGraw-Hill Science/ Engineering/Math.(2001).
80. J. Bond, K. Watson, and J. Welch, Atomic Theory of Gas Dynamics (Addison-Wesley, Reading, MA, 1965).
81. S. Horluck and P. Dimon, Phys. Rev. E **60,** 671 (1999).
82. R. Graham, Solids under High-Pressure Shock Compression (Springer-Verlag, New York, 1993).
83. R.Z. Sagdeev, Reviews of Plasma Physics (Consultants Bureau,New York) **4,** 2391 (1966).
84. H.K. Andersen, N. D' Angelo, and P. Michelsen, Phys. Fluids **11,** 606 (1968).
85. H. E. Petschek, Aerodynamic Dissipation, Rev. Mod. Phys. **30,** 966 (1958).
86. Fishman, F. J., A. R. Kantrowitz, and H. E. Petschek, Magnetohydrodynamic Shock Wave in a Collision-Free Plasma, Rev. Modern Phys. **32,** 959 (1960).
87. F. H. Shu, Physics of Astrophysics, Vol. II, University Science Books, (1992), ISBN 0-935702-65-2.
88. M. M. Mellott and E. W. Greenstadt, J. Geophys. Res. **89**, 2151 (1984).
89. V. V. Krasnoselskikh, B. Lembege, P. Savoini, and V. V. Lobzin, Phys. Plasmas **9,** 1192 (2002).
90. D. Sundkvist, V. Krasnoselskikh, S. D. Bale, S. J. Schwartz, J. Soucek, and F. Mozer, Phys. Rev. Lett. **108,** 025002 (2012).
91. R. Z. Sagdeev, Rev. Plasma Phys. **4,** 23 (1966).
92. S. P. Gary, J. Geophys. Res. **86,** 4331 (1981).

93. J. P. Edmiston and C. F. Kennel, J. Plasma Phys. **32,** 429 (1984).
94. C. F. Kennel, J. Geophys. Res. **92,** 427 (1987).
95. S. D. Bale et al., Space Sci. Rev. **118,** 161 (2005)
96. J. D. Scudder, T. L. Aggson, A. Mangeney, C. Lacombe, and C. C. Harvey, J. Geophys. Res. **91,**019 (1986a).
97. J. D. Scudder, T. L. Aggson, A. Mangeney, C. Lacombe, and C. C. Harvey, J. Geophys. Res. **91,** 053 (1986b).
98. J. D. Scudder, A. Mangeney, C. Lacombe, C. C. Harvey, and C. S. Wu, J. Geophys. Res. **91,** 075 (1986c).
99. S. A. Haver, In Proceedings of the Rogue Waves, Brest, France (2004), pp.1–8.
100. D. R. Solli, C. Ropers, P. Koonath, and B. Jalali, Nature **450,** 1054 (2007).
101. D.I. Yeom and B. J. Eggleton, Nature **450,** 953-954 (2007).
102. J. M. Dudley, G. Genty, F. Dias, B. Kibler, and N. Akhmediev, Optics Express, 21497 (2009).
103. M. S. Ruderman, Euro. Phys. J.: *Special Topics* **185,**57– 66(2010).
104. A. N. Ganshin, V. B. Efimov, G. V. Kolmakov, L. P. Mezhov- Deglin, and P. V. E. McClintock, Phys. Rev.Lett.**101,**(2008).
105. David Bohm, Rev.**85,** 166 (1952).
106. M.- J. Lee and Y.-D. Jung , Phys. Lett. A **381,** 636 (2017).
107. E. T. Meier and U. Shumlak, Phys. Plasmas **19,** 072508 (2012).
108. T. M. Davis and M. I. Scrimgeour, arXiv: 1405.0105v2 [astro-ph.CO] (2014).
109. R. Fitzpatrick, Thermodynamics and Statistical Mechanics, Lulu Enterprises, Inc, (2006).
110. R. Boström, et al., Phys. Rev. Lett. **61,** 82 (1988).
111. M. Temerin, K. Cerny, W. Lotko, and F. S. Mozer, Phys. Rev. Lett. **48,** 1175 (1982).
112. R .Lundin, et al., Nature, **341,** 609 (1989).
113. R. Boström, IEEE Trans. Plasma Sci. **20,** 756 (1992).
114. P. O. Dovner et al., Geophys. Res. Lett.**21,** 1827 (1994).
115. H. Matsumoto et al., Geophys. Res. Lett. **21,** 2915 (1994).
116. R. A. Cairns et al., Geophys. Res. Lett. **22,** 2709 (1995).
117. M. Maksimovic, V. Pierrard and P. Riley, Geophys. Res. Lett. **24,** 1151 (1997).
118. I. Zouganelis, J. Geophys. Res.: Space Physics (1978C2012) **113,** A8 (2008).

119. P. Chatterjee, U.N. Ghosh, K. Roy, S. V. Muniandy, C.S. Wong and B. Sahu, Phys. Plasmas **17,** 122314 (2010).
120. C. R. Choi, K. W. Min, and T. N. Rhee, Phys. Plasmas **18,** 092901 (2011).
121. D. Summers and R.M. Thorne, Phys. Fluids B **3,** 1835 (1991).
122. V. M. Vasyliunas, J. Geophys. Res. **73,** 2839 (1968).
123. T. K. Baluku and M. A. Hellberg, Phys. Plasmas **15,** 123705 (2008).
124. V. Pierrard · M. Lazar, Solar Phys. **267**, 153–174 (2010).
125. W.M. Moslem, Chaos Solitons Fractals **28,** 994 (2006).
126. M. Asaduzzaman, A.A. Mamun, J. Plasma Phys.**78,** 125 (2012).
127. M. Asaduzzaman, A.A. Mamun, Phys. Rev. E **86,** 016409 (2012).
128. M.P. Leubner, J. Geophys. Res. **87,** 6335 (1982).
129. S.K. Mishra, S. Misra, M.S. Sodha, Eur. Phys. J. D **67,** 210 (2013).
130. S.R. Cranmer, Astrophys. J. **508,** 925 (1998).
131. Z.Y. Meng, R. M. Thorne, and D. Summers, J. Plasma Phys. **47,** 445 (1992).
132. M.P. Leubner, Astrophys. Space Sci. **282,**573 (2002).
133. L.N. Guo, J.L. Du and Z.P. Liu, Phys. Lett. A **367,** 431 (2007).
134. C. Tsallis, J. Stat. Phys. **52,** 479 (1988).
135. M. Ferdousi, S. Yasmin, S. Ashraf and A A. Mamun, Astrophys. Space Sci.**352,** 579 (2014)
136. T. S. Gill, A. S. Bains, and N. S. Saini, Can. J. Phys. **87,** 861 (2009).
137. H. Washima and T. Taniuti, Phys. Rev. Lett.**17,** 996–998 (1966).
138. W. S. Duan, B. R. Wang, and R. J. Wei, J. Phys. Soc. Jpn. **65,** 945 (1996).
139. H. Ono, J. Phys. Soc. Jpn. **60,** 4127 (1991).
140. N. J. Zabusky and M. D. Kruskal, Phys. Rev. Lett. **15,** 240 (1965).
141. M. Wadati, J. Phys. Soc. Jpn. **59,** 4201 (1990).
142. X. Qi, Y. X. Xu, W. S. Duan, and L. Yang, Phys. Plasmas **21,** 013702(2014).
143. A. A. Mamun, R. A. Cairns, and P. K. Shukla, Phys. Plasmas **3,** 702 (1996).
144. C. H. Su and R. M. Mirie, J. Fluid Mech. **98,** 509 (1980).
145. C. S. Gardner, J. M. Greener, M. D. Kruskal, and R. M. Miura, Phys. Rev. Lett. **19,** 1095 (1967).
146. A. Jeery and T. Kawahawa, Asymptotic Methods in Nonlinear Wave Theory (Pitman, London, 1982).
147. G. X. Huang and M. G. Velarde, Phys. Rev. E **53,** 2988 (1996).

148. Y. X. Xu, Z. M. Liu, M. M. Lin, Y. R. Shi, J. M. Chen, and W. S. Duan, Phys. Plasmas, **18,** 052301 (2011).
149. J. N. Han, S. L. Du, and W. S. Duan, Phys. Plasmas **15,** 112104 (2008).
150. S. C. Li and W. S. Duan, Eur. Phys. J. B **62,** 485–491 (2008).
151. X. X. Yang, W. S. Duan, J. N. Han, and S. C. Li, Chin. Phys. B **17,** 2994 (2008).
152. Y. N. Nejoh, Phys. Fluids B **4,** 2830 (1992).
153. J. Zhang, Y. Yang, Y.-X. Xu, L. Yang, X. Qi, and W.-S. Duan, Phys. Plasmas **21**, 103706 (2014).
154. H. Poincare´, New Methods of Celestial Mechanics (NASA TTF, 1967), pp. 450.
155. M. J. Lighthill, Philos. Mag. **40,** 1120 (1949).
156. Y. H. Kuo, J. Math. Phys. **32,** 83 (1953).
157. H. S. Tsien, Adv. Appl. Math.**4,** 281 (1956).

Chapter 2

Interactions of ion acoustic multi-soliton and rogue wave with Bohm quantum potential in degenerate plasma

2.1 Introduction

It is well known that the dense electron–positron–ion (epi) plasmas are prevailed in the astrophysical environments, such as in white dwarfs, neutron stars, and active galactic nuclei[1–4], and are produced in the laboratory, such as in the intense laser–solid interaction experiments[5-6]. The relativistic or quantum effect becomes prominent due to the fact that the inter electron distance is comparable to the thermal de Broglie wave length [1] in such high density (of the order of 10^{30} cm^{-3}) plasmas, e.g., in white dwarfs. In such extremely high density plasmas, the electron thermal energy is much less the electron Fermi energy. According to Pauli's exclusion principle, the electron thermal pressure can thus be neglected [7] compared to the Fermi degeneracy pressure. The astrophysical objects sustain against the enormous gravitational forces due to the extremely dense degenerate electron pressure. In such case, the tunneling of the plasma species associated with the Bohm potential and statistical Fermi–Dirac pressure plays a significant role [8] on the structures and dynamics of the ion acoustic waves as observed in different astrophysical and space plasmas[9-10], such as in white dwarf[1] and magnetars [11].

References [4] and [12-21] have investigated the structures and nonlinear propagation of ion acoustic waves considering either degenerate or non-degenerate plasmas. Mamun and Shukla [12] investigated the structures of the shock waves in degenerate dense plasma in order to explain the phenomenon observed in white dwarfs. Rahman et al. [17] showed that the positron concentration and the relativistic plasma parameters significantly modify the amplitude, width, and phase velocity of the ion acoustic waves in epi plasmas. Haas *et al*.[18] found that the interaction of plasma particles with the Bohm potential significantly affects the properties of the nonlinear ion acoustic waves. Bhowmik *et al*. [19] studied the effects of quantum diffraction parameter (H) and equilibrium plasma species density ratio on the propagation of electron acoustic waves in the quantum plasmas. Recently, Hossen *et al*. [8] considered a degenerate epi plasma system consisting of inertial non-relativistic light ions,

degenerate electrons, and positrons and noted the effects of tunneling of the plasma particles with the Bohm potential on the propagation of ion acoustic waves by deriving the KdV, mKdV, and mixed mKdV (mmKdV) equations. On the other hand, many authors [22–29] have studied the propagation phenomena of the rogue waves by transforming the KdV, mKdV, and mmKdV equations to the corresponding NLS equations. Besides, Mandal *et al*. [30] have investigated only the overtaking collisions and phase shifts of dust acoustic multi-solitions in a four component dusty plasma. However, the interactions between single- and multi-solitons and hence the production of rogue waves along with their structures and dynamics are still unrevealed in the plasmas[8] for better understanding the physical issues observed in space plasmas [25–29,31–38]. Being motivated, for the significance of the problems related to the astrophysical and laboratory plasmas, we study the interaction processes of the ion acoustic single- and multi-solitons, and their phase shifts as well as rogue waves in an unmagnetized plasmas composing degenerate electrons and positrons including Bohm quantum potential and an inertial non-relativistic light ions. The effects of helium ion mass and density, degenerate electrons, and positrons densities and temperatures on the phase shift, interactions among the ion acoustic single- and multi-solitons, and the production of rogue waves are investigated.

In sequence of introduction, the theoretical model and derivations of two-sided KdV equations are presented in Section 2.2.The single- and multi-solitons solutions of the KdV equations and their corresponding phase shifts are illustrated in Section 2.3. Derivation of nonlinear Schrödinger equation (NLSE) along with the solution of its rational function is displayed in Section 2.4. The results and discussion are described in Section 2.5. Finally, the conclusion is drawn in Section 2.6.

2.2 Governing equations

2.2.1 Model equations

The electrons (positrons) remain non-relativistic if their Fermi energy is less than their rest mass energy [39] in high density plasmas. On the other hand, the electrons have Fermi energy that is comparable to or greater than their rest mass energy, and hence the electron Fermi speed turns out to be comparable to the speed of light in vacuum for the number densities in the range of $10^{29} - 10^{34}\mathrm{cm}^{-3}$. Chandrasekhar [4, 40] explained the equation of state for degenerate plasmas, as observed in an astrophysical compact object, namely, white dwarf, considering degenerate pressure exerted by plasma fluid as $P_s = K_s n_s^{\alpha} = K_s n_s^{\gamma}$, where $\alpha = 5/3$, $K_s \approx (3/5)\Lambda_c \hbar c$, $(\Lambda_c = \pi\hbar/m_s c = 1.2 \times 10^{-10}\mathrm{cm}, \hbar = h/2\pi)$ for the non-relativistic

and $\gamma = 4/3$, $K_s \approx (3/4)\hbar c$ for the ultra-relativistic cases, m_s and n_s are the plasma species mass and density, and h and c are the Planck constant and velocity of light in free space, respectively. In this report, an unmagnetized dense epi plasma system is considered composing both non-relativistic and relativistic degenerate electrons and positrons, and inertial non-relativistic light ions. $n_{e0} = n_{p0} + n_{i0}$ is considered as the quasi-neutrality condition, where n_{e0}, n_{p0}, and n_{i0} are the densities of the unperturbed electrons, positrons, and ions, respectively. To study the structures and dynamics of the ion acoustic waves including their electrostatic resonance phenomena, corresponding phase shifts, and production of rogue waves in the considered plasmas, the normalized fluid equations [8] can be written as

$$\frac{\partial n_i}{\partial t} + \frac{\partial}{\partial x}(n_i u_i) = 0 \ , \tag{2.1}$$

$$\frac{\partial u_i}{\partial t} + u_i \frac{\partial u_i}{\partial x} = -\frac{\partial \phi}{\partial x} - \frac{K_1}{n_i} \frac{\partial n_i^{\alpha}}{\partial x} \ , \tag{2.2}$$

$$n_e \frac{\partial \phi}{\partial x} - K_2 \frac{\partial n_e^{\gamma}}{\partial x} + \beta \frac{\partial}{\partial x}\left(\frac{1}{\sqrt{n_e}} \frac{\partial^2 \sqrt{n_e}}{\partial x^2}\right) = 0 \ , \tag{2.3}$$

$$n_p \frac{\partial \phi}{\partial x} + K_2 \eta_1 \frac{\partial n_p^{\gamma}}{\partial x} - \lambda \frac{\partial}{\partial x}\left(\frac{1}{\sqrt{n_p}} \frac{\partial^2 \sqrt{n_p}}{\partial x^2}\right) = 0 \ , \tag{2.4}$$

$$\frac{\partial^2 \phi}{\partial x^2} = \mu n_e - n_i - \sigma n_p. \tag{2.5}$$

Here, n_s ($\mathrm{s} = \mathrm{i}, e, p$) is normalized by their equilibrium counterparts n_{s0}, u_i is the ion fluid speed normalized by ion acoustic speed $C_i = (k_B T_{Fe}/m_i)^{1/2}$, ϕ is the electrostatic potential normalized by $(k_B T_{Fe}/e)$, $\eta_1 = (T_{Fp}/T_{Fe})$, $\mu = (n_{e0}/n_{i0})$, $\sigma = (n_{p0}/n_{i0})$, $K_1 = (n_{i0}^{\alpha-1} K_i/m_i c^2)$, $K_2 = (n_{j0}^{\gamma-1} K_j/m_i c^2), j = e, p$, k_B is the Boltzmann constant, m_i is the ion rest mass and $T_{Fp}(T_{Fe})$ is the Fermi temperature of positron (electron).The time and space variables are normalized by $\omega_{pm}^{-1} = (m_i/4\pi n_{i0} e^2)^{1/2}$ and $\lambda_{Di} = (k_B T_{Fe}/4\pi n_{i0} e^2)^{1/2}$, respectively. The remaining dimensionless quantum parameters are β ($= n_{i0} H_e^2/2\, n_{e0}$) and λ ($= n_{i0} H_p^2/2\, n_{p0}$), where $H_e = \hbar \omega_{pe}/k_B T_{Fe}$ and $H_p = \hbar \omega_{pp}/k_B T_{Fp}$ introduced in Eqs.(2.3) and (2.4) due to the tunneling effect associated with Bohm potential [41].

2.2.2 Derivation of two-sided KdV equations

The two-sided KdV equations are derived by employing the extended Poincaré-Lighthill-Kuo (ePLK) method [38]. According to the ePLK method, the scaling variables x and t are defined as

$$\left.\begin{aligned}\xi &= \varepsilon\left(x - V_p t\right) + \varepsilon^2 X_0(\eta,\tau) + \varepsilon^3 X_1(\eta,\xi,\tau) + \ \dots\dots \\ \eta &= \varepsilon\left(x + V_p t\right) + \varepsilon^2 Y_0(\xi,\tau) + \varepsilon^3 Y_1(\eta,\xi,\tau) + \ \dots\dots \\ \tau &= \varepsilon^3 t\end{aligned}\right\}, \tag{2.6}$$

and the perturbed quantities can be written as

$$\begin{bmatrix} n_s \\ u_i \\ \phi \end{bmatrix} = \begin{bmatrix} 1 \\ 0 \\ 0 \end{bmatrix} + \sum_{r=1}^{\infty} \varepsilon^{r+1} \begin{bmatrix} n_s^{(r)} \\ u_i^{(r)} \\ \phi^{(r)} \end{bmatrix} , \tag{2.7}$$

where ξ and η indicate the trajectories between the ion acoustic waves that are propagating toward each other, V_p is the unknown phase velocity of ion acoustic waves normalized by C_i, and ε is a small parameter. The unknown phase functions $X_0(\eta,\tau)$ and $Y_0(\xi,\tau)$ will be evaluated later. Substituting Eqs.(2.6) and (2.7) into Eqs. (2.1)-(2.5) and equating the quantities with the same orders of ε, one can obtain coupled equations. Taking the lowest order of ε gives the following equations:

$$\left(-V_p \frac{\partial n_i^{(1)}}{\partial \xi} + \frac{\partial u_i^{(1)}}{\partial \xi}\right) + \left(V_p \frac{\partial n_i^{(1)}}{\partial \eta} + \frac{\partial u_i^{(1)}}{\partial \eta}\right) = 0, \tag{2.8}$$

$$\left(-V_p \frac{\partial u_i^{(1)}}{\partial \xi} + K_1^{'} \frac{\partial n_i^{(1)}}{\partial \xi} + \frac{\partial \phi^{(1)}}{\partial \xi}\right) + \left(V_p \frac{\partial u_i^{(1)}}{\partial \eta} + K_1^{'} \frac{\partial n_i^{(1)}}{\partial \eta} + \frac{\partial \phi^{(1)}}{\partial \eta}\right) = 0, \tag{2.9}$$

$$\frac{\partial \phi^{(1)}}{\partial \xi} - K_2^{'} \frac{\partial n_e^{(1)}}{\partial \xi} + \frac{\partial \phi^{(1)}}{\partial \eta} - K_2^{'} \frac{\partial n_e^{(1)}}{\partial \eta} = 0 , \tag{2.10}$$

$$\frac{\partial \phi^{(1)}}{\partial \xi} + K_2^{'} \eta_1 \frac{\partial n_p^{(1)}}{\partial \xi} + \frac{\partial \phi^{(1)}}{\partial \eta} + K_2^{'} \eta_1 \frac{\partial n_p^{(1)}}{\partial \eta} = 0 , \tag{2.11}$$

$$\mu n_e^{(1)} - n_i^{(1)} - \sigma n_p^{(1)} = 0 \ , \tag{2.12}$$

where $K_1^{'} = K_1 \alpha$ and $K_2^{'} = K_2 \gamma$. One may define the relations along with different physical quantities $\phi_R^{(1)}(\xi,\tau) \approx \phi_R^{(1)}$ and $\phi_L^{(1)}(\eta,\tau) \approx \phi_L^{(1)}$ taking Eqs. (2.8) to (2.11) into account as

$$\phi^{(1)} = \phi_R^{(1)} + \phi_L^{(1)} , u_i^{(1)} = \frac{V_p}{V_p^2 - K_1^{'}}\left[\phi_R^{(1)} - \phi_L^{(1)}\right], n_i^{(1)} = \frac{1}{V_p^2 - K_1^{'}}\left[\phi_R^{(1)} + \phi_L^{(1)}\right],$$

$$n_e^{(1)} = \frac{1}{K_2^{'}}\left[\phi_R^{(1)} + \phi_L^{(1)}\right], n_p^{(1)} = -\frac{1}{K_2^{'}\eta_1}\left[\phi_R^{(1)} + \phi_L^{(1)}\right]. \tag{2.13}$$

Equation (2.13) indicates the two-sided electrostatic waves, one of which $\phi_R^{(1)}$ is propagating to the right direction from $\xi = 0, \eta \to -\infty$ to $\xi = 0, \eta \to +\infty$ and the other $\phi_L^{(1)}$ is propagating to the left direction from $\eta = 0, \xi \to +\infty$ to $\eta = 0, \xi \to -\infty$. By inserting Eq. (2.13) into Eq.(2.12), the phase velocity is obtained as

$$V_p = \left\{ K_1^{'} + \frac{K_2^{'}\eta_1}{\mu\eta_1 + \sigma} \right\}^{\frac{1}{2}} . \tag{2.14}$$

Again, the next order of ε provides a set of equations in terms of the second order perturbed quantities, similar to Eqs. (2.8)-(2.12). One may also define the physical quantities $\phi_R^{(2)}$ and $\phi_L^{(2)}$ similar to those of Eq. (2.13). Considering the next higher order of ε yields a set of nonlinear evolution equations that are presented in Appendix **A** (Eqs. (A1)-(A5)). Simplifying Eqs. (A1)-(A5) with the help of Eq. (2.13) and then integrating with regards to ξ and η yield

$$\int \left(\frac{\partial \phi_R^{(1)}}{\partial \tau} + A\phi_R^{(1)} \frac{\partial \phi_R^{(1)}}{\partial \xi} + B \frac{\partial^3 \phi_R^{(1)}}{\partial \xi^3} \right) d\eta + \frac{\partial}{\partial \eta} \int \left(\frac{\partial \phi_L^{(1)}}{\partial \tau} - A\phi_L^{(1)} \frac{\partial \phi_L^{(1)}}{\partial \eta} - B \frac{\partial^3 \phi_L^{(1)}}{\partial \eta^3} \right) d\xi$$
$$+ \iint \left(C \frac{\partial X_0}{\partial \eta} + D\phi_L^{(1)} \right) \frac{\partial^2 \phi_\xi^{(1)}}{\partial \xi^2} d\xi d\eta - \iint \left(C \frac{\partial Y_0}{\partial \xi} + D\phi_R^{(1)} \right) \frac{\partial^2 \phi_\eta^{(1)}}{\partial \eta^2} d\xi d\eta$$
$$= -2\left(V_p^2 - K_1^{'}\right) u_i^{(3)} , \tag{2.15}$$

where, $A = \frac{\left(V_p^2 - K_1^{'}\right)^2}{2V_p} \left\{ \frac{3V_p^2}{\left(V_p^2 - K_1^{'}\right)^3} + \frac{K_1^{'}(\alpha - 2)}{\left(V_p^2 - K_1^{'}\right)^3} + \frac{\mu(\gamma - 2)}{\left(K_2^{'}\right)^2} - \frac{\sigma(\gamma - 2)}{\left(K_2^{'}\eta_1\right)^2} \right\}$,

$$B = \frac{\left(V_p^2 - K_1^{'}\right)^2}{2V_p} \left\{ 1 - \frac{\mu\beta}{2\left(K_2^{'}\right)^2} - \frac{\lambda\sigma}{2\left(K_2^{'}\eta_1\right)^2} \right\},$$

$$C = \frac{\left(V_p^2 - K_1^{'}\right)^2}{2V_p} \left[\frac{3V_p^2}{\left(V_p^2 - K_1^{'}\right)^2} + \frac{1}{\left(V_p^2 - K_1^{'}\right)} - \frac{2\sigma}{K_2^{'}\eta_1} \right],$$

$$D = \frac{\left(V_p^2 - K_1^{'}\right)^2}{2V_p} \left[\frac{\mu(\gamma - 2)}{\left(K_2^{'}\right)^2} - \frac{\sigma(\gamma - 2)}{\left(K_2^{'}\eta_1\right)^2} - \frac{V_p^2 - K_1^{'}(\alpha - 2)}{\left(V_p^2 - K_1^{'}\right)^3} \right].$$

It is clearly seen that the first and second terms in the left hand side of Eq. (2.15) are proportional to η and ξ, respectively. Therefore, all the terms involved in the first two expressions of the left hand side of Eq. (2.15) become secular, which may be eliminated in

order to stay away from resonances [42]. The following two-sided KdV equations are obtained to study the resonance phenomena of the electrostatic potential:

$$\frac{\partial \phi_R^{(1)}}{\partial \tau} + A\phi_R^{(1)} \frac{\partial \phi_R^{(1)}}{\partial \xi} + B \frac{\partial^3 \phi_R^{(1)}}{\partial \xi^3} = 0, \tag{2.16}$$

$$\frac{\partial \phi_L^{(1)}}{\partial \tau} - A\phi_L^{(1)} \frac{\partial \phi_L^{(1)}}{\partial \eta} - B \frac{\partial^3 \phi_L^{(1)}}{\partial \eta^3} = 0. \tag{2.17}$$

The third and the fourth terms of the left hand side of Eq. (2.15) may become secular terms in the next higher order and yield the following equations:

$$C \frac{\partial X_0}{\partial \eta} = -D\phi_L^{(1)}, \tag{2.18}$$

$$C \frac{\partial Y_0}{\partial \xi} = -D\phi_R^{(1)}. \tag{2.19}$$

Equations (2.18) and (2.19) indicate that X_0 and Y_0 are the functions of η and ξ, respectively, which may be calculated with the help of analytical soliton solutions of KdV equations (2.16) and (2.17).

2.3 Soliton solutions and phase shifts

To study the nonlinear propagation characteristics of the interactions of ion acoustic solitons and their phase shifts in the plasmas, one has to derive the analytical soliton solutions of the KdV Eqs.(2.16) and (2.17) using the well established Hirota bilinear method [43-44]. According to this method, the single soliton solutions of Eqs.(2.16) and (2.17) can be obtained as

$$\phi_R^{(1)} = \frac{12B}{A} \frac{\partial^2}{\partial \xi^2} ln\left(1 + e^{\theta}\right), \tag{2.20}$$

$$\phi_L^{(1)} = \frac{12B}{A} \frac{\partial^2}{\partial \eta^2} ln(1 + e^{-\omega}), \tag{2.21}$$

where $\theta = \left(k_1 B^{-\frac{1}{3}} \xi - k_1^3 \tau\right)$ and $\omega = \left(k_1 B^{-\frac{1}{3}} \eta + k_1^3 \tau\right)$. Simplifying Eqs. (2.18) and (2.19) and taking Eqs. (2.20) and (2.21) into account, the leading phase changes due to the interaction of ion acoustic solitary waves that can be defined as

$$X_0 = -\frac{12BD}{CA}\frac{\partial}{\partial\eta}ln(1+e^{-\omega}) = \frac{12B^{2/3}Dk_1}{CA}\frac{e^{-\omega}}{1+e^{-\omega}}, \quad (2.22)$$

$$Y_0 = -\frac{12BD}{CA}\frac{\partial}{\partial\xi}ln\left(1+e^{\theta}\right) = -\frac{12B^{2/3}Dk_1}{CA}\frac{e^{\theta}}{1+e^{\theta}}. \quad (2.23)$$

The trajectories of solitary waves for weak interactions can be reduced to

$$\xi = \varepsilon\left(x - V_p t\right) + \varepsilon^2\frac{12B^{2/3}Dk_1}{CA}\frac{e^{-\omega}}{1+e^{-\omega}} + \cdots\cdots\cdots, \quad (2.24)$$

$$\eta = \varepsilon\left(x + V_p t\right) - \varepsilon^2\frac{12B^{2/3}Dk_1}{CA}\frac{e^{\theta}}{1+e^{\theta}} + \cdots\cdots\cdots. \quad (2.25)$$

To evaluate the phase shifts after interactions between ion acoustic solitons, one may assume that the solitons, say R and L are asymptotically far away from each other at the initial time, that is, soliton R is at $\xi = 0, \eta \to -\infty$ and L is at $\eta = 0, \xi \to +\infty$. After interaction, R is at $\xi = 0, \eta \to +\infty$ and L is at $\eta = 0, \xi \to -\infty$ to the right of L. The corresponding phase shifts are obtained as

$$\nabla X_0 = \varepsilon\left(x - V_p t\right)\big|_{\eta\to-\infty,\xi=0} - \varepsilon\left(x - V_p t\right)\big|_{\eta\to\infty,\xi=0} = \varepsilon^2\frac{12B^{2/3}Dk_1}{CA}, \quad (2.26)$$

$$\nabla Y_0 = \varepsilon\left(x + V_p t\right)\big|_{\xi\to-\infty,\eta=0} - \varepsilon\left(x + V_p t\right)\big|_{\xi\to\infty,\eta=0} = -\varepsilon^2\frac{12B^{2/3}Dk_1}{CA}. \quad (2.27)$$

Again, double- soliton solutions of the KdV equations can be written as

$$\phi_R^{(1)} = \frac{12B}{A}\frac{\partial^2}{\partial\xi^2}ln\left[1 + e^{\theta_1} + e^{\theta_2} + a_{12}e^{\theta_1+\theta_2}\right], \quad (2.28)$$

$$\phi_L^{(1)} = \frac{12B}{A}\frac{\partial^2}{\partial\eta^2}ln[1 + e^{\omega_1} + e^{\omega_2} + a_{12}e^{\omega_1+\omega_2}], \quad (2.29)$$

where $\theta_i = \left(k_i B^{-1/3}\xi - k_i^3\tau\right)$, $\omega_i = -\left(k_i B^{-1/3}\eta + k_i^3\tau\right)$ and $a_{12} = (k_2 - k_1)^2/(k_2 + k_1)^2$ with $i = 1, 2$. By using Eqs.(2.28) and (2.29), the solution of Eqs. (2.18) and (2.19) can written as

$$X_0 = \frac{12B^{2/3}D}{CA}\frac{k_1e^{\theta_1} + k_2e^{\theta_2} + a_{12}(k_1 + k_2)e^{\theta_1+\theta_2}}{1 + e^{\theta_1} + e^{\theta_2} + a_{12}e^{\theta_1+\theta_2}}, \quad (2.30)$$

$$Y_0 = -\frac{12B^{2/3}D}{CA}\frac{k_1 e^{\omega_1} + k_2 e^{\omega_2} + a_{12}(k_1+k_2)e^{\omega_1+\omega_2}}{1 + e^{\omega_1} + e^{\omega_2} + a_{12}e^{\omega_1+\omega_2}}, \quad (2.31)$$

and the corresponding phase shifts may be obtained due to the interactions of double soliton as

$$\nabla X_0 = \varepsilon^2 \frac{12B^{2/3}D}{CA}\sum_{i=1}^{2} k_i \,, \nabla Y_0 = -\varepsilon^2 \frac{12B^{2/3}D}{CA}\sum_{i=1}^{2} k_i \,. \quad (2.32)$$

Finally, triple-soliton solutions of the KdV equations can be written as

$$\phi_R^{(1)} = \frac{12B}{A}\frac{\partial^2}{\partial \xi^2} ln\big[1 + e^{\theta_1} + e^{\theta_2} + e^{\theta_3} + a_{12}e^{\theta_1+\theta_2} + a_{23}e^{\theta_2+\theta_3} + a_{13}e^{\theta_1+\theta_3} + a_{123}e^{\theta_1+\theta_2+\theta_3}\big], \quad (2.33)$$

$$\phi_L^{(1)} = \frac{12B}{A}\frac{\partial^2}{\partial \eta^2} ln[1 + e^{\omega_1} + e^{\omega_2} + e^{\omega_3} + a_{12}e^{\omega_1+\omega_2} + a_{23}e^{\omega_2+\omega_3} + a_{13}e^{\omega_1+\omega_3} + a_{123}e^{\omega_1+\omega_2+\omega_3}], \quad (2.34)$$

Where $\theta_i = \big(k_i B^{-1/3}\xi - k_i^3\tau\big)$, $\omega_i = -\big(k_i B^{-1/3}\eta + k_i^3\tau\big)$, $a_{12} = (k_1-k_2)^2/(k_1+k_2)^2$, $a_{23} = (k_2-k_3)^2/(k_2+k_3)^2$, $a_{13} = (k_1-k_3)^2/(k_1+k_3)^2$, and $a_{123} = a_{12}a_{23}a_{13}$ with $i = 1,2,3$, and their corresponding phase shifts due to the interaction of triple soliton may be written as

$$\nabla X_0 = \varepsilon^2 \frac{12B^{2/3}D}{A}\sum_{i=1}^{3} k_i \,, \nabla Y_0 = -\varepsilon^2 \frac{12B^{2/3}D}{CA}\sum_{i=1}^{3} k_i . \quad (2.35)$$

2.4 Derivation of NLSE with rogue wave solution

To study the behavior of weakly nonlinear wave packets in the plasmas, one can derive the NLSE considering the KdV equation as mentioned Eq.(2.16). For simplicity, one can use the following equation for the transformation of variables:

$$\phi(\xi,\tau) = \sum_{m=1}^{\infty}\varepsilon^m \sum_{l=-m}^{m}\phi_l^m(\xi,\tau)e^{il(k\xi-\omega\tau)}, \quad (2.36)$$

$$X = \varepsilon\big(\xi - v_g\tau\big), T = \varepsilon^2\tau \,, \quad (2.37)$$

where $\phi = \phi_{\xi}^{(1)}$, k is the wave number, ω is the angular frequency, and $\mathrm{v_g}$ is the group velocity of the nonlinear IA waves. By using the KdV Eq.(2.16), the following NLSE is obtained:

$$i\frac{\partial\psi}{\partial T} + \frac{1}{2}P\frac{\partial^2\psi}{\partial X^2} + Q\psi|\psi|^2 = 0\,, \tag{2.38}$$

where $P = 6Bk$ and $Q = -(A^2/6Bk)$. The rational function solution of Eq. (2.38) can be written as

$$\psi(X,T) = \sqrt{\frac{P}{Q}}\left[\frac{4(1+2iPT)}{1+4P^2T^2+4X^2} - 1\right]e^{iPT}. \tag{2.39}$$

It is seen that the ratio of P and Q obtained is always negative, that is $P/Q = -1/A^2$. Moreover, the weakly nonlinear theory predicts that quasi-monochromatic wave packets are always modulationally stable and the rogue waves cannot propagate due to the existence of the negative nonlinear coefficient terms in the NLSE. This indicates that the NLSE obtained from the KdV equation may not support the rogue wave solution.

On the other hand, there may arise the cases where the nonlinear coefficient (A) vanishes at the critical value (σ_c) for certain plasma parameters and equation (2.16) fails to study the nonlinear evolution of perturbation. For instance, A vanishes at $\sigma = \sigma_c \approx 0.0195$ for $\lambda = 0.10$, $\beta = 0.10$, $\gamma = 4/3$, $\mu = 0.1$ and $\eta_1 = 0.8$. In such a case, one can derive the mKdV equation by employing the stretched coordinates $\xi = \varepsilon(x - V_p t)$, $\tau = \varepsilon^3 t$ and perturbed quantities as $M = M_0 + \sum_{r=1}^{\infty}\varepsilon^r M^r$ into Eqs. (2.1)-(2.5), where $M = (n_s\, u_i\, \phi)'$, $M_0 = (1\ 0\ 0)'$, and $M^r = \left(n_s^{(r)} u_i^{(r)} \phi^{(r)}\right)'$. The lowest power of ε gives the first order perturbed quantities as $u_i^{(1)} = \left(V_p/(V_p^2 - K_1')\right)\phi^{(1)}$, $n_i^{(1)} = \phi^{(1)}/(V_p^2 - K_1')$, $n_e^{(1)} = \phi^{(1)}/K_2'$, and $n_p^{(1)} = -\phi^{(1)}/K_2'\eta_1$ [8]. The next higher power of ε provides the second order perturbed quantities $u_i^{(2)}$, $n_i^{(2)}$, $n_e^{(2)}$, and $n_p^{(2)}$ that are presented in appendix A(Eqs. (A6) and (A7)). Finally, the next higher order of ε gives the following mKdV equation by taking the first and the second order perturbed quantities into account [8]:

$$\frac{\partial\phi^{(1)}}{\partial\tau} + C\left(\phi^{(1)}\right)^2\frac{\partial\phi^{(1)}}{\partial\xi} + B\frac{\partial^3\phi^{(1)}}{\partial\xi^3} = 0 \tag{2.40}$$

Where

$$C = \frac{\left(V_p^2 - K_1'\right)^2}{2V_p}\left\{\frac{E}{2\left(V_p^2 - K_1'\right)^4} + \frac{F}{2\left(V_p^2 - K_1'\right)^5} + \frac{(\eta_1^3\mu + \sigma)(\gamma - 2)(3 - 2\gamma)}{2\left(K_2'\eta_1\right)^2}\right\},$$

$$E = 6V_p^2 + 6K_1'(\alpha - 2) + 6K_1'(\alpha - 2)(\alpha - 3),$$

$$F = 6V_p^2K_1' + 6(K_1')^2(\alpha - 2) + 18V_p^4 + 3K_1'V_p^2(\alpha - 2) + 3(K_1')^2(\alpha - 2)^2.$$

In order to obtain the rogue wave, substituting Eqs. (2.36) and (2.37) to the mKdV Eq. (2.40) and collect terms having the same order of ε. The lowest order approximation for $m = 1$ with the first harmonic $l = 1$ gives the dispersion relation of electrostatic waves as $\omega = -Bk^3$. The second order approximation for $m = 2$ with $l = 1$ predicts $v_g = -3Bk^2$.Finally, the compatibility condition for the equation that is obtained from the next order ($m = 3$,$l = 1$) provides the NLSE as mentioned in Eq. (2.38). The nonlinearity (Q) and dispersive coefficients (P) are obtained as

$$Q = -k\frac{\left(V_p^2 - K_1^{'}\right)^2}{2V_p}\left\{\frac{E}{2\left(V_p^2 - K_1^{'}\right)^4} + \frac{F}{2\left(V_p^2 - K_1^{'}\right)^5} + \frac{(\eta_1^3\mu + \sigma)(\gamma - 2)(3 - 2\gamma)}{2\left(K_2^{'}\eta_1\right)^2}\right\},$$

$$P = -6k\frac{\left(V_p^2 - K_1^{'}\right)^2}{2V_p}\left\{1 - \frac{\mu\beta}{2\left(K_2^{'}\right)^2} - \frac{\lambda\sigma}{2\left(K_2^{'}\eta_1\right)^2}\right\}.$$

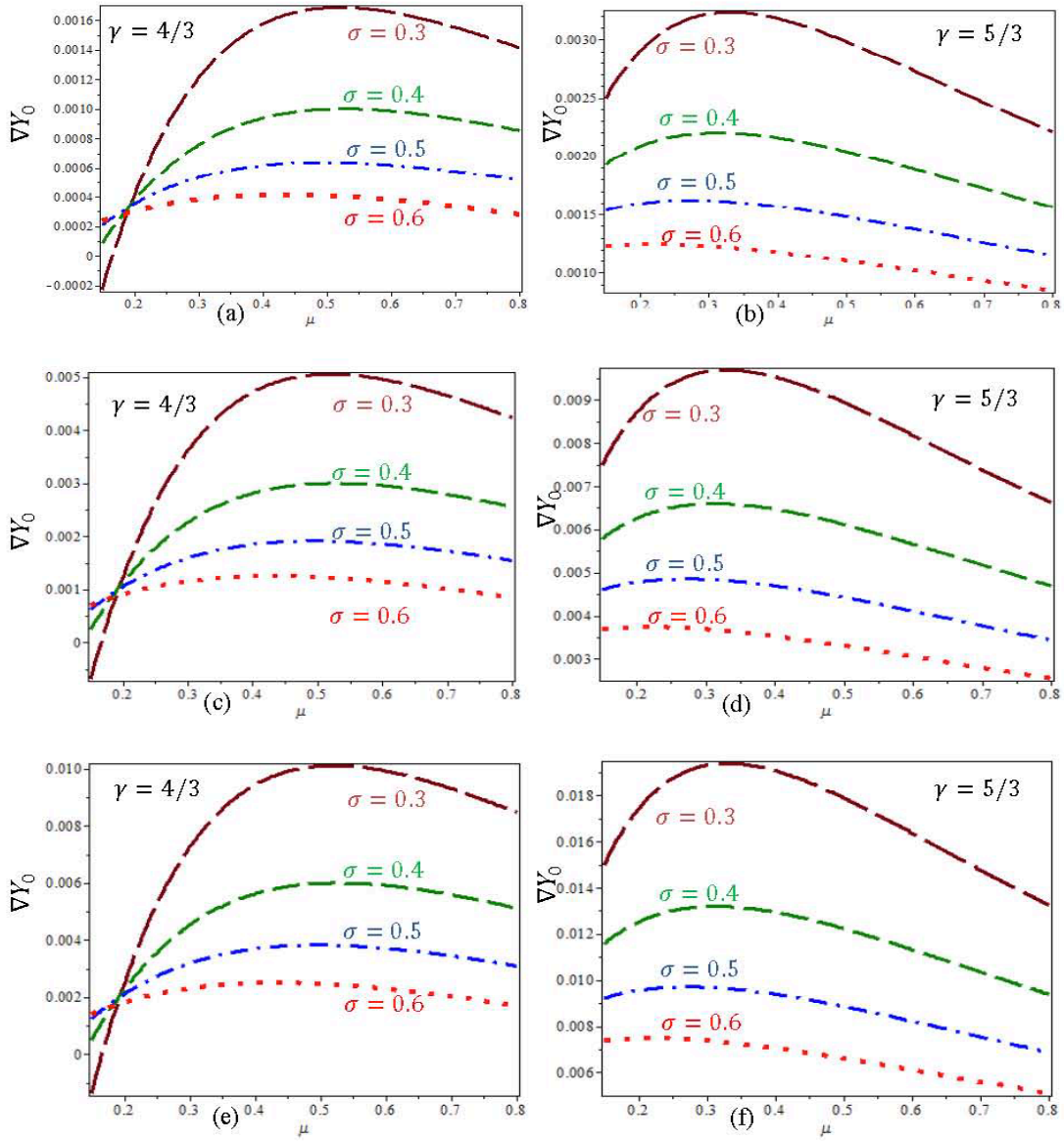

Figure 2.1 Effects of μ and σ on the phase shift ∇Y_0 due to the interaction between two ((a) and (b)), four ((c) and (d)) and six ((e) and (f)) equal amplitude ion acoustic solitons for non-relativistic helium light ions with $\alpha = 5/3$, ultra-relativistic ($\gamma = 4/3$), and non-relativistic ($\gamma = 5/3$) electrons and positrons, respectively, where $\eta_1 = 0.6, \lambda = 0.1, \beta = 0.1, k_1 = 1, k_2 = 2, k_3 = 3,$ and $\varepsilon = 0.1$.

2.5 Results and discussion

Two-sided KdV and NLSE equations are derived to investigate the unrevealed physical issues in the plasma considered, such as temporal evolution of electrostatic resonances and phase shifts due to the interaction of single- and multi-solitons, and modulus instability. The effects of plasma parameters on the temporal evolution of electrostatic resonances, phase shifts, and rogue waves are investigated considering helium ion mass $m_i = 6.68 \times 10^{-24}$ kg, ion density $n_{i0} = 3.0 \times 10^{31}\text{cm}^{-3}$, electron density $n_{e0} = 9.11 \times 10^{29}\text{cm}^{-3}$, positron density $n_{p0} = 1.5 \times n_{e0}$, quantum parameters $\beta = 0.01 - 0.5$ and $\lambda = 0.01 - 0.5$ which are for the relativistic degenerate astrophysical plasmas [4, 12, 45]. The results obtained from this study are described below.

When two or more solitary waves propagate toward each other, they will interact and exchange their energies among themselves, and then separate off, regain their original wave forms. During the whole process of the interactions, the solitary waves are remarkably stable entities, preserving their identities through interaction. Each soliton gains two phase shifts, one is due to the head-on interaction and the other one is due to overtaking one soliton by the other one. On the other hand, the unique effect is due to the interactions that change their phase shifts. The phase shifts become either positive or negative due to head-on and overtaking interactions of the solitons, which is independent of the wave modes [31-38]. Figures 2.1(a)-2.1(f) illustrate the effects of σ and μ on the phase shift ∇Y_0 due to the interaction among two, four, and six equal amplitude ion acoustic solitons in both ultra-relativistic and non-relativistic cases, respectively, taking the remaining parameters constant. It is seen that the changes of phase shifts are decreasing with the increase of positron to ion density ratio $\sigma = (n_{p0}/n_{i0})$. This means that with the increase of positrons density, their interaction with electrons increases having opposite charges due to the contribution to the higher restoring forces. On the other hand, the changes of phase shifts are increasing with the increase of $\mu = (n_{e0}/n_{i0})$ from 0.2 to 0.35 for ultra-relativistic and from 0.2 to 0.25 for non-relativistic cases due to interaction of oppositely propagating single- and multi-solitons, and then decreasing significantly.

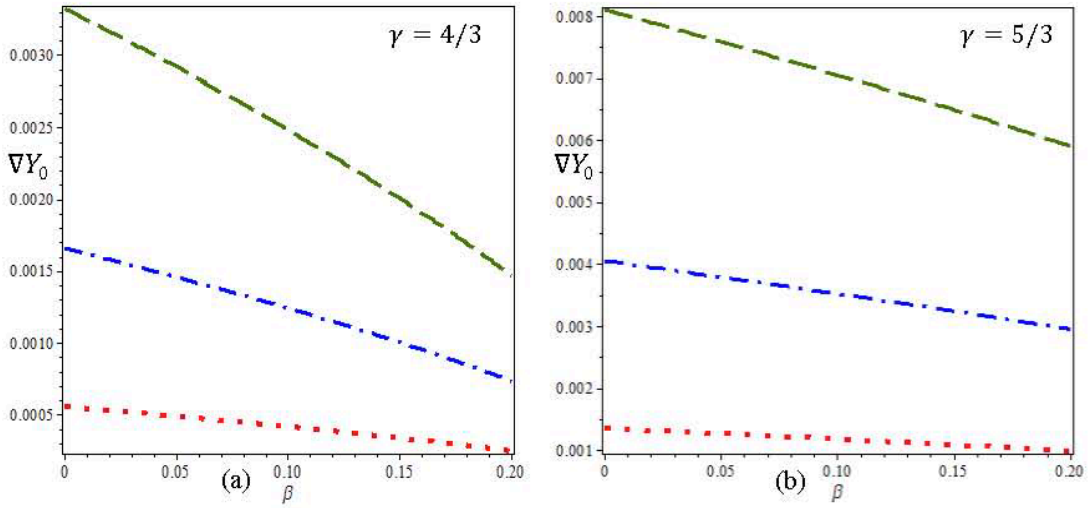

Figure 2.2 Effect of β on the phase shift ∇Y_0 due to the interaction between two (red color), four (blue color) and six (green color) same amplitudes ion acoustic solitons for non-relativistic helium light ions with $\alpha = 5/3$ and ultra-relativistic ($\gamma = 4/3$) as well as non-relativistic ($\gamma = 5/3$) electrons and positrons where $\eta_1 = 0.6$, $\lambda = 0.1$, $\mu = 0.4$, $\sigma = 0.6$, $k_1 = 1$, $k_2 = 2$, $k_3 = 3$, and $\varepsilon = 0.1$.

It is provided that the electrons can contribute to the restoring force due to their small number density in the range $0.2 \leq \mu \leq 0.35$ and then the restoring force increases due to the electrostatic interaction between electrons and positrons increases in the range $\mu > 0.35$. Figures 2.2(a)-2.2(b) show the changes of phase shifts ∇Y_0 with β for the interaction between equal amplitude single- and multi-solitons in both cases, respectively, considering the fixed values of the remaining parameters. The quantum parameter β is mainly arisen due to the Bohm potential, which is solely responsible for the tunneling effect of the corresponding plasma components. It is clear from Figs. 2.2 that the Bohm quantum potential significantly affects the phase shifts in which the changes of phase shifts are decreasing with the increase of quantum parameter β. This phenomenon indicates that the electrons interact more actively with the helium ions, causing the reduction in the magnitude changes of phase shift. Thus, it can be concluded that the phase shifts due to the interaction of two-sided single- and multi-solitons are strongly dependent on the plasma parameters and the wave numbers.

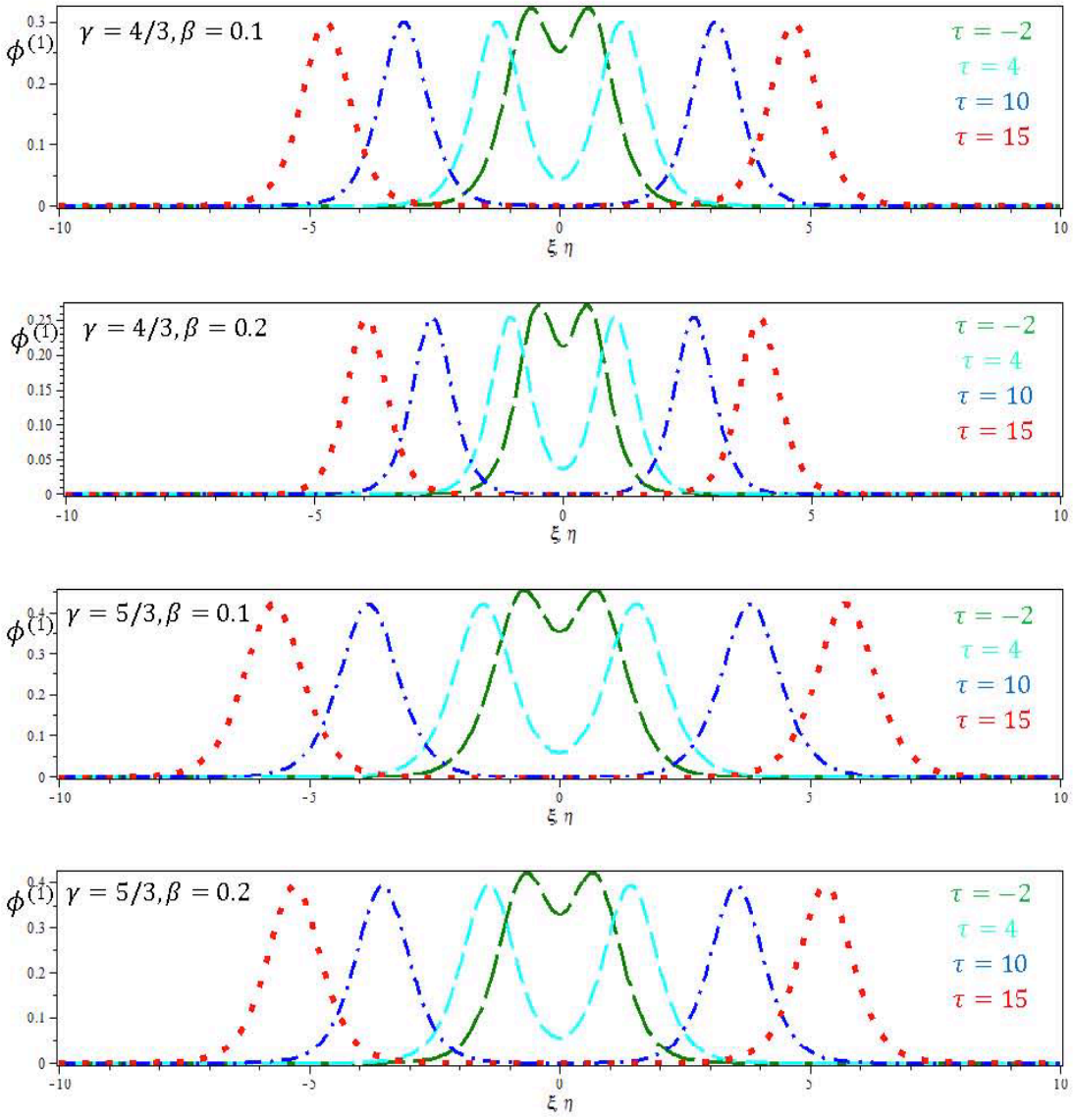

Figure 2.3 Electrostatic potential ($\phi^{(1)} = \phi_R^{(1)} + \phi_L^{(1)}$) profiles due to the interaction between equal amplitude single solitons at different τ and β with inertial non-relativistic helium ions for both ultra-relativistic ($\gamma = 4/3$) and non-relativistic ($\gamma = 5/3$) degenerate electrons and positrons, where $\eta_1 = 0.6$, $\lambda = 0.10$, $\mu = 0.40$, $k_1 = 1$ and $\sigma = 0.5$.

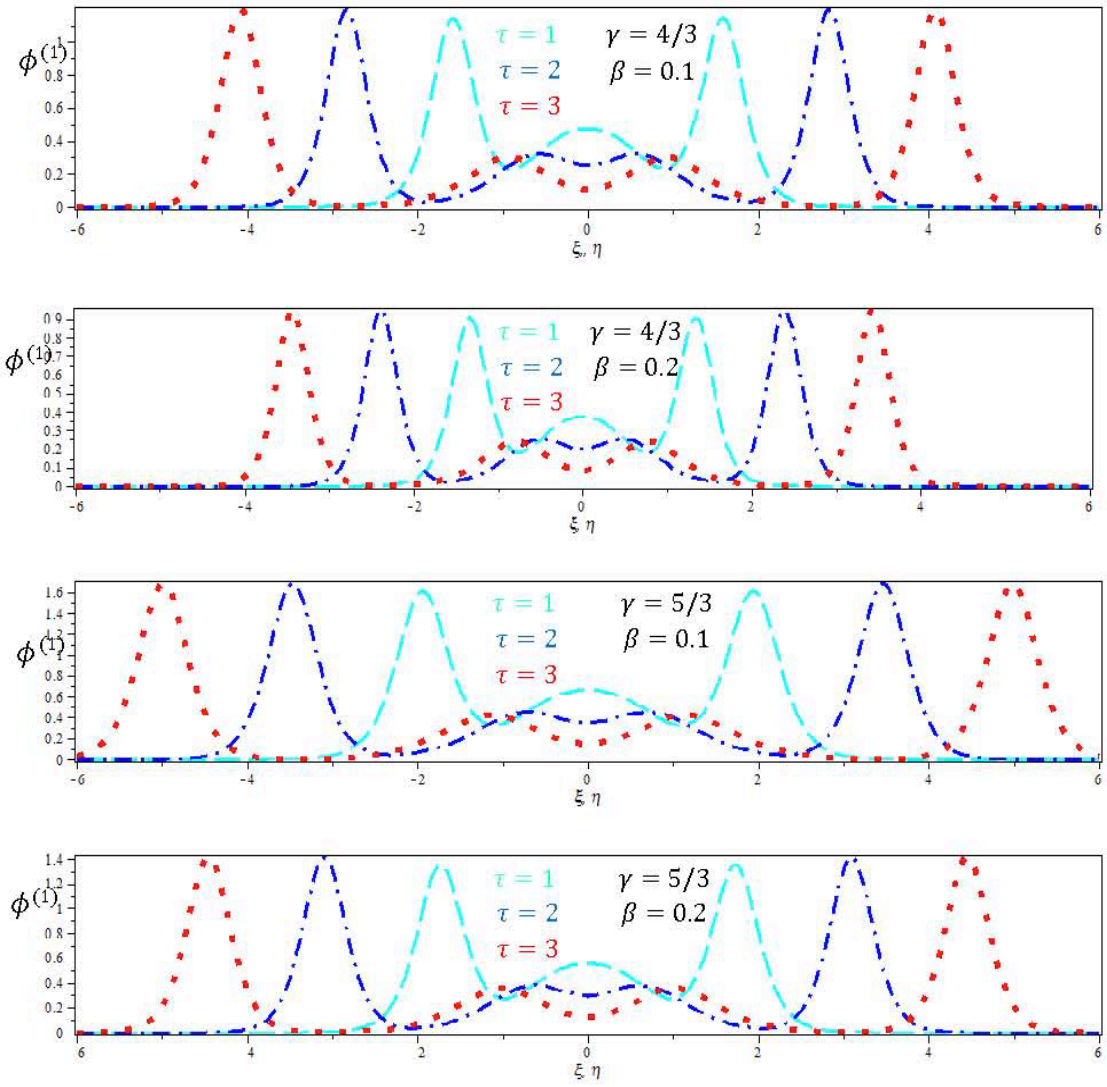

Figure 2.4 Electrostatic potential ($\phi^{(1)}$) profiles due to the interaction between equal amplitude double solitons at different τ and β for both ultra-relativistic ($\gamma = 4/3$) and non-relativistic ($\gamma = 5/3$) degenerate electrons and positrons, and inertial non-relativistic helium ions, where $\eta_1 = 0.6$, $\lambda = 0.10$, $\mu = 0.40$, $k_1 = 1$, $k_2 = 2$ and $\sigma = 0.5$.

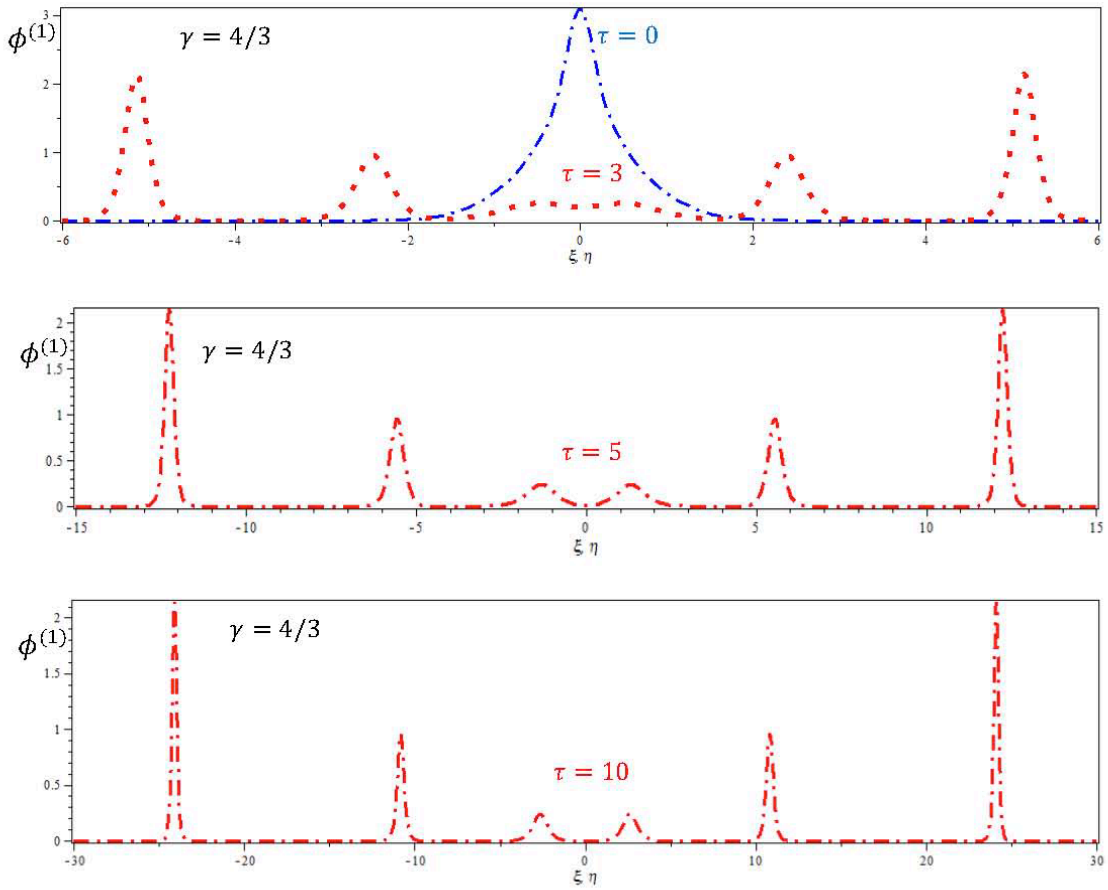

Figure 2.5 Electrostatic potential ($\phi^{(1)}$) profiles due to the interaction between equal amplitude triple solitons at different τ for ultra-relativistic ($\gamma = 4/3$) degenerate electrons and positrons, and inertial non-relativistic helium ions, where $\eta_1 = 0.6$, $\lambda = 0.10$, $\beta = 0.10$, $\mu = 0.40$, $k_1 = 1$, $k_2 = 2$, $k_3 = 3$, and $\sigma = 0.5$.

Figures 2.3(a)-2.3(d), 2.4(a)-2.4(d), and 2.5(a)-2.5(d) display the two-sided equal amplitude electrostatic potential structures $\phi^{(1)} = \phi_R^{(1)} + \phi_L^{(1)}$ for single-, double-, and tripple-solitons against ξ and η, respectively, with different values of β and τ taking the remaining parameters constant for both ultra-relativistic and non-relativistic cases. It is seen from these figures that the amplitudes and widths of both right and left moving solitons are decreasing with increasing β. The quantum parameter β is mainly arisen due to the influence of Bohm potential and exclusively related to the tunneling effect of the corresponding plasma component. The tunneling effect is also increasing with the increase of β. It is ensured that the electrons interact more actively with the ions, causing the reduction in amplitude and width of solitons, which is in agreement with the theoretical finding of Ref. [8]. Furthermore, the potential profiles $\phi_R^{(1)}(\xi, \tau)$ of the solitons are shifted towards the right, while $\phi_L^{(1)}(\eta, \tau)$ are

shifted towards the left with increasing τ. This dictates that the position of solitons R is at $\xi = 0, \eta \to -\infty$ and that of L is at $\eta = 0, \xi \to +\infty$ before interaction and they collide at time $t \to 0$ and then the soliton R is at $\xi = 0, \eta \to +\infty$ and L is at $\eta = 0, \xi \to -\infty$ after interaction, such interaction phenomena are displayed in Figs. 2.3-2.5.

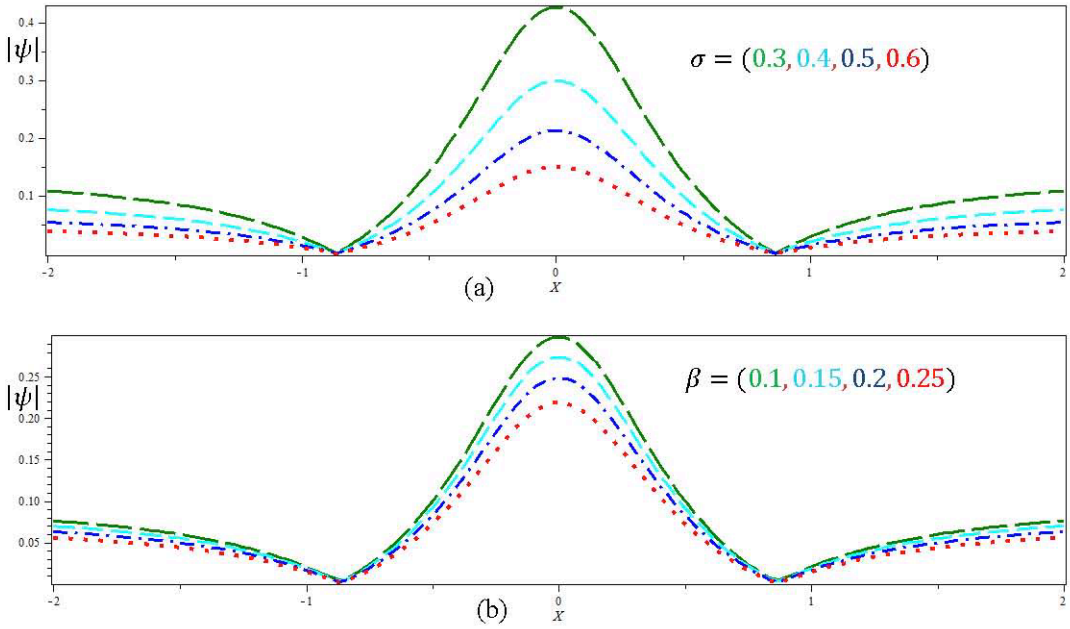

Figure 2.6 Effect of (a) σ ($\beta = 0.10$, $T = 0.01$) and (b) β ($\sigma = 0.4$, $T = 0.1$) on the rogue waves for ultra-relativistic ($\gamma = 4/3$) degenerate electrons, positrons, and inertial non-relativistic helium ions, where the remaining parameters are $\eta_1 = 0.6$, $\lambda = 0.10$ and $\mu = 0.40$.

On the other hand, it is found that the NLSE obtained from the KdV equation does not support rogue wave solutions due to modulational stability of the quasi-monochromatic wave packets. But, the NLSE obtained from the mKdV equation supports the rogue wave solutions for the considered plasma parameters as well as the critical value for which the nonlinear coefficient A of the KdV equation is zero. Figures 2.6(a) and 2.6(b) show the influences of σ and β on the rogue waves, respectively, taking different values of μ and remaining parameters constant for ultra-relativistic degenerate electrons and positrons. It is seen that the amplitudes of rogue waves are decreasing with increasing β, σ and μ in the plasmas. The quantum parameter β arises due to the Bohm potential which is solely responsible for the tunneling effect of the corresponding plasma component. The tunneling effect becomes pronounced with the increase of β, which dictates that the electrons interact more actively with the ions, causing the reduction of amplitude of rogue waves. Furthermore, the amplitude of rogue waves decreases significantly due to the increase of σ and μ in the aforementioned plasma

system, which predicts that the electrostatic interaction between electrons and positrons increases, and thus their contribution to the restoring force increases in the plasmas.

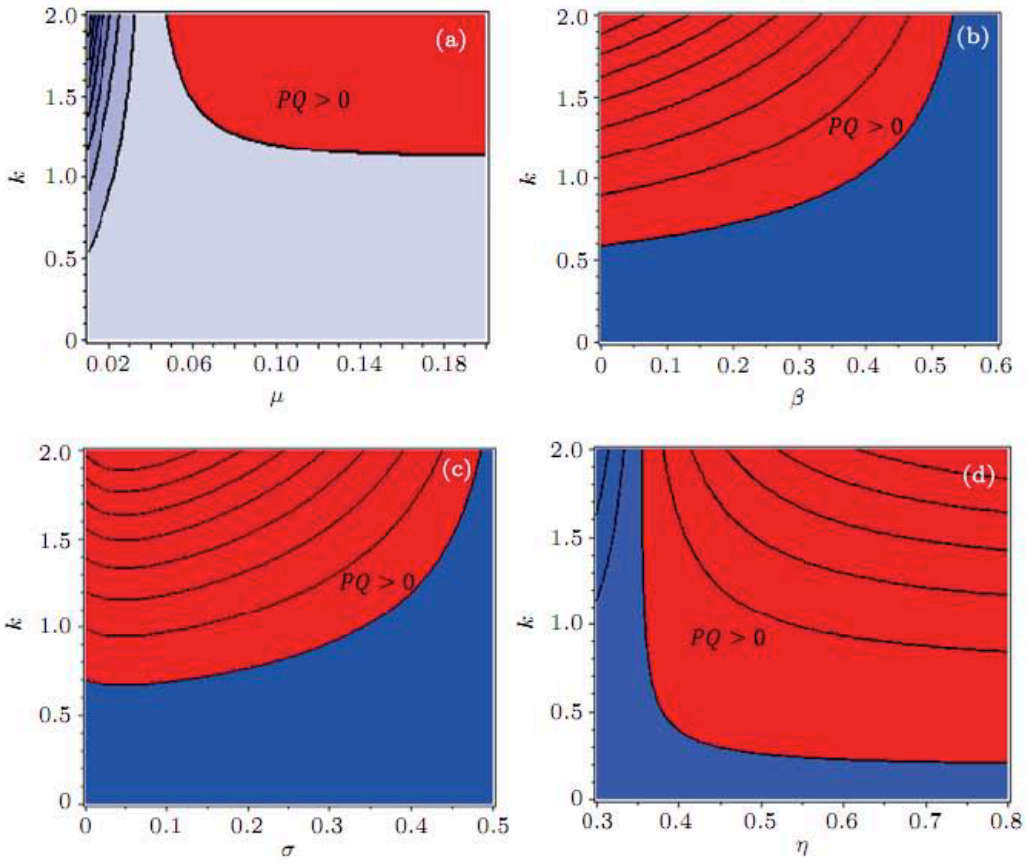

Figure 2.7 Contour plot of PQ for the existence regions (red color) of the rogue waves against (a) μ and k ($\beta = 0.10, \lambda = 0.10, \eta_1 = 0.45, \sigma = 0.01$), (b) β and k ($\lambda = 0.10, \eta_1 = 0.8, \sigma = 0.3, \mu = 0.4$), (c) σ and k ($\beta = 0.3, \lambda = 0.3, \eta_1 = 0.8, \mu = 0.1$), and (d) η_1 and k ($\beta = 0.10, \lambda = 0.10, \mu = 0.4, \sigma = 0.3$).

Finally, Figs. 2.7(a)-2.7(d) display the existence regions (red color) of the rogue waves with respect to μ, β, σ, and η_1 along with k, respectively, taking the remaining parameters as constant for ultra-relativistic degenerate electrons and positrons.

2.6 Conclusions

The interactions between the ion acoustic solitons, their phase shifts, and the production of rogue waves are investigated by considering the soliton solution of the two-sided KdV equations and the rational function solution of the NLSE, respectively. It is found that the

quantum parameters become prominent due to the Bohm potential, which significantly modifies the propagation characteristics due to the interactions of the small amplitude long-lived solitons as well as large amplitude short-lived rogue waves in the plasmas. The results obtained in this study might be useful for the understanding of the effects of electrostatic resonance and phase shifts after weak interaction between multi-solitons and rogue waves for astrophysical compact objects, e.g., white dwarfs, neutron stars, etc., and for laboratory plasmas like intense laser–solid matter interaction experiments.

Appendix A

$$-V_p\,\frac{\partial n_i^{(3)}}{\partial \xi}+V_p\,\frac{\partial n_i^{(3)}}{\partial \eta}+\frac{\partial n_i^{(1)}}{\partial \tau}+\frac{\partial u_i^{(3)}}{\partial \xi}+\frac{\partial u_i^{(3)}}{\partial \eta}+\frac{\partial}{\partial \xi}\left(n_i^{(1)}\,u_i^{(1)}\right)+\frac{\partial}{\partial \eta}\left(n_i^{(1)}\,u_i^{(1)}\right)+V_p\,\frac{\partial X_0}{\partial \eta}\frac{\partial n_i^{(1)}}{\partial \xi}$$
$$-V_p\frac{\partial Y_0}{\partial \xi}\frac{\partial n_i^{(1)}}{\partial \eta}+\frac{\partial X_0}{\partial \eta}\frac{\partial u_i^{(1)}}{\partial \xi}+\frac{\partial Y_0}{\partial \xi}\frac{\partial u_i^{(1)}}{\partial \eta}\;=0 \qquad (A1)$$

$$-V_p\,\frac{\partial u_i^{(3)}}{\partial \xi}+V_p\,\frac{\partial u_i^{(3)}}{\partial \eta}+\frac{\partial u_i^{(1)}}{\partial \tau}+u_i^{(1)}\frac{\partial u_i^{(1)}}{\partial \xi}+u_i^{(1)}\frac{\partial u_i^{(1)}}{\partial \eta}+\frac{\partial \phi_i^{(3)}}{\partial \xi}+\frac{\partial \phi_i^{(3)}}{\partial \eta}+K_1^{'}\frac{\partial n_i^{(3)}}{\partial \xi}+K_1^{'}\frac{\partial n_i^{(3)}}{\partial \eta}$$
$$+K_1^{'}(\alpha-2)n_i^{(1)}\frac{\partial n_i^{(1)}}{\partial \xi}+K_1^{'}(\alpha-2)n_i^{(1)}\frac{\partial n_i^{(1)}}{\partial \eta}+V_p\,\frac{\partial X_0}{\partial \eta}\frac{\partial u_i^{(1)}}{\partial \xi}-V_p\frac{\partial Y_0}{\partial \xi}\frac{\partial u_i^{(1)}}{\partial \eta}$$
$$+\frac{\partial X_0}{\partial \eta}\frac{\partial \phi^{(1)}}{\partial \xi}+\frac{\partial Y_0}{\partial \xi}\frac{\partial \phi^{(1)}}{\partial \eta}=0 \qquad (A2)$$

$$n_e^{(1)}\,\frac{\partial \phi^{(1)}}{\partial \xi}+n_e^{(1)}\,\frac{\partial \phi^{(1)}}{\partial \eta}+\frac{\partial \phi^{(3)}}{\partial \xi}+\frac{\partial \phi^{(3)}}{\partial \eta}-K_2^{'}\frac{\partial n_e^{(3)}}{\partial \xi}-K_2^{'}\frac{\partial n_e^{(3)}}{\partial \eta}-K_2^{'}(\gamma-1)n_e^{(1)}\frac{\partial n_e^{(1)}}{\partial \xi}$$
$$-K_2^{'}(\gamma-1)n_e^{(1)}\frac{\partial n_e^{(1)}}{\partial \eta}+\frac{1}{2}\beta\frac{\partial^3 n_e^{(1)}}{\partial \xi^3}+\frac{1}{2}\beta\frac{\partial^3 n_e^{(1)}}{\partial \eta^3}+\frac{\partial X_0}{\partial \eta}\frac{\partial \phi^{(1)}}{\partial \xi}+\frac{\partial Y_0}{\partial \xi}\frac{\partial \phi^{(1)}}{\partial \eta}$$
$$-K_2^{'}\frac{\partial X_0}{\partial \eta}\frac{\partial n_e^{(1)}}{\partial \xi}-K_2^{'}\frac{\partial Y_0}{\partial \xi}\frac{\partial n_e^{(1)}}{\partial \eta}=0 \qquad (A3)$$

$$n_p^{(1)}\,\frac{\partial \phi^{(1)}}{\partial \xi}+n_p^{(1)}\,\frac{\partial \phi^{(1)}}{\partial \eta}+\frac{\partial \phi^{(3)}}{\partial \xi}+\frac{\partial \phi^{(3)}}{\partial \eta}+K_2^{'}\eta_1\frac{\partial n_p^{(3)}}{\partial \xi}+K_2^{'}\eta_1\frac{\partial n_p^{(3)}}{\partial \eta}+K_2^{'}\eta_1(\gamma-1)n_p^{(1)}\frac{\partial n_p^{(1)}}{\partial \xi}$$
$$+K_2^{'}\eta_1(\gamma-1)n_p^{(1)}\frac{\partial n_e^{(1)}}{\partial \eta}-\frac{1}{2}\lambda\frac{\partial^3 n_p^{(1)}}{\partial \xi^3}-\frac{1}{2}\lambda\frac{\partial^3 n_p^{(1)}}{\partial \eta^3}+\frac{\partial X_0}{\partial \eta}\frac{\partial \phi^{(1)}}{\partial \xi}+\frac{\partial Y_0}{\partial \xi}\frac{\partial \phi^{(1)}}{\partial \eta}$$
$$-K_2^{'}\,\eta_1\frac{\partial X_0}{\partial \eta}\frac{\partial n_p^{(1)}}{\partial \xi}-K_2^{'}\eta_1\frac{\partial Y_0}{\partial \xi}\frac{\partial n_p^{(1)}}{\partial \eta}$$
$$=0 \qquad (A4)$$

$$\frac{\partial^2 \phi^{(1)}}{\partial \xi^2}\;+2\frac{\partial^2 \phi^{(1)}}{\partial \xi \partial \eta}+\frac{\partial^2 \phi^{(1)}}{\partial \eta^2}\;=\mu n_e^{(3)}-n_i^{(3)}-\sigma n_p^{(3)} \qquad (A5)$$

$$\left.\begin{aligned} n_i^{(2)}&=\frac{3V_p^2+K_1'(\alpha-2)}{2\left(V_p^2-K_1'\right)^3}\left\{\phi^{(1)}\right\}^2+\frac{\phi^{(2)}}{\left(V_p^2-K_1'\right)},\\ n_e^{(2)}&=\frac{(2-\gamma)}{2K_1'^{\,2}}\left\{\phi^{(1)}\right\}^2\frac{\phi^{(2)}}{K_2'},\\ n_p^{(2)}&=\frac{(2-\gamma)}{2\left(\eta_1K_2'\right)^2}\left\{\phi^{(1)}\right\}^2-\frac{\phi^{(2)}}{\eta_1K_2'},\end{aligned}\right\} \qquad (A6)$$

$$-\frac{1}{2}\left\{\frac{3V_p^2}{\left(V_p^2-K_1'\right)^3}+\frac{K_1'(\alpha-2)}{\left(V_p^2-K_1'\right)^3}+\frac{\mu(\gamma-2)}{\left(K_2'\right)^2}-\frac{\sigma(\gamma-2)}{\left(\eta_1K_2'\right)^2}\right\}\left\{\phi^{(1)}\right\}^2=0. \qquad (A7)$$

References

1. S. L. Shapiro and S. A. Teukolsky, Black Holes, White Dwarfs and Neutron Stars: The Physics of Compact Objects (New York: John Wiley & Sons) (1983).
2. E. Garcia-Berro, S. Torres, L. G. Althaus, I. Renedo, P. Lorn-Aguiltar, A.H. Crsico, R.D. Rohrmann, M. Salaris and J. Isern, Nature **465,194** (2010).
3. N. C. Woolsey, C. Courtois and R. O. Dendy, Plasma Phys. Control. Fusion **46, B397** (2004).
4. A. A. Mamun and P. K. Shukla, Phys. Lett. A **374,** 4238 (2010).
5. M. Murklund and P. K. Shukla, Rev. Mod. Phys.**78,** 591 (2006).
6. V. I. Berezhiani, D. D. Tskhakaya and P. K. Shukla Phys. Rev. A **46,** 6608 (1992).
7. Ata-ur-Rahman, M. M. Kerr, W. F. El-Taibany, I. Kourakis and A. Qamar, Phys Plasmas, **22,** 022305 (2015).
8. M. M. Hasan, M. A. Hossen, A. Rafat and A. A. Mamun, Chin. Phys.B **25,** 105203 (2016).
9. N. El-Bedwehy and W. M Moslem, Astrophys. Space Sci. **335,** 435 (2011).
10. N. Shatashvili, J. Javakhishvili and H. Kaya, Astrophys. Space Sci. **250,** 109 (1997).
11. M. Opher, L. O. Silva, D. Dauger, V. K. Decyk and J. M. Dawson, Phys. Plasmas **8,** 2454 (2001).
12. A. A. Mamun, and P. K. Shukla, Phys. Plasmas **17,** 104504 (2010).
13. S. I. Popel, S.V. Vladimirov and P. K. Shukla, Phys. Plasmas **2,** 716 (1995).
14. W. F. El-Taibany and M. Tribeche, Phys. Plasmas **19,** 024507 (2012).
15. M. Shahmansouri and M. Tribeche, Astrophys. Space Sci. **349,** 781 (2014).
16. M. A. Hossen and A. A. Mamun, Phys. Plasmas **22,** 102710 (2015).
17. Ata-ur-Rahman, S. Ali, A. Mushtaq and A. Qamar J. Plasma Phys.**79**, 817 (2013).
18. F. Haas, L. G. Garcia, J. Goedert and G. Manfredi, Phys. Plasmas **10,** 3858 (2003).
19. C. Bhowmik, A. P. Misra and P. K. Shukla, Phys. Plasmas **14,** 12210 (2007).
20. M. G. Hafez, M. R. Talukder and M. H. Ali, Waves in Random and Complex Media **26,** 68 (2016).
21. M. G. Hafez, R. Sakthivel and M. R. Talukder, Chinese J. Phys. **53,** 120901 (2015).
22. M. S. Ruderman, T. Talipova and E. Pelinovsky, J. Plasma Phys.**74,** 639 (2008).
23. M. S. Rudermana, Eur. Phys. J. Special Topics **185,** 57 (2010).
24. R. Grimshaw, D. Pelinovsky, E. Pelinonsky and T. Talipova, Physica D **159,** 35 **(**2001).
25. S. A. El-Tantawy and W. M. Moslem, Phys. Plasmas **21,** 052112 (2014).

26. S. A. El-Tantawy, A. M. Wazwaz and R. Schlickeiser, Plasma Phys. Control. Fusion **57,** (1250122015).
27. S. A. El-Tantawy, E. I. El- Awady and M. Tribeche, Phys. Plasmas **22**, 113705 (2015).
28. S. A. El- Tantawy, E. I. El-Awady and R. Schlickeiser, Astrophys. Space Sci. **360,** 49 (2015).
29. S. A. El-Tantawy, Astrophys. Space Sci. **361,** 164 (2016).
30. G. Mandal, K. Roy, A. Paul, A. Saha and P. Chatterjee, Z. Naturforsch. **70,** 703 (2015).
31. U. N. Ghosh, K. Roy and P. Chatterjee, Phys. Plasmas **18,** 103703 (2011).
32. S. Parveen, S. Mahmood, M. Adnan and A. Qamar, Phys. Plasmas **23,** 092122 (2016).
33. K. Roy, M. K. Ghorui, P. Chatterjee and M. Tribeche, Commun. Theor. Phys. **65,** 237 (2016).
34. J. N. Han, S. C. Li, X. X. Yang and W. S. Duan, Eur. Phys. J. D **47,** 197 (2008).
35. J. N. Han, S. L. Du and W. S. Duan, Phys. Plasmas **15,** 112104 (2008).
36. S. K. El-Labany, E. F. El-Shamy, R. Sabry and M. Shokry, Astrophys. Space Sci. **325,** 201 (2010).
37. A. Saha and P. Chatterjee, Astrophys. Space Sci. **353,** 169 (2014).
38. J. K. Xue, Phys. Rev. E **69**, 016403 (2004).
39. S. Sadiq, S. Mahmood, Q. Haque and M. Z. Ali, The Astrophysical J. **793,** 27 (2014).
40. S. Chandrasekhar, Mon. Not. R. Astron. Soc. **170,** 405 (1935).
41. M. A. Hossen and A. A. Mamun, Phys. Plasmas **22,** 073505 (2015).
42. P. Chatterjee, U. N. Ghosh, K. Roy, S.V. Muniandy, C. S. Wong and B. Sahu, Phys. Plasmas **17,** 122314 (2010).
43. R. Hirota, The Direct Method in The Soliton Theory (Cambridge: Cambridge University Press), (2004).
44. M. S. Alam, M. G. Hafez, M. R. Talukder and M. H. Ali, arXiv: **1611**, 10225 (2016).
45. D. Koester and G. Chanmugam, Rep. Prog. Phys. **53**, 837 (1990).

Abbreviation and Nomenclature:

KdV= Korteweg-de Vries

mKdV= modified Korteweg-de Vries

mmKdV= mixed modified Korteweg-de Vries

NLSE= nonlinear Schrödinger equation

PLK = Poincaré-Lighthill-Kuo

H= quantum diffraction parameter

m_s= mass of plasma spesies

n_s= density of plasma species(s = i,e,p)

h = Plank constant

c = velocity of light

C_i = ion acoustic speed

n_i = density of ion

n_e = density of electron

n_p = density of positron

u_i = ion fluid speed

ϕ = electrostatic potential

η_1 = Fermi temperature ratio of positron to electron

T_{F_p} = Fermi temperature of positron

T_{F_e} = Fermi temperature of electron

k_B = Boltzmann constant

m_i = mass of rest ion

ω_{pm} = plasma frequency

λ_{Di} = ion Debye length

$\beta = n_{i0}H_e^2/2n_{e0}$ = dimensionless quantum parameter for electron

$\lambda = n_{i0}H_p^2/2n_{p0}$ = dimensionless quantum parameter for positron

$H_e = \hbar\omega_{pe}/k_B\,T_{F_e}$

$H_p = \hbar\omega_{pp}/k_B\,T_{F_p}$

$\hbar = \mathrm{h}/2\pi$

V_p = unknown phase velocity

ξ, η, τ = stretched coordinates

ε = small parameter, measure the strength of nonlinearity

k_i = wave number, $i = 1,2,3$

ω = angular velocity

v_g = group velocity

$\sigma = n_{p0}/n_{i0}$ = density ratio of unperturbed positron to ion

$\mu = n_{e0}/n_{i0}$ = density ratio of unperturbed electron to ion

A = coefficient of nonlinearity in KdV equation

B = coefficient of dispersion in KdV equation

P = coefficient of nonlinearity in NLSE

Q = coefficient of dispersion in NLSE

∇X_0 = phase shift of right moving soliton

∇Y_0 = phase shift of left moving soliton

Chapter 3

Head-on collision of ion acoustic solitary waves in electron-positron-ion nonthermal plasmas for weakly and highly relativistic regimes

3.1 Introduction

It is well established that the electron–positron (ep) plasmas are observed both in the laboratory, e.g., in inertial confinement fusion experiments [1-3] and in nature, e.g., in the relativistic wind of pulsar magnetosphere [4], polar regions of neutron stars [5], pulsar magnetospheres [6], active galactic nuclei [7], at the centre of the Milky Way galaxy [8], in the early universe [9-10], and so on by pair production through high-energy processes. For instance, the solar wind and cosmic rays are the sources of highly energy particles that exist in the Van Allen belts, which are trapped by the earth magnetic field. These highly energetic cosmic protons and heavy nuclei interact with the molecules of the earth's upper atmosphere and produce nonthermal electrons and positrons [11-12]. Further, the hot ep plasma exists in the sheet boundary layer of the earth's magneto-tail, outflows from the pulsar, and interacts with the interstellar cold, low density electron-ion plasmas [13]. Besides, the nonthermal charge particles gain high energy due to stochastic heating, and this effect may arise in the pulsar magnetosphere [4, 6]. The electric field may generate due to the rotation of pulsar and extracts electrons from the pulsar surface. These electrons lose their energies through the pair production process to generate ep plasma. Moreover, the plasma particles may gain relativistic energies under the influences of high-power laser interaction [14-15]. The ratio of ion-electron temperature is found to be greater than unity as observed in solar flares [16], the solar wind [17] and interplanetary space [18]. It is therefore important to consider finite ion temperature and relativistic effects which significantly affect the propagation characteristics of the solitons. Furthermore, most of the astrophysical plasmas contain ions as well as electrons and positrons, and forming electron-position-ion (epi) plasmas. Therefore, it is reasonable to consider that the relativistic effects in such plasmas prevail because the particles having streaming velocities approach to the velocity of light. It is considered that the weakly relativistic effects of ions are considered in the range of 0.1–4.7MeV for the appropriate description, whereas the highly relativistic effects are taken into account in the range of 4.7–

100MeV that are frequently observed in astrophysical and space environments. Therefore, the propagation of ion acoustic waves in the epi relativistic plasmas plays a vital role for the understanding of physical scenarios concerned in space environments, Van Allen radiation belts, plasma sheet boundary layer of Earth's magnetosphere and laser plasma interaction, and so on [11-19]. Several authors [20-32] have studied, considering their significance and potentiality for understanding the physical issues involved, the characteristics of ion acoustic waves for epi relativistic plasmas, taking two as well as three-term expansion of the Lorentz relativistic factor for ions assuming different plasma conditions. It was noted in Refs. 27-31 that the three-term expansion of the Lorentz relativistic factor [the so called highly relativistic regime (HRR) of ions], rather than two-term of the Lorentz relativistic factor [the so called weakly relativistic regime (WRR) of ions], significantly modify the ion acoustic wave dynamics in the plasmas. On the other hand, the high-energy particles are produced by the nonthermal particles, which reached higher than thermal energies [33]. In such a situation, the plasma particles have long range interactions that are characterized by different distribution functions except Boltzmann distribution. The Cairns distribution function [34],is one of the most important distributions and applies to evaluate nonthermal particle concentration. Hafez et al. [28] have investigated the oblique nonlinear propagation of ion acoustic shock waves both for the weakly and highly relativistic regimes consisting of nonthermal electrons, positrons, and relativistic thermal ions. They showed that the effect of obliqueness, nonthermal electrons, and positrons significantly modifies the ion acoustic shock waves in epi plasmas in highly relativistic rather than weakly relativistic regimes. Therefore, the existence of relativistic ions and nonthermal electrons and positrons in the pulsar magnetosphere and laser–plasma interaction is a well established phenomenon [35-38] for studying the properties of nonlinear waves in epi plasmas.

However, the interaction between nonlinear ion acoustic solitary waves is one of the most important physical phenomena as observed in space plasmas [39-41]. A few authors [42-44] have investigated the head-on collision and their corresponding phase shifts considering the unit amplitude of the solitons in weakly relativistic epi plasmas. Khaled [43] has studied the head-on collision and their corresponding phase shift between ion acoustic solitary waves in plasmas consisting of relativistic cold ions and nonextensive electrons and positrons in WRR. Saini and Singh [44] have considered the head-on collision between dust acoustic solitary waves in plasmas with relativistic cold ions, Kappa distributed electrons, and positrons in WRR. In such situations, the phase shift and trajectories [45] play a significant role in the

formation of solitary waves after head-on collision. The extended Poincaré-Lighthill-Kuo (ePLK) method [40] can be employed to derive two-sided KdV equations for investigating the interaction of solitary waves and their corresponding phase shifts. The solitary wave solutions of the two-sided KdV equations reveal important physical phenomena, including resonances due to its wide application and potentiality as mentioned earlier. Therefore, head-on collision deserves significant importance for revealing the propagation characteristics of nonlinear ion acoustic solitary waves in the plasmas consisting of relativistic ions, nonthermal electrons, and positrons both for WRR and HRR. The effect of plasma parameters on the interaction between electrostatic ion acoustic solitary waves, the corresponding phase shifts and bell-shaped structures are investigated. In sequence of introduction, the hydrodynamic fluid equations are presented in Section 3.2. Derivations of two-sided KdV equations for weakly and highly relativistic regimes are mentioned in Section 3.3. The stationary solutions of two-sided KdV equations and phase shift are displayed in Section 3.4. The results along with relevant discussion are depicted in Section 3.5. Finally, the conclusion is drawn in section 3.6.

3.2 Theoretical model equations

An unmagnetized collisionless epi plasma is considered consisting of nonthermal electrons, positrons, and relativistic warm ions. The electrons and positrons are assumed to follow Cairns nonthermal distribution [34], and their velocity distribution functions can be written in the following form:

$$f_j(v_j) = \frac{n_{j0}}{(1+3\alpha_j)\sqrt{2\pi}}\left[1+\frac{\alpha_j}{v_{tj}^4}(v_j^2-2\phi)^2\right]\exp\left(-\frac{v_j^2-2\phi}{2v_{tj}^2}\right), v_{tj} = \left(T_j/m_j\right)^{1/2}, \quad (3.1)$$

where, ϕ, v_j, T_j, m_j, n_{j0}, and α_j are the electrostatic potential, velocity, temperature, mass, unperturbed densities, and population of the particles. The densities of electrons and positrons can be obtained by integrating Eq. (3.1) over the volume space as

$$n_e = n_{e0}\left\{1-\beta_e\left(\frac{e\phi}{T_e}\right)+\beta_e\left(\frac{e\phi}{T_e}\right)^2\right\}\exp\left(\frac{e\phi}{T_e}\right), \quad (3.2)$$

and

$$n_p = n_{p0}\left\{1+\beta_p\left(\frac{e\phi}{T_p}\right)+\beta_p\left(\frac{e\phi}{T_p}\right)^2\right\}\exp(-\frac{e\phi}{T_p}), \quad (3.3)$$

where $\beta_e = 4\alpha_e/(1+3\alpha_e)$, $\beta_p = 4\alpha_p/(1+3\alpha_p)$, and $n_{e0}(n_{p0})$ are the unperturbed electron (positron) concentration, $T_e(T_p)$ is the electron (positron) temperature, e is the

electronic charge, and $\alpha_{e,p} > -1/3$ determines the population of nonthermal electrons and positrons, respectively. It is seen that Eqs. (3.2) and (3.3) can be reduced to the isothermally distributed electrons and positrons by inserting $\alpha_{e,p} = 0$. It is also considered that $v_{thi} \ll C_s \ll v_{the}, v_{thp}$, so that the Landau damping can be ignored, where v_{thi} is the ion thermal velocity, $C_s = \sqrt{(T_e/m_i)}$ is the ion acoustic speed, m_i is the ion mass, and $v_{the}(v_{thp})$ is the electron (positron) thermal velocity. On the other hand, the plasma instabilities are characterized, in general, by a solution in which initially small perturbations of an equilibrium configuration are predicted to grow exponentially with time or space. Thus, such growing perturbations will not remain small. The linearization procedure breaks down, and the nonlinear effects tend to limit the growth of instabilities (nonlinear saturation), provided that the amplitude of the wave becomes sufficiently large [46-47].The nonlinear terms in the equations become eventually significant for describing system dynamics. Further, the dispersion relation of ion acoustic wave can be counter-balanced by nonlinearity, and an ion acoustic pulse-like solitary perturbation can propagate without appreciable deformation. Besides, the nonlinearities may also occur from the harmonic generation involving fluid advection, the nonlinear Lorentz force, trapping of particles in the wave potential, ponderomotive force, and so on [46]. In such situation, one may study the nonlinear propagation characteristics without considering two-stream instability in the considered plasmas. Thus, to study the nonlinear dynamics of ion acoustic solitary waves, the normalized fluid equations can be defined to the following forms:

$$\frac{\partial n_i}{\partial t} + \frac{\partial (n_i u_i)}{\partial x} = 0, \qquad (3.4)$$

$$\frac{\partial (\gamma u_i)}{\partial t} + u_i \frac{\partial (\gamma u_i)}{\partial x} + \frac{j n_i^{j-2} T_{ie}}{(1-n_{pe})^{j-1}} \frac{\partial n_i}{\partial x} = -\frac{\partial \phi}{\partial x}, \qquad (3.5)$$

$$\frac{\partial^2 \phi}{\partial x^2} = (1 - \beta_e \phi + \beta_e \phi^2) e^{\phi} - n_{pe}\left(1 + \beta_p T_{ep}\, \phi + \beta_p T_{ep}^2 \phi^2\right) e^{-T_{ep}\, \phi} - n_i\,. \qquad (3.6)$$

Here, n_i, u_i, T_{ie}, T_{ep}, and n_{pe} denote the normalized ion density, ion fluid velocity, ion-electron temperature ratio ($T_{ie} = T_i/T_e$), electron-positron temperature ratio ($T_{ep} = T_e/T_p$), and fractional concentration of positrons with respect to electron ($n_{pe} = n_{p0}/n_{e0}$), respectively. The perturbed quantities n_i, u_i, and ϕ are normalized as $n_i \to n_i/n_{e0}$, $u_i \to u_i/C_s$, $\phi \to (T_e/e)\phi$. The space variable is normalized by the electron Debye radius $\lambda_{De} = \sqrt{(T_e/4\pi n_{e0} e^2)}$, and the time variable is normalized by λ_{De}/C_s. The equation of state for the

adiabatic ions is considered as $P_{i0}/n_{i0}^{j} = P_i/n_i^{j}$, P_i is ion pressure, $j = (N+2)/N$ (N is the number of degrees of freedom), and $N = 1$ for one-dimensional case. The parameter $\gamma = 1/\sqrt{1 - u_i^2/c^2}$ in Eq. (3.5) is the Lorentz relativistic factor, where the non-relativistic limit $\gamma = 1$ and $n_{i0} = 1 - n_{pe}$ is the normalized quasi-neutrality condition.

3.3 Formation of two-sided KdV equations

To investigate the interaction of two ion acoustic solitary waves for WRR and HRR regimes, one can apply the ePLK method [40], which leads to the scaling of independent variables through the stretched coordinates as

$$\left.\begin{array}{c} \xi = \varepsilon(x - V_1 t) + \varepsilon^2 P_0(\eta,\tau) + \varepsilon^3 P_1(\eta,\xi,\tau) + \ \ldots\ldots\ldots \\ \eta = \varepsilon(x + V_2 t) + \varepsilon^2 Q_0(\xi,\tau) + \varepsilon^3 Q_1(\eta,\xi,\tau) + \ \ldots\ldots\ldots \\ \tau = \varepsilon^3 t. \end{array}\right\} \tag{3.7}$$

where ξ and η indicate the trajectories of two solitary waves traveling toward to each other, and V_1 and V_2 are the unknown phase velocities of ion acoustic solitary waves. The mysterious phase functions $P_0(\eta,\tau)$ and $Q_0(\xi,\tau)$ will be evaluated later. The perturbed quantities may be expanded as

$$\left.\begin{array}{c} n_i = (1 - n_{pe}) + \varepsilon^2 n_i^{(1)} + \varepsilon^3 n_i^{(2)} + \varepsilon^4 n_i^{(3)} + \cdots\cdots\cdots\cdots \\ u_i = u_{i0} + \varepsilon^2 u_i^{(1)} + \varepsilon^3 u_i^{(2)} + \varepsilon^4 u_i^{(3)} + \ \cdots\cdots\cdots\cdots\cdots \\ \phi = 0 + \varepsilon^2 \phi^{(1)} + \varepsilon^3 \phi^{(2)} + \varepsilon^4 \phi^{(3)} + \ \cdots\cdots\cdots\cdots\cdots \end{array}\right\}. \tag{3.8}$$

The relativistic Lorentz factor involved in the momentum [Eq.(3.5)] is considered to be weak and taking up to two-term, that is, for WRR as

$$\gamma \approx 1 + \frac{u_i^2}{2c^2}. \tag{3.9}$$

Inserting Eqs. (3.7)-(3.9) into Eqs. (3.4)-(3.6) and separating the perturbed quantities with the similar power of ε, one can derive a set of equations in various power of ε. The lowest power of ε yeilds

$$(-V_1 + u_{i0})\frac{\partial n_i^{(1)}}{\partial \xi} + (V_2 + u_{i0})\frac{\partial n_i^{(1)}}{\partial \eta} + (1 - n_{pe})\frac{\partial u_i^{(1)}}{\partial \xi} + (1 - n_{pe})\frac{\partial u_i^{(1)}}{\partial \eta} = 0,$$

(3.10)

$$(-V_1+u_{i0})\gamma_1\frac{\partial u_i^{(1)}}{\partial\xi}+(V_2+u_{i0})\gamma_1\frac{\partial u_i^{(1)}}{\partial\eta}+\frac{3T_{ie}}{(1-n_{pe})}\frac{\partial n_i^{(1)}}{\partial\xi}+\frac{3T_{ie}}{(1-n_{pe})}\frac{\partial n_i^{(1)}}{\partial\eta}$$

$$=-\left(\frac{\partial\phi^{(1)}}{\partial\xi}+\frac{\partial\phi^{(1)}}{\partial\eta}\right), \tag{3.11}$$

$$n_i^{(1)}=\left[(1-\beta_e)+n_{pe}T_{ep}(1-\beta_p)\right]\phi^{(1)}. \tag{3.12}$$

Solving Eqs. (3.10)-(3.12), one may define the relations along with the different physical quantities as

$$\phi^{(1)}=\phi_\xi^{(1)}(\xi,\tau)+\phi_\eta^{(1)}(\eta,\tau) \tag{3.13}$$

$$n_i^{(1)}=\frac{(1-n_{pe})}{[(V_1-u_{i0})^2\gamma_1-3T_{ie}]}\phi_\xi^{(1)}(\xi,\tau)+\frac{(1-n_{pe})}{[(V_2+u_{i0})^2\gamma_1-3T_{ie}]}\phi_\eta^{(1)}(\eta,\tau), \tag{3.14}$$

$$u_i^{(1)}=\frac{(V_1-u_{i0})}{[(V_1-u_{i0})^2\gamma_1-3T_{ie}]}\phi_\xi^{(1)}(\xi,\tau)-\frac{(V_2+u_{i0})}{[(V_2+u_{i0})^2\gamma_1-3T_{ie}]}\phi_\eta^{(1)}(\eta,\tau). \tag{3.15}$$

It is seen from Eq. (3.13) that two electrostatic solitary waves may be obtained, one of which $\phi_\xi^{(1)}(\xi,\tau)$ is propagating from left to right and the other $\phi_\eta^{(1)}(\eta,\tau)$ is propagating from right to left. Using the solvability condition, the phase velocities are obtained as

$$V_1=\sqrt{\frac{3T_{ie}}{\gamma_1}+\frac{(1-n_{pe})}{\gamma_1K_1}}+u_{i0},\ V_2=\sqrt{\frac{3T_{ie}}{\gamma_1}+\frac{(1-n_{pe})}{\gamma_1K_1}}-u_{i0}\ , \tag{3.16}$$

where $K_1=[(1-\beta_e)+n_{pe}T_{ep}(1-\beta_p)]$. The next power of ε provides another set of equations whose solutions are also defined by the following relations:

$$\phi^{(2)}=\phi_\xi^{(2)}(\xi,\tau)+\phi_\eta^{(2)}(\eta,\tau) \tag{3.17}$$

$$n_i^{(2)}=\frac{(1-n_{pe})}{[(V_1-u_{i0})^2\gamma_1-3T_{ie}]}\phi_\xi^{(2)}(\xi,\tau)+\frac{(1-n_{pe})}{[(V_2+u_{i0})^2\gamma_1-3T_{ie}]}\phi_\eta^{(2)}(\eta,\tau), \tag{3.18}$$

$$u_i^{(2)}=\frac{(V_1-u_{i0})}{[(V_1-u_{i0})^2\gamma_1-3T_{ie}]}\phi_\xi^{(2)}(\xi,\tau)-\frac{(V_2+u_{i0})}{[(V_2+u_{i0})^2\gamma_1-3T_{ie}]}\phi_\eta^{(2)}(\eta,\tau). \tag{3.19}$$

Finally, the next higher order of ε gives the following relation taking Eqs.(3.13)-(3.16) into account:

$$\frac{\partial}{\partial\xi}\left(\frac{\partial\phi_\xi^{(1)}}{\partial\tau}+A_1\phi_\xi^{(1)}\frac{\partial\phi_\xi^{(1)}}{\partial\xi}+B_1\frac{\partial^3\phi_\xi^{(1)}}{\partial\xi^3}\right)+\frac{\partial}{\partial\eta}\left(\frac{\partial\phi_\eta^{(1)}}{\partial\tau}-A_2\phi_\eta^{(1)}\frac{\partial\phi_\eta^{(1)}}{\partial\eta}-B_2\frac{\partial^3\phi_\eta^{(1)}}{\partial\eta^3}\right)$$
$$+\left(C_1\frac{\partial P_0}{\partial\eta}-D_1\phi_\eta^{(1)}\right)\frac{\partial^2\phi_\xi^{(1)}}{\partial\xi^2}-\left(C_2\frac{\partial Q_0}{\partial\xi}-D_2\phi_\xi^{(1)}\right)\frac{\partial^2\phi_\eta^{(1)}}{\partial\eta^2}$$
$$=-\left\{\frac{L(V_1+V_2)}{2(V_1-u_{i0})}+\frac{M(V_1+V_2)}{2(V_2+u_{i0})}\right\}\frac{\partial^2u_i^{(3)}}{\partial\xi\partial\eta}\ , \qquad (3.20)$$

where

$$A_1=\left\{\frac{(V_1-u_{i0})}{L}+\left\{\gamma_1-\gamma_2\left(\frac{V_1-u_{i0}}{u_{i0}}\right)\right\}\frac{(V_1-u_{i0})}{2\gamma_1L}+\frac{3T_{ie}}{2\gamma_1(V_1-u_{i0})L}-\frac{K_2L}{\gamma_1(V_1-u_{i0})K_1}\right\},$$

$$B_1=\frac{L}{2\gamma_1(V_1-u_{i0})K_1},$$

$$C_1=\left[\frac{(V_1-u_{i0})}{2}+(V_2+u_{i0})+\frac{3T_{ie}}{2\gamma_1(V_1-u_{i0})}+\frac{L}{2\gamma_1(V_1-u_{i0})}\right],$$

$$D_1=\left[\left\{\gamma_1-\gamma_2\left(\frac{V_1-u_{i0}}{u_{i0}}\right)\right\}\frac{(V_2+u_{i0})}{2\gamma_1M}-\frac{3T_{ie}}{2\gamma_1(V_1-u_{i0})M}+\frac{K_2L}{\gamma_1(V_1-u_{i0})K_1}\right],$$

$$A_2=\left\{\frac{(V_2+u_{i0})}{M}+\left\{\gamma_1+\gamma_2\left(\frac{V_2+u_{i0}}{u_{i0}}\right)\right\}\frac{(V_2+u_{i0})}{2\gamma_1M}+\frac{3T_{ie}}{2\gamma_1(V_2+u_{i0})M}-\frac{K_2M}{\gamma_1(V_2+u_{i0})K_1}\right\},$$

$$B_2=\frac{M}{2\gamma_1(V_2+u_{i0})K_1},$$

$$C_2=\left[(V_1-u_{i0})+\frac{(V_2+u_{i0})}{2}+\frac{3T_{ie}}{2\gamma_1(V_2+u_{i0})}+\frac{M}{2\gamma_1(V_2+u_{i0})}\right],$$

$$D_2=\left[\left\{\gamma_1+\gamma_2\left(\frac{V_2+u_{i0}}{u_{i0}}\right)\right\}\frac{(V_1-u_{i0})}{2\gamma_1L}-\frac{3T_{ie}}{2\gamma_1(V_2+u_{i0})L}+\frac{K_2M}{\gamma_1(V_2+u_{i0})K_1}\right],$$

$$L=[(V_1-u_{i0})^2\gamma_1-3T_{ie}],$$

$$M=[(V_2+u_{i0})^2\gamma_1-3T_{ie}],$$

$$K_2=\left(1-n_{pe}T_{ep}^2\right)/2, \text{ and } \gamma_2=3\beta^2.$$

Integrating Eq. (3.20) twice with regards to ξ and η, respectively, one obtains

$$\int\left(\frac{\partial\phi_{\xi}^{(1)}}{\partial\tau}+A_1\phi_{\xi}^{(1)}\frac{\partial\phi_{\xi}^{(1)}}{\partial\xi}+B_1\frac{\partial^3\phi_{\xi}^{(1)}}{\partial\xi^3}\right)d\eta+\int\left(\frac{\partial\phi_{\eta}^{(1)}}{\partial\tau}-A_2\phi_{\eta}^{(1)}\frac{\partial\phi_{\eta}^{(1)}}{\partial\eta}-B_2\frac{\partial^3\phi_{\eta}^{(1)}}{\partial\eta^3}\right)d\xi$$
$$+\int\left(C_1\frac{\partial P_0}{\partial\eta}-D_1\phi_{\eta}^{(1)}\right)\frac{\partial^2\phi_{\xi}^{(1)}}{\partial\xi^2}d\xi d\eta-\int\left(C_2\frac{\partial Q_0}{\partial\xi}-D_2\phi_{\xi}^{(1)}\right)\frac{\partial^2\phi_{\eta}^{(1)}}{\partial\eta^2}d\xi d\eta$$
$$=-\left\{\frac{L(V_1+V_2)}{2(V_1-u_{i0})}+\frac{M(V_1+V_2)}{2(V_2+u_{i0})}\right\}u_i^{(3)}. \qquad (3.21)$$

Eq. (3.21) shows that the perturbed quantity $u_i^{(3)}$ contains both secular and non-secular terms that are obtained by solving only the secular terms. It is noted that two-sided KdV equations can only be obtained when the secular terms are considered. The first and second terms on the left side of Eq. (3.21) are proportional to η and ξ, respectively, because the integrands involving the first and second terms in the left side of Eq.(3.21) are independent of η and ξ, respectively. Since the first two expressions are all secular terms those can be eliminated in order to avoid unexpected resonances. Thus, one can find the following two-sided KdV equations:

$$\frac{\partial\phi_{\xi}^{(1)}}{\partial\tau}+A_1\phi_{\xi}^{(1)}\frac{\partial\phi_{\xi}^{(1)}}{\partial\xi}+B_1\frac{\partial^3\phi_{\xi}^{(1)}}{\partial\xi^3}=0\,, \qquad (3.22)$$

$$\frac{\partial\phi_{\eta}^{(1)}}{\partial\tau}-A_2\phi_{\eta}^{(1)}\frac{\partial\phi_{\eta}^{(1)}}{\partial\eta}-B_2\frac{\partial^3\phi_{\eta}^{(1)}}{\partial\eta^3}=0\,. \qquad (3.23)$$

Further, the third and fourth expressions on the left side of Eq. (3.21) may become secular terms in the next higher order and yields the following equations:

$$C_1\frac{\partial P_0}{\partial\eta}-D_1\phi_{\eta}^{(1)}=0\,, \qquad (3.24)$$

$$C_2\frac{\partial Q_0}{\partial\xi}-D_2\phi_{\xi}^{(1)}=0\,. \qquad (3.25)$$

For improved accuracy of the potential profiles due to the interaction between ion acoustic solitary waves, the three-term expansion of the Lorentz relativistic factor (γ) involved in the momentum Eq. (3.5) can be considered as

$$\gamma\approx 1+\frac{u_i^2}{2c^2}+\frac{3u_i^4}{8c^4}\ . \qquad (3.26)$$

Again, inserting Eqs.(3.7), (3.8), and (3.26) into Eqs. (3.4)-(3.6) and separating the perturbed quantities with equal powers of ε, one can obtain a set equations in various powers of ε. The lowest power of ε gives a set of equations whose solutions may be defined by the following relations:

$$\phi^{(1)} = \phi_{\xi}^{(1)}(\xi,\tau) + \phi_{\eta}^{(1)}(\eta,\tau)\ , \tag{3.27}$$

$$n_i^{(1)} = \frac{(1-n_{pe})}{[(V_1-u_{i0})^2\gamma_3 - 3T_{ie}]}\phi_{\xi}^{(1)}(\xi,\tau) + \frac{(1-n_{pe})}{[(V_2+u_{i0})^2\gamma_3 - 3T_{ie}]}\phi_{\eta}^{(1)}(\eta,\tau), \tag{3.28}$$

$$u_i^{(1)} = \frac{(V_1-u_{i0})}{[(V_1-u_{i0})^2\gamma_3 - 3T_{ie}]}\phi_{\xi}^{(1)}(\xi,\tau) - \frac{(V_2+u_{i0})}{[(V_2+u_{i0})^2\gamma_3 - 3T_{ie}]}\phi_{\eta}^{(1)}(\eta,\tau), \tag{3.29}$$

where $\gamma_3 = \gamma_1 + \frac{15}{8}\beta^4$. The phase velocities in Eq. (3.16) can be converted to

$$V_1 = \sqrt{\frac{3T_{ie}}{\gamma_3} + \frac{(1-n_{pe})}{\gamma_3 K_1}} + u_{i0},\ V_2 = \sqrt{\frac{3T_{ie}}{\gamma_3} + \frac{(1-n_{pe})}{\gamma_3 K_1}} - u_{i0}\ . \tag{3.30}$$

Similarly, one can derive Eqs. (3.22)-(3.25) in the above forms. But, the coefficients of Eqs. (3.22)-(3.25) can be obtained as

$$A_1 = \left\{\frac{(V_1-u_{i0})}{L_1} + \left\{\gamma_3 - \gamma_4\left(\frac{V_1-u_{i0}}{u_{i0}}\right)\right\}\frac{(V_1-u_{i0})}{2\gamma_3 L_1} + \frac{3T_{ie}}{2\gamma_3(V_1-u_{i0})L_1} - \frac{K_2 L_1}{\gamma_3(V_1-u_{i0})K_1}\right\},$$

$$B_1 = \frac{L_1}{2\gamma_3(V_1-u_{i0})K_1},$$

$$C_1 = \left[\frac{(V_1-u_{i0})}{2} + (V_2+u_{i0}) + \frac{3T_{ie}}{2\gamma_3(V_1-u_{i0})} + \frac{L_1}{2\gamma_3(V_1-u_{i0})}\right],$$

$$D_1 = \left[\left\{\gamma_3 - \gamma_4\left(\frac{V_1-u_{i0}}{u_{i0}}\right)\right\}\frac{(V_2+u_{i0})}{2\gamma_3 M_1} - \frac{3T_{ie}}{2\gamma_3(V_1-u_{i0})M_1} + \frac{K_2 L_1}{\gamma_3(V_1-u_{i0})K_1}\right],$$

$$A_2 = \left\{\frac{(V_2+u_{i0})}{M_1} + \left\{\gamma_3 + \gamma_4\left(\frac{V_2+u_{i0}}{u_{i0}}\right)\right\}\frac{(V_2+u_{i0})}{2\gamma_3 M_1} + \frac{3T_{ie}}{2\gamma_3(V_2+u_{i0})M_1} - \frac{K_2 M_1}{\gamma_3(V_2+u_{i0})K_1}\right\},$$

$$B_2 = \frac{M_1}{2\gamma_3(V_2+u_{i0})K_1},$$

$$C_2 = \left[(V_1-u_{i0}) + \frac{(V_2+u_{i0})}{2} + \frac{3T_{ie}}{2\gamma_3(V_2+u_{i0})} + \frac{M_1}{2\gamma_3(V_2+u_{i0})}\right],$$

$$D_2 = \left[\left\{\gamma_3 + \gamma_4\left(\frac{V_2 + u_{i0}}{u_{i0}}\right)\right\}\frac{(V_1 - u_{i0})}{2\gamma_3 L_1} - \frac{3T_{ie}}{2\gamma_3(V_2 + u_{i0})L_1} + \frac{K_2 M_1}{\gamma_3(V_2 + u_{i0})K_1}\right],$$

$L_1 = [(V_1 - u_{i0})^2\gamma_3 - 3T_{ie}]$, $M_1 = [(V_2 + u_{i0})^2\gamma_3 - 3T_{ie}]$, and $\gamma_4 = \gamma_2 + \frac{15}{2}\beta^4$.

3.4 Solitary wave solutions and phase shifts

It is seen from Eqs. (3.22) and (3.23) that the KdV equations represent the two-sided traveling waves for the considered frame of references ξ and η, respectively. The stationary solutions of the KdV equations can be obtained as

$$\phi_{\xi}^{(1)}(\xi, \tau) = \phi_R \text{sech}^2\left\{\frac{(\xi - U_0\tau)}{W_R}\right\}, \tag{3.31}$$

$$\phi_{\eta}^{(1)}(\eta, \tau) = \phi_L \text{sech}^2\left\{\frac{(\eta + U_0\tau)}{W_L}\right\}, \tag{3.32}$$

where $\phi_R = (3U_0/A_1)$ and $W_R = \sqrt{((4B_1/U_0)}$ are the amplitude and width of the right moving solitons in their initial positions, $\phi_L = (3U_0/A_2)$ and $W_L = \sqrt{(4B_2/U_0)}$ are the amplitude and width of the left moving solitons in their initial positions, and U_0 is the constant velocity of the solitons. The leading phase functions due to the collision can be obtained solving Eqs. (3.24) and (3.25) with the help of the analytical solutions of Eqs. (3.31) and (3.32) as

$$P_0(\eta, \tau) = \frac{D_1}{C_1}\phi_L W_L\left[\tanh\left(\frac{\eta + U_0\tau}{W_L}\right) + 1\right], \tag{3.33}$$

$$Q_0(\xi, \tau) = \frac{D_2}{C_2}\phi_R W_R\left[\tanh\left(\frac{\xi - U_0\tau}{W_R}\right) - 1\right]. \tag{3.34}$$

Therefore, the trajectories of the two ion acoustic solitary waves for weak head-on collision can be obtained up to order of ε^2 as follows:

$$\xi = \varepsilon(x - V_1 t) + \varepsilon^2\frac{D_1}{C_1}\phi_L W_L\left[\tanh\left(\frac{\eta + U_0\tau}{W_L}\right) + 1\right] + \cdots, \tag{3.35}$$

$$\eta = \varepsilon(x + V_2 t) + \varepsilon^2\frac{D_2}{C_2}\phi_R W_R\left[\tanh\left(\frac{\xi - U_0\tau}{W_R}\right) - 1\right] + \cdots \quad . \tag{3.36}$$

In order to obtain the phase shift after the head-on collision between two solitons, say S_R and S_L, one can assume that the solitons S_R at $\xi = 0, \eta \to -\infty$ and S_L at $\eta = 0, \xi \to +\infty$ are

asymptotically far away from each other at the initial time ($t \to -\infty$). After collision ($t \to +\infty$), S_R is far to the right of S_L, that is, S_R is at $\xi = 0, \eta \to +\infty$ and S_L is at $\eta = 0, \xi \to -\infty$ .Using Eqs. (3.35) and (3.36), one can obtain their corresponding phase shifts as

$$\nabla P_0 = -2\varepsilon^2 \frac{D_1}{C_1} \phi_L W_L \,, \tag{3.37}$$

$$\nabla Q_0 = 2\varepsilon^2 \frac{D_2}{C_2} \phi_R W_R \,. \tag{3.38}$$

Equations(3.37) and (3.38) show that the magnitudes of phase shifts depend on the amplitude and width of the solitons.

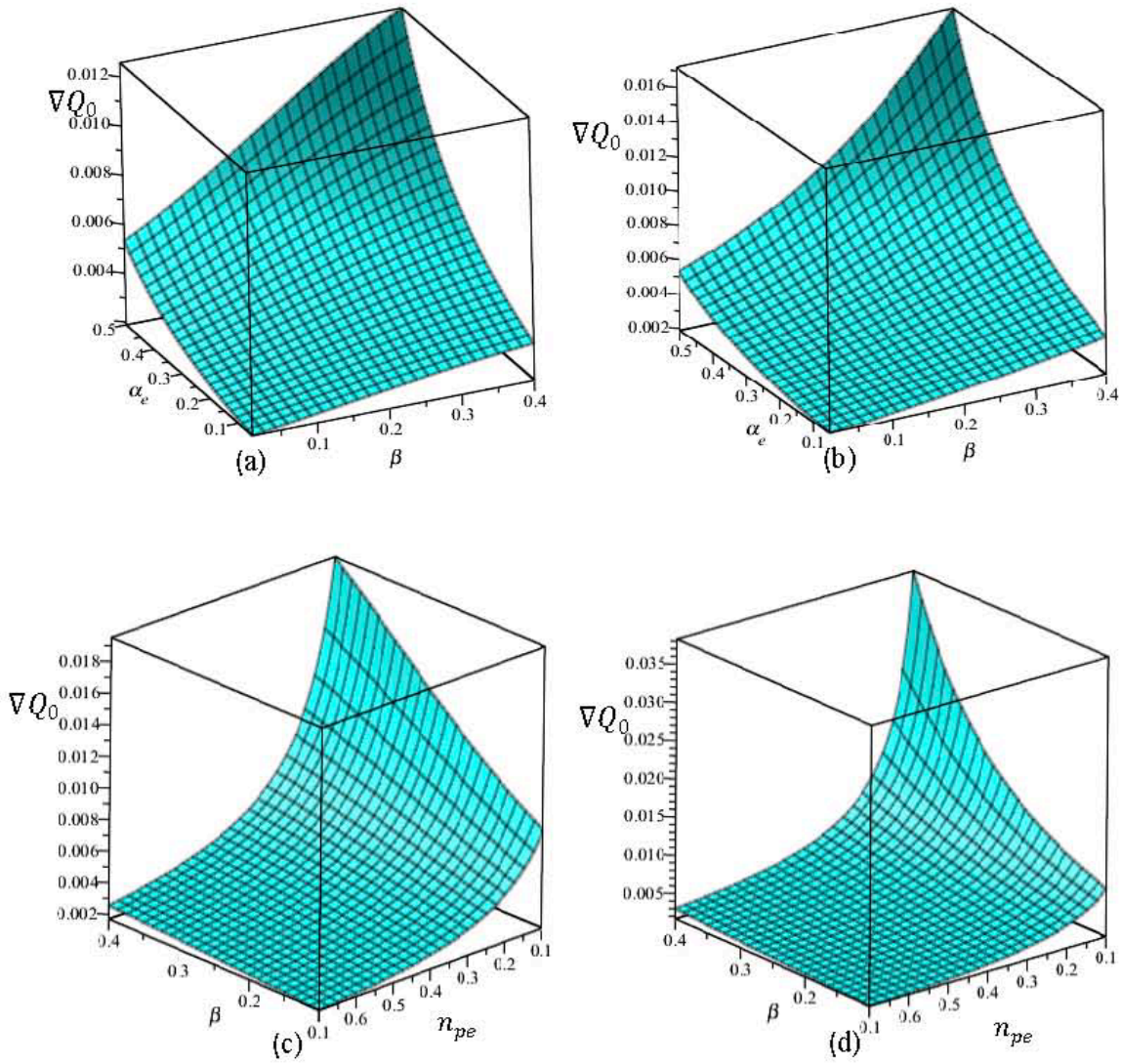

Figure 3.1 Effect of α_e((a) and (b)) taking $T_{ie} = T_i/T_e = 0.001, T_{ep} = T_e/T_p = 1, \alpha_p = 0.5, U_0 = 0.0075$, and $\epsilon = 0.1$; and $n_{pe} = n_{p0}/n_{e0}$ ((c) and (d)) taking $T_{ie} = 0.001, T_{ep}1, \alpha_{e,p} = 0.1, U_0 = 0.0075$, and $\epsilon = 0.1$ along with relativistic streaming factor $\beta = u_{i0}/c$ on the positive phase shift ∇Q_0 for both of WRR (left column) and HRR (right column).

3.5 Results and discussion

The interaction of ion acoustic solitary waves and their phase shift, time evolution, and pulse like electrostatic ion acoustic solitary waves are studied in the considered plasmas composing relativistic ions and high-energy nonthermal electrons and positrons. It is known that the high-energy particles are produced through the collisions among nonthermal particles, which reached high energies rather than their thermal energies [33]. In such situation, the relativistic ions are produced by the nonthermal electrons and positrons. Furthermore, the energetic streaming ions with energies 0.1-100 MeV are observed in solar atmosphere and interstellar space [20, 22]. To study the effect on phase shift after head-on collision between ion acoustic solitary waves, the time evolution and hump-shape structures of ion acoustic solitary waves in the considered plasmas both for WRR and HRR, the two-sided KdV equations are derived using the ePLK method. On the other hand, many authors [39-44] have studied the head-on collision between two solitons and their corresponding phase shift considering the unit amplitude of the solitons, whereas the amplitude of solitons strongly depends on the plasma parameters. In addition, the phase shifts are constructed in terms of the amplitude and width of the solitons using the well established stationary solitary wave solutions of KdV equations. Therefore, the influence of positron concentration (n_{pe}), relativistic streaming factor (β), electron to positron temperature ratio (T_{ep}), ion to electron temperature ratio (T_{ie}), and $\alpha_e(\alpha_p)$, which are responsible for the production of nonthermal electrons and positrons, on the phase shift, evolution and propagation of electrostatic potentials, and hump shape electrostatic ion acoustic solitary waves are investigated.

Figures 3.1(a) and 3.1(b) display the effects of α_e and n_{pe} along with relativistic streaming factor β $(= u_{i0}/c)$ on the phase shift ∇Q_0 both for WRR (left column) and HRR (right column) taking the remaining plasma parameters constant. On the other hand, Figs. 3.2(a) and 3.2(b) depict the effect of ∇Q_0 on the $\beta - T_{ie}$ and $\beta - T_{ep}$ planes both for WRR (left column) and HRR (right column), respectively, considering the remaining parameters constants. It is seen that the magnitudes of phase shift are increasing with increasing relativistic streaming factor, while it is decreasing with positron concentration, ion-electron temperature ratio, and electron-positron temperature ratio for both cases. This phenomenon can be attributed as follows. The electronic pressure depends on electron temperature as well as on electron density. Thus, the restoring force, as produced by electronic pressure, reduces

with increasing positron density and ion temperature, and hence, the magnitude of phase shift is decreasing. This means that the increase in positron concentration can be interpreted as

depopulation of ions from the plasma system, and as a result, the driving force (provided by ions inertia) of ion acoustic solitary waves decreases. It is also seen that the magnitudes of phase shift are almost the same for $\beta \leq 0.1$ and slightly larger for $\beta > 0.1$ in HRR rather

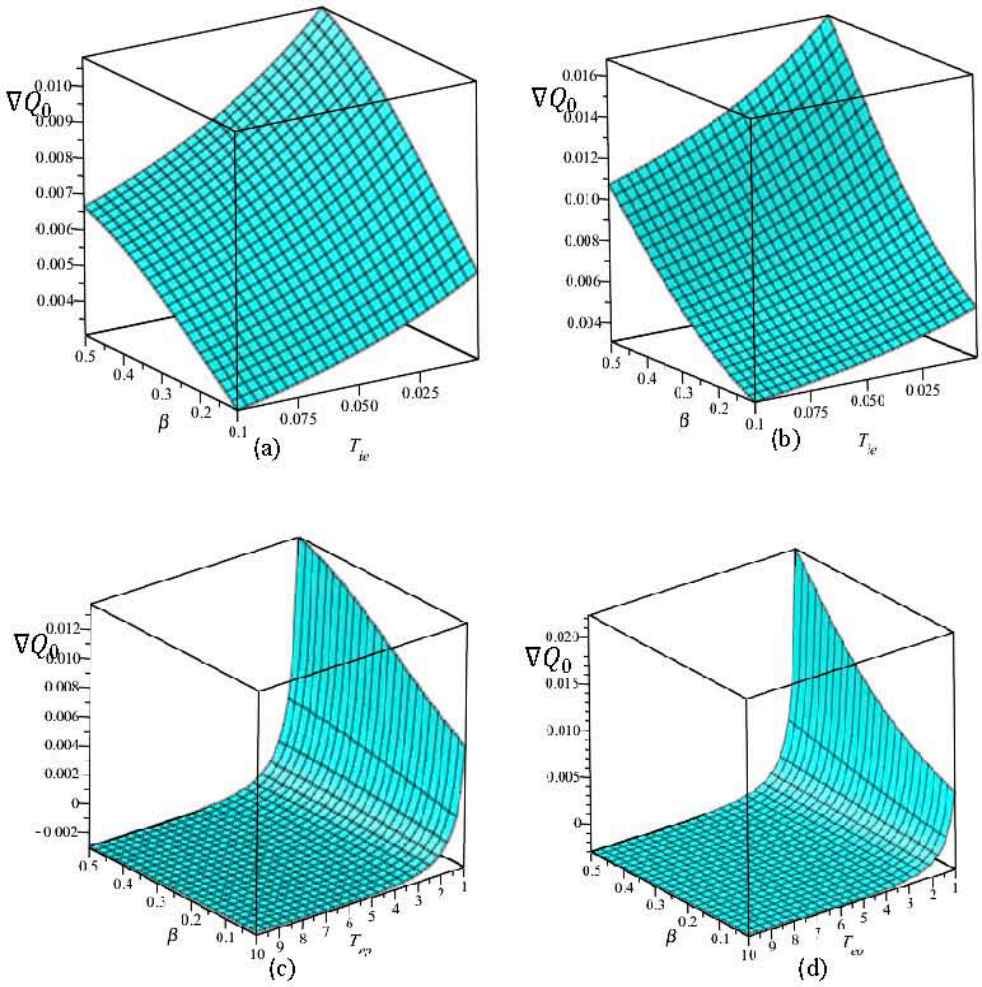

Figure 3.2 Effect of T_{ie} for $T_{ep} = 1.05$ ((a) and (b)) and T_{ep} for $T_{ie} = 0.01$ ((c) and 3(d)) along with relativistic streaming factor β on the positive phase shift ∇Q_0 for both of WRR (left column) and HRR (right column). The remaining parameters are considered as $n_{pe} = 0.7$, $T_e = 0.01$ MeV, $\alpha_e = \alpha_p = 0.5$, and $\epsilon = 0.1$.

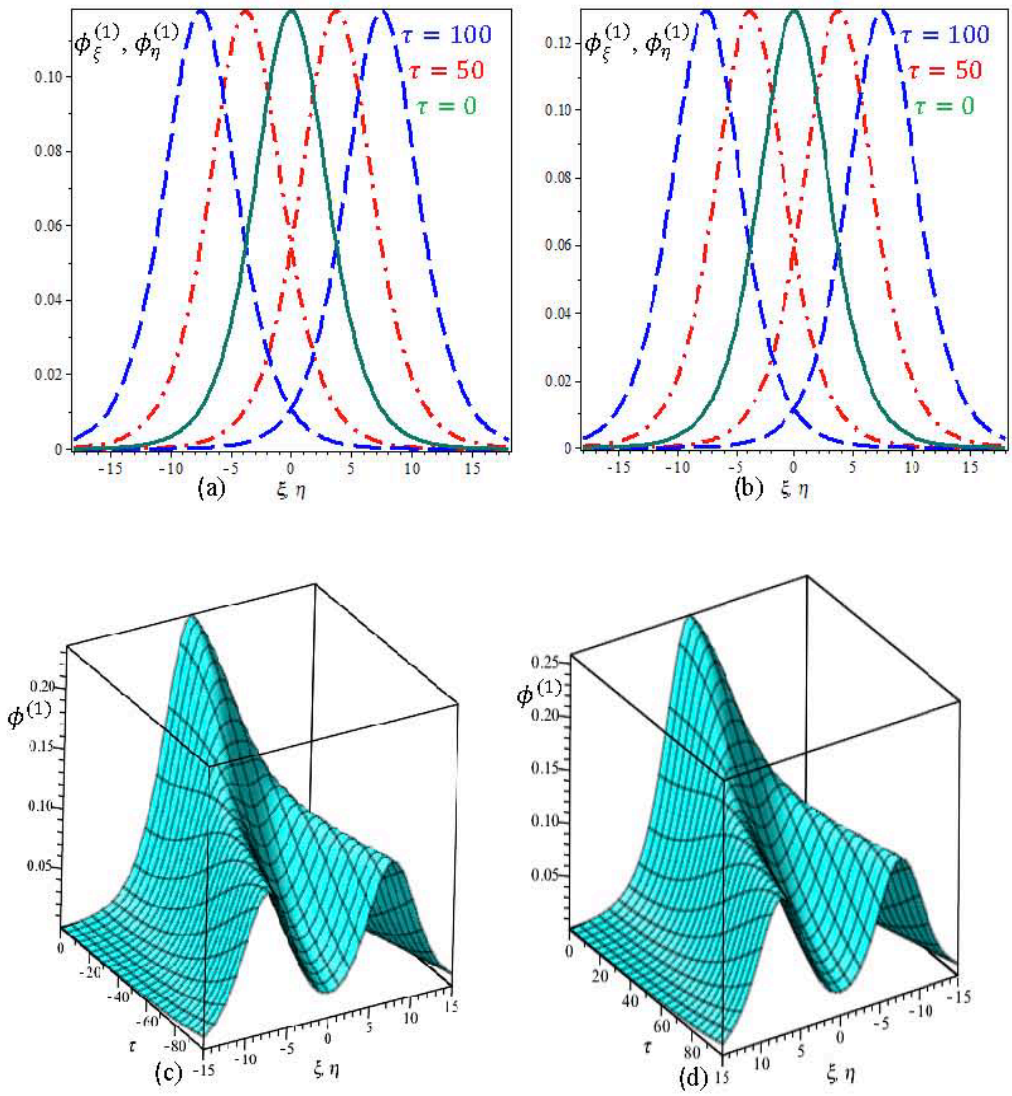

Figure 3.3 Electrostatic right $\phi_\xi^{(1)}$ and left $\phi_\eta^{(1)}$ moving profiles at $\tau = 0$ (green color), $\tau = 50$ (red color), and $\tau = 100$ (blue color) for both of (a) WRR and (b) HRR. Electrostatic profile ($\phi^{(1)}$) with different values of τ for both of (c) WRR and (d)HRR. The remaining parameters are considered as $n_{pe} = 0.7, T_{ep} = 1$, $\alpha_e = \alpha_p = 0.2, U_0 = 0{,}075$, and $\beta = 0.4$.

than WRR. Furthermore, it is seen from Fig. 3.2(b) that the magnitudes of phase shift is decreasing with the decrease of positron temperature in the range $T_{ep} = 1 - 5$ and then saturating in the range $T_{ep} > 5$ in both cases. It is noticed that the phase shift is independent of the wave modes [48].The coefficients D_1 and D_2 of Eqs. (3.24) and (3.25), respectively, dictate the types of phase shift, that is, positive or negative after head-on collision between

two solitary waves. It is observed from Figs. 3.1 and 3.2 that the magnitudes of phase shifts significantly modify for HRR rather than WRR and positive phase shift is obtained due to influences of plasma parameters in the plasma system.

Figures 3.3(a) and 3.3(b) show the temporal evolutions of compressive electrostatic potential structures $\phi_{\xi}^{(1)}$and $\phi_{\eta}^{(1)}$ against ξ and η, respectively, whereas Figs. 3.3(c) and 3.3(d) show the temporal evolution of compressive electrostatic potential $\phi^{(1)} = \phi_{\xi}^{(1)}(\xi,\tau) + \phi_{\eta}^{(1)}(\eta,\tau)$ against ξ and η , respectively, taking the remaining plasma parameters constant.

It is clearly seen from Figs. 3.3(a) and 3.3(b) that $\phi_{\xi}^{(1)}$ and $\phi_{\eta}^{(1)}$ are shifted towards the right and left direction, respectively, with increasing time τ. The two electrostatic ion acoustic solitary waves are propagating toward each other. This means that before collision, that is, at the initial time $t \to -\infty$, the soliton S_R is at $\xi = 0, \eta \to -\infty$ and S_L is at $\eta = 0, \xi \to +\infty$, and at time $t \to 0$, they collide, and then after collision, that is, at the time $t \to +\infty$, the soliton S_R is at $\xi = 0, \eta \to +\infty$ and S_L is at $\eta = 0, \xi \to -\infty$, such collision phenomena are shown in Figs. 3.3, as expected. On the other hand, the phase shifts combine to yield a single composite structure after interaction between the solitons, and then they propagate along the trajectories which deviate from the initial trajectories. Figs. 3.3(c) and 3.3(d) clearly indicate that the phase shift is approximately zero within $-10 < \tau < 10$ and then increasing with time τ ($\tau < -10, \tau > 10$) for both cases.

One can study the effect of plasma parameters on the hump shape structures of electrostatic potentials of ion acoustic solitary waves both for WRR and HRR considering the stationary solution $\phi_{\xi}^{(1)}(\xi,\tau) = \phi_R \mathrm{sech}^2(\chi/W_R)$ of the KdV equation, [Eq. (3.22)]. The effects of β, n_{pe}, and T_{ie} on the spatial electrostatic potential profiles of ion acoustic solitary waves are illustrated in Figs. 3.4(a)-3.4(f) both for WRR [Figs. 3.4(a), 3.4(c), 3.4(e)] and HRR [3.4(b),3.4 (d), 3.4(f)], respectively, taking the remaining plasma parameters constant into account. It is observed from Fig. 3.4 that the amplitudes and widths of the ion acoustic solitary waves are decreasing with the increase in n_{pe} and T_{ie}, and increasing with the increase in β. The relativistic streaming factor significantly affects the amplitude of ion acoustic solitary

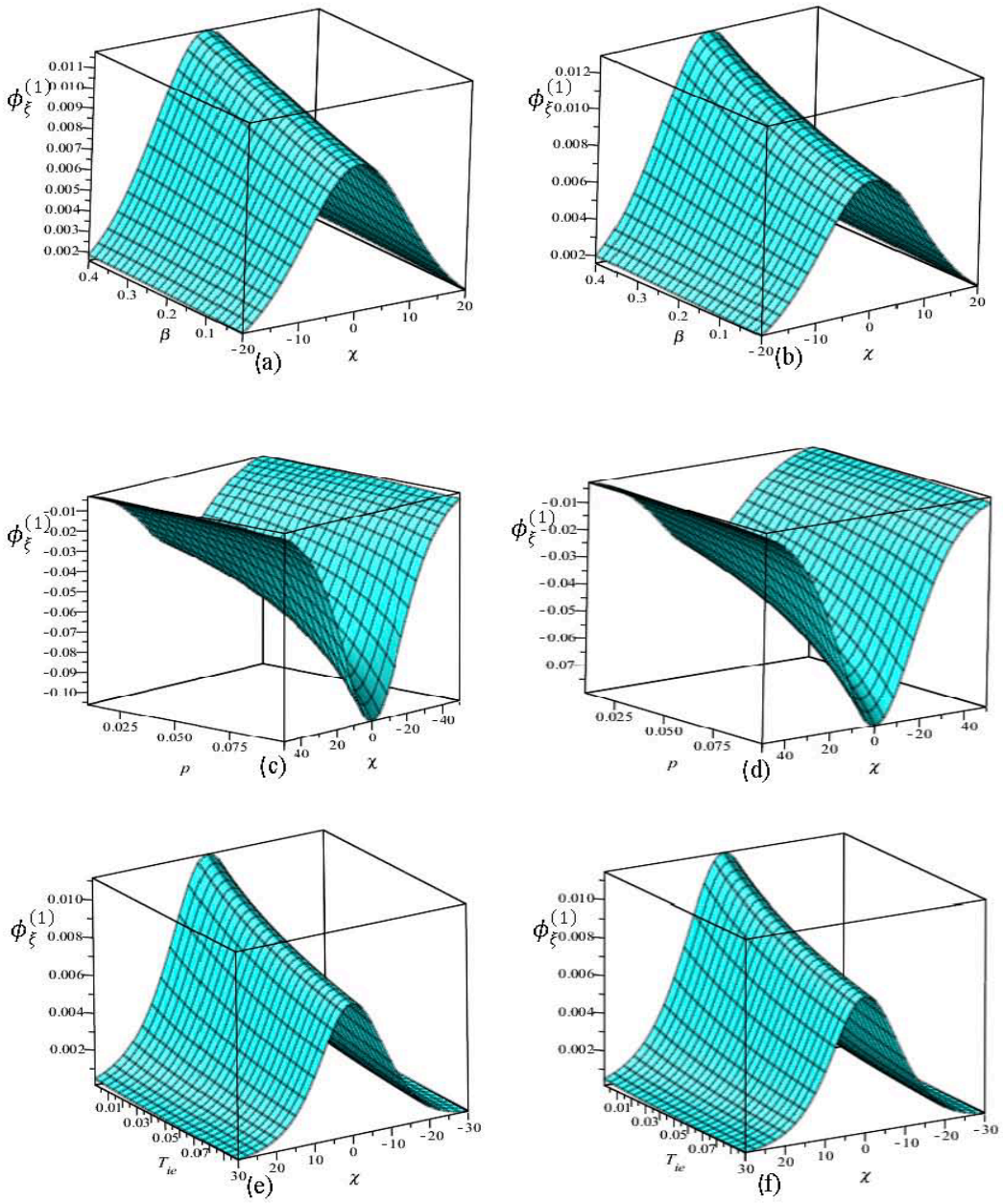

Figure 3.4 Effect of β ($n_{pe} = 0.7, T_{ie} = 0.01$), n_{pe} ($\beta = 0.3, T_{ie} = 0.01$), and T_{ie} ($n_{pe} = 0.7, \beta = 0.25$), on the electrostatic bell-shaped potential for both WRR ((a),(c), (e)) and HRR ((b), (d), (f)). The remaining parameters are considered as $T_{ep} = 1$, $\alpha_e = \alpha_p = 0.2$, and $U_0 = 0{,}075$.

waves in which the amplitudes are almost similar when $\beta \geq 0.1$ for both cases, but higher for HRR rather than WRR when $\beta < 0.1$. It is also provided that the HRR significantly modifies the wave dynamics rather than WRR in the plasmas. Furthermore, it is found that the compressive and rarefactive ion acoustic solitary waves are obtained in the plasmas. The rarefective ion acoustic solitary waves are only found in both cases of plasmas for $n_{pe} \leq 0.1$.

The normalized electric fields can be investigated using the relation $\boldsymbol{E} = (2\phi_R/W_R)\mathrm{sech}^2(\chi/W_R)\tanh(\chi/W_R)$. The behaviors of normalized electric fields are illustrated both for WRR and HRR in Figs. 3.5(a) and 3.5(b), respectively. It is observed that the electric field behaves like a semi-kink shape structure in the plasmas.

3.6 Conclusions

The electrostatic nonlinear propagation and head-on collision of ion acoustic solitary waves are investigated taking different plasma parameters into account both for the weakly and highly relativistic regimes by deriving the two-sided KdV equations employing the ePLK method. The phase shift is observed in terms of plasma parameters considering the stationary solutions of the KdV equations. It is found that the change in phase shift, magnitude of amplitude, and width of ion acoustic solitary waves are decreasing with the increase of positron concentration, ion-electron temperature ratio, electron-positron temperature ratio, but increasing with the increase of relativistic streaming factor. On the other hand, the nonlinear propagation characteristics of electrostatic ion acoustic solitary waves are almost same for $\beta \leq 0.1$ and slightly larger for $\beta > 0.1$ in HRR rather than WRR. It is concluded that the ion acoustic solitary waves are propagating faster in highly relativistic rather than weakly relativistic plasmas. The results revel that the propagation characteristics including electrostatic resonances of ion acoustic solitary waves are useful for understanding the physical issues of highly energetic nonthermal particles with relativistic warm ions in astrophysical and laboratory plasmas, especially in pulsar magnetosphere, laser produced, inertial confinement plasmas, pulsar relativistic winds with supernova ejecta, etc. This work is done to study the interaction of ion acoustic solitary waves and their corresponding phase shift derived from two-sided KdV equations. It is to be noted that there can be a possibility of producing instabilities due to higher order nonlinearity that may require further investigation.

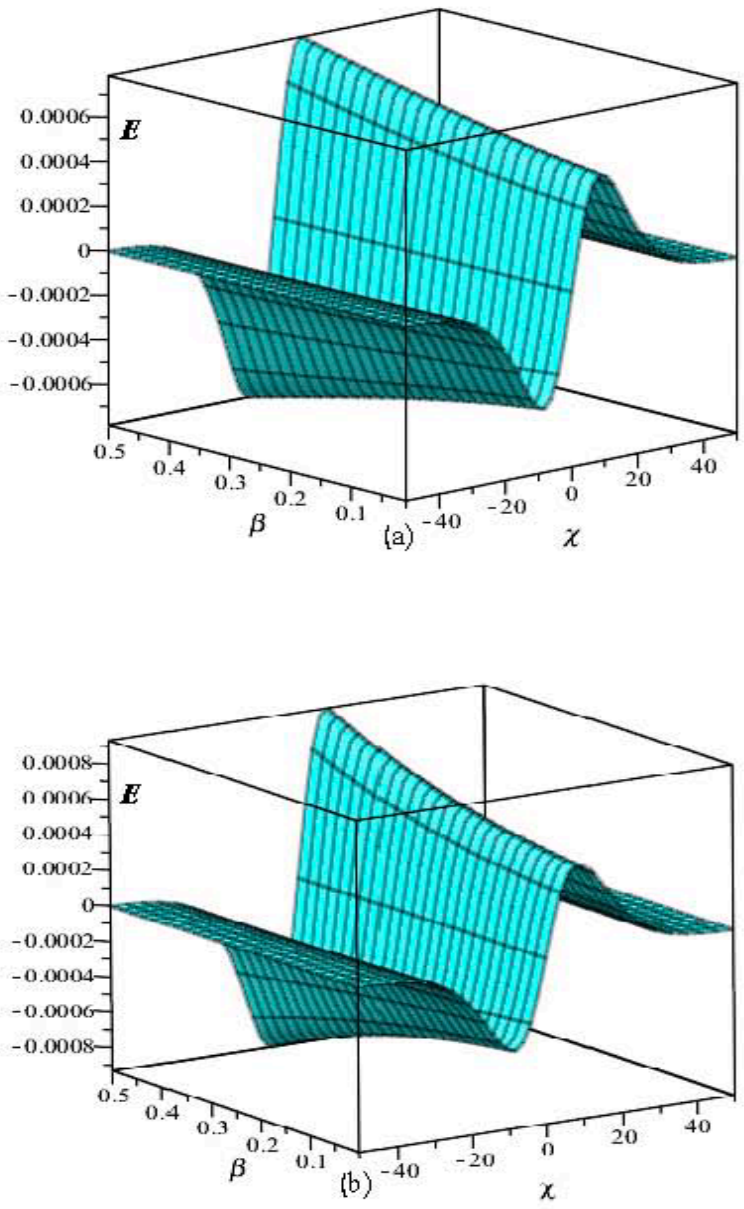

Figure 3.5 Behaviors of normalized electric field for both of (a) WRR and (b) HRR taking $\alpha_e = \alpha_p = 0.2$, $n_{pe} = 0.7$, $T_{ie} = 0.01$, $T_{ep} = 1$, and $U_0 = 0.0075$ into account.

References

1. M. D. Tinkle, R. G. Greaves, C. M. Surko, R. L. Spencer, and G. W. Mason, Phys. Rev. Lett. **72**, 352 (1994).
2. R. G. Greaves, and C. M. Surko, Phys. Rev. Lett. **75**, 3846 (1995).
3. D. B. Doumaz, and M. Djebli, Phys. Plasmas **17,** 074501(2010).
4. J. E. Gunn, and J. P. Ostriker, Astrophys. J. **165**, 523 (1971).
5. F. C. Michel, Theory of Neutron Star Magnetosphere (Chicago University Press, Chicago, 1991)
6. F. C. Michel, Rev. Mod. Phys. **54,** 1(1982).
7. H. R. Miller, and P. J. Wiita, Active Galactic Nuclei (Springer, Berlin, 1987).
8. M. L. Burns, Positron–Electron Pairs in Astrophysics (American Institute of Physics, Melville, NY, 1983)
9. S. W. Weinberg, Gravitation and Cosmology (Wiley, New York, 1972).
10. M. J. Rees, The Very Early Universe (Cambridge University Press, Cambridge,1983)
11. A. M. Galper, S. V. Koldashov, V. V. Mikhailov, and S. A. Voronov, Radiat. Meas. **26**, 375 (1996).
12. E. Fiandrini, J. Geophys. Res. **108**, 1402 (2003).
13. F. Verheest, T. Cattaert, and M. Hellberg, Space Sci. Rev. **121**, 299 (2005).
14. V. I. Berezhiani, D. P. Garuchava, and P. K. Shukla, Phys. Lett. A **360**, 624 (2007).
15. B. Bhattacharyya, Phys. Rev. A **27**, 568 (1983).
16. D. F. Smith, and S. H. Brecht, J. Geophys. Res. **90**, 205 (1985).
17. R. P. Lin, W. K. Levedahl, D. A. Gurnett, and F. L. Scarf, Astrophys. J. 308, 954 (1986).
18. L. R. Lyons, and D. J. Williams, in Quantitative Aspects of Magnetospheric Physics (Reidel, Dordrecht, 1984).
19. J. Arons, Space Sci. Rev. **24**, 437 (1979).
20. Y. Nejoh, Phys. Fluid B 4, 2830 (1992).
21. M. G. Hafez, M. R. Talukder, and M. H. Ali, Astrophys. Space Sci. **361,** 154 (2016).
22. T. S. Gill, A. Singh, H. Kaur, N. S. Saini, and P. Bala, Phys. Lett. A. **361**, 364 (2007).
23. T. S. Gill, A. S. Bains, and N. S. Saini, Can. J. Phys. **87**, 861(2009).
24. M. G. Hafez, and M. R. Talukder, Astrophys. Space Sci. **359**, 27 (2015).
25. H. K. Malik, Phys. Rev. E **54,** 5844 (1996).
26. M. G. Hafez, M. R. Talukder, and R. Sakthivel, Indian J. Phys. **90**, 603 (2016).
27. M. G. Hafez, M. R. Talukder, and M. H. Ali, Phys. Plasmas **23**, 012902 (2016).

28. M. G. Hafez, N. C. Roy, M. R. Talukder, and M. H. Ali, Astrophys. Space Sci. **361,** 312 (2016).
29. H. R. Pakzad, and K. Javidan, Astrophys. Space Sci. **333**, 257 (2011).
30. M. G. Hafez, N. C. Roy, M. R. Talukder, and M. H. Ali, Plasma Sci. Technol. **19,** 015002 (2017).
31. K. Javidan, and H. R. Pakzad, Indian J. Phys. **86**, 1037 (2012).
32. M. G. Hafez, M. R. Talukder, and M. H. Ali, Pramana-J. Phys. **87,** 70 (2016).
33. T. Cattaert, M. A. Helberg, and R. L. Mace, Phys. Plasmas **14,** 082111(2007).
34. R. A. Cairns, A. A. Mamun, R. Bingham, R. O. Dendy, R. Bostrom, C. M. C. Nairn, and P. K. Shukla, Geophys. Res. Lett. **22**, 2709 (1995).
35. L. Arons, Astrophys. Space Sci. Library **357,** 373 (2009).
36. M. E. Dieckmann, B. Elisson, and P. K. Shukla, Phys. Rev. E **70,** 036401 (2004).
37. S. Usami, H. Hasegawa, and Y. Ohsawa, Phys. Plasmas **8,** 2666 (2001).
38. D. B. Doumaz, and M. Djebli, Phys. Plasmas **17,** 074501 (2010).
39. K. E. Lonngren, Opt. Quantum Electron. **30**, 615 (1998).
40. J. K. Xue, Phys. Rev. E **69**, 016403 (2004).
41. J. N. Han, S. L. Du, and W. S. Duan, Phys. Plasmas **15**, 112104 (2008).
42. J. N. Han, X. X. Yang, D. X. Tian, and W. S. Duan, Phys. Lett. A **372**, 4817 (2008).
43. M. A. Khaled, Astrophys. Space Sci. **350**, 607 (2014).
44. N. S. Saini, and K. Singh, Phys. Plasmas **23**, 103701 (2016).
45. N. J. Zabusky, and M. D. Kruskal, Phys. Rev. Lett. **15**, 240 (1965).
46. P. K. Shukla and A. A. Mamun, Introduction to Dusty Plasma Physics (IOP, Bristol, 2002).
47. A. Mushtaq and R. Khan, Phys. Scr. **78**, 015501(2008).
48. U. N. Ghosh, K. Roy, and P. Chatterjee, Phys. Plasmas **18**, 103703 (2011).

Abbreviation and Nomenclature:

KdV= Korteweg-de Vries

ePLK = extended Poincaré-Lighthill-Kuo

WRR= weakly relativistic regime

HRR= highly relativistic regime

DA= dust acoustic

ϕ = electrostatic potential

v_j = velocity of jth species

T_j = temperature of jth species

m_j = mass of jth species

n_{j0} = unperturbed density of jth species

α_j = population of jth particle

v_{tj} = thermal speed of jth species

β_e = thermality of electron

β_p = thermality of positron

m_i = mass of ion

v_{thi} = ion thermal velocity

v_{thp} = positron thermal velocity

n_i = ion density

u_i = ion fluid velocity

$T_{ie} = T_i/T_e$ = temperature ratio of ion to electron

$T_{ep} = T_e/T_p$ = temperature ratio of electron to positron

P_i = ion pressure

N = degrees of freedome

γ = Lorentz relativistic factor

c = velocity of light

$V_1 (V_2)$ = unknown phase velocity

ε = small parameter, measure the strength of nonlinearity

β = relativistic streaming factor

$A_1 (A_2)$ = coefficient of nonlinearity

$B_1 (B_2)$ = coefficient of dispersion

$\phi_R(\phi_L)$ = amplitude of right (left) moving soliton

$W_R(W_L)$ = width of right (left) moving soliton

U_0 = constant velocity of soliton

u_{i0} = unperturbed ion dencity

M eV= mega electron volt

E = electric field

$\nabla P_0(\nabla Q_0)$ = phase shift of right (left) moving soliton

Chapter 4

Effects of two-temperature ions on head-on collision and phase shifts of dust acoustic single- and multi-solitons in dusty plasma

4.1 Introduction

Dusty plasmas are composed of electrons, ions, and micron or submicron size massively charged dust with masses in the range from $10^6 - 10^{12}$ of proton masses [1]. These plasmas are considered for understanding several types of collective processes that are existed in the lower and upper mesosphere, cometary tails, planetary rings, interstellar media, planetary magnetosphere, interplanetary spaces [1–4], as well as in laboratory dusty plasmas [5–7]. The nonlinear collective effects of plasmas cannot appropriately be studied without tedious mathematical techniques. The localization of waves produces several types of important structures, namely: solitary waves, shock waves, double layers, vortices, etc., due to nonlinearity with dispersion or dissipation, which deserve both theoretical and experimental studies to get insight knowledge of the physical phenomena. Rao et al.[5] have investigated the characteristics of low phase speed dust acoustic waves in dusty plasmas that are observed in space and laboratory. They have found that the inertia is provided by the mass of the dust particles, while the pressure of the inertialess electrons and ions provides restoring force due to the production of dust acoustic waves in the plasmas. Many authors [8–17] have investigated the propagation characteristics of dust acoustic waves in dusty plasmas considering different plasma assumptions. On the other hand, the effect of dust charge fluctuation plays a significant role only for the wave whose time period (T_ω) is comparable to the dust charging time period (T_{cw}) [18]. But T_ω (= 0.01-0.1s) is much larger than $T_{c\omega}$ ($= 1 - 10\mu s$) , and in such case, one can neglect the effect of dust charge fluctuation of the dust acoustic waves. Bandyopadhyay et al. [19] have studied the nonlinear dust acoustic solitary waves experimentally with constant dust charge fluctuation in dusty plasmas and determined ion density $n_i = 7 \times 10^{13}\mathrm{m}^{-3}$, dust density $n_d = 1 \times 10^{10}\mathrm{m}^{-3}$, ion temperature $T_i = 0.3\mathrm{eV}$, dust charge number $Z_d = 3 \times 10^3$, and dust mass $m_d = 1 \times 10^{-13}$ kg. They have mentioned, taking the propagation of two solitary structures of different heights moving with different

velocities into account, that the dynamics of solitary pulses are similar to those of theoretical findings for compressive solitary waves of the Korteweg–de Vries (KdV).

However, the interactions among nonlinear waves, including resonances, carry important physical phenomena that are observed in space plasmas [20–28]. When two or more solitary waves propagate toward each other, they will interact and exchange their energies among themselves and then separate off. During the process of interactions, the solitary waves become stable and preserve their identities. Each soliton gains two phase shifts (either positive or negative) that is independent of wave modes [22]. One is due to the head-on collision [29] and the other is due to the overtaking collision [30] of one soliton by another. The asymptotic conservation, which is one of the salient properties of solitons, forms when two or more waves undergo collision. It provides two important effects: phase shifts and trajectories [31-32]. In such case, one can employ the extended Poincaré-Lighthill-Kuo (ePLK) method with strained coordinates [33-34] to derive the two-sided nonlinear evolution equations. On the other hand, the multi-soliton solutions of the evolution equations may properly describe how greater amplitude (with higher velocity) solitons overtake the smaller (with lower velocity) one, in the presence of nonlinearity during the interaction phase. However, many authors [20–28] have investigated the effects of plasma parameters on equal-amplitude colliding solitons and time delay considering the square root of the initial amplitude. Harvey et al. [35] have investigated experimentally the interaction of two counter-propagating equal initial amplitude solitons in a complex plasma. They have found that the propagation velocity of the soliton becomes slower after the collision and the time delay is not proportional to the square root of the initial amplitude. They are unable to verify their experimental findings due to theoretical limitations [20–28]. Theoretical predictions of colliding solitons considering appropriate initial amplitude are important for understanding the electrostatic resonances and their time delay in the plasmas. Thus, the study of interactions of nonlinear solitons and their phase shifts becomes one of the most important topics due to its wide applications and potentiality.

Considering two-temperature (cold and hot) ions of equal masses and charge numbers following Boltzmann distribution function, Xie et al.[36] have found that the energy exchange rate is much smaller than the characteristic frequency of the plasma system. The Soviet Phobos 2 spacecraft [37] and the Japanese Nozomi spacecraft [38] have detected nonthermal ions having a partial ring structure in the velocity phase space.

Besides, Tagare et al.[39] have noted that the electron becomes isothermal if the electron temperature is much smaller than the effective ion temperature. Zhang and Wang [40] have

studied the effect of two-temperature nonthermally distributed ions on dust acoustic solitary waves. Tasnim et al.[41] have also considered the distinct nonthermal ion temperature in a dusty plasma system using the Gardner equation to study the properties of dust acoustic solitary waves. Later on, Tasnim et al.[18] have studied the properties of dust acoustic solitary waves in unmagnetized quasi-neutral dusty plasma neglecting the effect of dust charge fluctuation considering that the surface charge of the extremely massive mobile dust particles is composed of Boltzmann distributed electrons, and two distinct ion temperatures, where the cold and hot ions follow the nonextensive and nonthermal distributions, respectively. They have derived the KdV, modified KdV (mKdV), and standard Gardner (SG) equations to study the nonlinear physical phenomena in the aforementioned plasmas. They have also determined how the Gardner solution differs from the KdV and mKdV solutions based on the typical data of Refs. 19, 40, and 41, and mentioned that these plasmas may exist in various cosmic dust laden plasmas [42-43], where two distinct temperature ions [41, 44-45] can significantly modify the wave dynamics. However, the role of the head-on collisions between the dust acoustic waves may not be ignored, because it plays an important role in understanding physical scenarios of plasmas. Being motivated by the potentiality of the problems related to the astrophysical, space, and laboratory plasmas, the head-on collisions among the dust acoustic single- and multi-solitons and their phase shifts in unmagnetized plasmas consisting of massive negatively charged mobile dust particles, Boltzmann distributed electrons, and two-temperature nonthermal ions are investigated; the two temperature nonthermal cold and hot ions occupy two different regions of phase space. The effects of cold and hot ions temperature ratio (σ_1), cold ion-electron temperature ratio (σ_2), unperturbed cold ion-dust density ratio (μ_{i1}), unperturbed hot ion-dust density ratio (μ_{i2}), population of cold ion nonthermality (β_{i1}) and population of hot ion nonthermality (β_{i2}) on the phase shift, and head-on collisions among the dust acostic single- and multi-solitons are examined. In sequence of introduction, theoretical model and derivations of two different types of KdV equations are presented in Section 4.2. The single- and multi-soliton solutions of KdV equations and their corresponding phase shifts are displayed in Section 4.3. The results along with the relevant discussion are presented in Section 4.4. Finally, the conclusion is drawn in Section 4.5.

4.2 Basic equations

4.2.1 Model equations

Let us consider a one-dimensional unmagnetized plasma system consisting of negatively charged mobile dust, two temperature ions, and Boltzmann-distributed electrons. Yu and Luo

[46] have shown that the different species occupy different regions of phase space, and therefore, it is reasonable to consider different temperatures of the species in the multispecies fluid model to construct quasi-stationary nonlinear structures. So, the two temperature (cold and hot) ions may occupy two different regions of the phase space. Further, the distribution of charged particles does not follow the Boltzmann-Gibbs statistics for the systems with the long-range interactions, where the non-equilibrium stationary states exist. In such situations, one can consider the non-Maxwellian distributions (e.g., Cairns, nonextensive, and kappa distributions [47]) for the charge particles. The cold and hot ions are assumed to follow the nonthermal distribution [48] due to the production of two temperature nonthermal ions in the satellite missions [37-38]. According to the Cairns distribution [48], the nonthermal concentrations of cold and hot ions are obtained [41] as

$$n_{i1(i2)} = n_{i10,(i20)}\left[1 + \beta_{i1(i2)}\left(\frac{e\phi}{T_{i1(i2)}}\right) + \beta_{i1(i2)}\left(\frac{e\phi}{T_{i1(i2)}}\right)^2\right] \times exp\left(-\frac{e\phi}{T_{i1(i2)}}\right),$$

where $\beta_{i1(i2)} = 4\alpha_{i1(i2)}/\left(1 + 3\alpha_{i1(i2)}\right)$, $n_{i10,(i2)}$ are the unperturbed cold (hot) ions concentration, $T_{i1(i2)}$ is the cold (hot) ion temperature, e is the electron charge, and $\alpha_{i1(i2)} > -1/3$ determines the population of nonthermal cold (hot) ions, respectively. The nonthermal cold and hot ions become isothermal for $\alpha_{i1(i2)} \to 0$. At equilibrium, the charge neutrality condition $n_{i10} + n_{i20} = n_{e0} + Z_d n_{d0}$ is obtained, where n_{e0} and n_{d0} are the densities of unperturbed electrons and surface electrons of the dust grain, respectively, and Z_d is the charge number. To study the head-on collision dynamics of the low phase velocity dust acoustic waves, the normalized governing fluid equations can be defined as

$$\frac{\partial n_d}{\partial t} + \frac{\partial}{\partial x}(n_d\, u_d) = 0\,, \tag{4.1}$$

$$\frac{\partial u_d}{\partial t} + u_d \frac{\partial u_d}{\partial x} = \frac{\partial \phi}{\partial x}\,, \tag{4.2}$$

$$\frac{\partial^2 \phi}{\partial x^2} = n_d + \mu e^{T_s \sigma_2 \phi} - \mu_{i1}(1 + \beta_{i1} T_s \phi + \beta_{i1} T_s^2 \phi^2) e^{-T_s \phi} - \mu_{i2}(1 + \beta_{i2} T_s \sigma_1 \phi + \beta_{i2} T_s^2 \sigma_1^2 \phi^2) e^{-T_s \sigma_1 \phi}. \tag{4.3}$$

Here, n_d is dust particle density normalized by n_{d0} , u_d is the dust fluid speed normalized by dust acoustic speed $C_d = (Z_d k_B T_{i1}/m_d)^{1/2}$, ϕ is the electrostatic potential normalized by T_{eff}/e, $\sigma_1 = T_{i1}/T_{i2}$, $\sigma_2 = T_{i1}/T_e$, $\mu_{i1(i2)} = n_{i10(i20)}/Z_d n_{d0}$, $T_s = T_{eff}/T_{i1} = 1/(\mu\sigma_2 + \mu_{i1} + \mu_{i2}\sigma_1)$, k_B is the Boltzmann constant, m_d is the dust particle mass and T_{eff} is the effective ion temperature which is obtained from the relation

$1/T_{eff} = (1/Z_d n_{d0})\,(n_{e0}/T_e + n_{i10}/T_{i1} + n_{i20}/T_{i2})$. The time variable t is normalized by dust particle period $\omega_{pd}^{-1} = (m_d/4\pi n_{d0} Z_d^2 e^2)^{1/2}$ and the space variable x is normalized by the Debye length $\lambda_{Dm} = \left(k_B T_{eff}/4\pi n_{d0} Z_d e^2\right)^{1/2}$. The equilibrium charge neutrality condition in the plasmas is obtained by taking the Poisson's relation into account as $\mu = n_{e0}/Z_d n_{d0} = \mu_{i1} + \mu_{i2} - 1$. It is to be noted that the electrons may become isothermal for $T_e \ll T_{eff}$.

4.2.2 Formation of two-sided KdV equations via the extended PLK method

The ePLK method [33-34] of stretched coordinates is employed to derive the two-sided KdV equations for studying the interactions of dust acoustic solitons in the considered plasma system. According to this method, the scaling variables x and t can be the following coordinate system:

$$\left.\begin{array}{c} \xi = \varepsilon(x - Vt) + \varepsilon^2 P_0(\eta,\tau) + \varepsilon^3 P_1(\eta,\xi,\tau) + \ \ldots\ldots \\ \eta = \varepsilon(x + Vt) + \varepsilon^2 Q_0(\xi,\tau) + \varepsilon^3 Q_1(\eta,\xi,\tau) + \ \ldots\ldots \\ \tau = \varepsilon^3 t \end{array}\right\}, \tag{4.4}$$

where ξ and η are the trajectories between the solitons which are traveling toward each other, and V is the unknown phase velocity of dust acoustic waves and ε is a small parameter measuring the strength of nonlinearity and dissipation. The unknown variables $P_0(\eta,\tau)$ and $Q_0(\xi,\tau)$ will be determined later. Using Eq. (4.4), the operators can be defined as

$$\left.\begin{array}{l} \dfrac{\partial}{\partial t} \approx \varepsilon^3 \dfrac{\partial}{\partial \tau} + \varepsilon V\left(-\dfrac{\partial}{\partial \xi} + \dfrac{\partial}{\partial \eta}\right) + \varepsilon^3 V\left(\dfrac{\partial P_0}{\partial \eta}\dfrac{\partial}{\partial \xi} - \dfrac{\partial Q_0}{\partial \xi}\dfrac{\partial}{\partial \eta}\right) + \cdots\cdots \\ \dfrac{\partial}{\partial x} \approx \varepsilon\left(\dfrac{\partial}{\partial \xi} + \dfrac{\partial}{\partial \eta}\right) + \varepsilon^3\left(\dfrac{\partial P_0}{\partial \eta}\dfrac{\partial}{\partial \xi} + \dfrac{\partial Q_0}{\partial \xi}\dfrac{\partial}{\partial \eta}\right) + \cdots\cdots\cdots\cdots\cdots\cdots \end{array}\right\}. \tag{4.5}$$

The perturbed quantities can be expanded in power series of ε as

$$\begin{bmatrix} n_d \\ u_d \\ \phi \end{bmatrix} = \begin{bmatrix} 1 \\ 0 \\ 0 \end{bmatrix} + \varepsilon^2 \begin{bmatrix} n_d^{(1)} \\ u_d^{(1)} \\ \phi^{(1)} \end{bmatrix} + \varepsilon^3 \begin{bmatrix} n_d^{(2)} \\ u_d^{(2)} \\ \phi^{(2)} \end{bmatrix} + \varepsilon^4 \begin{bmatrix} n_d^{(3)} \\ u_d^{(3)} \\ \phi^{(3)} \end{bmatrix} + \cdots \ . \tag{4.6}$$

Inserting Eqs.(4.5) and (4.6) into Eqs. (4.1)-(4.3) and equating the quantities with equal powers of ε, one may obtain a set of equations in different orders of ε. To the lowest order of ε yeilds

$$\left(-V\frac{\partial n_d^{(1)}}{\partial \xi} + \frac{\partial u_d^{(1)}}{\partial \xi}\right) + \left(V\frac{\partial n_d^{(1)}}{\partial \eta} + \frac{\partial u_d^{(1)}}{\partial \eta}\right) = 0, \tag{4.7}$$

$$\left(-V\frac{\partial u_d^{(1)}}{\partial \xi}-\frac{\partial \phi^{(1)}}{\partial \xi}\right)+\left(V\frac{\partial u_d^{(1)}}{\partial \eta}-\frac{\partial \phi^{(1)}}{\partial \eta}\right)=0, \tag{4.8}$$

$$n_d^{(1)}=-C_1\phi^{(1)}, \tag{4.9}$$

where $C_1=T_s[\mu\sigma_2-\mu_{i1}(\beta_{i1}-1)-\mu_{i2}\sigma_1(\beta_{i2}-1)]$. One may define the relations along with the different physical quantities, taking Eqs. (4.7)-(4.9) into account as

$$\phi^{(1)}=\phi_\xi^{(1)}(\xi,\tau)+\phi_\eta^{(1)}(\eta,\tau), \tag{4.10}$$

$$n_d^{(1)}=-C_1\left[\phi_\xi^{(1)}(\xi,\tau)+\phi_\eta^{(1)}(\eta,\tau)\right], \tag{4.11}$$

$$u_d^{(1)}=\frac{1}{V}\left[-\phi_\xi^{(1)}(\xi,\tau)+\phi_\eta^{(1)}(\eta,\tau)\right]. \tag{4.12}$$

The normalized phase velocity is obtained as $V=\sqrt{1/C_1}$ by taking the solvability condition into account. The functions $\phi_\xi^{(1)}(\xi,\tau)$ and $\phi_\eta^{(1)}(\eta,\tau)$ may be determined taking the next order of ε. Relations (4.10)-(4.12) provide the two-sided electrostatic waves, one of which ($\phi_\xi^{(1)}$) is traveling to right direction and the other ($\phi_\eta^{(1)}$) is traveling to left direction.

To the next order of ε, one can obtain another set of equations whose solutions are defined as

$$\phi^{(2)}=\phi_\xi^{(2)}(\xi,\tau)+\phi_\eta^{(2)}(\eta,\tau), \tag{4.13}$$

$$n_d^{(2)}=-C_1\left[\phi_\xi^{(2)}(\xi,\tau)+\phi_\eta^{(2)}(\eta,\tau)\right], \tag{4.14}$$

$$u_d^{(2)}=\frac{1}{V}\left[-\phi_\xi^{(2)}(\xi,\tau)+\phi_\eta^{(2)}(\eta,\tau)\right]. \tag{4.15}$$

Finally, the next higher order of ε gives

$$\begin{aligned}&\frac{\partial {n_d}^{(1)}}{\partial \tau}-V\frac{\partial n_d^{(3)}}{\partial \xi}+V\frac{\partial n_d^{(3)}}{\partial \eta}+\frac{\partial u_d^{(3)}}{\partial \xi}+\frac{\partial u_d^{(3)}}{\partial \eta}+\frac{\partial}{\partial \xi}\left({n_d}^{(1)}{u_d}^{(1)}\right)+\frac{\partial}{\partial \eta}\left({n_d}^{(1)}{u_d}^{(1)}\right)\\&\quad+V\frac{\partial P_0}{\partial \eta}\frac{\partial n_d^{(1)}}{\partial \xi}+\frac{\partial P_0}{\partial \eta}\frac{\partial u_d^{(1)}}{\partial \xi}-V\frac{\partial Q_0}{\partial \xi}\frac{\partial n_d^{(1)}}{\partial \eta}+\frac{\partial Q_0}{\partial \xi}\frac{\partial u_d^{(1)}}{\partial \eta}\\&\quad=0,\end{aligned} \tag{4.16}$$

$$\frac{\partial u_d{}^{(1)}}{\partial \tau} - V\frac{\partial u_d^{(3)}}{\partial \xi} + V\frac{\partial u_d^{(3)}}{\partial \eta} + u_d{}^{(1)}\frac{\partial u_d{}^{(1)}}{\partial \xi} + u_d{}^{(1)}\frac{\partial u_d{}^{(1)}}{\partial \eta} - \frac{\partial \phi^{(3)}}{\partial \xi} - \frac{\partial \phi^{(3)}}{\partial \eta} + V\frac{\partial P_0}{\partial \eta}\frac{\partial u_d^{(1)}}{\partial \xi}$$
$$- \frac{\partial P_0}{\partial \eta}\frac{\partial \phi^{(1)}}{\partial \xi} - V\frac{\partial Q_0}{\partial \xi}\frac{\partial u_d^{(1)}}{\partial \eta} - \frac{\partial Q_0}{\partial \xi}\frac{\partial \phi^{(1)}}{\partial \eta} = 0, \qquad (4.17)$$

$$\frac{\partial^2 \phi^{(1)}}{\partial \xi^2} + \frac{\partial^2 \phi^{(1)}}{\partial \eta^2} + 2\frac{\partial^2 \phi^{(1)}}{\partial \xi \partial \eta} = n_d{}^{(3)} + C_1\phi^{(3)} + C_2\{\phi^{(1)}\}^2, \qquad (4.18)$$

where $C_2 = \frac{T_s^2}{2}[\mu\sigma_2^2 - \mu_{i1} - \mu_{i2}\sigma_1^2]$. Simplifying Eqs.(4.16)-(4.18) using Eqs. (4.10)-(4.12) and then integrating with regards to ξ and η provide

$$2V^2 u_d^{(3)} = \int\left(\frac{\partial \phi_\xi^{(1)}}{\partial \tau} + A\phi_\xi^{(1)}\frac{\partial \phi_\xi^{(1)}}{\partial \xi} + B\frac{\partial^3 \phi_\xi^{(1)}}{\partial \xi^3}\right)d\eta$$
$$+ \int\left(\frac{\partial \phi_\eta^{(1)}}{\partial \tau} - A\phi_\eta^{(1)}\frac{\partial \phi_\eta^{(1)}}{\partial \eta} - B\frac{\partial^3 \phi_\eta^{(1)}}{\partial \eta^3}\right)d\xi$$
$$+ \iint\left(2V\frac{\partial P_0}{\partial \eta} - \left[C_2V^3 - \frac{1}{2V}\right]\phi_\eta^{(1)}\right)\frac{\partial^2 \phi_\xi^{(1)}}{\partial \xi^2}d\xi d\eta$$
$$- \iint\left(2V\frac{\partial Q_0}{\partial \xi} - \left[C_2V^3 - \frac{1}{2V}\right]\phi_\xi^{(1)}\right)\frac{\partial^2 \phi_\eta^{(1)}}{\partial \eta^2}d\xi d\eta, \qquad (4.19)$$

where $A = -[(3/2V) + V^3C_2]$ and $B = V^3/2$. The first and second terms on the right side of Eq.(4.19) are proportional to η and ξ, respectively, because the integrands of these two terms are independent of η and ξ. All the terms of the first two expressions on the right side of Eq.(4.19) become secular and they may be eliminated in order to stay away from spurious resonances. Thus, one finds the following KdV equations:

$$\frac{\partial \phi_\xi^{(1)}}{\partial \tau} + A\phi_\xi^{(1)}\frac{\partial \phi_\xi^{(1)}}{\partial \xi} + B\frac{\partial^3 \phi_\xi^{(1)}}{\partial \xi^3} = 0, \qquad (4.20)$$

$$\frac{\partial \phi_\eta^{(1)}}{\partial \tau} - A\phi_\eta^{(1)}\frac{\partial \phi_\eta^{(1)}}{\partial \eta} - B\frac{\partial^3 \phi_\eta^{(1)}}{\partial \eta^3} = 0. \qquad (4.21)$$

Equations (4.20) and (4.21) dictate two- sided traveling wave KdV equations in the considered frame of references ξ and η, respectively. Moreover, the third and fourth terms in the right side of Eq. (4.19) may become secular on the next higher order and yield the following equations, respectively:

$$\frac{\partial P_0}{\partial \eta} = D\phi_{\eta}^{(1)}, \tag{4.22}$$

$$\frac{\partial Q_0}{\partial \xi} = D\phi_{\xi}^{(1)}, \tag{4.23}$$

where,

$$D = \left[\frac{C_2 V^2}{2} - \frac{1}{4V^2}\right]. \tag{4.24}$$

The leading phase functions $P_0(\eta, \tau)$ and $Q_0(\xi, \tau)$ can be obtained by solving Eqs.(4.22) and (4.23) with the help of analytical solutions of the KdV equations (4.20) and (4.21).

4.3 Soliton solutions and phase shifts

4.3.1 Soliton solutions via Hirota bilinear method

The Hirota bilinear method [49] is employed to construct the single- and multi-soliton solutions of the KdV equations (4.20) and (4.21). By introducing the variable transform $\xi \to \xi B^{\frac{1}{3}}$, $\eta \to -\eta B^{\frac{1}{3}}$, $\phi_{\xi}^{(1)} \to 6\phi_{\xi}^{(1)} A^{-1} B^{\frac{1}{3}}$, and $\phi_{\eta}^{(1)} \to 6\phi_{\eta}^{(1)} A^{-1} B^{\frac{1}{3}}$ into Eqs. (4.20) and (4.21), one obtains

$$\frac{\partial u}{\partial \tau} + 6u\frac{\partial u}{\partial X} + \frac{\partial^3 u}{\partial X^3} = 0,$$

where u is used for $\phi_{\xi}^{(1)}$ and $\phi_{\eta}^{(1)}$, and X is used for ξ and η. Now, one can use the transformation $u = 2(lnf)_{XX}$ to reduce the above KdV equation into the Hirota bilinear form $(D_X D_\tau + D_X^4)(f.f) = 0$. The N-soliton is therefore obtained as $f_1 = \sum_{i=1}^{N} \exp(\theta_i)$, where $\theta_i = k_i X - \omega_i \tau$, k_i is the wave number, and ω_i is an arbitrary constant. Inserting $\phi_{\xi}^{(1)} = \exp(k_i X - \omega_i \tau)$ into the linear terms of the above KdV equation gives the dispersion relation $\omega_i = k_i^3$. Therefore, the single-soliton solutions of the KdV equations (4.20) and (4.21) considering $f = 1 + \exp(k_1 X - k_1^3 \tau)$ can be written, respectively, as

$$\phi_{\xi}^{(1)} = \frac{12B}{A}\frac{\partial^2}{\partial \xi^2}\left[\mathrm{In}\left\{1 + \exp\left(k_1 B^{-\frac{1}{3}}\xi - k_1^3 \tau\right)\right\}\right], \tag{4.25}$$

$$\phi_{\eta}^{(1)} = \frac{12B}{A}\frac{\partial^2}{\partial \eta^2}\left[\mathrm{In}\left\{1 + \exp\left(-k_1 B^{-\frac{1}{3}}\eta - k_1^3 \tau\right)\right\}\right]. \tag{4.26}$$

Again, double-soliton solutions of Eqs.(4.20) and (4.21) can be written, respectively, as

$$\phi_{\xi}^{(1)} = \frac{12B}{A}\frac{\partial^2}{\partial \xi^2}[\mathrm{In}\{1 + \exp(\vartheta_1) + \exp(\vartheta_2) + a_{12}\exp(\vartheta_1 + \vartheta_2)\}], \tag{4.27}$$

$$\phi_{\eta}^{(1)} = \frac{12B}{A}\frac{\partial^2}{\partial\eta^2}[\mathrm{In}\{1 + \exp(\Omega_1) + \exp(\Omega_2) + a_{12}\exp(\Omega_1 + \Omega_2)\}], \qquad (4.28)$$

where $\vartheta_i = k_i B^{-1/3}\xi - k_i^3\tau$, $\Omega_{\mathrm{i}} = -k_i B^{-1/3}\eta - k_i^3\tau$ and $a_{12} = (k_2 - k_1)^2/(k_2 + k_1)^2$ with $i = 1, 2$.

Finally, triple-soliton solutions of the Eqs.(4.20) and (4.21) can be written, respectively as

$$\begin{aligned}\phi_{\xi}^{(1)} = \frac{12B}{A}\frac{\partial^2}{\partial\xi^2}[\mathrm{In}\{1 &+ \exp(\vartheta_1) + \exp(\vartheta_2) + \exp(\vartheta_3) + a_{12}\exp(\vartheta_1 + \vartheta_2)\\ &+ a_{23}\exp(\vartheta_2 + \vartheta_3) + a_{13}\exp(\vartheta_1 + \vartheta_3)\\ &+ a_{123}\exp(\vartheta_1 + \vartheta_2 + \vartheta_3)\}], \qquad (4.29)\end{aligned}$$

$$\begin{aligned}\phi_{\eta}^{(1)} = \frac{12B}{A}\frac{\partial^2}{\partial\eta^2}[\mathrm{In}\{1 &+ \exp(\Omega_1) + \exp(\Omega_2) + \exp(\Omega_3) + a_{12}\exp(\Omega_1 + \Omega_2)\\ &+ a_{23}\exp(\Omega_2 + \Omega_3) + a_{13}\exp(\Omega_1 + \Omega_3)\\ &+ a_{123}\exp(\Omega_1 + \Omega_2 + \Omega_3)\}], \qquad (4.30)\end{aligned}$$

where $\vartheta_i = k_i B^{-1/3}\xi - k_i^3\tau$, $\Omega_{\mathrm{i}} = -k_i B^{-1/3}\eta - k_i^3\tau$, $i = 1 - 3$, $a_{12} = (k_1 - k_2)^2/(k_1 + k_2)^2$, $a_{23} = (k_2 - k_3)^2/(k_2 + k_3)^2$, $a_{13} = (k_1 - k_3)^2/(k_1 + k_3)^2$ and $a_{123} = a_{12}a_{23}a_{13}$.

4.3.2 Phase shifts

The phase shift can be determined after head-on single- as well multi-soliton collisions considering the soliton solutions of the two-sided KdV equations as follows:

Using Eqs.(4.25) and (4.26), Eqs. (4.22) and (4.23) can be converted to

$$\frac{\partial P_0}{\partial\eta} = \frac{12BD}{A}\frac{\partial^2}{\partial\eta^2}\left[\mathrm{In}\left\{1 + \exp\left(-k_1 B^{-1/3}\eta - k_1^3\tau\right)\right\}\right], \qquad (4.31)$$

$$\frac{\partial Q_0}{\partial\xi} = \frac{12BD}{A}\frac{\partial^2}{\partial\xi^2}\left[\mathrm{In}\left\{1 + \exp\left(k_1 B^{-1/3}\xi - k_1^3\tau\right)\right\}\right]. \qquad (4.32)$$

Solving Eqs. (4.31) and (4.32), the leading phase changes due to the collisions of two-sided solitary waves can be obtained as

$$P_0(\eta, \tau) = -\frac{12B^{2/3}Dk_1}{A}\frac{\exp\left(-k_1 B^{-1/3}\eta - k_1^3\tau\right)}{1 + \exp(-k_1 B^{-1/3}\eta - k_1^3\tau)}, \qquad (4.33)$$

$$Q_0(\xi,\tau)=\frac{12B^{2/3}Dk_1}{A}\frac{\exp\left(k_1B^{-\frac{1}{3}}\xi-k_1^3\tau\right)}{1+\exp\left(k_1B^{-\frac{1}{3}}\xi-k_1^3\tau\right)}. \quad (4.34)$$

The trajectories of two solitary waves for weak head-on collision can be written as

$$\xi=\varepsilon(x-Vt)-\varepsilon^2\frac{12B^{2/3}Dk_1}{A}\frac{\exp\left(-k_1B^{-1/3}\eta-k_1^3\tau\right)}{1+\exp(-k_1B^{-1/3}\eta-k_1^3\tau)}+\cdots, \quad (4.35)$$

$$\eta=\varepsilon(x+Vt)+\varepsilon^2\frac{12B^{2/3}Dk_1}{A}\frac{\exp\left(k_1B^{-\frac{1}{3}}\xi-k_1^3\tau\right)}{1+\exp\left(k_1B^{-\frac{1}{3}}\xi-k_1^3\tau\right)}+\cdots. \quad (4.36)$$

To evaluate the phase shifts after a head-on collision of the two solitons, one may consider the solitons, say, S_1 and S_2, are asymptotically far from each other at the initial time. After collision, S_1 is far to the right of S_2. Using the relation $\nabla P_0=\varepsilon(x-Vt)|_{\eta\to-\infty,\xi=0}-\varepsilon(x-Vt)|_{\eta\to\infty,\xi=0}$ and $\nabla Q_0=\varepsilon(x+Vt)|_{\xi\to-\infty,\eta=0}-\varepsilon(x+Vt)|_{\xi\to\infty,\eta=0}$, the corresponding phase shifts may be obtained as

$$\nabla P_0=-\varepsilon^2\frac{12B^{2/3}D}{A}k_1,\nabla Q_0=\varepsilon^2\frac{12B^{2/3}D}{A}k_1. \quad (4.37)$$

Again, using the double-soliton solutions of the KdV equations given by Eqs.(4.27) and (4.28) of the KdV equations, the solution of Eqs. (4.22) and (4.23) can be determined as

$$P_0=-\frac{12B^{2/3}D}{A}\frac{k_1\exp(\vartheta_1)+k_2\exp(\vartheta_2)+a_{12}(k_1+k_2)\exp(\vartheta_1+\vartheta_2)}{1+\exp(\vartheta_1)+\exp(\vartheta_2)+a_{12}\exp(\vartheta_1+\vartheta_2)}, \quad (4.38)$$

$$Q_0=\frac{12B^{2/3}D}{A}\frac{k_1\exp(\Omega_1)+k_2\exp(\Omega_2)+a_{12}(k_1+k_2)\exp(\Omega_1+\Omega_2)}{1+\exp(\Omega_1)+\exp(\Omega_2)+a_{12}\exp(\Omega_1+\Omega_2)}, \quad (4.39)$$

and the corresponding phase shifts may be obtained as

$$\nabla P_0=-\varepsilon^2\frac{12B^{2/3}D}{A}\sum_{i=1}^{2}k_i,\quad \nabla Q_0=\varepsilon^2\frac{12B^{2/3}D}{A}\sum_{i=1}^{2}k_i. \quad (4.40)$$

Finally, the phase shifts after head-on collisions between two-sided triple-solitons, given by Eqs. (4.29) and (4.30), may be evaluated as

$$\nabla P_0=-\varepsilon^2\frac{12B^{2/3}D}{A}\sum_{i=1}^{3}k_i,\qquad \nabla Q_0=\varepsilon^2\frac{12B^{2/3}D}{A}\sum_{i=1}^{3}k_i. \quad (4.41)$$

The interactions among the dust acoustic solitons and their corresponding phase shifts on plasma parameters are discussed in section 4.4.

4.4 Results and discussion

The head-on collision phenomena among the dust acoustic solitons and their corresponding phase shifts have been investigated by deriving two-sided KdV equations involving nonlinearity (A) and dispersion (B) cofficients with the ePLK method for a dusty plasma as mentioned earlier. The coefficients A and B strongly depend on the plasma parameters $\sigma_1 = T_{i1}/T_{i2}$, $\sigma_2 = T_{i1}/T_e$, $\mu_{i1} = n_{i10}/Z_d n_{d0}$, $\mu_{i2} = n_{i20}/Z_d n_{d0}$, β_{i1}, and β_{i2}.It is seen that the compressive and rarefactive dust acoustic solitons may exist when $A > 0$ and $A < 0$, respectively. Besides, the phase shifts may become either positive or negative due to the head-on collision between the solitons which are independent of the wave mode. For instance, Ghosh et al. [22] have noted that the positive or negative phase shift does not depend on the type of wave mode, but depends on the co-efficient D in Eq. (4.24). Furthermore, Han et al.[26], Xue [32], and Liang et al.[50] have mentioned that the colliding acoustic waves produce positive phase shift, while El-Labany et al. [27] have illustrated that the colliding dust acoustic solitary waves produce negative phase shift; both of these phases are shifted in the direction of propagation. It is found that the positive phase shifts are obtained only if $A > 0$ and $D < 0$, otherwise negative. The parametric effects considering the typical data of Refs.18, 40, and 41 on the head-on collisions among the electrostatic dust acoustic single- and multi-solitons and their corresponding phase shifts are discussed.

Figures 4.1(a)-4.1(c) show the effects on phase shift ∇P_0 for the interaction between the two equal amplitude single- solitons propagating toward each other with respect to μ_{i1} and μ_{i2}, σ_1 and σ_2, and β_{i1} and β_{i2}, respectively, taking the remaining parameters constant. On the other hand, Figs. 4.2(a)-4.2(c) show the changes of phase shifts ∇P_0 for the interaction between the equal amplitude double-solitons propagating toward each other with respect to μ_{i1} and μ_{i2}, σ_1 and σ_2, and β_{i1} and β_{i2}, respectively, considering the same values as in Fig.4.1 except the wave numbers $k_1 = 1$ and $k_2 = 2$. It is seen that the phase shifts due to the interaction of two-sided single- and multi-solitons are strongly dependent on the plasma parameters and the

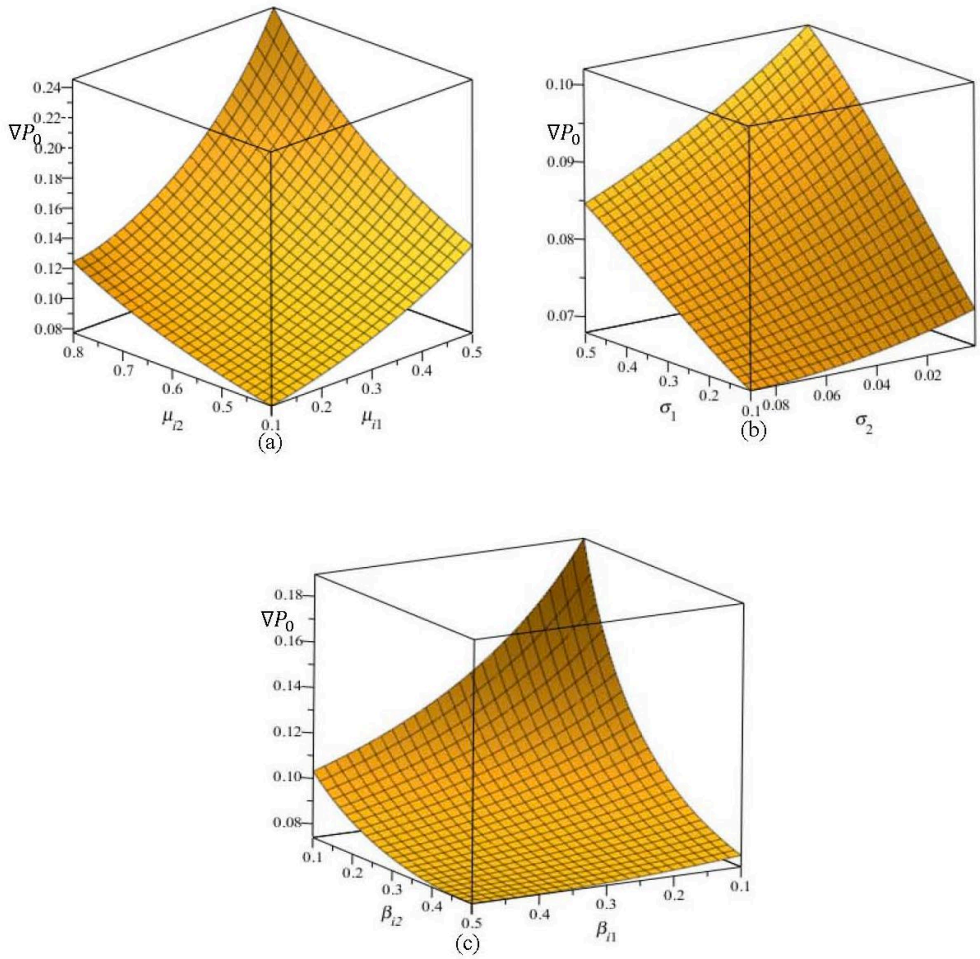

Figure 4.1 Influence on phase shifts due to head-on collision for single-soliton (a) μ_{i1} and μ_{i2} taking $\sigma_1 = 0.3$, $\sigma_2 = 0.01$, and $\beta_{i1} = \beta_{i2} = 0.5$, (b) σ_1 and σ_2 taking $\mu_{i1} = 0.2$, $\mu_{i2} = 0.41$, and $\beta_{i1} = \beta_{i2} = 0.5$, , and (c) β_{i1} and β_{i2} taking $\sigma_1 = 0.5$, $\sigma_2 = 0.1$, $\mu_{i1} = 0.1$, and $\mu_{i2} = 0.41$.

wave numbers, and are increasing with increasing μ_{i1}, μ_{i2},and σ_1, and are decreasing with increasing σ_2, β_{i1}, and β_{i2}. Figures 4.1 and 4.2 obviously indicate that the inertialess electrons and two-temperature nonthermal ions significantly contribute to the restoring force with increasing the temperature and number density of cold ions, but decreasing with the temperature of electrons due to the electrostatic interaction of producing dust acoustic solitons for extremely massive negatively charged mobile dust. This physical phenomenon provides that the time delay is increasing with increasing restoring force. On the other hand, the population of two-temperature nonthermal ions significantly affects the phase shifts in which the changes of phase shifts are decreasing. This phenomenon indicates that the cold and hot ions interact more actively with the other plasma species, causing the reduction in the

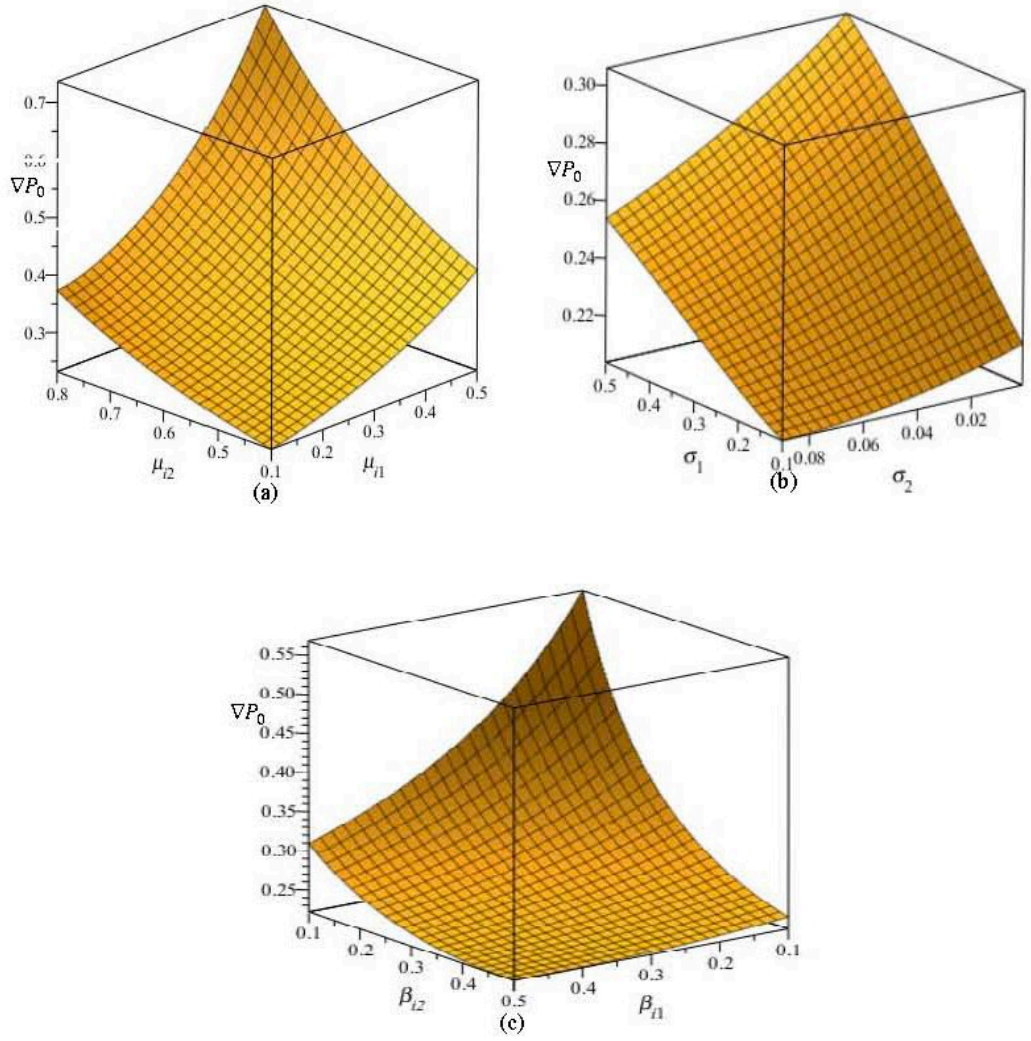

Figure 4.2 Influence on phase shifts due to head-on collision for double-soliton (a) μ_{i1} and μ_{i2}, (b) σ_1 and σ_2, and (c) β_{i1} and β_{i2} considering typical values as of Fig.4.1.

magnitude of phase shift. It is also found that the phase shifts for head-on collision for multi-solitons are higher rather than single-solitons due to increase of wave numbers.

Figures 4.3(a)-4.3(d) display the electrostatic potential (ϕ) structures consisting of $\phi_{\xi}^{(1)}$ and $\phi_{\eta}^{(1)}$ approaching toward each other for single-soliton as obtained from Eqs. (4.25) and (4.26) against ξ and η, considering the different values of the plasma parameters and time τ. It is seen that the amplitudes of the colliding dust acoustic solitary waves are increasing with the increase of μ_{i1}, μ_{i2}, and σ_1, and are decreasing with the increase of σ_2; hence the nonlinear

coefficients A is proportional to σ_2, but it is inversely proportional to μ_{i1}, μ_{i2}, and σ_1. Further, Fig. 4.3(d) is the mirror image of Fig. 4.3(b) as is expected. It is also seen from Fig. 4.3(a)

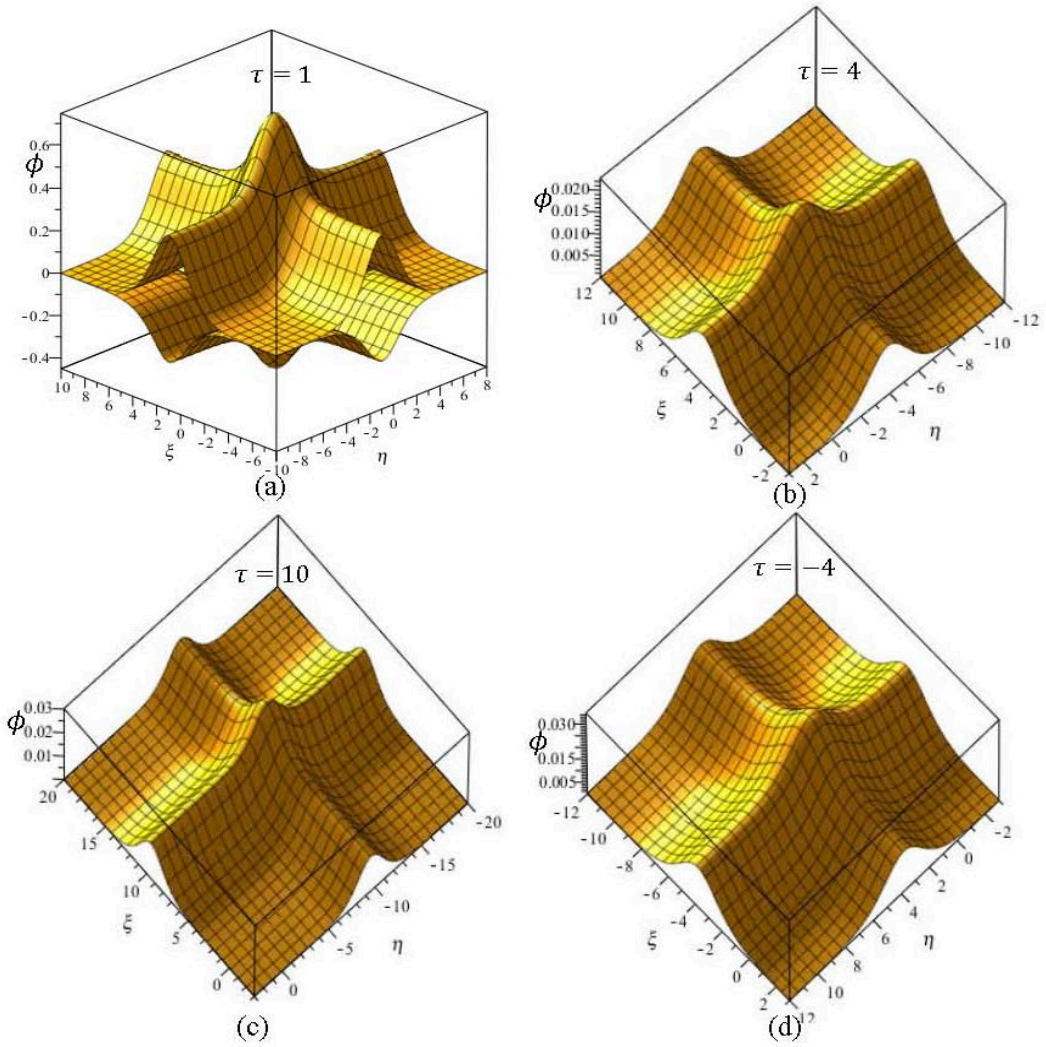

Figure 4.3 Electrostatic potential (ϕ) profiles single-soliton traveling toward right $\left(\phi_{\xi}^{(1)}\right)$ and left $\left(\phi_{\xi}^{(1)}\right)$ due to head-on collisions taking (a) $\mu_{i1} = 0.5$ (compressive), $\mu_{i1} = 0.6$ (rarefactive), $\mu_{i2} = 0.41$ $\sigma_1 = 0.2$, $\sigma_2 = 0.05$,and $\beta_{i1} = \beta_{i2} = 0.3$, (b) $\mu_{i1} = 0.2$, $\mu_{i2} = 0.41$, $\sigma_1 = 0.1$, $\sigma_2 = 0.05$, and $\beta_{i1} = \beta_{i2} = 0.3$, (c) as of (b) but $\sigma_2 = 0.01$, and (d) as of (c) but $\mu_{i2} = 0.5$.

that the compressive and rarefactive potential structures are found for $\mu_{i1} < 0.5$ and $\mu_{i1} > 0.5$, respectively, due to the interaction between two-solitons which are in good agreement with the investigations of Ref.42. Figures 4.4(a)-4.4(d) display the electrostatic potential (ϕ) structures consisting of $\phi_{\xi}^{(1)}$ and $\phi_{\eta}^{(1)}$ traveling toward each other for double-solitons as obtained from Eqs. (4.27) and (4.28) against ξ and η, respectively, taking the different values

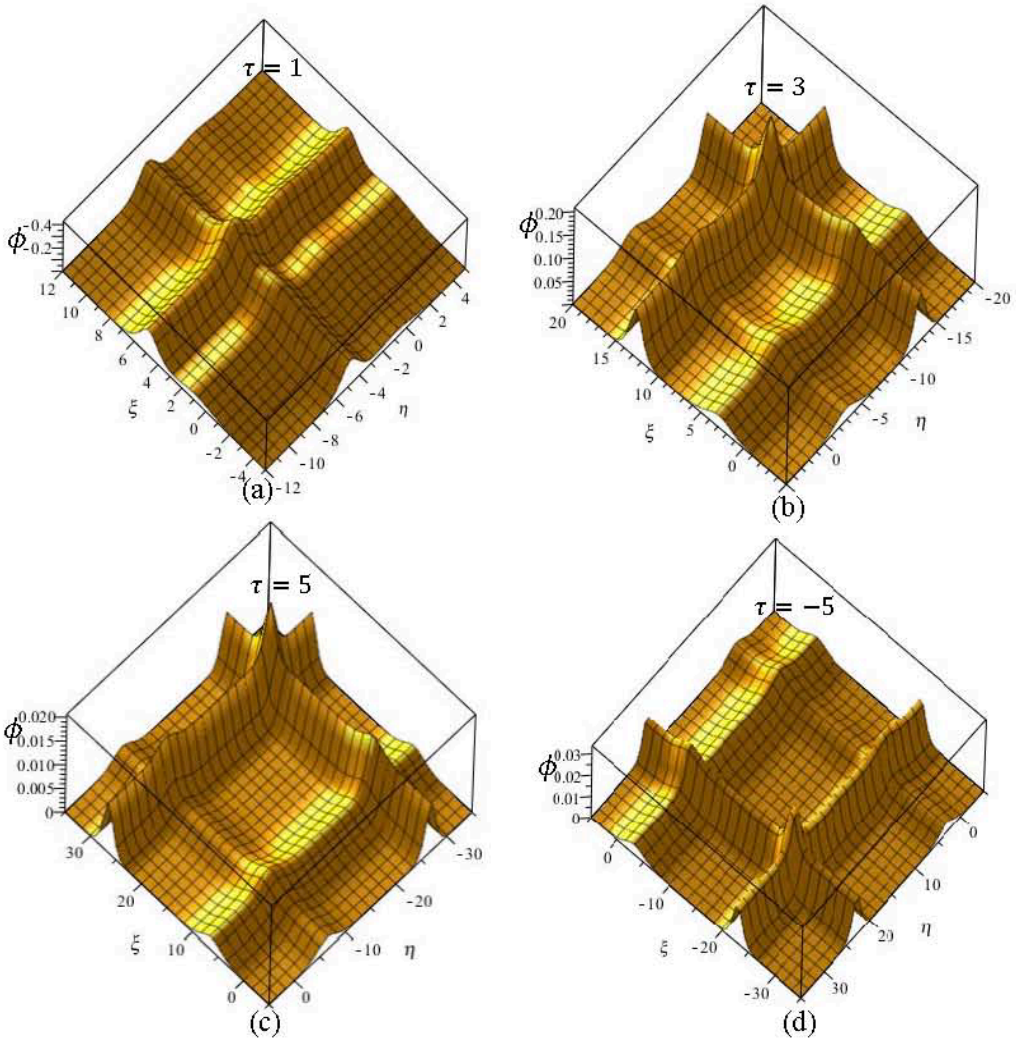

Figure 4.4 Electrostatic potential (ϕ) profiles of double-soliton traveling toward right $\left(\phi_{\xi}^{(1)}\right)$ and left $\left(\phi_{\eta}^{(1)}\right)$ due to head-on collisions taking (a) $\mu_{i1} = 0.78$, $\mu_{i2} = 0.41$ $\sigma_1 = 0.5$, $\sigma_2 = 0.05$,and $\beta_{i1} = \beta_{i2} = 0.3$, (b) as of (a) except $\mu_{i1} = 0.1$, (c) $\mu_{i1} = 0.1$, $\mu_{i2} = 0.41$, $\sigma_1 = 0.1$, $\sigma_2 = 0.05$, and $\beta_{i1} = \beta_{i2} = 0.3$, and (d) as of (b) except $\sigma_2 = 0.01$.

of the plasma parameters and time τ. It is seen that the amplitude of dust acoustic double-solitons is increasing with the increase of μ_{i1}, μ_{i2}, and σ_1, and is decreasing with the increase of σ_2. Figures 4.4(a)-4.4(d) clearly dictate that the four compressive and rarefactive scattered solitons are produced due to head-on collisions of double-solitons, of which of two are propagating from left to right and remaining two are propagating in the opposite direction. Figures 4.5(a)-4.5(d) display the electrostatic potential (ϕ) structures consisting of $\phi_{\xi}^{(1)}$ and $\phi_{\eta}^{(1)}$ traveling toward each other for triple-soliton as obtained from Eqs. (4.29) and (4.30) against ξ and η, respectively, considering different values of the plasma parameters and τ. It

is also seen that the amplitudes of dust acoustic solitary waves are increasing with the increase of μ_{i1}, μ_{i2}, and σ_1, and are decreasing with the increase of σ_2. Figures 4.5(a)-4.5(d) show that the compressive and rarefactive six scattered solitons are produced due to head-on collisions of triple-soliton, of which three are propagating from left to right and the remaining three are

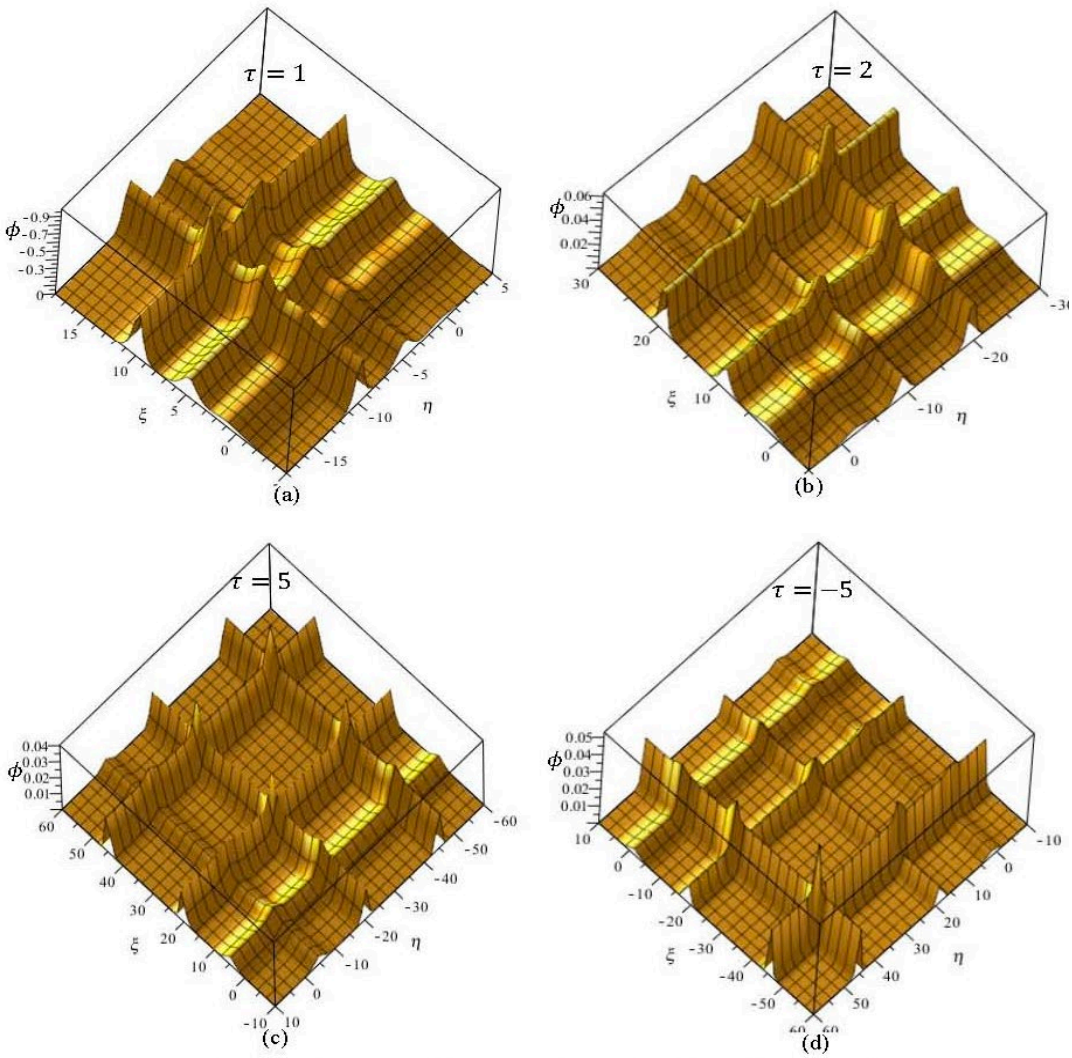

Figure 4.5 Electrostatic potential (ϕ) profiles of triple-soliton traveling toward right $\left(\phi_{\xi}^{(1)}\right)$ and left $\left(\phi_{\xi}^{(1)}\right)$ due to head-on collisions (a) $\mu_{i1} = 0.78$, $\mu_{i2} = 0.41$ $\sigma_1 = 0.5$, $\sigma_2 = 0.05$, and $\beta_{i1} = \beta_{i2} = 0.3$, (b) $\mu_{i1} = 0.1$, $\mu_{i2} = 0.41$, $\sigma_1 = 0.1$, $\sigma_2 = 0.05$, and $\beta_{i1} = \beta_{i2} = 0.3$, (c) as of (b) but $\beta_{i1} = 0.25$, and (d) as of (b) but $\mu_{i2} = 0.31$.

propagating in the opposite direction. It is observed from Figs.4.3-4.5 that the amplitudes of dust acoustic solitons are increasing with increasing β_{i1} and T_{i1}, which provide that the nonextensive cold ions contribute significantly to the restoring force and then the restoring

force increases due to the interactions among the extremely massive mobile dust and inertialess electrons as mentioned earlier. However, the nonthermal hot ions interact more actively with the remaining plasma species, causing a reduction in magnitudes of the dust acoustic solitons with the increase of β_{i2}. This means that the increase in concentrations of cold and hot ions can be interpreted due to the depopulation of extremely massive negative mobile dusts from the plasma system, and as a result the resulting force, as provided by the inertial mass of the dust particles, of dust acoustic waves decreases. Finally, Figs. 4.6 (a)-4.6(c) show the contour plot for better visualization of the variation of electrostatic potential profiles with respect to space and time for the head-on collisions among the single-,double-,and triple-solitons, respectively, considering $\mu_{i1} = 0.1$, $\mu_{i2} = 0.41$, $\sigma_1 = 0.5$, $\sigma_2 = 0.05$, $\beta_{i1} = 0.3$,and $\beta_{i2} = 0.3$.

This work concerns the electrostatic resonance phenomena of dust acoustic solitons, time evolution, and their phase shifts, taking the plasma parameters $n_{d0} = 1 \times 10^{10}\mathrm{m}^{-3}$, $n_{i20} = 7 \times 10^{13}\mathrm{m}^{-3}$, $T_{i2} = 0.3\mathrm{eV}$, $T_{i1} = 0.01 - 0.1\mathrm{eV}$, and $Z_d = 3 \times 10^3$ into account as obtained in Ref. 19 by deriving the analytical soliton solutions of the two-sided KdV equations (4.20) and (4.21). The results show that the compressive and rarefactive scattered dust acoustic solitons are produced for $A > 0$ and $A < 0$, respectively, but no soliton is observed for $A = 0$. Besides, the phase shifts combine to yield a single composite structure after the interaction among the solitons, and they propagate along the trajectories which deviate from the initial trajectories. The sum of the phase shifts is zero for oppositely propagating solitons. It is clearly seen that the estimated phase shifts, as mentioned in Eqs. (4.37), (4.40), and (4.41), satisfy the phase conservation law, that is $\nabla P_0 + \nabla Q_0 = 0$ for both compressive and rarefactive scattered dust acoustic solitons. Furthermore, many authors [22-28, 50] have investigated the phase shifts between two scattered solitons which are only valid for $A > 0$. It is to be noted that the phase shifts estimated of the scattered dust acoustic two-, four-, and six-solitons are valid both for $A > 0$ and $A < 0$. It is also seen from Figs. 4.3-4.5 that the potential profiles $\phi_{\xi}^{(1)}(\xi, \tau)$ of the solitons are shifted towards the right, while the other $\phi_{\eta}^{(1)}(\eta, \tau)$ are shifted towards the left directions with increasing time τ. This means that the dust acoustic scattered solitons propagate toward each other, collide, and then depart, which are in good agreement with the theoretical findings of Harvey et al.[35]. It is also observed that the multi-soliton solutions of the evolution equations provide that the taller (and faster) solitons overtake the smaller (and slower) one, with nonlinearity during the interaction phase.

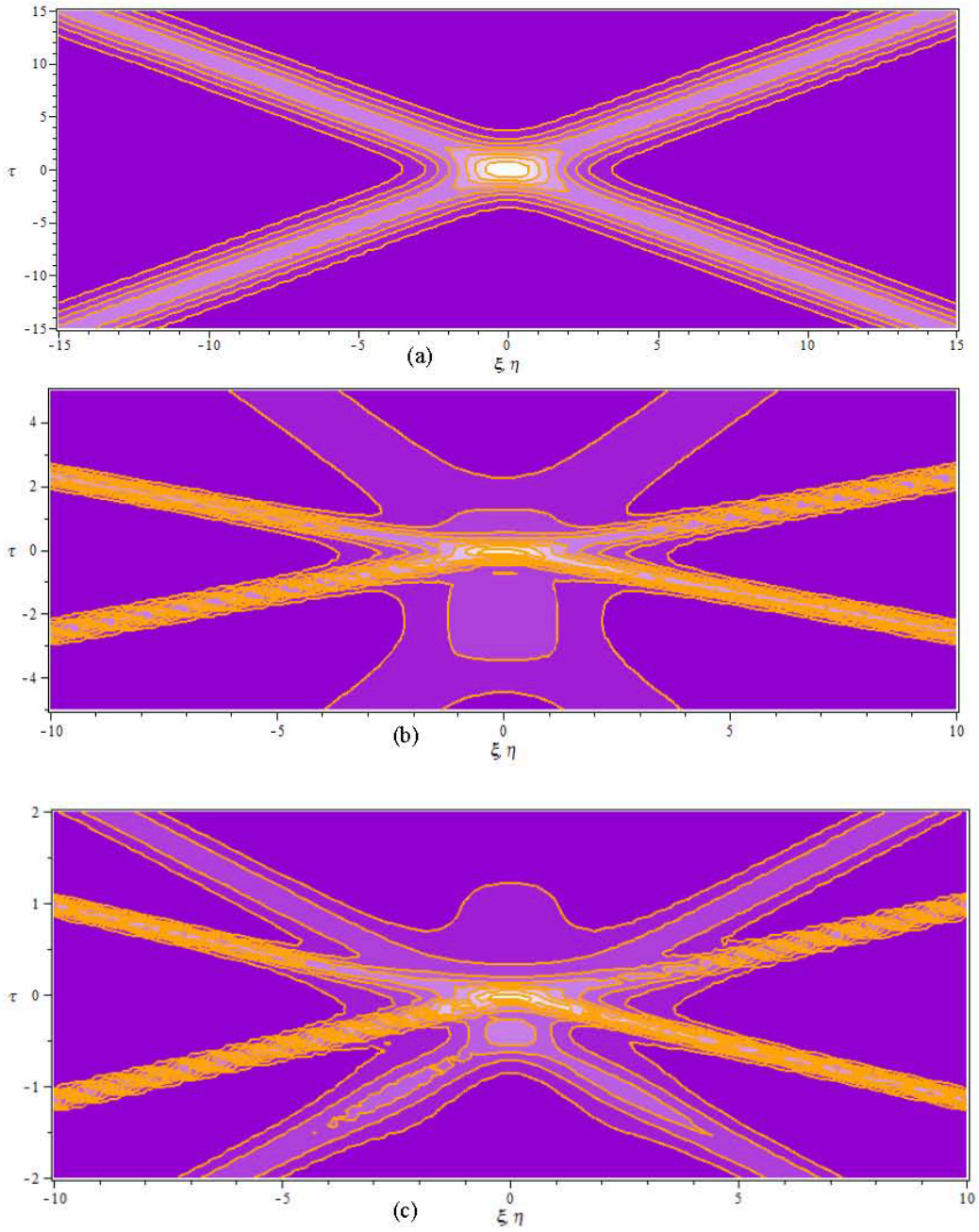

Figure 4.6 Contour plot of electrostatic potential (ϕ) due to head-on collisions among (a) single-soliton, (b) double-soliton, and (c) triple-soliton with respect to space and time taking $\mu_{i1} = 0.1$, $\mu_{i2} = 0.41$, $\sigma_1 = 0.5$, $\sigma_2 = 0.05$, and $\beta_{i1} = \beta_{i2} = 0.3$.

Thus, the results obtained may be useful for better understanding the electrostatic resonances and phase shifts due to interactions of nonlinear waves in various cosmic dust-laden plasma [18,40-43] as well as in laboratory dusty plasmas [19,35].

4.5 Conclusions

The paper is concerned with the study of the propagation characteristics due to the interactions among the dust acoustic solitons composed of negatively charged mobile dust, Boltzmann-distributed electrons, and two-temperature nonthermal cold and hot ions, occupying two different regions of velocity phase space. The KdV equations are derived using the ePLK method. The analytical solutions for solitons are constructed using the well established Hirota bilinear method. The phase shifts due to head-on collisions among the dust acoustic single-, double-, and triple-solitons are determined analytically from the solutions of the two-sided KdV equations. The effects of plasma parameters on the head-on collisions among the electrostatic dust acoustic single-and multi-solitons and their corresponding phase shifts are discussed. The compressive and rarefactive scattered two-, four-, and six- dust acoustic waves are obtained for $A > 0$ and $A < 0$, respectively. The phase shifts due to head-on collision of dust acoustic single- and multi-solitons are strongly dependent on the plasma parameters and the wave numbers, are increasing with increasing μ_{i1}, μ_{i2}, σ_1, and q , and are decreasing with the increase of σ_2, and β . One may conclude that the results obtained in this investigation might be useful for understanding electrostatic resonance disturbances and phase shifts after weak head-on collision among the solitons in space and laboratory plasma systems, such as Saturn's E-ring, Saturn's F-ring, noctilucent clouds, Halley's comet, interstellar molecular clouds in cosmic dust laden plasma, laboratory dusty plasmas, etc., where major plasma species are negatively charged massive mobile dust, Boltzmann distributed electrons, and two-temperature ions following the nonthermal distributions. This work is done to study the interaction of dust acoustic solitons and their corresponding phase shift (time delay) through the two-sided KdV equations. The quadratic nonlinearity of the KdV equations may disappear for a certain critical value; in such case, one may study the interactions among solitons using modified KdV equations.

References

1. P. K. Shukla and A. A. Mamun, Introduction to Dusty Plasma Physics (IOP, Bristol, 2002).
2. P. K. Shukla, Phys. Plasmas **8,** 1791 (2001).
3. D. A. Mendis and M. Rosenberg, Annu. Rev. Astron. Astrophys. **32,** 419 (1994).
4. F. Verheest, Waves in Dusty Plasmas (Kluwer, Dordrecht, 2000).
5. N. N. Rao, P. K. Shukla, and M. Y. Yu, Planet. Space Sci. **38,** 543 (1990).
6. A. Barkan, R. L. Merlino, and N. D'Angelo, Phys. Plasmas **2,** 3563 (1995).
7. J. T. Mendonc¸a, N. N. Rao, and A. Guerreiro, Euro-Phys. Lett. **54,**741(2001).
8. Y. Nakamura, H. Bailung, and P. K. Shukla, Phys. Rev. Lett. **83,** 1602 (1999).
9. A. A. Mamun, R. A. Cairns, and P. K. Shukla, Phys. Plasmas **3,** 702 (1996).
10. A. A. Mamun, Astrophys. Space Sci. **260,** 507 (1998).
11. A. A. Mamun, S. M. Russel, C. A. M. Briceno, M. N. Alam, T. K. Datta, and A. K. Das, Planet. Space Sci. **48,** 599 (2000).
12. C. A. Mendoza-Briceno, S. M. Russel, and A. A. Mamun, Planet. Space Sci. **48,** 599 (2000).
13. W. S. Duan, H. Y. Wang, and P. John, Commun. Theor. Phys. **45,** 1112 (2006).
14. M. M. Lin and W. S. Duan, Chaos Solitons Fractals **33,** 1189 (2007).
15. H. Y. Wang and K. B. Zhang, Can. J. Phys. **86,** 1381 (2008).
16. M. Tribeche and A. Merriche, Phys. Plasmas **18,** 034502 (2011) .
17. Sahu and M. Tribeche, Astrophys. Space Sci.**338,** 259 (2012) .
18. I. Tasnim, M. M. Masud, and A. A. Mamun, Plasma Phys. Rep. **40,** 723 (2014).
19. P. Bandyopadhyay, G. Prasad, A. Sen, and P. K. Kaw, Phys. Rev. Lett. **101,** 065006 (2008)
20. G. Mandal, K. Roy, A. Paul, A. Saha, and P. Chatterjee, Z. Naturforsch. **70,** 703 (2015).
21. K. E. Lonngren, Opt. Quantum Electron. **30,** 615 (1998).
22. U. N. Ghosh, K. Roy, and P. Chatterjee, Phys. Plasmas **18,** 103703 (2011).
23. S. Parveen, S. Mahmood, M. Adnan, and A. Qamar, Phys. Plasmas **23,** 092122 (2016).
24. K. Roy, M. K. Ghorui, P. Chatterjee, and M. Tribeche, Commun. Theor. Phys. **65,** 237 (2016).
25. N. S. Saini, and K. Singh, Phys. Plasmas **23,** 103701 (2016).
26. J. N. Han, S. L. Du, and W. S. Duan, Phys. Plasmas **15,** 112104 (2008).
27. S. K. El-Labany, E. F. El-Shamy, R. Sabry, and M. Shokry, Astrophys. Space Sci.**325,** 201 (2010).
28. A. Saha and P. Chatterjee, Astrophys. Space Sci. **353,** 169 (2014).
29. C. H. Su and R. M. Miura, J. Fluid Mech. **98,** 509 (1980).

30. C. S. Gardner, J. M. Greener, M. D. Kruskal, and R. M. Miura, Phys. Rev. Lett. **19,** 1095 (1967).
31. N. J. Zabusky and M. D. Kruskal, Phys. Rev. Lett. **15,** 240 (1965).
32. J. K. Xue, Phys. Rev. E **69,** 016403 (2004).
33. M. Van Dyke, Perturbation Methods in Fluid Mechanics, 2nd ed. (Parabolic, Stanford, CA, (1975), 108–112.
34. F. Verheest, M. A. Hellberg, and W. A. Hereman, Phys. Plasmas **19,** 092302 (2012)
35. P. Harvey, C. Durniak, D. Samsonov, and G. Morfill, Phys. Rev. E **81,** 057401 (2010).
36. B. Xie, K. He, and Z. Huang, Phys. Plasmas **6,** 3808 (1999).
37. R. Lundin, A. Zakharov, R. Pellinen, H. Borg, B. Hultqvist, N. Pissarenko, E. M. Dubinin, S. W. Barabash, I. Leide, and H. Koskinen, Nature **341,** 609 (1989).
38. Y. Futaana, S. Machida, Y. Saito, A. Matsuoka, and H. Hayakawa, J. Geophys. Res. **108,** 1025 (2003).
39. S. G. Tagare, S. V. Singh, R. V. Reddy, and G. S. Lakhina, Nonlinear Processes Geophys. **11,** 215 (2004).
40. K. B. Zhang and H. Y. Wang, J. Korean Phys. Soc. **55,** 1461 (2009).
41. I. Tasnim, M. M. Masud, M. Asaduzzaman, and A. A. Mamun, Chaos **23,** 013147 (2013).
42. S. Imada, H. Hara, and T. Watanabe, Astrophys. J. Lett.**705,** L208 (2009).
43. W. M. Moslem, Chaos Solitons Fractals **23,** 939 (2005).
44. I. Tasnim, M. M. Masud, and A. A. Mamun, Astrophys. Space Sci. **343,** 647 (2013).
45. D. Dorranian and A. Sabetkar, Phys. Plasmas **19,** 013702 (2012).
46. M. Y. Yu and H. Luo, Phys. Plasmas **15,** 024504 (2008).
47. A. A. Abid, M. Z. Khan, Quanming Lu, and S. L. Yap, Phys. Plasmas **24,** 033702 (2017).
48. R. A. Cairns, A. A. Mamun, R. Bingham, R. O. Dendy, R. Bostrom, C. M. C. Nairn, and P. K. Shukla, Geophys. Res. Lett. **22,** 2709 (1995).
49. R. Hirota, The Direct Method in the Soliton Theory (Cambridge University Press, Cambridge, 2004).
50. G. Z. Liang, J. N. Han, M. M. Lin, J. N. Wei, and W. S. Duan, Phys. Plasmas **16,** 073705(2009).

Abbreviation and Nomenclature:

KdV= Korteweg-de Vries

mKdV = modify Korteweg-de Vries

ePLK = extended Poincaré-Lighthill-Kuo

SG = standard Gardner

T_ω = time period

$T_{c\omega}$ = dust charging time period

T_i = ion temperature

Z_d = duat charge number

σ_1 = temperature ratio of cold ion to hot ion temperature

σ_{21} = temperature ratio of cold ion to electron temperature

μ_{i1} = density ratio of unperturbed cold ion to dust density

μ_{i2} = density ratio of unperturbed hot ion to dust density

$n_{i1}(n_{i2})$ = concentration of cold (hot) ion

$T_{i1}(T_{i2})$ = temperature of cold (hot) ion

$\alpha_{i1}(\alpha_{i2})$ = population of cold (hot) ion

n_{i1} (n_{i2}) = density of cold (hot) ion

$\beta_{i1}(\beta_{i2})$ = nonthermality of cold (hot) ion

n_d = density of dust ion

u_d = speed of dust fluid

C_d = dust acoustic speed

e = electronic charge

ϕ = electrostatic potential

T_{eff} = effective ion temperature

k_B= Boltzmann constant

m_d = dust mass

ε = small parameter, measure the strength of nonlinearity

k_i= wave number, $i = 1,2,3$

ω_i = angular velocity

A = coefficient of nonlinearity in KdV equation

B = coefficient of dispersion in KdV equation

$\nabla P_0(\nabla Q_0)$ = phase shift of right (left) moving soliton

Chapter 5

Head-on collision of ion acoustic shock waves in electron-positron-ion nonextensive plasmas for weakly and highly relativistic regimes

5.1 Introduction

Electron-positron (ep) plasmas are observed in astrophysical environments such as in the polar region of neutron stars [1], pulsar magnetospheres [2], active galactic nuclei [3], at the center of Milky Way galaxy [4], in the early universe [5], accretion disk [6] and black holes [7], and in the laboratory as in the intense laser fields [8]. Such plasmas are produced through pair production due to the high energy processes. Experimentally, it has established that at electron density of 10^{12} cm^{-3} and temperature as low as 1 eV, the positron annihilation time is greater than 1s [9]. Due to its longer life time, a numerous low frequency waves can be produced in the ep plasmas. Arons [10] has reported that the stochastic acceleration process generates the super-thermal/nonthermal tail on the thermal distribution of particles. In contrast, Livadiotis and McComas [11] have reported that Tsallis statistical mechanics is more suitable for describing superthermal tails in astrophysical and space plasmas. Since most of the astrophysical plasmas [12-13] contain positrons along with ions and electrons, and they form electron-position-ion (epi) plasmas. Besides, the Advanced Satellite for Cosmology and Astrophysics (ASCA) satellite [14] has observed the existence a fraction of ions in astrophysical ep plasmas. In addition, the pulsar relativistic wind is produced with electrons and positrons, and a small fraction of energetic ions. It is reasonable to model high-energy (non-thermal/super-thermal) electrons and positrons with the nonextensive distribution. The pulsar relativistic wind is one of the examples where relativistic ions exist. Several authors [15-19] have reported that the ion acoustic waves in relativistic plasmas exist due to simultaneous appearance of ep plasmas with relativistic ions. It is noted that the epi relativistic plasmas is also the well established phenomenon in pulsar magnetosphere and laser–plasma interaction [10, 20-22]. Pakzad *et al*. [23-24], Tribeche *et al*. [25], and Munoz [26] have already mentioned that the ion acoustic waves exist in epi plasma simultaneously with nonextensive and relativistic effects.

It was observed experimentally that the plasma particles attain relativistic speeds [27-28] due to the interaction with ultra-intense laser pulses. It is evident [29] that the excitations of nonlinear structures such as shock and solitary waves are produced for the high-speed streaming ions, electrons, and positrons. Moreover, the epi relativistic plasmas plays crucial role in the formation of ion acoustic shocks which are concerned in space environments [30], Van Allen radiation belts [31], and plasma sheet boundary layer of Earth's magnetosphere. Therefore, it is reasonable to consider that the relativistic effects in such plasmas prevail as the particles having streaming velocities approach to the velocity of light. A number of authors have investigated the nonlinear wave propagation in epi plasmas theoretically to explore the dynamic behaviors of double layers [15, 32] in astrophysical, cosmological [33], and laboratory plasmas [34]. The weakly relativistic effects of ions are considered [35] in the range 0.1–4.7MeV, and the highly relativistic effects are considered [35] in the range 4.7–100MeV that are frequently observed in astrophysical and space environments. Alam *et al*. [35] have reported that the effects of head-on collision between two solitary waves in epi nonthermal relativistic plasmas by deriving Korteweg-de-Vries (KdV) equations. In this report, we studied the effects of positron concentration, temperature ratios, relativistic streaming factor, and population of electron and positron nonthermality on the electrostatic resonance and their corresponding phase shifts. They found that the plasma parameters play a vital role to produce ion acoustic solitary waves. Considering the importance of the physical issues concerned, the characteristics ion acoustic waves for epi relativistic plasmas are investigated [16,32,36] taking two- and three-term expansions of the Lorentz relativistic factor for ions assuming different plasma conditions. It is established [17, 37] that the Lorentz relativistic factor for ions significantly modifies the ion acoustic wave dynamics in the e-p-i relativistic plasmas. Hafez et al. [37] have studied the oblique nonlinear propagation of ion acoustic shock waves in case of weakly and highly relativistic regimes (WRR/HRR) composed nonthermal electrons, positrons, and relativistic thermal ions. They have found that the nonthermal electrons and positrons significantly modify the structures of ion acoustic shock waves in epi plasmas in highly relativistic rather than in weakly relativistic regimes. Han et al. [38] have studied the head-on collision in dense epi quantum plasmas without considering the relativistic effects and found that the two colliding shocks change the plane of propagation after head-on collision. Thus, the relativistic effect plays a significant role in the propagation characteristics for the head-on collisions between the two ion acoustic shock waves. Taking into consideration, the key importance of the epi plasmas with nonextensive effects for long-range interaction, as observed in the interstellar medium while the cosmic-

rays interact with nuclei [39], astrophysics [40] etc., the head-on collision between the two ion acoustic shock waves propagating toward each other in weakly and highly relativistic plasmas consisting of relativistic ions, nonextensive electrons and positrons. Being motivated due to the significance of the above-mentioned physical issues concerned and to fill up the gap, the head-on collision of ion acoustic shock waves in epi nonextensive plasmas is investigated for weakly and highly relativistic regimes employing the extended Poincaré-Lighthill-Kuo (ePLK) method. In sequence of introduction, in section 5.2, the model equations for relativistic plasmas are presented. Derivations of two-sided KdV Burger (KdVB) equations along with ePLK technique are given in section 5.3. The solutions of shock wave are displayed in section 5.4. The results are discussed in section 5.5, and conclusion is drawn in section 5.6.

5.2 Theoretical model equations

Unmagnetized collisionless epi plasma is considered consisting of nonextensive electrons, positrons, and relativistic ions. The nonextensive distribution function for species α can be defined [41] as

$f_\alpha(v_\alpha) = C_{q\alpha}\left[1-(q_\alpha-1)\left(\frac{m_\alpha v_\alpha^2}{2k_BT_\alpha}+\frac{e_\alpha\Phi}{k_BT_\alpha}\right)\right]^{\frac{1}{q_\alpha-1}}$, with $C_{q\alpha} = n_{\alpha0}\frac{\Gamma\left(\frac{1}{1-q_\alpha}\right)}{\Gamma\left(\frac{1}{1-q_\alpha}-\frac{1}{2}\right)}\sqrt{\frac{m_\alpha(1-q_\alpha)}{2\pi k_BT_\alpha}}$ for $1 < q_\alpha < 1$ and $C_{q\alpha} = n_{\alpha0}\left(\frac{1+q_\alpha}{2}\right)\frac{\Gamma\left(\frac{1}{1-q_\alpha}+\frac{1}{2}\right)}{\Gamma\left(\frac{1}{1-q_\alpha}\right)}\sqrt{\frac{m_\alpha(1-q_\alpha)}{2\pi k_BT_\alpha}}$, for $q_\alpha > 1$, where $C_{q\alpha}$ and Γ are the normalization constant and Gamma function, respectively. Here, Φ, m_α, e_α, $n_{\alpha0}$, v_α, T_α and k_B , are the electrostatic potential, mass, charge, unperturbed particle density, velocity, and temperature of the species α, Boltzmann constant, respectively. $\alpha = i, e,$ and p are for ions, electrons, and positrons, respectively. It is noticed that the nonextensive velocity distribution function gives a thermal cutoff at the maximum velocities of the species considered as $v_{max} = \sqrt{\frac{2k_BT_\alpha}{m_\alpha}\left(\frac{e_\alpha\Phi}{k_BT_\alpha}+\frac{1}{q_\alpha-1}\right)}$. Using the relation $n_\alpha = \int_{-\infty}^{\infty} f_\alpha(v)dv$, for $1 < q_\alpha < 1$ and $n_\alpha = \int_{-v_{max}}^{v_{max}} f_\alpha(v)dv$ for $q_\alpha > 1$, the population of nonextensive electrons and positrons can be obtained [17] in the form $n_e = n_{e0}\left[1+(q_e-1)\frac{\Phi}{k_BT_e}\right]^{\frac{q_e+1}{2(q_e-1)}}$ and $n_p = \left[1+(q_p-1)\frac{\Phi}{k_BT_p}\right]^{\frac{q_p+1}{2(q_p-1)}}$ respectively. q_e and q_p indicate nonextensive parameters which characterize the degree of nonextensivity. For superthermality $-1 < q_{e,p} < 1$ and for subthermality $q_{e,p} > 1$ and in the limit $q_{e,p} \to 1$, the nonextensive velocity distribution function transforms into the

Maxwell-Boltzmann distribution. The normalized continuity and momentum equations which are governed by the nonlinear dynamics of ion acoustic shock waves as

$$\frac{\partial n_i}{\partial t}+\frac{\partial (n_i u_i)}{\partial x}=0, \tag{5.1}$$

and

$$\frac{\partial (\gamma u_i)}{\partial t}+u_i\frac{\partial (\gamma u_i)}{\partial x}+\frac{T_{ip}}{n_i}\frac{\partial n_i}{\partial x}+\frac{\partial \phi}{\partial x}=\eta_i\frac{\partial^2 u_i}{\partial x^2}, \tag{5.2}$$

where n_i, u_i, ϕ indicate the normalized ion number density, ion fluid velocity, and electrostatic potential, respectively. n_i, u_i, and ϕ are normalized as $n_i \to n_i/n_{e0}$, $u_i \to u_i/C_s$, and $\phi \to \phi e/k_B T_e$, with $C_s=\sqrt{k_B T_e/m_i}$. The temperature ratios are defined as $T_{ip}=T_i/T_p$ and $T_{ep}=T_e/T_p$. The space and time variables are normalized by electron Debye length $\lambda_{De}=(T_e/4\pi n_{e0}e^2)^{1/2}$ and $t=\omega_{pi}^{-1}=(m_i/4\pi n_{e0}e^2)^{1/2}$, respectively, where ω_{pi} is the ion plasma frequency. η_i is the viscosity coefficient of ions, normalized by $\eta_i=\lambda_{De}^2 m_i n_{i0}/\omega_{pi}^{-1}$. η_i is responsible for nonlinear shock wave propagation in the plasma. The kinematic viscosities of electrons and positrons are neglected because they are of the order of m_e/m_i. In the range of ion densities $3.9\times10^{28}<n_i(cm^{-3})<1.4\times10^{37}$, the annihilation effects of electrons and positrons can be neglected [42]. The Lorentz factor $\left(\gamma=1/\sqrt{1-u_i^2/c^2}\right)$ for weakly and highly relativistic effect are defined as $\gamma=1+u_i^2/2c^2$ and $=1+u_i^2/2c^2+3u_i^4/8c^4$, respectively, where c is the speed of light, $\gamma=1$ in the non-relativistic limit. The Poisson's equation in such plasma is defined as

$$\frac{\partial^2\phi}{\partial x^2}=n_e-n_p-n_i. \tag{5.3}$$

The normalized nonextensive electrons and positrons densities can be expanded as

$$n_e=\frac{1}{1-p}\left[1+\frac{q+1}{2}\phi+\frac{(q+1)(3-q)}{8}\phi^2+\cdots\cdots\right], \tag{5.4}$$

$$n_p=\frac{p}{1-p}\left[1-\frac{q+1}{2}T_{ep}\phi+\frac{(q+1)(3-q)}{8}T_{ep}^2\phi^2-\cdots\cdots\right], \tag{5.5}$$

where $p=n_{p0}/n_{e0}$ at equilibrium.

5.3 Derivation of two-sided KdV Burger equations

Initially the two shock waves at $t \to -\infty$ are asymptotically far apart and propagate toward each other. After some time, they collide and then depart from each other in the opposite direction. To study the interaction of two ion acoustic shock waves for WRR and HRR, one can consider the extended Poincare- Lighthill- Kuo (ePLK) method [43]. The independent variables ξ and η are expanded in light of the ePLK method as

$$\left.\begin{aligned} \xi &= \epsilon(x - \lambda_p t) + \epsilon^2 P_0(\eta, \tau) + \cdots\cdots\cdots\cdots\cdots\cdots\cdots\cdots \\ \eta &= \epsilon(x + \lambda_p t) + \epsilon^2 Q_0(\xi, \tau) + \cdots\cdots\cdots\cdots\cdots\cdots\cdots\cdots \\ \tau &= \epsilon^3 t \end{aligned}\right\}, \tag{5.6}$$

where ξ and η denote the trajectories of two shock waves traveling toward each other and λ_p is the unknown phase velocity of ion acoustic shock waves and the unknown phase function determined earlier. The dependent variables are expanded as

$$\left.\begin{aligned} n_i &= 1 + \epsilon^2 n_i^{(1)} + \epsilon^3 n_i^{(2)} + \epsilon^4 n_i^{(3)} + \cdots\cdots \\ u_i &= u_{i0} + \epsilon^2 u_i^{(1)} + \epsilon^3 u_i^{(2)} + \epsilon^4 u_i^{(3)} + \cdots\cdots \\ \phi &= \epsilon^2 \phi^{(1)} + \epsilon^3 \phi^{(2)} + \epsilon^4 \phi^{(3)} + \cdots\cdots \end{aligned}\right\}, \tag{5.7}$$

where ε is a small parameter characterizing the strength of nonlinearity. As the value of ion kinematic viscosity η_i infinitesimal be considered in many experimental situation, so we take $\eta_i = \varepsilon\eta_1$. Considering the stretched coordinates (5.6) one can obtain

$$\frac{\partial}{\partial t} = \varepsilon\lambda_p\left(\frac{\partial}{\partial\eta} - \frac{\partial}{\partial\xi}\right) + \varepsilon^3\lambda_p\left(\frac{\partial P_0}{\partial\eta}\frac{\partial}{\partial\xi} - \frac{\partial Q_0}{\partial\xi}\frac{\partial}{\partial\eta}\right) + \varepsilon^3\frac{\partial}{\partial\tau}, \tag{5.8}$$

$$\frac{\partial}{\partial x} = \varepsilon\left(\frac{\partial}{\partial\eta} + \frac{\partial}{\partial\xi}\right) + \varepsilon^3\left(\frac{\partial P_0}{\partial\eta}\frac{\partial}{\partial\xi} + \frac{\partial Q_0}{\partial\xi}\frac{\partial}{\partial\eta}\right). \tag{5.9}$$

Inserting the value of n_i , u_i , and ϕ from Eq.(5.7) into the Eqs. (5.1)-(5.3) and using Eq. (5.8) and Eq. (5.9), one can derive a set of partial differential equations (PDEs) in various powers of ε . The smallest power of ε gives

$$-(\lambda_p - u_{i0})\frac{\partial n_i^{(1)}}{\partial\xi} + (\lambda_p + u_{i0})\frac{\partial n_i^{(1)}}{\partial\eta} + \frac{\partial u_i^{(1)}}{\partial\xi} + \frac{\partial u_i^{(1)}}{\partial\eta} = 0, \tag{5.10}$$

$$-(\lambda_p - u_{i0})\gamma_1\frac{\partial u_i^{(1)}}{\partial\xi} + (\lambda_p + u_{i0})\gamma_1\frac{\partial u_i^{(1)}}{\partial\eta} + T_{ip}\frac{\partial n_i^{(1)}}{\partial\xi} + T_{ip}\frac{\partial n_i^{(1)}}{\partial\eta} + \frac{\partial\phi^{(1)}}{\partial\xi} + \frac{\partial\phi^{(1)}}{\partial\eta} = 0 \tag{5.11}$$

and

$$R_1\phi^{(1)} - n_i^{(1)} = 0. \tag{5.12}$$

Solving Eqs. (5.10)-(5.12) for n_i , u_i, and ϕ, one can obtain

$$\phi^{(1)} = \phi_\xi^{(1)}(\xi,\tau) + \phi_\eta^{(1)}(\eta,\tau)\,, \tag{5.13}$$

$$n_i^{(1)} = \frac{1}{\gamma_1\left(\lambda_p - u_{i0}\right)^2 - T_{ip}}\phi_\xi^{(1)}(\xi,\tau) + \frac{1}{\gamma_1\left(\lambda_p + u_{i0}\right)^2 - T_{ip}}\phi_\eta^{(1)}(\eta,\tau)\,, \tag{5.14}$$

$$u_i^{(1)} = \frac{\lambda_p - u_{i0}}{\gamma_1\left(\lambda_p - u_{i0}\right)^2 - T_{ip}}\phi_\xi^{(1)}(\xi,\tau) - \frac{\lambda_p + u_{i0}}{\gamma_1\left(\lambda_p + u_{i0}\right)^2 - T_{ip}}\phi_\eta^{(1)}(\eta,\tau), \tag{5.15}$$

and the phase velocity is

$$\lambda_p = \pm u_{i0} + \left\{\frac{T_{ip}}{\gamma_1} + \frac{1}{\gamma_1 R_1}\right\}^{1/2}, \tag{5.16}$$

where $R_1 = \frac{1+q}{2(1-p)} + \frac{p(q+1)T_{ip}}{2(1-p)}$, $\gamma_1 = 1 + \frac{3}{2}\beta^2$ and $\beta = \frac{u_{i0}}{c}$.

From Eq. (5.13) it is observed that two electrostatic shock waves may be obtained, one of which $\phi_\xi^{(1)}(\xi,\tau)$ travels from left to right and the other $\phi_\eta^{(1)}(\eta,\tau)$ travels from right to left.

For the next order of ε yields

$$\phi^{(2)} = \phi_\xi^{(2)}(\xi,\tau) + \phi_\eta^{(2)}(\eta,\tau)\,, \tag{5.17}$$

$$n_i^{(2)} = \frac{1}{\gamma_1\left(\lambda_p - u_{i0}\right)^2 - T_{ip}}\phi_\xi^{(2)}(\xi,\tau) + \frac{1}{\gamma_1\left(\lambda_p + u_{i0}\right)^2 - T_{ip}}\phi_\eta^{(2)}(\eta,\tau), \tag{5.18}$$

and

$$u_i^{(2)} = \frac{\lambda_p - u_{i0}}{\gamma_1\left(\lambda_p - u_{i0}\right)^2 - T_{ip}}\phi_\xi^{(2)}(\xi,\tau) - \frac{\lambda_p + u_{i0}}{\gamma_1\left(\lambda_p + u_{i0}\right)^2 - T_{ip}}\phi_\eta^{(2)}(\eta,\tau). \tag{5.19}$$

Finally, considering the next higher order of ε one can be obtained the following relation using Eqs. (5.13)- (5.16) into account

$$-2\lambda_p\left[\frac{1}{b_1+a_1(\lambda_p-u_{i0})}+\frac{1}{b_2+a_2(\lambda_p-u_{i0})}\right]u_i^{(3)}$$

$$=\int\left[\frac{\partial\phi_\xi^{(1)}}{\partial\tau}+A\phi_\xi^{(1)}\frac{\phi_\xi^{(1)}}{\partial\xi}+B\frac{\partial^3\phi_\xi^{(1)}}{\partial\xi^3}-C\frac{\partial^2\phi_\xi^{(1)}}{\partial\xi^2}\right]d\eta$$

$$+\int\left[\frac{\partial\phi_\eta^{(1)}}{\partial\tau}-A_1\phi_\eta^{(1)}\frac{\phi_\eta^{(1)}}{\partial\eta}-B_1\frac{\partial^3\phi_\eta^{(1)}}{\partial\eta^3}+C_1\frac{\partial^2\phi_\eta^{(1)}}{\partial\eta^2}\right]d\xi$$

$$-\iint\left[L\phi_\eta^{(1)}-M\frac{\partial P_0}{\partial\eta}\right]\frac{\partial^2\phi_\xi^{(1)}}{\partial\xi^2}d\xi d\eta$$

$$+\iint\left[L_1\phi_\xi^{(1)}-M_1\frac{\partial Q_0}{\partial\xi}\right]\frac{\partial^2\phi_\eta^{(1)}}{\partial\eta^2}d\xi d\eta\ , \qquad (5.20)$$

where $A=\frac{\frac{b_1^2}{2}(2+3\gamma_2+\gamma_2\lambda_p)-T_{ip}a_1+2\gamma_1a_1b_1(\lambda_p-u_{i0})-2R_2\left\{T_{ip}-\gamma_1(\lambda_p-u_{i0})^2\right\}}{\gamma_1[b_1+a_1(\lambda_p-u_{i0})]}$,

$B=\frac{T_{ip}-\gamma_1(\lambda_p-u_{i0})^2}{\gamma_1[b_1+a_1(\lambda_p-u_{i0})]}$,

$C=\frac{b_1\eta_1}{\gamma_1[b_1+a_1(\lambda_p-u_{i0})]}$, $A_1=\frac{\frac{b_2^2}{2}(2+3\gamma_2+\gamma_2\lambda_p)-T_{ip}a_2+2\gamma_1a_2b_2(\lambda_p+u_{i0})-2R_2\left\{T_{ip}-\gamma_1(\lambda_p+u_{i0})^2\right\}}{\gamma_1[b_2+a_2(\lambda_p+u_{i0})]}$,

$B_1=\frac{T_{ip}-\gamma_1(\lambda_p+u_{i0})^2}{\gamma_1[b_2+a_2(\lambda_p+u_{i0})]}$, $C_1=\frac{b_2\eta_1}{\gamma_1[b_2+a_2(\lambda_p+u_{i0})]}$,

$L=\frac{\frac{b_1b_2}{2}\left(2+3\gamma_2+\frac{2\gamma_2\lambda_p}{u_{i0}}\right)+\gamma_1(a_1b_2-a_2b_1)(\lambda_p-u_{i0})+T_{ip}a_1a_2+2\left\{T_{ip}-\gamma_1(\lambda_p-u_{i0})^2\right\}}{\gamma_1[b_1+a_1(\lambda_p-u_{i0})]}$,

$M=\frac{b_1\gamma_1(\lambda_p+u_{i0})+T_{ip}a_1+1+\gamma_1a_1(\lambda_p-u_{i0})^2+b_1\gamma_1(\lambda_p-u_{i0})}{\gamma_1[b_1+a_1(\lambda_p-u_{i0})]}$,

$L_1=\frac{\frac{b_1b_2}{2}\left(2+3\gamma_2+\frac{2\gamma_2\lambda_p}{u_{i0}}\right)+\gamma_1(a_1b_2-a_2b_1)(\lambda_p-u_{i0})+T_{ip}a_1a_2+2\left\{T_{ip}-\gamma_1(\lambda_p-u_{i0})^2\right\}}{\gamma_1[b_2+a_2(\lambda_p-u_{i0})]}$,

$M_1=\frac{b_2\gamma_1(\lambda_p+u_{i0})+T_{ip}a_2+1+\gamma_1a_2(\lambda_p^2-u_{i0}^2)+b_2\gamma_1(\lambda_p+u_{i0})}{\gamma_1[b_2+a_2(\lambda_p+u_{i0})]}$,

$a_1=\frac{1}{\gamma_1(\lambda_p-u_{i0})^2-T_{ip}}$, $a_2=\frac{1}{\gamma_1(\lambda_p+u_{i0})^2-T_{ip}}$, $b_1=\frac{\lambda_p-u_{i0}}{\gamma_1(\lambda_p-u_{i0})^2-T_{ip}}$, $b_2=\frac{\lambda_p+u_{i0}}{\gamma_1(\lambda_p+u_{i0})^2-T_{ip}}$,

$R_2=\frac{(1+q)(3-q)}{8(1-p)}-\frac{p(1-q)(3-q)T_{ep}^2}{8(1-p)}$, and $\gamma_2=3\beta^2$.

The first and second terms in the right hand side of Eq. (5.20) are proportional to $\eta(\xi)$, for this reason, the integrand is independent of $\eta(\xi)$. Thus, these two terms are secular, which should be eliminated in order to avoid unexpected resonances and yields

$$\frac{\partial \phi_{\xi}^{(1)}}{\partial \tau} + A\phi_{\xi}^{(1)}\frac{\phi_{\xi}^{(1)}}{\partial \xi} + B\frac{\partial^3 \phi_{\xi}^{(1)}}{\partial \xi^3} - C\frac{\partial^2 \phi_{\xi}^{(1)}}{\partial \xi^2} = 0 \tag{5.21}$$

and

$$\frac{\partial \phi_{\eta}^{(1)}}{\partial \tau} - A_1\phi_{\eta}^{(1)}\frac{\phi_{\eta}^{(1)}}{\partial \eta} - B_1\frac{\partial^3 \phi_{\eta}^{(1)}}{\partial \eta^3} + C_1\frac{\partial^2 \phi_{\eta}^{(1)}}{\partial \eta^2} = 0\,. \tag{5.22}$$

Equations (5.21) and (5.22) represent the two-sided traveling KdV Burger equations in the frame of references ξ and η, where A (A_1), B (B_1), and C (C_1) are the coefficients of nonlinearity, dispersion, and dissipation, respectively. The dissipation term (Burger term) C (C_1) exists for the effect of ion kinematic viscosity η_1. The reduced form of Eq. (5.21) has already been derived [18]: relativistic plasma with Boltzmann distributed electrons [15], dissipation free relativistic thermal ei plasma [44], weakly and highly relativistic plasmas with nonextensivity, and [16] dissipation free relativistic thermal epi plasmas. On the other hand, the results obtained employing reductive perturbation method [15, 16, 18, 44- 46] recovering classical limit for the ei [45] and the epi [46] plasmas. The third and fourth terms of Eq. (5.20) are not secular, it would be secular in the next order [47], and one can obtain the following relations:

$$\frac{\partial P_0}{\partial \eta} = \frac{L}{M}\phi_{\eta}^{(1)}, \tag{5.23}$$

and

$$\frac{\partial Q_0}{\partial \xi} = \frac{L_1}{M_1}\phi_{\xi}^{(1)}\,. \tag{5.24}$$

To investigate the better accuracy for the interactions of two ion acoustic shock waves, one can consider the following expansion of the Lorentz factor (γ) for the case of highly relativistic regime as:

$$\gamma \approx 1 + \frac{u_i^2}{2c^2} + \frac{3u_i^4}{8c^4}. \tag{5.25}$$

Inserting Eqs. (5.4)-(5.7) and (5.25) into the Eqs. (5.1)- (5.3), a set of PDEs in various powers of ε can be derived. The smallest power of ε yield a set of equations whose solution can be expressed by the following relations:

$$\phi^{(1)} = \phi_{\xi}^{(1)}(\xi,\tau) + \phi_{\eta}^{(1)}(\eta,\tau), \tag{5.26}$$

$$n_i^{(1)} = \frac{1}{\gamma_3\left(\lambda_p - u_{i0}\right)^2 - T_{ip}}\phi_{\xi}^{(1)}(\xi,\tau) + \frac{1}{\gamma_3\left(\lambda_p + u_{i0}\right)^2 - T_{ip}}\phi_{\eta}^{(1)}(\eta,\tau), \tag{5.27}$$

$$u_i^{(1)} = \frac{\lambda_p - u_{i0}}{\gamma_3\left(\lambda_p - u_{i0}\right)^2 - T_{ip}}\phi_{\xi}^{(1)}(\xi,\tau) - \frac{\lambda_p + u_{i0}}{\gamma_3\left(\lambda_p + u_{i0}\right)^2 - T_{ip}}\phi_{\eta}^{(1)}(\eta,\tau), \tag{5.28}$$

and the phase velocity

$$\lambda_p = \pm u_{i0} + \left\{\frac{T_{ip}}{\gamma_3} + \frac{1}{\gamma_3 R_1}\right\}^{1/2}, \tag{5.29}$$

where $\gamma_3 = \gamma_1 + \frac{15}{8}\beta^4$. Continuing the above procedure one can derive the evolution equations in the same form as of Eqs. (5.21)-(5.24) except coefficients. The coefficients can be written in the follow form:

$$A = \frac{\frac{b_1^2}{2}\left(2 + 3\gamma_4 + \gamma_4\lambda_p\right) - T_{ip}a_1 + 2\gamma_3 a_1 b_1\left(\lambda_p - u_{i0}\right) - 2R_2\left\{T_{ip} - \gamma_3\left(\lambda_p - u_{i0}\right)^2\right\}}{\gamma_3\left[b_1 + a_1\left(\lambda_p - u_{i0}\right)\right]}$$

$$B = \frac{T_{ip} - \gamma_3\left(\lambda_p - u_{i0}\right)^2}{\gamma_3\left[b_1 + a_1\left(\lambda_p - u_{i0}\right)\right]}, C = \frac{b_1\eta_1}{\gamma_3\left[b_1 + a_1\left(\lambda_p - u_{i0}\right)\right]},$$

$$A_1 = \frac{\frac{b_2^2}{2}\left(2 + 3\gamma_4 + \gamma_4\lambda_p\right) - T_{ip}a_2 + 2\gamma_3 a_2 b_2\left(\lambda_p + u_{i0}\right) - 2R_2\left\{T_{ip} - \gamma_3\left(\lambda_p + u_{i0}\right)^2\right\}}{\gamma_3\left[b_2 + a_2\left(\lambda_p + u_{i0}\right)\right]},$$

$$B_1 = \frac{T_{ip} - \gamma_3\left(\lambda_p + u_{i0}\right)^2}{\gamma_3\left[b_2 + a_2\left(\lambda_p + u_{i0}\right)\right]}, C_1 = \frac{b_2\eta_1}{\gamma_3\left[b_2 + a_2\left(\lambda_p + u_{i0}\right)\right]},$$

$$L = \frac{\frac{b_1 b_2}{2}\left(2 + 3\gamma_4 + \frac{2\gamma_4\lambda_p}{u_{i0}}\right) + \gamma_3(a_1 b_2 - a_2 b_1)\left(\lambda_p - u_{i0}\right) + T_{ip}a_1 a_2 + 2\left\{T_{ip} - \gamma_3\left(\lambda_p - u_{i0}\right)^2\right\}}{\gamma_3\left[b_1 + a_1\left(\lambda_p - u_{i0}\right)\right]},$$

$$M = \frac{b_1\gamma_3\left(\lambda_p + u_{i0}\right) + T_{ip}a_1 + 1 + \gamma_3 a_1\left(\lambda_p - u_{i0}\right)^2 + b_1\gamma_3\left(\lambda_p - u_{i0}\right)}{\gamma_1\left[b_1 + a_1\left(\lambda_p - u_{i0}\right)\right]},$$

$$L_1 = \frac{\frac{b_1 b_2}{2}\left(2 + 3\gamma_4 + \frac{2\gamma_4\lambda_p}{u_{i0}}\right) + \gamma_3(a_1 b_2 - a_2 b_1)\left(\lambda_p - u_{i0}\right) + T_{ip}a_1 a_2 + 2\left\{T_{ip} - \gamma_3\left(\lambda_p - u_{i0}\right)^2\right\}}{\gamma_3\left[b_2 + a_2\left(\lambda_p - u_{i0}\right)\right]},$$

$M_1 = \frac{b_2\gamma_3(\lambda_p+u_{i0})+T_{ip}a_2+1+\gamma_3 a_2(\lambda_p^2-u_{i0}^2)+b_2\gamma_3(\lambda_p+u_{i0})}{\gamma_3[b_2+a_2(\lambda_p+u_{i0})]}$, and $\gamma_4 = \gamma_2 + \frac{15}{2}\beta^4$.

5.4 Solutions of shock wave

Equations (5.21) and (5.22) are represent the two-sided KdV Burger equations for the two sided traveling waves in the considering frame of references ξ and η. Putting C(C_1) = 0 we get KdV equations, and for B (B_1) = 0, we obtain Burger equations. The KdV Burger equation is extensively used in plasma physics. The tangent hyperbolic method seems to be a significant tool for the computation of exact traveling wave solutions. The solutions of ion acoustic shock waves governed by the Eqs.(5.21) and (5.22) can be obtained as [48]

$$\phi_{\xi}^{(1)} = \frac{3C^2}{25AB}\left\{1 - tanh\left[\frac{C}{10B}\left(\xi - \frac{6C^2}{25B}\tau\right)\right]\right\}^2, \tag{5.30}$$

and

$$\phi_{\eta}^{(1)} = \frac{3C_1^2}{25A_1B_1}\left\{1 + tanh\left[\frac{C_1}{10B_1}\left(\eta + \frac{6C_1^2}{25B_1}\tau\right)\right]\right\}^2, \tag{5.31}$$

where τ denotes the stretched time coordinate in case of the slow time scale. The functions P_0 and Q_0 can be determined from Eqs.(5.23) and (5.24), respectively. The electrostatic wave potential $\phi^{(1)}$ for weak head-on collision is given by

$$\phi^{(1)} = \varepsilon^2\frac{3C^2}{25AB}\left\{1 - tanh\left[\frac{C}{10B}\left(\xi - \frac{6C^2}{25B}\tau\right)\right]\right\}^2 + \varepsilon^2\frac{3C_1^2}{25A_1B_1}\left\{1 + tanh\left[\frac{C_1}{10B_1}\left(\eta + \frac{6C_1^2}{25B_1}\tau\right)\right]\right\}^2. \tag{5.32}$$

It is evident that the solution (5.32) depends thoughtfully on the plasma parameters p, q, $T_{ep,}$ T_{ip}, β, ξ, η, τ, and η_1.

To explain the head-on collision of ion acoustic shock waves asymptotically, it is necessary to find the solution of Eqs.(5.23) and (5.24) with suitable boundary conditions. The phase change, which occurs due to the collision, can be obtained solving Eqs. (5.23) and (5.24) and can be written as

$$P_0(\eta,\tau) = \frac{6LC_1}{5MA_1}\left\{tanh\left[\frac{C_1}{25B_1}(\eta + 6C_1^2\tau/25B_1)\right] + 1\right\} - \frac{12LC_1}{5MA_1}\left\{ln\left[-1 + tanh\left(\frac{C_1}{25B_1}(\eta + 6C_1^2\tau/25B_1)\right)\right]\right\}$$

and

$$Q_0(\xi,\tau) = \frac{6L_1C}{5M_1A}\left\{tanh\left[\frac{C}{25B}(\xi - 6C^2\tau/25B)\right] - 1\right\} + \frac{12L_1C}{5M_1A}\left\{ln\left[1 + tanh\left(\frac{C}{25B}(\xi - 6C^2\tau/25B)\right)\right]\right\}.$$

Therefore, up to $O(\varepsilon^2)$, the trajectories of the two shock waves due to head-on collision are

$$\xi = \varepsilon(x - \lambda_p t) + \varepsilon^2\frac{6LC_1}{5MA_1}\left\{tanh\left[\frac{C_1}{25B_1}(\eta + 6C_1^2\tau/25B_1)\right] + 1\right\} - \varepsilon^2\frac{12LC_1}{5MA_1}\left\{ln\left[-1 + tanh\left(\frac{C_1}{25B_1}(\eta + 6C_1^2\tau/25B_1)\right)\right]\right\}$$

and

$$\eta = \varepsilon(x + \lambda_p t) + \varepsilon^2\frac{6L_1C}{5M_1A}\left\{tanh\left[\frac{C}{25B}(\xi - 6C^2\tau/25B)\right] - 1\right\} + \varepsilon^2\frac{12L_1C}{5M_1A}\left\{ln\left[1 + tanh\left(\frac{C}{25B}(\xi - 6C^2\tau/25B)\right)\right]\right\}.$$

To find the phase shifts due to head-on collision of two solitons, it is assumed that initially ($t \to -\infty$), they are asymptotically far from each other, that is, one (the right traveling soliton) is at $\xi = 0$, $\eta \to -\infty$, and other (the left traveling soliton) is at $\eta = 0$, $\xi \to +\infty$. After head-on collision ($t \to +\infty$), the right traveling soliton is far to the right of left traveling soliton, that is, the right traveling soliton is at $\xi = 0$, $\eta \to +\infty$, and the left traveling soliton is at $\eta = 0$, $\xi \to -\infty$. So one can obtain the corresponding phase shifts Δv_+ and Δv_- as follows:

$$\Delta v_+ = \varepsilon(x + \lambda_p t)\big|_{\xi=0,\eta=\infty} - \varepsilon(x + \lambda_p t)\big|_{\xi=0,\eta=-\infty} = \varepsilon^2\frac{12CL_1}{5AM_1}$$

$$\text{and } \Delta v_- = \varepsilon(x - \lambda_p t)\big|_{\eta=0,\xi=\infty} - \varepsilon(x - \lambda_p t)\big|_{\eta=0,\xi=-\infty} = -\varepsilon^2\frac{12C_1L}{5A_1M}.$$

Therefore,

$$\Delta v_+ = \varepsilon^2\frac{12CL_1}{5AM_1}, \qquad \Delta v_- = -\varepsilon^2\frac{12C_1L}{5A_1M}\ . \tag{5.33}$$

5.5 Results and discussion

It is well known that the most important characteristic of solitons after collision is the asymptotic maintenance of their structures. A number of researchers [49-51] have studied the head-on collision between solitons along with their corresponding phase shift considering unit amplitude. But the phase shifts are produced due to non-coherent amplitudes of the interacting solitons and so that our main interest is to investigate the effects of plasma parameters such as temperature ratio, kinematic viscosity, ion density, relativistic streaming factor on the properties as well as on trajectories of ion acoustic shock waves after collision. Besides, the coefficients of nonlinearity, dispersion, and dissipation are depended on plasma parameters, so it is also important to study the effects of these parameters on the structures of ion acoustic shock waves. To study the properties and structures of ion acoustic shock waves, the KdV Burger equations are derived both for weakly and highly relativistic regimes considering the plasma system composing relativistic warm ions, nonextensive electrons, and positions. The effects of plasma parameters on nonlinearity and dispersion coefficients, the evolution of electrostatic resonance, and phase shifts, as well as amplitudes and collision processes involved, are investigated considering T_e= 0.2-140 MeV, T_p= 0.2-40 MeV, and T_i = 2-100 MeV [39]. The effects of electron to positron temperature ratio (T_{ep}) on the nonlinearity coefficient (A) with the relativistic streaming factor (β) are displayed in Figs.5.1 (a) and 5.1(b). It is observed that A increases with increasing T_{ep} and β for both weakly and highly relativistic regimes. It is noticed that the change in A of the ion acoustic shock waves in the highly relativistic regime (HRR) is rather higher than that of the weakly relativistic regime (WRR). Figures 5.1(c) and 5.1(d) show the influence of the nonextensivity parameter (q) on A with the ion to the positron temperature ratio (T_{ip}). It is observed from these figures that A of the ion acoustic shock are also increasing with the increase in q in both weakly and highly relativistic regimes, but A increases with T_{ip} [Fig.5.1(c)] only in weakly relativistic regimes, and A is insignificant [Fig.1(d)] in highly relativistic regime.

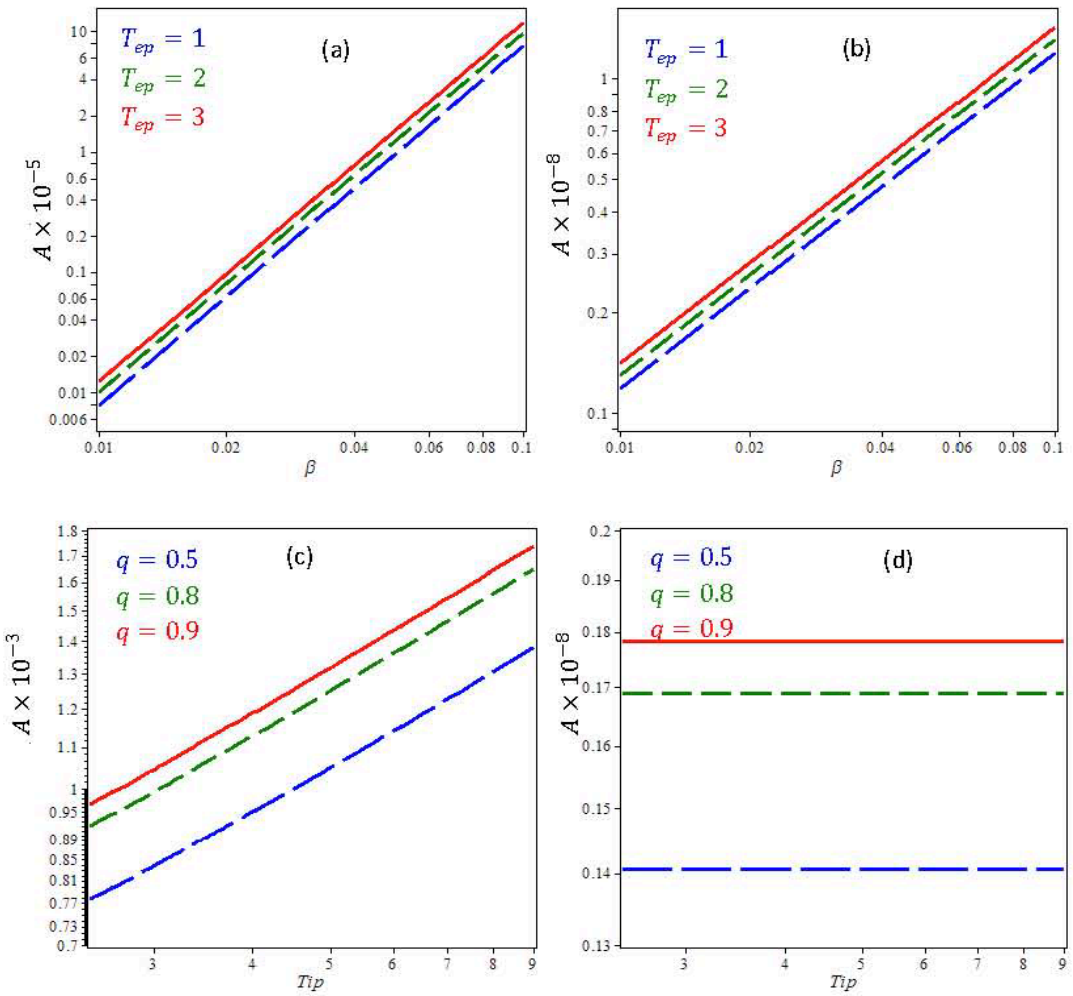

Figure 5.1 Effect on A of T_{ep} ((a), (b)) with β taking $p = 0.6$, $q = 0.5$, η_1= 0.09,and T_{ip} = 2.5 and q ((c), (d)) with T_{ip}, remaining parameters are considered as (a), β = 0.01and T_{ep} = 1 in case of weakly relativistic (left column) and highly relativistic (right column) regimes.

Figure 5.2 depicts the influence on the dispersion coefficient (B) with β for T_{ep} = 1.0, 1.3, and 1.6 [5.2(a) and 5.2(b)] taking the typical values of the remaining plasma parameters as $q = 0.5$, T_{ip}=2.5, η_1= 0.09, p = 0.45, and $T_{ip} = 2.5$ for $q = 0.5, 0.8, 0.9$ [Figs.5.2(c) and 5.2(d)] and $p = 0.45$, η_1= 0.09, β = 0.01, and $T_{ep} = 1.0$. Figures 5.2(a) and 5.2(b) reveal that B is increasing with the increase in T_{ep} in both HRR and WRR, but there is no effect observed of β on B in both cases. B is smaller for weakly relativistic than that of highly relativistic regimes for T_{ep}, which indicates that the ion acoustic shock waves propagate faster in weakly relativistic regime rather than highly relativistic case. Figures 5.2(c) and 5.2(d) show that B is increasing with q and T_{ip} for HRR and WRR. It is noted that B is negative; therefore, only negative electrostatic potential of ion acoustic shock waves are

investigated. This means that the energy is absorbed by the solitons for the phase shift due to collisions without the change of their shapes and velocities.

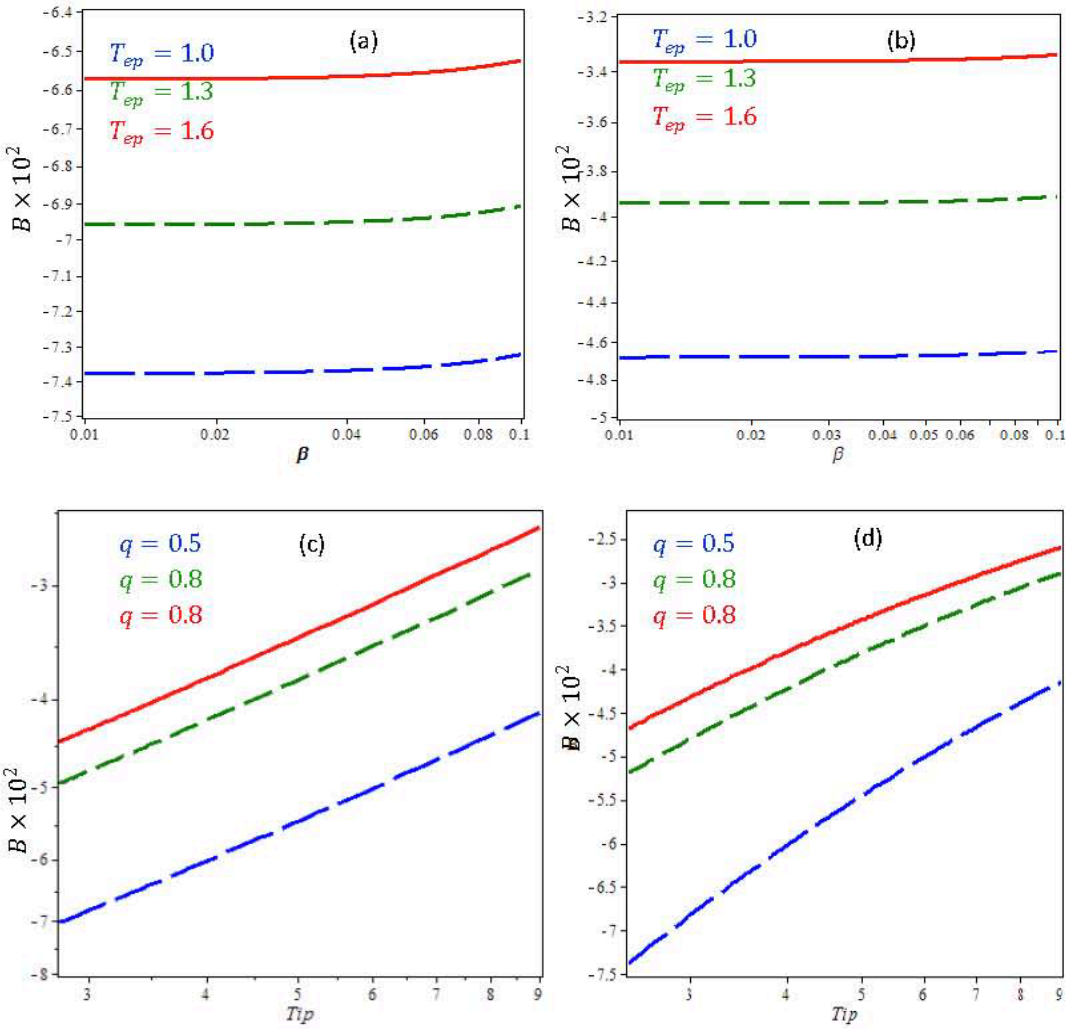

Figure 5.2 Effect on B of T_{ep} ((a), (b)) with β, other parameters considered as q =0.5, T_{ip}=2.5, η_1= 0.09, and p = 0.45, and q ((c), (d)) with T_{ip} remaining parameters are considered as (a),β = 0.01and $T_{ep} = 1.0$ in the case of weakly relativistic (right column) and highly relativistic (left column) regimes.

Figures. 5.3(a) and 5.3(b) illustrate the effects of kinematic viscosity (η_1) and β on phase shifts taking typical values of the remaining plasma parameter as $= 0.18$, $p =$ 0.3, $T_{ip} = 2.5$, and $T_{ep} = 2$. It is found that the phase shifts are decreasing monotonically with increasing β. On the other hand, the phase shifts are increasing with the increase in η_1 for both WRR and HRR. The increment (decrement) of phase shift depends on the gain (loss) of energy during

the collisions.

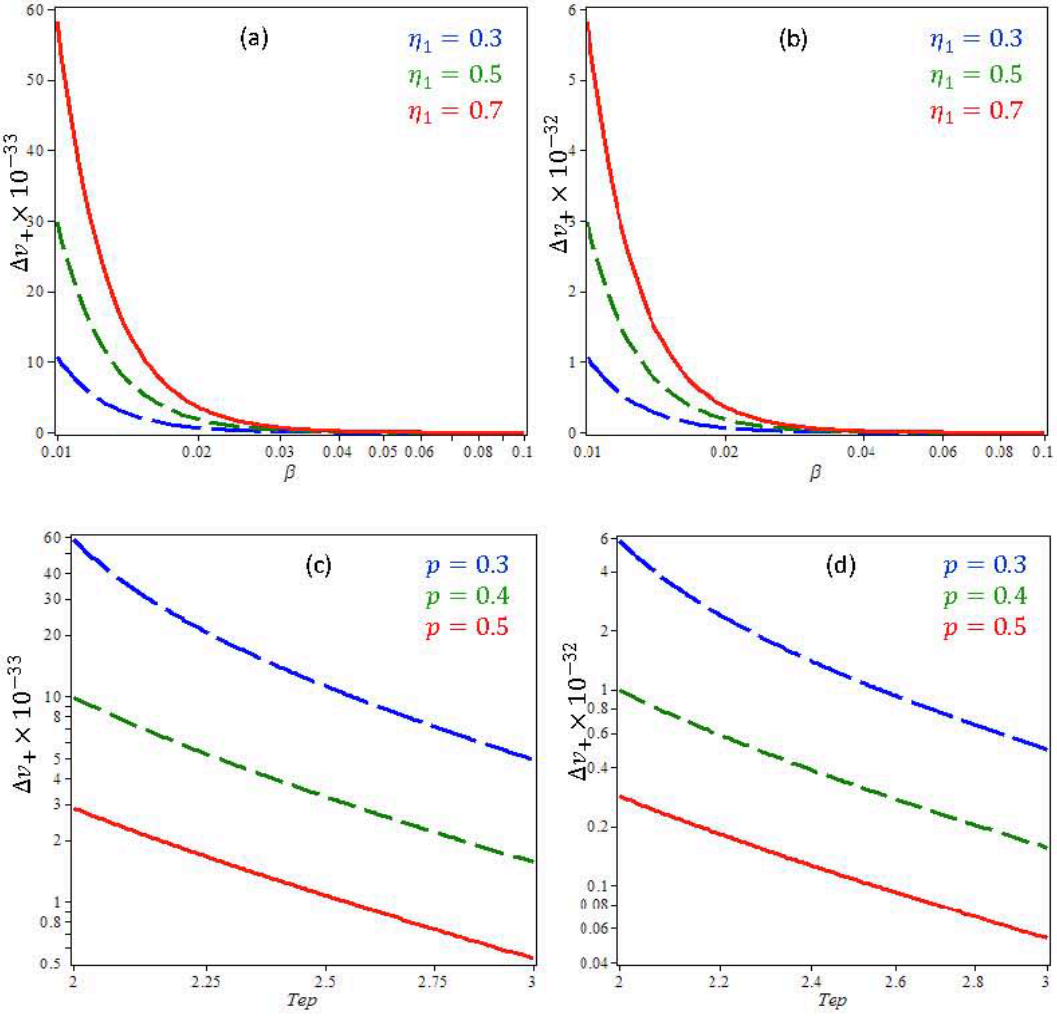

Figure 5.3 Effect on Δv_+ of η_1 ((a), (b)) with β taking remaining parameters $q = 0.18$, $p = 0.3$, $T_{ip} = 2.5$ and T_{ep}=2 and p ((c), (d)) with T_{ep} taking as(a), $\beta = 0.01$ and $\eta_1 = 0.3$ in case of HRR (left column) and WRR (right column).

The phase velocity decreases due to the increase in η_1; as a result, A, the coefficient (L), and the dissipation coefficient (C) turn to increase, which further enhances the phase shift (Δv_+) and the soliton gains energy in the collision processes. Figures 5.3(c) and 5.3(d) elucidate the change of phase shifts due to the effects of p and T_{ep} considering $p = 0.3$, 0.4, and 0.5, and the remaining parameters are kept constant. From the figures, it is observed that the phase shift is decreasing for the effects of both p and T_{ep} in WRR and HRR. It is evident that the phase shift is positive which dictates that the post collisional part of the soliton moves ahead of the initial trajectory. The collision process between two ion acoustic shock waves is illustrated in Fig.5.4 for $T_{ep} = 0.1$ [Fig. 5.4(a)] and $T_{ep} = 0.2$ [Fig. 5.4(b)] in WRR, taking $p = 0.6$, $q = 0.5$, $\beta = 0.01$, $\eta_1 = 0.09$, and $T_{ip} = 2.5$. From these figures, it is seen that the

width of the ion acoustic shock waves are increasing with increasing T_{ep}. Figures 5.4(c) and 5.4(d) represent the contour plot of Fig.5.4 (a) and Fig. 5.4(b), respectively.

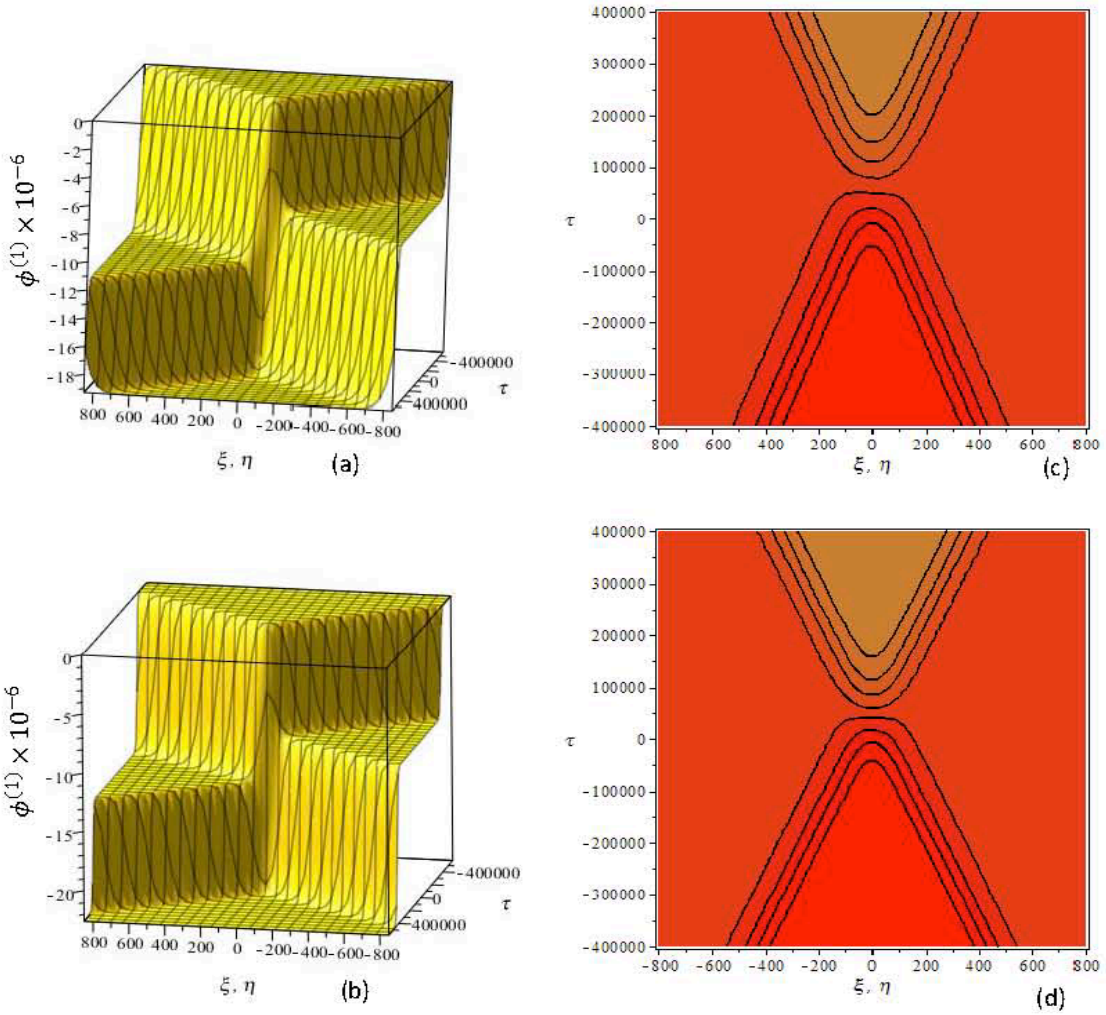

Figure 5.4 The electrostatic potential ($\phi^{(1)}$) for (a) $T_{ep} = 0.1$, (b) $T_{ep} = 0.2$, (c) is the contour plot of (a), and (d) is the contour plot of (b), respectively, with various values of τ considering q=0.5, p= 0.6, β=0.01, η_1= 0.09, and T_{ip}=2.5 in the weakly relativistic regime.

Figures 5.5(a) and 5.5(b) reveal that the widths of the ion acoustic shock waves remain unchanged with increasing η_1 while the widths of the ion acoustic shock waves are increasing due to the effect of T_{ip} which are shown in Figs. 5.6(a) and 5.6(b) in case of WRR. The figures in the right hand columns of Figs. 5.5 and Figs. 5.6 represent the contour plots of the left hand columns, respectively.

The widths of the ion acoustic shock waves in HRR are increasing with increasing T_{ep} that can be observed from Figs. 5.7(a) and 5.7(b). Similar results are also found for the effect of η_1

as shown in Figs. 5.8(a) and 5.8(b). Figures 5.7(c), 5.7(d), 5.8(c), and 5.8(d) are the contour plots of Figs. 5.7(a), 5.7(b), 5.8(a), and 5.8(b), respectively, in HRR.

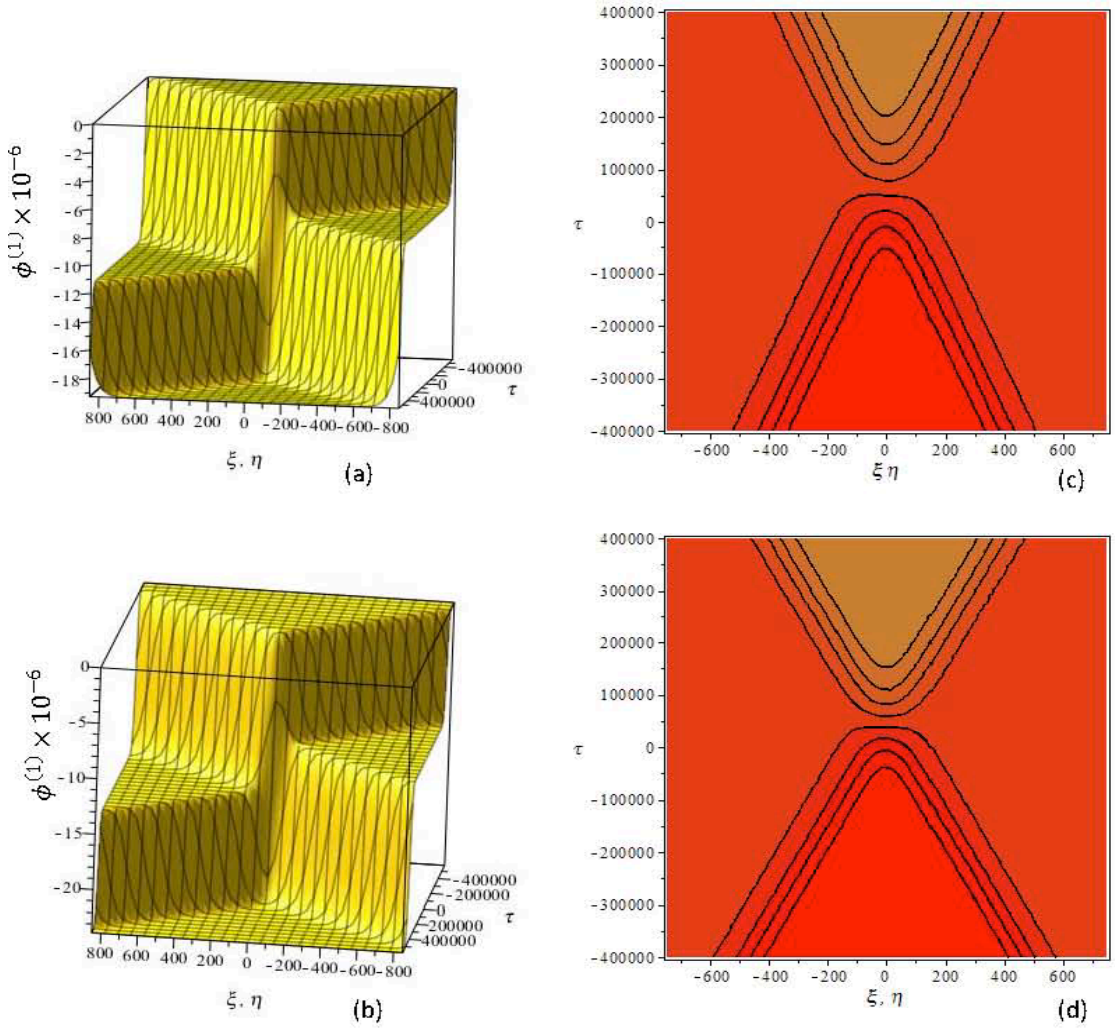

Figure 5.5 The electrostatic potential ($\phi^{(1)}$) for (a) η_1=0.09, (b) η_1 = 0.15, and (c) is the contour plot of (a), and (d) is the contour plot of (b), respectively, with various values of τ considering $q = 0.5$, $p = 0.6$, $\beta = 0.01$, T_{ep}= 1.0, and T_{ip}=2.5 in the weakly relativistic regime.

Figures 5.9(a) and 5.9(b) display the effect of T_{ip} on the electrostatic potential ($\phi^{(1)}$). It is observed that the width of the soliton remains unchanged in HRR. Figures 5.9(c) and 5.9(d) are also the contour plots of Figs. 5.9(a) and 5.9(b), respectively. It has to be mentioned that T_{ip} plays a crucial role to form ion acoustic shocks in WRR rather than HRR. Besides, only the rarefactive electrostatic ion acoustic shocks are found for different values of T_{ep}, T_{ip}, and η_1 in both the cases of WRR and HRR in the plasmas considered.

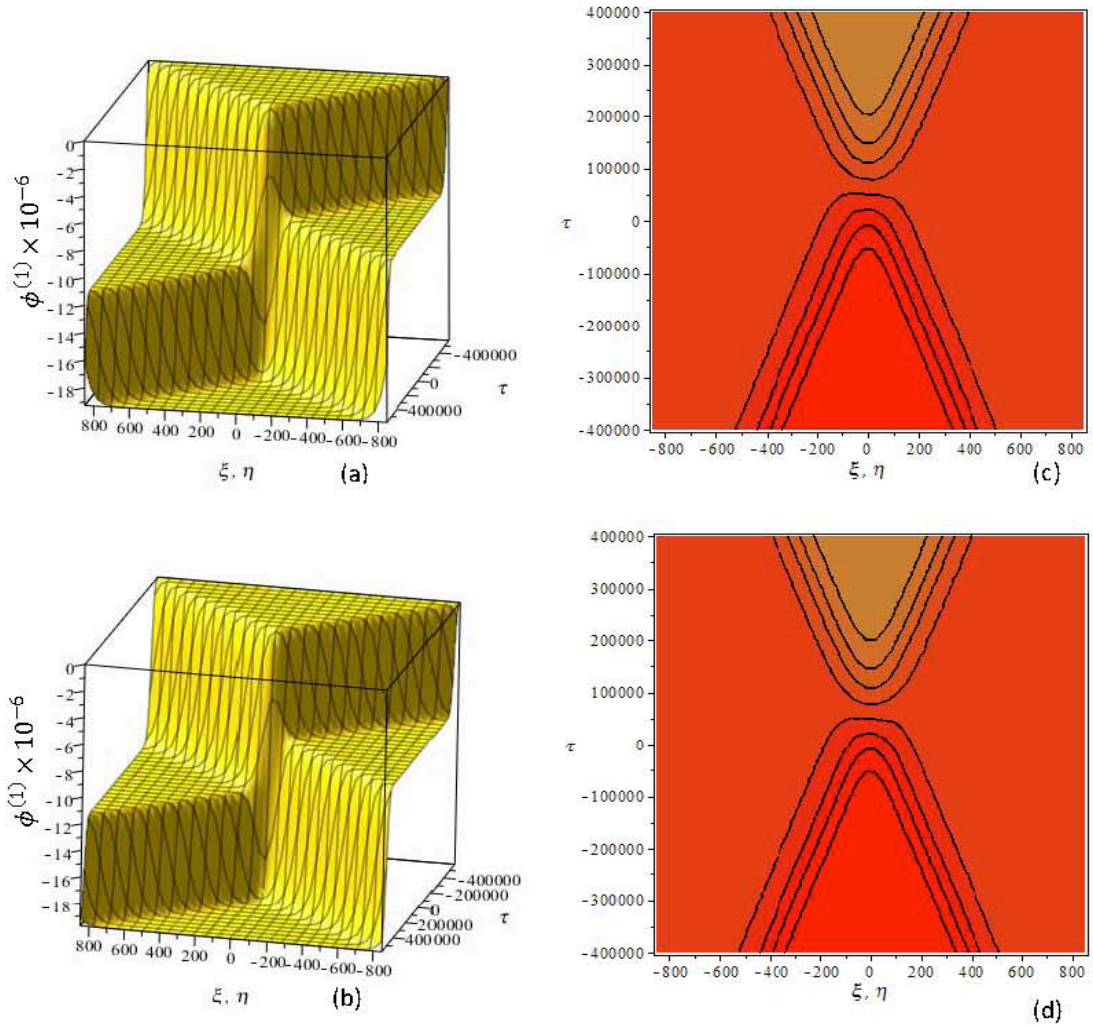

Figure 5.6 The electrostatic potential ($\phi^{(1)}$) for (a) $T_{ip} = 2.5$, (b) $T_{ip} = 3.0$, and (c) is the contour plot of (a), and (d) is the contour plot of (b), respectively, with various values of τ considering q=0.5, p= 0.6, β=0.01, T_{ep}= 1.0, and η_1=0.09 in the weakly relativistic regime.

The changes in amplitudes ($\phi_0 = 3C^2/25AB$) are depicted in Figs. 5.10(a)-5.10(f) for β, η_1, and p, taking $p = 0.6$, $q = 0.4$, $\beta = 0.001$, $T_{ip} = 2.5$, $\eta_1 = 0.1$, and $T_{ep} = 1$, respectively. It is seen from Figs. 5.10(a) and 5.10(b) that the amplitudes of ion acoustic shock waves are increasing due to the effects of β but are decreasing due to the effect of T_{ep} in both regimes. However, the amplitudes of ion acoustic shock waves are relatively higher for HRR than those of WRR due to the increase of β and T_{ep}. The two- and three-term expansions of Lorentz factor are considered for the weakly and highly relativistic cases, respectively. Due to the increasing relativistic streaming factor, the nonlinearity (convection) in the considered plasma system becomes weaken, and the solitons gain the energies; consequently, the peak amplitude of the shock wave grows up.

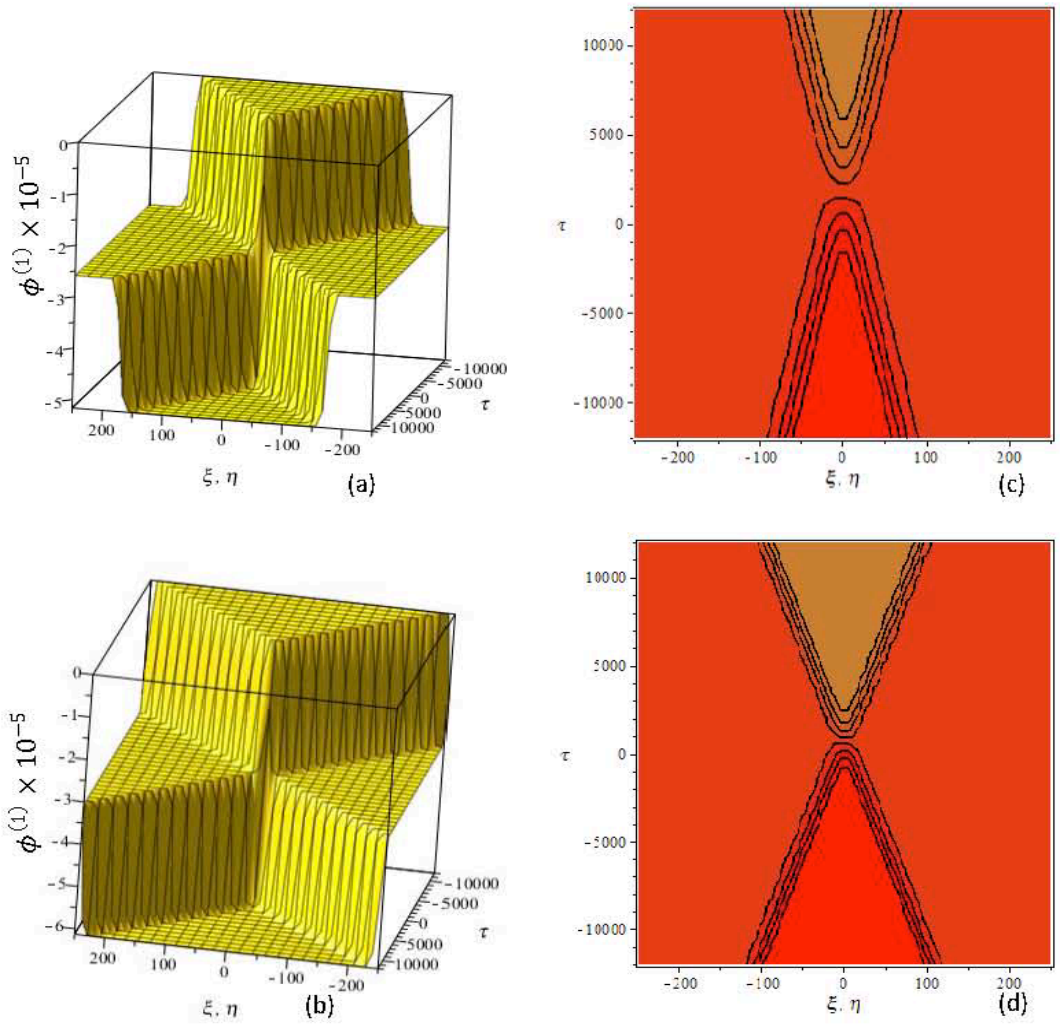

Figure 5.7 The electrostatic potential ($\phi^{(1)}$) for (a) $T_{ep} = 1.0$, (b) $T_{ep} = 2.0$, and (c) is the contour plot of (a), and (d) is the contour plot of (b), respectively, with various values of τ considering q= 0.5, p= 0.6, β=0.01,η_1= 0.09, and $T_{ip} = 2.5$ in the highly relativistic regime.

As a result, the amplitudes of ion acoustic shock waves are relatively higher for HRR than that of WRR due to the increase in β.The effects of η_1 and q on the amplitudes of ion acoustic shock waves are presented in Figs.5.10(c) and 5.10(d). It is found that in both cases of WRR and HRR, the amplitudes of ion acoustic shock waves are reduced for the effects of both η_1 and q. Figures 5.10(e) and 5.10(f) show the influence of p and T_{ip} on the amplitudes of ion acoustic shock waves in the case of WRR and HRR. It is found that the amplitudes are decreasing with the increase in p in both cases. It is interesting to note that the amplitudes are increasing in WRR, but it is decreasing in HRR due to the effect of T_{ip}.

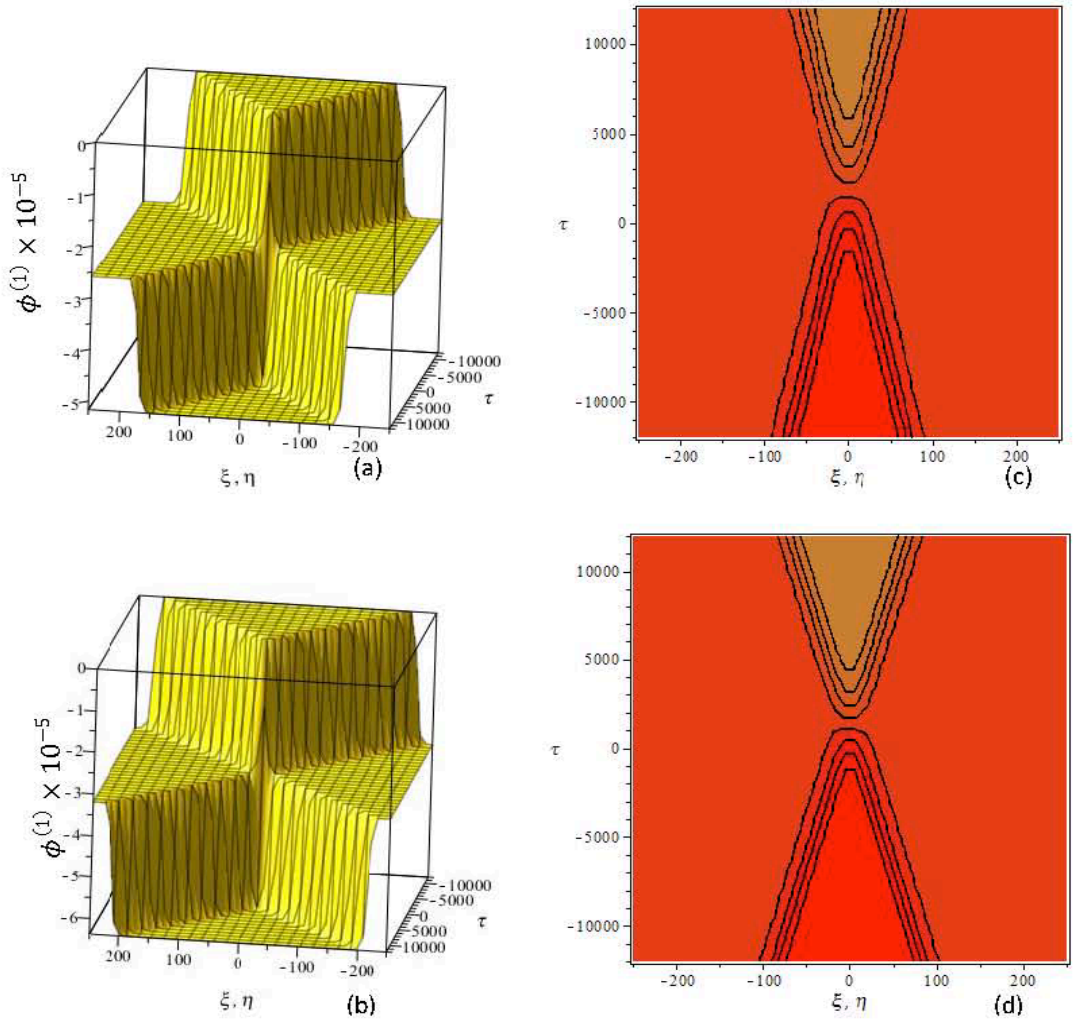

Figure 5.8 The electrostatic potential ($\phi^{(1)}$) for (a) η_1=0.09, (b)η_1= 0.10, and (c) is the contour plot of (a), and (d) is the contour plot of (b), respectively, with various values of τ considering q=0.5, p= 0.6, β=0.01, $T_{ep} = 1.0$ and $T_{ip} = 2.5$ in the highly relativistic regime.

The reason is that with the increase in T_i, the convection exceeds dispersion in the system, and consequently, the amplitudes of the solitons are decreasing. Further, the amplitudes of the solitons are restraining due to the increase of positron concentration. In fact, the increase in positron concentration can be interpreted as the depopulation of ions due to which the driving force (for the ion inertia) decreases. As a result, the amplitudes of the solitons are decreasing, and hence, the ion acoustic shock waves are generated. Figures 5.11(a) and 5.11(b) display the time evolution potential profiles of the spatial soliton solutions $\phi_\xi^{(1)}$ and $\phi_\eta^{(1)}$ for numerous values of τ for the head-on collision. It is observed that the soliton $\phi_\xi^{(1)}$ is traveling toward right direction, while $\phi_\eta^{(1)}$ towards left direction with increasing time. This result is in good agreement with the analytical solution [52].

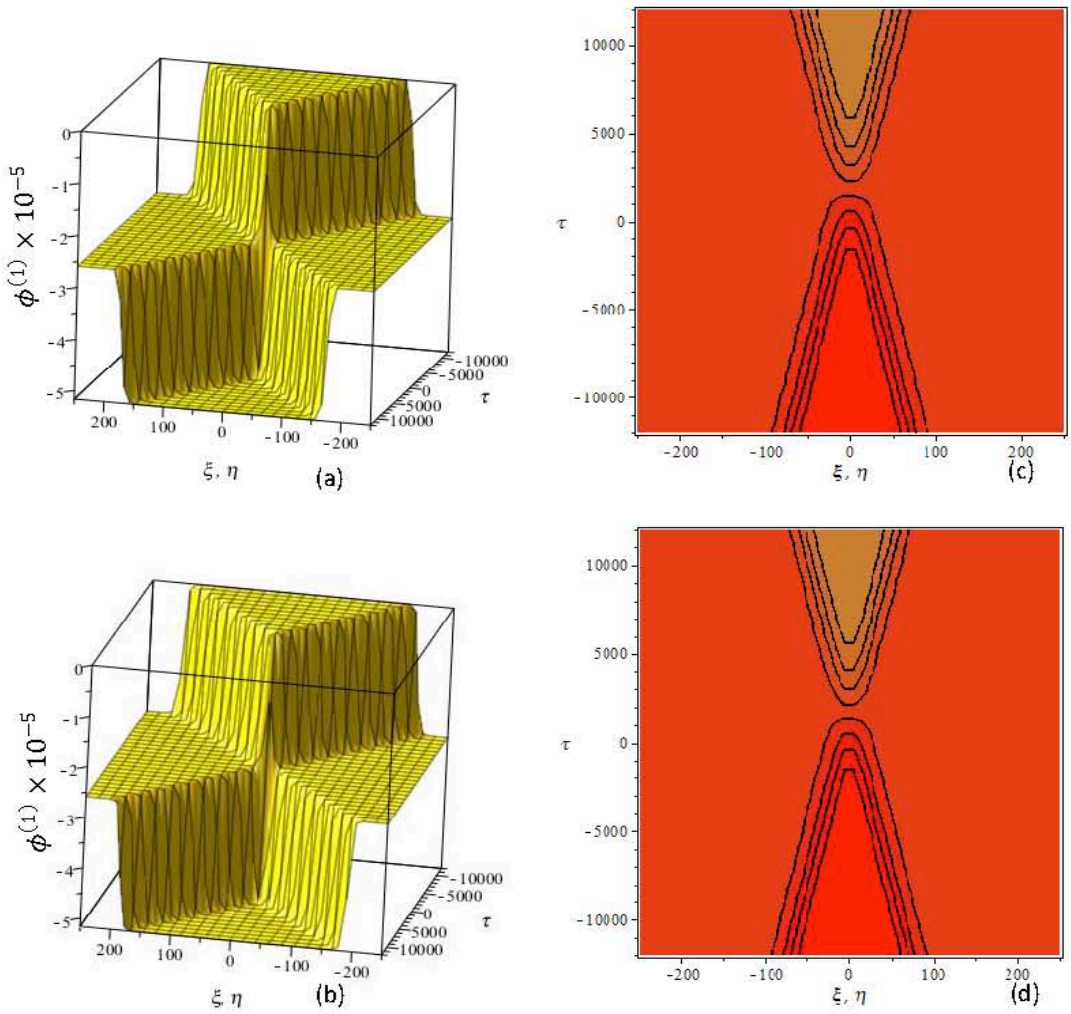

Figure 5.9 The electrostatic potential ($\phi^{(1)}$) for (a)$T_{ip} = 2.5$, (b) $T_{ip} = 3.0$, and (c) is the contour plot of (a), and (d) is the contour plot of (b), respectively, with various values of τ considering $q = 0.5$, $p = 0.6$, β=0.01, $T_{ep} = 1.0$ and $\eta_1 = 0.09$ in the highly relativistic regime.

5.6 Conclusions

The plasma system consisting of relativistic warm ions, nonextensive electrons, and positions are considered to investigate the head-on collision between ion acoustic shock waves, the change of phase shifts and amplitudes, taking into account the effects of nonlinearity and dispersion. To do so, two-sided KdV Burger equations are derived with help of ePLK method.

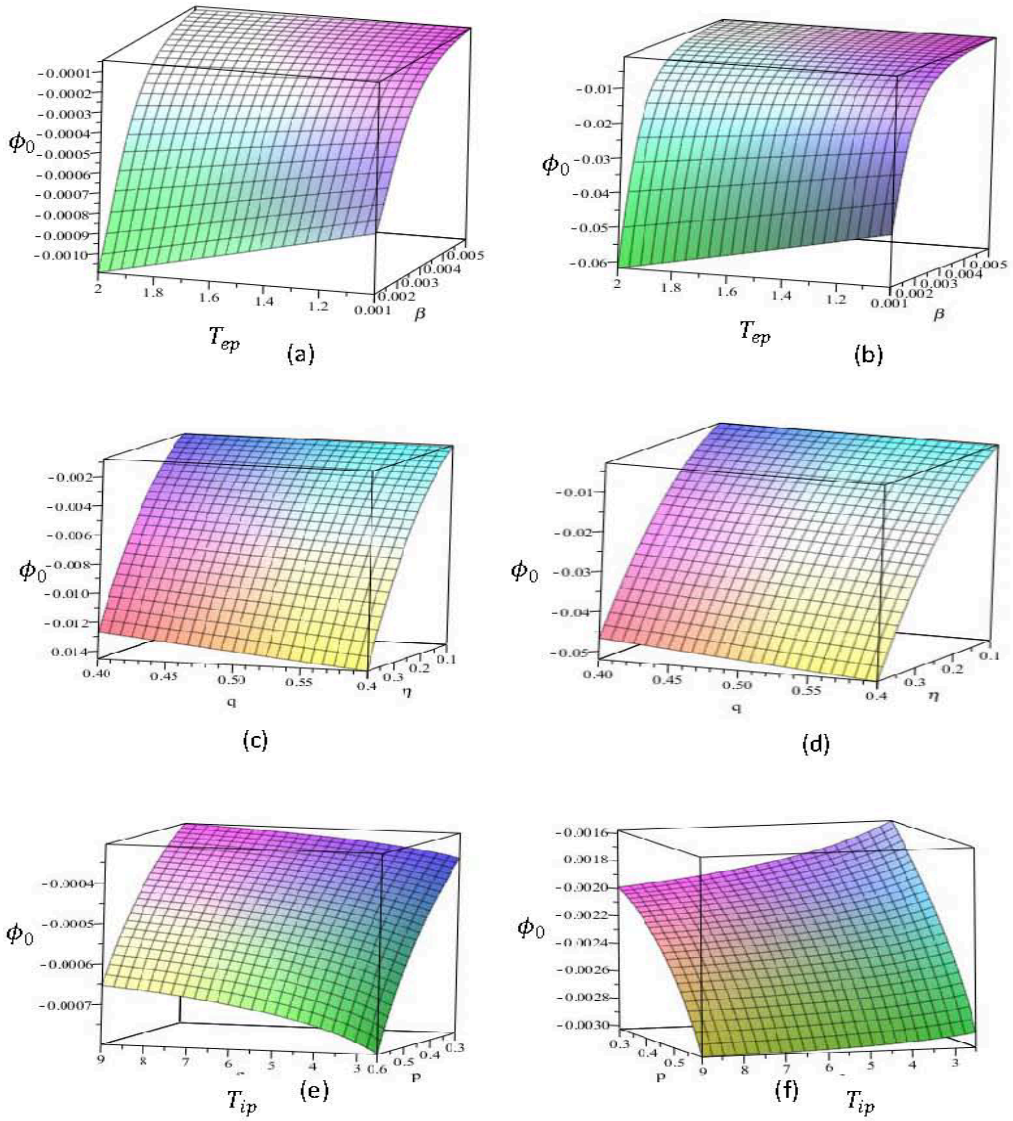

Figure 5.10 Effect of T_{ep} and β ((a), (b)) taking $p = 0.6, \eta_1 = 0.1, T_{ip} = 2.5$, and $q = 0.4$, q and η_1 ((c), (d)) considering $p = 0.6, T_{ep} = 1$, $\beta = 0.001$, and $T_{ip} = 2.5$, and $T_{ip}$and p ((e), (f)) for $\beta = 0.001$, $T_{ep} = 1, q = 0.5$, and $\eta_1 = 0.1$on the amplitudes of ion acoustic shock waves in case of weakly (left column) and highly (right column) relativistic regimes.

Two shock waves, one is at $\xi = 0, \eta \to -\infty$ and the other at $\eta = 0, \xi \to +\infty$ are traveling toward each other and collide at $t = 0$ and then depart from each other. It is observed that T_{ep}, T_{ip}, η_1, p, β, and q significantly modify the structures of the shock waves. The phase shifts are found to change due to the effects of T_{ep}, β, η_1, and p. The results reveal that the electrostatic ion acoustic shock waves become rarefactive for the temperature ratios, kinematic viscosity, and superthermality in both WRR and HRR.

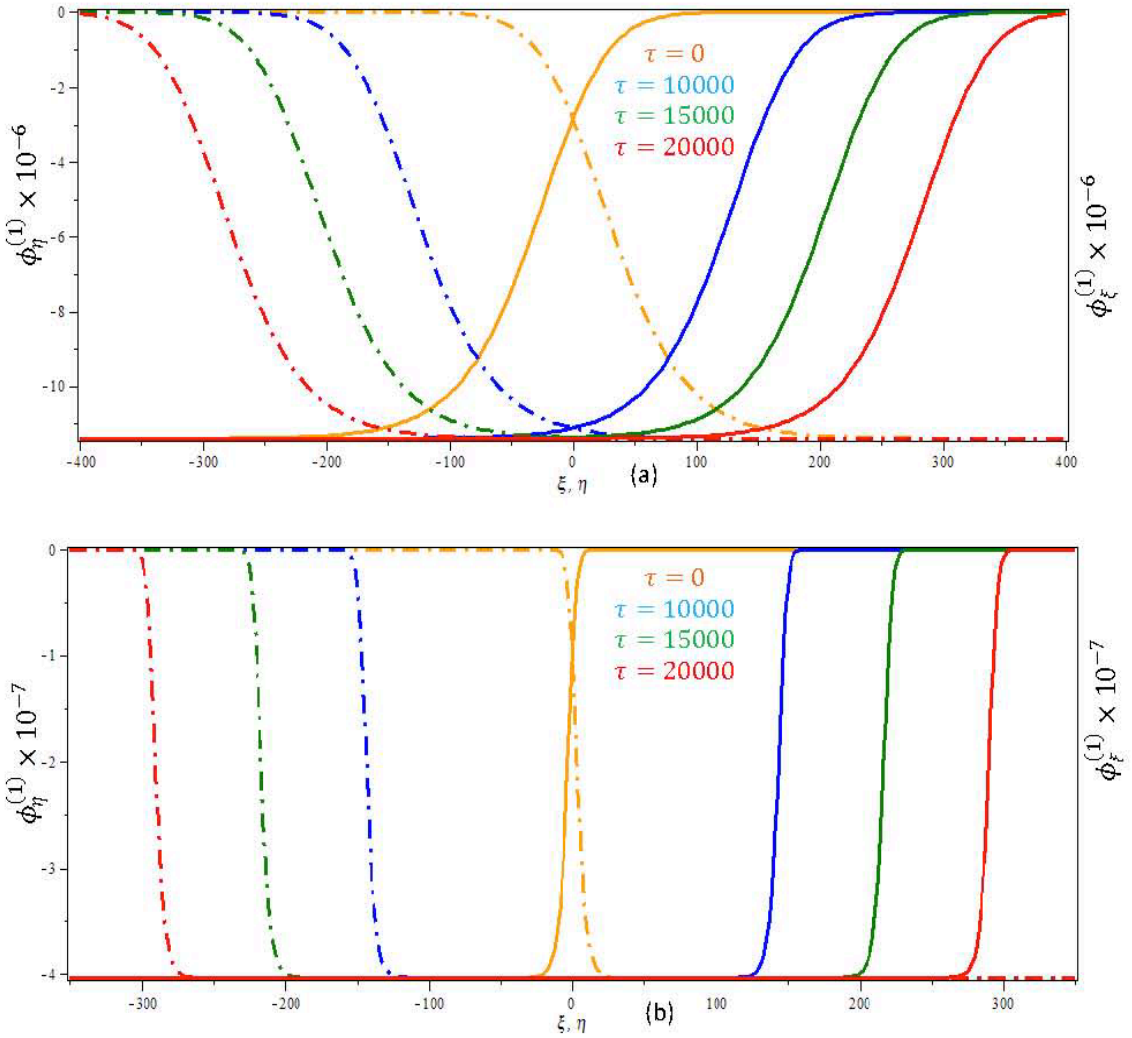

Figure 5.11 Effects of τ, p, q, β, T_{ip}, and T_{ep} on the potential profiles of the soliton $\phi_\xi^{(1)}$(solid lines) and $\phi_\eta^{(1)}$ (dash- dotted lines) for (a) weakly and (b) highly relativistic regimes, taking the typical of the parameters as in Fig. 5.9 and $T_{ip} = 2.5$.

The amplitudes of ion acoustic shock waves are increasing for WRR but decreasing for HRR due to increasing ion thermal velocities. Besides, the amplitudes of the solitons are detaining due to the increase in the positron concentration for the depopulation of ions. The results obtained may be useful for the clarifications of interactions between ion acoustic shock waves in astrophysical, especially in pulsar magnetosphere and laser produced plasmas in laboratory where nonextensive electrons, positrons and relativistic ions exist.

References

1. F. C. Michel, Theory of Neutron Star Magnetosphere, Chicago University Press, Chicago, (1991).
2. F. C. Michel, Rev. Mod. Phys. **54**, 1 (1982).
3. H. R. Miller and P. J. Wiita, Active Galactic Nuclei*, Springer*, Berlin, (1987).
4. M. L. Burns, Positron-Electron Pairs in Astrophysics*,* American Institute of Physics, Melville, NY, (1983).
5. S. Weinberg, Gravitation and Cosmology, Wiley, New York, (1972).
6. J.R. Orsoz, R.A. Remillard, C. D. Baiyn, and J.E. Clintock, Astrophys. J. Lett. **478**, L83 (1997).
7. J. Daniel and T. Tajima, Astrophys. J. **498**, 296 (1998).
8. V. Berezhiani, D. D. Tskhakaya, and P. K. Shukla, Phys. Rev. A **46**, 6608 (1992).
9. C. M. Surko and T. Murphy, Phys. Fluids B **2**, 1372 (1990).
10. L. Arons, Astrophys. Space Sci. *Library* **357***,* 373 (2009).
11. G. Livadiotis, D. J. Mc Comas, J. Geophys. Res. **114**, A11105 (2009).
12. J. Arons, Space Sci. Rev. **24**, 417 (1979).
13. J. I. Vette, Particle and Fields in the Magnetosphere, Reidel Dordrecht (1970).
14. T. Kotani, N. Kawai, M. Matsuoka, and W. Brinkmann, Publ. Astron. Soc. Jpn. **48**, 619 (1996
15. Y. Nejoh, J. Plasma Phys. **37**, 487 (1987).
16. S. Gill, A. Singh, H. Kaur, N.S. Saini, P. Bala, Phys. Lett. A. **361**, 364 (2007).
17. M. G. Hafez, M. R. Talukder, and M. H. Ali, Phys. Plasmas **23**, 012902 (2016).
18. A. Shah, R. Saeed, Phys. Lett. A **373**, 4164 **(**2009).
19. G. C. Das and S. N. Paul, Phys. Fluid,28,823(1985)
20. D. B. Doumaz, M. Djebli, Phys. Plasmas **17**, 074501 **(**2010).
21. M. E. Dieckmann, B. Elisson, P. K. Shukla, Phys. Rev. E **70**, 036401 (2004).
22. S. Usami, H. Hasegawa and Y. Ohsawa, Phys. Plasmas **8**, 2666 (2001).
23. H. R. Pakzad, R. Hamid Astrophys. and Space Sci. **334**, 337 (2011).
24. H. R. Pakzad, K. Javidan, Indian J. Phys. **87,** 705 (2013).
25. M. Tribeche, H. R. Pakzad, R. Hamid, Astrophys. Space Sci. **339**, 237 (2012).
26. V. Munoz, arXiv.org: Physics 041020 (2004).
27. F. L. Scraf, F. V. Coroniti, C. F. Kennel, E. J. Smith, J. A. Slavin, B.T. Tsurutani, S. J. Bame, and W. C. Feldman, Geophys. Ress. Lett. **11**, 1050 (1984).

28. F. L. Scraf, F. V. Coroniti, C. F. Kennel, R. W. Fredricks, D.A. Gurnett, and E. J. Smith, Geophys. Ress. Lett. **11**, 335 (1984).
29. W. Masood, H. Rizvi, Phys. Plasmas **17**, 052314 (2010).
30. W. Masood, N. Jehan, A. M. Mirza, P.H. Sakanaka, Phys. Lett. A **372**, 4279 (2008).
31. H. Ikezi, R. Taylor, and D. Baker, Phys. Rev. Lett. **25**, 11 (1970).
32. Y. Nejoh, Phys. Fluids B **4**, 2830 (1992).
33. H. Alfven and P. Carlqvist, Solar Phys. **1**, 220 (1967).
34. Y. N. Nejoh, Phys. Plasmas **3**, 1447 (1996).
35. M. S. Alam, M. G. Hafez, M. R. Talukder, M. H. Ali, Phys. Plasmas **24**, 072901 (2017).
36. M. G. Hafez, and M. R. Talukder, Astrophys. Space Sci. **359**, 27 (2015).
37. M. G. Hafez, N. C. Roy, M. R. Talukder, M. H. Ali, Astrophys. Space Sci. **361**, 312 (2016).
38. J. N. Han, L. He, N. X. Yang, Z. H. Han, X. X. Wang, Physics Lett. A **375**, 3794 (2011).
39. I.V. Moskalenko, A. W. Strong, Astrophys. J. **493**, 694 (1998); O. Adriani, G. C. Barbarino, G. A. Bazilevskaya, Nature **458**, 607 (2009).
40. M. R. Brown, Phys. Plasmas **6**, 1717 (1999).
41. M. G. Hafez, M. R. Talukder, M. H. Ali, Phys. Plasmas **23**, 012902 (2016).
42. S. Ali, W. M. Moslem, P. K. Shukla, R. Schlickeiser, Phys. Plasmas **14**, 082307 (2007).
43. J. K. Xue, Phys. Rev. E **69**, 016403 (2004).
44. M. G. Hafez, N. C. Roy, M. R. Talukder, M. H. Ali, Plasma Sci. Technol. **19**, 015002 (2017).
45. H. Washimi, T. Taniuti, Phys. Rev. Lett. **17**, 996 (1996).
46. S. I. Popel, S. V. Vladimirov, P. K. Shukla, Phys. Plasmas **2**, 716 (1995).
47. C.H. Su, R.M. Mirie, J. Fluid Mech. **98**, 509 (1980).
48. W. Masood, A. M. Mirza, M. Hanif, Phys. Plasmas **15**, 072106 (2008).
49. J. N. Han, X. X. Yang, D. X. Tian, and W. S. Duan, Phys. Lett. A **372**, 4817 (2008).
50. M. A. Khaled, Astrophys. Space Sci. **350**, 607 (2014).
51. N. S. Saini and K. Singh, Phys. Plasmas **23**, 103701 (2016).
52. P. Chatterjee, U. N. Ghosh, J. Eur. Phys. **64**, 413 (2011).

Abbreviation and Nomenclature:

KdV = Korteweg-de Vries

ePLK = extended Poincaré-Lighthill-Kuo

WRR (HRR) = weakly (highly) relativistic regime

ASCA = Advanced Satellite for Cosmology and Astrophysics

ep = electron-positron

epi = electron-positron-ion

M eV = mega electron volt

$n_i(u_i)$ = number density (fluid velocity) of relativistic ion

$n_e(n_p)$ = concentration of nonextensive electron (positron)

ϕ/Φ = electrostatic potential

C_s = thermal speed

Γ = Gamma function

T_i = ion temperature

T_p = positron temperature

T_e = electron temperature

m_α= mass of α species

e_α= charge of α species

k_B= Boltzmann constant

$n_{\alpha 0}$ = unperturbed density of α species

v_α = velocity of α species

T_α = temperature of α species

q_e = nonextensive parameter of electron

q_p = nonextensive parameter of positron

T_{ip} = temperature ratio of ion to electron temperature

T_{ep} = temperature ratio of electron to positron temperature

λ_{De} = electron Debye length

ω_{pi} = ion plasma frequency

η_i = viscosity coefficient of ion

$\eta_1 = \eta_i/\varepsilon$

γ = Lorentz factor

$p = n_{p0}/n_{e0}$ = density ratio of unperturbed positron to electron density

β = relativistic streaming factor

λ_p = phase velocity of ion acoustic shock waves

A (A_1) = coefficient of nonlinearity in KdVB equation

B (B_1) = coefficient of dispersion in KdVB equation

C (C_1) = coefficient of dissipation in KdVB equation

$\nabla v_-(\nabla v_+)$ = phase shift of right (left) moving soliton

Chapter 6

Head-on collision between positron acoustic waves in homogeneous and inhomogeneous plasmas

6.1 Introduction

It is well known that the electron–positron (ep) and electron–positron–ion (epi) plasmas are existed in astrophysical and space plasmas, especially in the ionosphere [1], auroral acceleration regions [2], solar wind [3], quasar and pulsar magnetosphere [4], active galactic nuclei [4], Van Allen radiation belts [5], polar cup of fast rotating neutron stars [6], semiconductor plasmas [7], intense laser fields [8] and so on. The ep plasmas are not only existed in astrophysical objects, but also produced in laboratory in which the positrons may be used to probe the particle transport in tokamak plasmas [9-10]. However, it is not an easy task to the researchers for the production of astrophysical or space like plasmas in the laboratory for better understanding of the basic characteristics of plasmas. Further, one may frequently encounters nonlinear collective influences to the plasmas, which cannot appropriately be considered without tedious mathematical techniques. The dispersion and dissipation of waves along with nonlinearities are produced several consistent structures in the plasmas, such as solitary waves, shock waves, double layer, vortices, etc., which play important roles for understanding physical phenomena from both the theoretical and experimental point of views. Therefore, the studies of nonlinear wave propagation in the epi plasmas become one of the most essential aspects in recent years due to its broad applications and potentiality as mentioned earlier. A number of researchers [11-22] have studied the nonlinear wave propagation in different epi plasmas. Ghosh and Bharuthram [15] have described the small but finite amplitude ion acoustic solitons and double layers in plasmas consisting of Boltzmann electrons, Boltzmann positrons, singly charged cold positive ions, and negatively charged static dusts and found the existence of both compressive and rarefactive solitons as well as double layers in the considered plasma system. Besides, plasmas in space or in laboratories may contain substantially high energy particles. The high energy particles may arise due to the influence of external forces acting on the natural space plasmas or wave particle interactions. Adriani et al. [23] observed the abundance of positrons in the cosmic

radiation in the energy range from 1.5–100 GeV through PAMELA satellite. Surko et al. [24] carried out experiment for the development of materials for conversion from fast (several hundred keV), through either radioactive decay or pair production, to slow (few eV) positrons. The annihilation, for the interaction of electrons and positrons, usually occurs at much longer characteristic time scales compared to the time of collective interaction between the charged particles [25-26]. Yu and Luo [27] have showed that the different species occupy different regions of phase space and therefore it is reasonable to consider different temperatures of the species in the multi-species plasma model for constructing quasi-stationary nonlinear structures. Jilani et al. [28] have investigated the properties of fully nonlinear electron acoustic solitary waves in an unmagnetized and collisionless epi plasma and considered cold electron density $n_{e0c} \approx (0.1-0.4)\mathrm{cm}^{-3}$, positron density $n_{p0} \approx (1.5-3)\mathrm{cm}^{-3}$, hot electron density $n_{e0h} \approx 1.53\ \mathrm{cm}^{-3}$, temperature of hot electrons $T_{eh} \approx (200-1000)$ eV,and temperature of positrons $T_p \approx (200-1000)$ eV to satisfy various plasma systems from laboratory level to astrophysical environments. Moreover, astrophysical and space plasmas with an excess of superthermal electrons or positrons are generally characterized by a long tail in the high energy region, which can be studied by considering generalized Lorentzian or kappa distributions [29-31]. The presence of a significant number of superthermal particles follow kappa distribution, but not the Maxwellian one, can significantly change the rate of resonant energy transfer between particles and plasma waves [32-33**]**.

Positron acoustic waves are mainly acoustic-type, where the inertia is provided by the cold positron mass and the restoring force is provided by the thermal pressure of hot positrons and electrons. Besides, the phase speed between the thermal speed of hot positrons (v_{hp}) or electrons (v_e) and cold positrons (v_{cp}) is considered as $v_{cp} \ll \omega/k \ll v_{hp,e}$ and their frequency is much higher than ion plasma frequency. This phenomenon is allowed us to consider the dynamics of inertial cold positrons, non-Maxwellian hot positrons and electrons, and stationary ions. For instance, Tribeche et al. [34], Tribeche [35] and Sahu [36] have investigated the nonlinear positron acoustic solitary waves and double layers dynamics of mobile cold positrons in four-component epi plasmas consisting of immobile positive ions, mobile cold positrons, and Maxwell-Boltzmann distributed hot positrons and electrons. El-Shamy et al. [26] have studied the head-on collision between two positron acoustic solitary

waves by deriving two-sided KdV equations. Recently, Alam et al. [37] have studied the positron acoustic KdV solitary waves, mKdV solitary waves, Gardner solitary waves, and double layers in the epi plasmas composing immobile positive ions, mobile cold and hot positrons, and superthermal hot electrons, in unmagnetized homogeneous plasmas and have found that the kappa distributed electrons and positrons significantly modify amplitudes, widths, polarity, and phase speed of positron acoustic KdV solitary waves, mKdV solitary waves, Gardner solitary waves, and double layers in the plasmas. The nonlinear dynamics of positron acoustic waves in epi plasmas are considered for describing the physical issues in astrophysical and space environments [38-41]. Shah and Rakha [41] have studied the solitary waves excited by positron showers in naturally doped superthermal astrophysical plasmas. Shah et al. [42] have studied the nonlinear positron acoustic shock waves in astrophysical plasmas. They have mentioned that positron acoustic wave propagation is useful for better understanding the behaviors of several astrophysical objects, such as neutron starts [43], pulsar magnetosphere [4], active galactic nuclei [6], and so on. Very recently, Saha et al. [40] have investigated nonlinear excitations of positron acoustic waves in auroral acceleration regions. Saha [44] has studied qualitative changes in the dynamics of nonlinear small amplitude and fully nonlinear arbitrary amplitude positron acoustic waves in solar wind, ionosphere, lower part of magnetosphere, and auroral acceleration regions. Saha and Tamang [45] have analyzed positron acoustic waves in epi plasmas for understanding the qualitative behavior of the cosmic rays. However, the head-on collisions between KdV and mKdV solitary waves with their corresponding phase shifts, subsequently the production of rogue waves in unmagnetized homogeneous as well as KdV and mKdV solitary waves in inhomogeneous plasmas are considered for understanding the unrevealed physical issues in the plasma system [37]. When two solitary waves interact, they exchange their energies, and consequently produce phase shifts [46]. The phase shift, can be either positive or negative, depends on the velocity during the collision stage. Collision occurs in two ways: the overtaking collision [47] occurs when the angle between the interacting waves is zero, while the head-on collision [48-50] occurs when the angle between the interacting solitons is π. In such collision, the nonlinear evolution equations can be derived using the extended Poincaré-Lighthill-Kuo (ePLK) method [51].The solitary wave solutions of these equations are useful for better understanding the electrostatic resonance phenomena that are observed in plasma experiments [52]. Being motivated, for the significance of the problems related to the

astrophysical and laboratory plasmas, the head-on collision among KdV solitary waves, mKdV solitary waves and rogue waves (RWs) in unmagnetized homogeneous plasmas consisting of immobile positive ions, mobile cold positrons, and kappa distributed hot positrons and electrons are investigated. The influence of plasma inhomogeneity on the propagation of positron acoustic KdV solitary waves and mKdV solitary waves are also investigated in the considered plasmas. In sequence of introduction, theoretical model and derivations of two-sided KdV and mKdV equations with their corresponding phase shifts are presented in Section 6.2. Derivation of nonlinear Schrödinger equation (NLSE) along with its rational function solution is displayed in Section 6.3. Formations of KdV and mKdV equations in inhomogeneous plasmas with analytical solutions are presented in Section 6.4. The results and discussion are described in Section 6.5. Finally, the conclusion is drawn in section 6.6.

6.2 Governing equations

6.2.1 Model equations

Let us consider a four-component plasma system consisting of immobile positive ions, mobile cold positron, and kappa distributed hot positrons, and hot electrons. The charge neutrality condition is as $n_{e0} = n_{pc0} + n_{ph0} + n_{i0}$, where n_{i0} ,n_{e0}, n_{pc0} ,and n_{ph0} are the unperturbed number density of ions, electrons, cold positrons, and hot positrons, respectively. The nonlinear dynamics of positron acoustic waves in the plasmas [37], the normalized hydrodynamic fluids can be written as

$$\frac{\partial n_{pc}}{\partial t} + \frac{\partial}{\partial x}(n_{pc}\, u_{pc}) = 0\,, \tag{6.1}$$

$$\frac{\partial u_{pc}}{\partial t} + u_{pc}\frac{\partial u_{pc}}{\partial x} = -\frac{\partial \phi}{\partial x}, \tag{6.2}$$

$$\frac{\partial^2 \phi}{\partial x^2} = -n_{pc} - \mu_{ph}\left(1 + \frac{\sigma_1 \phi}{K_p - \frac{3}{2}}\right)^{-K_p+\frac{1}{2}} + \mu_e\left(1 - \frac{\sigma_2 \phi}{K_e - \frac{3}{2}}\right)^{-K_e+\frac{1}{2}} - \mu_i. \tag{6.3}$$

Here, n_{pc} is the cold positron number density normalized by n_{pc0} ,u_{pc} is the cold positron fluid speed normalized by positron acoustic speed $C_{pc} = \left(k_B T_{ef}/m_p\right)^{1/2}$, ϕ is the electrostatic wave potential normalized by $k_B T_{ef}/e$, $\sigma_1 = T_{ef}/T_{ph}$, $\sigma_2 = T_{ef}/T_e$, $\mu_{ph} = n_{ph0}/n_{pc0}$, $\mu_e = n_{e0}/n_{pc0}$, $\mu_i = n_{i0}/n_{pc0}$, where $T_{ef} = T_e T_{ph}/(\mu_e T_{ph} + \mu_{ph} T_e)$ is the

effective temperature, k_B is the Boltzmann constant, m_p is the positron mass, e is the magnitude of electron charge and $\kappa_{e(p)} > 3/2$ is the superthermal parameter for hot electrons (positrons), respectively. The time t is normalized by the period $\omega_{pc}^{-1} = \left(m_p/4\pi n_{pc0}e^2\right)^{1/2}$ of cold positron plasma and the space x is normalized by the positron Debye length $\lambda_{Dm} = \left(k_B T_{ef}/4\pi n_{pc0}e^2\right)^{1/2}$.

6.2.2 Formation of two-sided KdV equations and phase shift

In order to investigate the resonance of electrostatic potential and their corresponding phase shift, one needs to transform the normalized fluid Eqs. (6.1)-(6.3) considering the following coordinate [51] that give away the separation of variables and allows successful elimination of the seculars terms from the desired evolution equations:

$$\left.\begin{aligned} \xi &= \varepsilon\left(x - \lambda_p t\right) + \varepsilon^2 P_0(\xi,\eta,\tau) + \cdots \\ \eta &= \varepsilon\left(x + \lambda_p t\right) + \varepsilon^2 Q_0(\xi,\eta,\tau) + \cdots \\ \tau &= \varepsilon^3 t \end{aligned}\right\}, \tag{6.4}$$

where ξ and η are the trajectories of solitons traveling toward to each other, and λ_p is the unknown phase velocity of positron acoustic waves and ε is the proper fraction parameter measuring the limitation of the dispersion. The other variables $P_0(\xi,\eta,\tau)$ and $Q_0(\xi,\eta,\tau)$ involved in Eq. (6.4) will be evaluated later. The dependent perturbed quantities are expanded taking the small deviations from the equilibrium state [51] as

$$\mathcal{H} = \mathcal{H}^0 + \sum_{i=1}^{\infty} \varepsilon^i \mathcal{H}^{(i)} \tag{6.5}$$

where $\mathcal{H} = (n_{pc} \quad u_{pc} \quad \phi)'$, $\mathcal{H}^0 = (1 \quad 0 \quad 0)'$ and $\mathcal{H}^{(i)} = \left(n_{pc}^{(i)} \quad u_{pc}^{(i)} \quad \phi^{(i)}\right)'$. Inserting Eqs.(6.4) and (6.5) into Eqs. (6.1)-(6.3) and separating the quantities with the different power of ε, one can obtain the set of coupled equations in terms of ε. To the lowest order of ε yeilds

$$-\lambda_p \frac{\partial n_{pc}^{(1)}}{\partial \xi} + \lambda_p \frac{\partial n_{pc}^{(1)}}{\partial \eta} + \frac{\partial u_{pc}^{(1)}}{\partial \xi} + \frac{\partial u_{pc}^{(1)}}{\partial \eta} = 0, \tag{6.6}$$

$$-\lambda_p \frac{\partial u_{pc}^{(1)}}{\partial \xi} + \lambda_p \frac{\partial u_{pc}^{(1)}}{\partial \eta} + \left(\frac{\partial \phi^{(1)}}{\partial \xi} + \frac{\partial \phi^{(1)}}{\partial \eta}\right) = 0, \tag{6.7}$$

$$n_{pc}^{(1)} = \left\{ \frac{\mu_{ph}\left(\kappa_p - \frac{1}{2}\right)\sigma_1}{\kappa_p - \frac{3}{2}} + \frac{\mu_e\left(\kappa_e - \frac{1}{2}\right)\sigma_2}{\kappa_e - \frac{3}{2}} \right\} \phi^{(1)} . \tag{6.8}$$

One may define the physical relations along with the different quantities, say $\phi_{\xi}^{(1)}(\xi,\tau) \approx \phi_{\xi}^{(1)}$ and $\phi_{\eta}^{(1)}(\eta,\tau) \approx \phi_{\eta}^{(1)}$ as

$$\phi^{(1)} = \phi_{\xi}^{(1)} + \phi_{\eta}^{(1)}, n_{pc}^{(1)} = R_1\left[\phi_{\xi}^{(1)} + \phi_{\eta}^{(1)}\right], u_{pc}^{(1)} = \frac{1}{\lambda_p}\left[\phi_{\xi}^{(1)} - \phi_{\eta}^{(1)}\right], \quad (6.9)$$

with

$$R_1 = \left\{\frac{\mu_{ph}\left(\kappa_p - \frac{1}{2}\right)\sigma_1}{\kappa_p - \frac{3}{2}} + \frac{\mu_e\left(\kappa_e - \frac{1}{2}\right)\sigma_2}{\kappa_e - \frac{3}{2}}\right\},$$

which stratifies Eqs. (6.6)-(6.8). Here, $\phi_{\xi}^{(1)}$ and $\phi_{\eta}^{(1)}$ denote the two-sided electrostatic solitary waves, one of which $\phi_{\xi}^{(1)}$ propagates to the right and $\phi_{\eta}^{(1)}$ propagates to the left directions. Using the solvability condition, the phase velocity can be obtained as $\lambda_p = \sqrt{1/R_1}$. To the second order of ε gives

$$-\lambda_p\frac{\partial n_{pc}^{(2)}}{\partial\xi} + \lambda_p\frac{\partial n_{pc}^{(2)}}{\partial\eta} + \frac{\partial u_{pc}^{(2)}}{\partial\xi} + \frac{\partial u_{pc}^{(2)}}{\partial\eta} + \frac{\partial}{\partial\xi}\left(n_{pc}^{(1)}u_{pc}^{(1)}\right) + \frac{\partial}{\partial\eta}\left(n_{pc}^{(1)}u_{pc}^{(1)}\right) = 0, \quad (6.10)$$

$$-\lambda_p\frac{\partial u_{pc}^{(2)}}{\partial\xi} + \lambda_p\frac{\partial u_{pc}^{(2)}}{\partial\eta} + \frac{1}{2}\frac{\partial}{\partial\xi}\left\{u_{pc}^{(1)}\right\}^2 + \frac{1}{2}\frac{\partial}{\partial\eta}\left\{u_{pc}^{(1)}\right\}^2 + \left(\frac{\partial\phi^{(2)}}{\partial\xi} + \frac{\partial\phi^{(2)}}{\partial\eta}\right) = 0, \quad (6.11)$$

$$-n_{pc}^{(2)} + R_1\phi^{(2)} - R_2\left\{\phi^{(1)}\right\}^2 = 0\,, \quad (6.12)$$

where $R_2 = \left\{\frac{\mu_{ph}\left(\kappa_p-\frac{1}{2}\right)\left(\kappa_p+\frac{1}{2}\right)\sigma_1^2}{2\left(\kappa_p-\frac{3}{2}\right)^2} - \frac{\mu_e\left(\kappa_e-\frac{1}{2}\right)\left(\kappa_e+\frac{1}{2}\right)\sigma_2^2}{2\left(\kappa_e-\frac{3}{2}\right)^2}\right\}$, which can be simplified with the help of Eq. (6.9) along with the different quantities, say $\phi_{\xi}^{(2)}(\xi,\tau) \approx \phi_{\xi}^{(2)}$ and $\phi_{\eta}^{(2)}(\eta,\tau) \approx \phi_{\eta}^{(2)}$ as

$$\left.\begin{aligned} \phi^{(2)} &= \phi_{\xi}^{(2)} + \phi_{\eta}^{(2)} + \widetilde{\phi^{(2)}} \\ n_{pc}^{(2)} &= \frac{1}{\lambda_p^2}\left[\phi_{\xi}^{(2)} + \phi_{\eta}^{(2)}\right] + \frac{3}{2\lambda_p^4}\left[\left\{\phi_{\xi}^{(1)}\right\}^2 + \left\{\phi_{\eta}^{(1)}\right\}^2\right] + \widetilde{n_{pc}^{(2)}} \\ u_{pc}^{(2)} &= \frac{1}{\lambda_p}\left[\phi_{\xi}^{(2)} - \phi_{\eta}^{(2)}\right] + \frac{1}{2\lambda_p^3}\left[\left\{\phi_{\xi}^{(1)}\right\}^2 - \left\{\phi_{\eta}^{(1)}\right\}^2\right] + \widetilde{u_{pc}^{(2)}} \end{aligned}\right\} \quad (6.13)$$

Equations (6.13) are coupled through

$$-\left(\frac{3}{2\lambda_p^4} + R_2\right)\left\{\phi_{\xi}^{(1)}\right\}^2 = -\left(\frac{3}{2\lambda_p^4} + R_2\right)\left\{\phi_{\eta}^{(1)}\right\}^2 = 0 \quad (6.14)$$

and

$$\frac{\partial^2}{\partial\xi\partial\eta}\widetilde{\phi^{(2)}} - \lambda_p^2\left(R_2+\frac{1}{2}R_1\right)\frac{\partial\phi_\xi^{(1)}}{\partial\xi}\frac{\partial\phi_\eta^{(1)}}{\partial\eta} - \frac{\lambda_p^4}{4}(R_1^2-2R_2)\left[\phi_\eta^{(1)}\frac{\partial^2\phi_\xi^{(1)}}{\partial\xi^2}+\phi_\xi^{(1)}\frac{\partial^2\phi_\eta^{(1)}}{\partial\eta^2}\right]=0.$$

It is observed from Eq. (6.14) that there can arise two cases, such as $\phi_\xi^{(1)}=\phi_\eta^{(1)}=0$ which is the generic case and $\frac{3}{2\lambda_p^4}+R_2=0$. Considering the generic case, Eq. (6.13) are converted to

$$\phi^{(2)}=\phi_\xi^{(2)}+\phi_\eta^{(2)}, n_{pc}^{(2)}=R_1\left[\phi_\xi^{(2)}+\phi_\eta^{(2)}\right], u_{pc}^{(2)}=\frac{1}{\lambda_p^3}\left[\phi_\xi^{(2)}-\phi_\eta^{(2)}\right]. \quad (6.15)$$

The third order of ε gives

$$\left.\begin{aligned} -\lambda_p\frac{\partial n_{pc}^{(3)}}{\partial\xi}+\lambda_p\frac{\partial n_{pc}^{(3)}}{\partial\eta}+\frac{\partial u_{pc}^{(3)}}{\partial\xi}+\frac{\partial u_{pc}^{(3)}}{\partial\eta}=0\\ -\lambda_p\frac{\partial u_{pc}^{(3)}}{\partial\xi}+\lambda_p\frac{\partial u_{pc}^{(3)}}{\partial\eta}+\left(\frac{\partial\phi^{(3)}}{\partial\xi}+\frac{\partial\phi^{(3)}}{\partial\eta}\right)=0\\ n_{pc}^{(3)}=R_1\phi^{(3)}\end{aligned}\right\}. \quad (6.16)$$

Since the variables involved in Eqs.(6.16) will not occur for the fourth order in ε, thus one may consider $n_{pc}^{(3)}=u_{pc}^{(3)}=\phi^{(3)}=0$. Finally, the fourth order of ε gives the following relation:

$$\begin{aligned}\int\left(\frac{\partial\phi_\xi^{(2)}}{\partial\tau}+A\phi_\xi^{(2)}\frac{\partial\phi_\xi^{(2)}}{\partial\xi}+B\frac{\partial^3\phi_\xi^{(2)}}{\partial\xi^3}\right)d\eta+\int\left(\frac{\partial\phi_\eta^{(2)}}{\partial\tau}-A\phi_\eta^{(2)}\frac{\partial\phi_\eta^{(2)}}{\partial\eta}-B\frac{\partial^3\phi_\xi^{(2)}}{\partial\eta^3}\right)d\xi\\ +\iint\left\{\left(C\frac{\partial P_0}{\partial\eta}-D\phi_\eta^{(2)}\right)\frac{\partial^2\phi_\xi^{(2)}}{\partial\xi^2}-\left(C\frac{\partial Q_0}{\partial\xi}-D\phi_\xi^{(2)}\right)\frac{\partial^2\phi_\eta^{(2)}}{\partial\eta^2}\right.\\ \left.+\frac{\partial^2}{\partial\xi\partial\eta}\left[C\widetilde{\phi^{(2)}}+4D\phi_\xi^{(2)}\phi_\eta^{(2)}\right]\right\}d\xi d\eta=-2\lambda_p^2u_{pc}^{(4)}, \quad (6.17)\end{aligned}$$

where $A=\left[\frac{3}{2\lambda_p}+R_2\lambda_p^3\right], B=\frac{\lambda_p^3}{2}, C=2\lambda_p$ and $D=\left[\frac{1}{2\lambda_p}-R_2\lambda_p^3\right]$.

The integrands in the first and second terms in the left hand side of (6.17) do not depend on η and ξ, respectively. So, all the terms of the first two expressions in the left hand side of Eq. (6.17) become secular, which should be eliminated in order to avoid unexpected resonances. Hence, one can derive the following two-sided KdV equations:

$$\frac{\partial\phi_\xi^{(2)}}{\partial\tau}+A\phi_\xi^{(2)}\frac{\partial\phi_\xi^{(2)}}{\partial\xi}+B\frac{\partial^3\phi_\xi^{(2)}}{\partial\xi^3}=0, \quad (6.18)$$

$$\frac{\partial \phi_\eta^{(2)}}{\partial \tau} - A\phi_\eta^{(2)} \frac{\partial \phi_\eta^{(2)}}{\partial \eta} - B \frac{\partial^3 \phi_\xi^{(2)}}{\partial \eta^3} = 0. \quad (6.19)$$

The stationary solutions of the two-sided KdV equations obtained can be written as

$$\phi_\xi^{(2)} = \phi_0 \ \mathrm{sech}^2 \left\{ \frac{(\xi - U_0\tau)}{W_0} \right\}, \phi_\eta^{(2)} = \phi_0 \mathrm{sech}^2 \left\{ \frac{(\eta + U_0\tau)}{W_0} \right\}, \quad (6.20)$$

where $\phi_0 = (3U_0/A)$ and $W_0 = \sqrt{((4B/U_0)}$ are the amplitudes and widths of the solitary waves traveling in the opposite direction from their initial positions and U_0 is the constant velocity of the reference frame. It is also seen that the third term in Eq. (6.17) is dependent on both ξ and η, except τ, provides

$$\left(C \frac{\partial P_0}{\partial \eta} - D\phi_\eta^{(2)} \right) \frac{\partial^2 \phi_\xi^{(2)}}{\partial \xi^2} - \left(C \frac{\partial Q_0}{\partial \xi} - D\phi_\xi^{(2)} \right) \frac{\partial^2 \phi_\eta^{(2)}}{\partial \eta^2} + \frac{\partial^2}{\partial \xi \partial \eta} \left[C\widetilde{\phi^{(2)}} + 4D\phi_\xi^{(2)} \phi_\eta^{(2)} \right] = 0 \quad (6.21)$$

The first and second terms in the left hand side of Eq. (6.21) may become secular in the next power of ε and provide the following relations:

$$P_0 = \frac{D}{C} \int_{-\infty}^{\eta} \phi_\eta^{(1)}(\chi, \tau) d\chi \ ; Q_0 = \frac{D}{C} \int_{\infty}^{\xi} \phi_\xi^{(1)}(\chi, \tau) d\chi \ . \quad (6.22)$$

It is clearly seen that the leading phase functions in Eq. (6.22) due to the weak interactions among the solitons can be obtained with the help of Eq. (6.20) as

$$P_0 = \frac{D}{C} \phi_0 W_0 \left[\tanh \left(\frac{\eta + U_0\tau}{W_0} \right) + 1 \right], Q_0 = \frac{D}{C} \phi_0 W_0 \left[\tanh \left(\frac{\xi - U_0\tau}{W_0} \right) - 1 \right]. \quad (6.23)$$

Therefore, the trajectories of the two positron acoustic solitary waves for weak head-on collision are obtained up to the order of ε^2 as:

$$\xi = \varepsilon(x - \lambda_p t) + \varepsilon^2 \frac{D}{C} \phi_0 W_0 \left[\tanh \left(\frac{\eta + U_0\tau}{W_0} \right) + 1 \right] + \cdots, \quad (6.24)$$

$$\eta = \varepsilon(x + \lambda_p t) + \varepsilon^2 \frac{D}{C} \phi_0 W_0 \left[\tanh \left(\frac{\xi - U_0\tau}{W_0} \right) - 1 \right] + \cdots \ . \quad (6.25)$$

In order to obtain the phase shift after the head-on collision between two solitons, say S_R and S_L, one can assume that the solitons S_R at $\xi = 0, \eta \to -\infty$ and S_L at $\eta = 0, \xi \to +\infty$ are asymptotically far away from each other at the initial time ($t \to -\infty$). After collision ($t \to$

$+\infty$), S_R is far to the right of S_L, that is, S_R is at $\xi = 0, \eta \to +\infty$ and S_L is at $\eta = 0, \xi \to -\infty$ .Using Eqs. (6.24) and (6.25), one can obtain the corresponding phase shifts as

$$\nabla P_0 = -2\varepsilon^2 \frac{D}{C}\phi_0 W_0, \nabla Q_0 = 2\varepsilon^2 \frac{D}{C}\phi_0 W_0 \ . \tag{6.26}$$

On the other hand, the dispersion coefficient (B) of the coupled KdV equations is always positive. Therefore, the positron acoustic waves are obtained compressive for $A > 0$ and rarefactive for $A < 0$ depanding on the physical parameters. It is clearly seen that the amplitudes of the two-sided KdV solitons of Eqs. (6.18) and (6.19) and their corresponding magnitudes of phase shifts approaches to infinity, when $A \to 0$. Under this condition, the validity of the reductive perturbation technique breaks down. In order to find the parametric regimes for which the compressive and rarefactive electrostatic potential of the solitary waves may exist, one can obtain the following condition for $\mu_{ph} = \mu_c$ taking $A(\mu_{ph} = \mu_c) = 0$ into account:

$$\mu_{pc} = \mu_c = -\frac{(2\kappa_p + 1)}{6(2\kappa_p - 1)} - \frac{(2\kappa_p - 3)(2\kappa_e - 1)\mu_2\sigma_2}{(2\kappa_p - 1)(2\kappa_e - 3)\sigma_1} + \frac{(2\kappa_p + 1)(-2\kappa_e + 3)}{6(2\kappa_p - 1)(2\kappa_e - 3)} + \frac{\sigma_1\sqrt{g_1} + \sqrt{g_2}}{6(2\kappa_p - 1)(2\kappa_e - 3)\sigma_1}, \tag{6.27}$$

where $g_1 = 12(2\kappa_p + 1)(2\kappa_e - 3)(4\kappa_e^2 - 8\kappa_3 + 3)\mu_2\sigma_2$ and $g_2 = 12(-2\kappa_p + 3)^2(4\kappa_e^2 - 1)\mu_2\sigma_2^2$. For instance, one can obtain the critical values from the above relation, say $\mu_{pc} = \mu_c \cong 0.0818$ taking $\mu_e = 0.2$, $\sigma_1 = 1$, $\sigma_2 = 0.8$, $\kappa_e = 3$ and $\kappa_p = 10$ for which the coefficient A of the KdV equations vanishes. In such case, one can consider the higher order nonlinearity to study the head-on collision between two solitary waves and their phase shift around the critical values in the plasmas.

6.2.3 Derivation of two-sided mKdV equations and phase shift

It is found that the coefficient of quadratic nonlinearity in Eqs. (6.18) and (6.19) are vanishes at the critical values $\mu_{ph} = \mu_c$ as mentioned in Eq. (6.27). In order to study the head-on collision between the solitary waves propagating toward each other and phase shift around the critical values μ_c. One may insert $\phi_\xi^{(2)} = \phi_\eta^{(2)} = 0$ and $\widetilde{\phi^{(2)}} \neq 0$ [51] and Eqs. (6.13) can be converted to

$$n_{pc}^{(2)} = \frac{3}{2}R_1^2\left[\left\{\phi_\xi^{(1)}\right\}^2 + \left\{\phi_\eta^{(1)}\right\}^2\right], u_{pc}^{(2)} = \frac{1}{2\lambda_p^3}\left[\left\{\phi_\xi^{(1)}\right\}^2 - \left\{\phi_\eta^{(1)}\right\}^2\right] \quad (6.28)$$

where $\left(\frac{3}{2\lambda_p^4} + R_2\right) = 0$.

Finally, combining the contributions around the critical region as obtained in Eqs. (6.28) for the third order term of ε yield the following relation:

$$\int\left(\frac{\partial\phi_\xi^{(1)}}{\partial\tau} + \alpha B\left\{\phi_\xi^{(1)}\right\}^2\frac{\partial\phi_\xi^{(1)}}{\partial\xi} + B\frac{\partial^3\phi_\xi^{(1)}}{\partial\xi^3}\right)d\eta + \int\left(\frac{\partial\phi_\eta^{(1)}}{\partial\tau} - \alpha B\left\{\phi_\eta^{(1)}\right\}^2\frac{\partial\phi_\eta^{(1)}}{\partial\eta} - B\frac{\partial^3\phi_\eta^{(1)}}{\partial\eta^3}\right)d\xi + \iint\left(C\frac{\partial P_0}{\partial\eta} - D^*\left\{\phi_\eta^{(1)}\right\}^2\right)\frac{\partial^2\phi_\xi^{(1)}}{\partial\xi^2}d\xi d\eta - \iint\left(C\frac{\partial Q_0}{\partial\xi} - D^*\left\{\phi_\xi^{(1)}\right\}^2\right)\frac{\partial^2\phi_\eta^{(1)}}{\partial\eta^2}d\xi d\eta + \cdots = -2\lambda_p^2 u_{pc}^{(3)}, \quad (6.29)$$

where, $\alpha = \left[\frac{15}{2\lambda_p^6} - 3R_3\right], D^* = \left[3R_3 - \frac{1}{2\lambda_p^6}\right]B,$

$$R_3 = \left\{\frac{\mu_{ph}\left(\kappa_p - \frac{1}{2}\right)\left(\kappa_p + \frac{1}{2}\right)\left(\kappa_p + \frac{3}{2}\right)\sigma_1^3}{6\left(\kappa_p - 3/2\right)^3} + \frac{\mu_e\left(\kappa_e - \frac{1}{2}\right)\left(\kappa_e + \frac{1}{2}\right)\left(\kappa_e + \frac{3}{2}\right)\sigma_2^3}{6(\kappa_e - 3/2)^3}\right\}.$$

Since, all the terms of the first two expressions in the left hand side of Eq. (6.29) become secular and should be eliminated in order to avoid unexpected resonances around the critical values. Hence, one can obtain the following two-sided coupled mKdV equations:

$$\frac{\partial\phi_\xi^{(1)}}{\partial\tau} + \alpha B\left\{\phi_\xi^{(1)}\right\}^2\frac{\partial\phi_\xi^{(1)}}{\partial\xi} + B\frac{\partial^3\phi_\xi^{(1)}}{\partial\xi^3} = 0, \quad (6.30)$$

$$\frac{\partial\phi_\eta^{(1)}}{\partial\tau} - \alpha B\left\{\phi_\eta^{(1)}\right\}^2\frac{\partial\phi_\eta^{(1)}}{\partial\eta} - B\frac{\partial^3\phi_\eta^{(1)}}{\partial\eta^3} = 0. \quad (6.31)$$

The stationary solutions of the two-sided mKdV equations can be written as

$$\phi_\xi^{(1)} = \phi_1\mathrm{sech}\left\{\frac{(\xi - U_0\tau)}{W_1}\right\}, \phi_\eta^{(1)} = \phi_1\mathrm{sech}\left\{\frac{(\eta + U_0\tau)}{W_1}\right\}, \quad (6.32)$$

where $\phi_1 = \left(\sqrt{6U_0/\alpha B}\right)$ and $W_1 = \phi_1\sqrt{(\alpha/6)}$ are the amplitudes and widths of the mKdV solitary waves approaching each other from their initial positions. On the other hand, the third

and fourth terms in the left hand side of Eq. (6.29) will become secular in the next higher order of ε and provides the following relations

$$P_0(\eta,\tau)=\frac{D^*}{C}\int_{-\infty}^{\eta}\left\{\phi_\eta^{(1)}(\chi,\tau)\right\}^2 d\chi\ , Q_0(\xi,\tau)=\frac{D^*}{C}\int_{\infty}^{\xi}\left\{\phi_\xi^{(1)}(\chi,\tau)\right\}^2 d\chi\ . \quad (6.33)$$

Finally, one can obtain the phase shifts after weak head-on collision between two mKdV solitons having equal amplitudes propagating in opposite directions as

$$\nabla P_0=-2\varepsilon^2\frac{D^*}{C}\phi_1 W_1, \nabla Q_0=2\varepsilon^2\frac{D^*}{C}\phi_1 W_1\ . \quad (6.34)$$

6.3 Derivation of NLS equation with rogue wave solution

The envelope of the soliton is investigated theoretically [53-54] and observed experimentally [55] in the multi-component plasmas for the determination of critical value for typical plasma parameters by deriving the NLSE from the mKdV equation. Further, a new type of unstable soliton, so called the peregrine solitons or RWs, has been predicted in multi-component plasmas to obtaion critical value considering certain parameters. A few authors [54, 56-59] have shown that the behavior of weakly nonlinear wave packets can be studied by employing the NLSE, which can be derived from the mKdV equation at critical plasma parameter.

In order to study the behavior of weakly nonlinear wave packets in the plasmas, one needs to derive the NLSE considering the mKdV Eq. (6.30). For simplicity, one has to transform the variables [60] as

$$\phi(\xi,\tau)=\sum_{m=1}^{\infty}\varepsilon^m\sum_{l=-m}^{m}\phi_l^m(\xi,\tau)e^{il(k\xi-\omega\tau)}, X=\varepsilon\left(\xi-v_g\tau\right), T=\varepsilon^2\tau\ , \quad (6.35)$$

where $\phi=\phi_\xi^{(1)}$, k is the wave number, ω is the angular frequency, and v_g is the group velocity of the nonlinear ion acoustic waves. Inserting Eq. (6.35) to the mKdV Eq. (6.30), collecting and equating the terms with equal order of ε. The lowest order approximation for $m=1$ with the first harmonic $l=1$ gives the dispersion relation of electrostatic waves as $\omega=-Bk^3$. The second order approximation for $m=2$ with $l=1$ predicts $v_g=-3Bk^2$. Finally, the compatibility condition can be found solving the equations considering the next higher order approximation ($m=3$) with first harmonic ($l=1$) yields the NLSE as

$$i\frac{\partial \Psi}{\partial T}+\frac{1}{2}P\frac{\partial^2 \Psi}{\partial X^2}+Q\Psi|\Psi|^2=0\,, \tag{6.36}$$

where $\phi_{\xi}^{(1)} \approx \Psi$, $P=-6Bk$ and $Q=-\alpha Bk$. It is known that the stability or instability of the envelope for external perturbations depends on the ratio of $P/Q=6/\alpha$, which indicates that the plane wave becomes stable for $\alpha<0$ and unstable for $\alpha>0$. One can study the profiles of rogue waves within the modulational unstable region ($\alpha>0$) considering the rational function solution of Eq. (6.36) as

$$\Psi(X,T)=\sqrt{\frac{P}{Q}}\left[\frac{4(1+2iPT)}{1+4P^2T^2+4X^2}-1\right]e^{iPT}. \tag{6.37}$$

On the other hand, one can derive NLS equation (6.36) to the KdV equation taking Eq. (6.35) into account. In such case, the dispersive coefficients (P) and nonlinearity (Q) coefficients are obtained as $P=6Bk$ and $Q=-(A^2/6Bk)$. It is seen that the ratio of P and Q obtained is always negative, that is $P/Q=-1/A^2$. Moreover, the weakly nonlinear theory predicts that the quasi-monochromatic wave packets are always modulationally stable and the rogue waves cannot propagate due to the existence of the negative nonlinear coefficient terms in the NLSE. This indicates that the NLSE that obtained from the KdV equation does not support the rogue wave solution.

6.4 Derivation of KdV and mKdV equations with variable coefficients

To study the effects of plasma inhomogeneity on the propagation of positron acoustic waves, one can consider stretched variables which applicable for spatially inhomogeneous plasmas [61] as

$$\xi=\varepsilon^{1/2}\left(\int\frac{dx}{V}-t\right), X=\varepsilon^{3/2}x, \tag{6.38}$$

where, V is the speed of wave propagation and the perturbed quantities can be expanded according to the well known reductive perturbation method as

$$\mathcal{H}=\sum_{i=0}^{\infty}\varepsilon^i\mathcal{H}^{(i)}\,, \tag{6.39}$$

taking only spatial gradients $\frac{\partial \mathcal{H}^{(0)}}{\partial \xi}=0$ and $\frac{\partial V}{\partial \xi}=0$, where $\mathcal{H}^{(0)}=\begin{pmatrix} n_{pc}^{(0)} & u_{pc}^{(0)} & \phi^{(0)}\end{pmatrix}'$.

Substituting Eqs.(6.38) and (6.39) into Eqs. (6.1)-(6.3) and collecting the quantities based on the equal powers of ε, one can obtain a set of equations in terms of ε. The first order of ε gives the following relations:

$$\left.\begin{aligned} n_{pc}^{(1)} = \frac{n_{pc}^{(0)}\phi^{(1)}}{\left(V-u_{pc}^{(0)}\right)^2}, u_{pc}^{(1)} = \frac{\phi^{(1)}}{\left(V-u_{pc}^{(0)}\right)}, \\ n_{pc}^{(0)}/\left(V-u_{pc}^{(0)}\right)^2 - R_1 + 2R_2\phi^{(0)} - 3R_3\{\phi^{(0)}\}^2 = 0 \end{aligned}\right\}. \quad (6.40)$$

Finally, eliminating $n_{pc}^{(2)}$, $u_{pc}^{(2)}$, and $\phi^{(2)}$ from the set of equations that can be obtained taking the next higher order of ε,one can derive the following partial differential equation (PDE) with variable coefficients as

$$\frac{\partial\phi^{(1)}}{\partial X} + \frac{A_3}{A_2}\phi^{(1)}\frac{\partial\phi^{(0)}}{\partial X} + \frac{A_1}{A_2}\phi^{(1)}\frac{\partial\phi^{(1)}}{\partial\xi} + \frac{1}{V^2A_2}\frac{\partial^3\phi^{(1)}}{\partial\xi^3} = 0, \quad (6.41)$$

where $A_1 = R_2 - 2R_3\phi^{(0)} + \frac{6n_{pc}^{(0)}}{\left(V-u_{pc}^{(0)}\right)^4}$, $A_2 = \frac{2V^2n_{pc}^{(0)}}{\left(V-u_{pc}^{(0)}\right)^3}$, $A_3 = \frac{Vn_{pc}^{(0)}(V-3u_{pc}^{(0)})}{\left(V-u_{pc}^{(0)}\right)^3\{u_{pc}^{(0)}\}^2}$.

To obtain the solitary wave solution of Eq. (6.41), one can convert Eq. (6.41) considering the transform $\phi^{(1)} = \varphi(\xi, X)e^{(-A_3/A_2)\phi^{(0)}}$as

$$\frac{\partial\varphi}{\partial X} + L\varphi\frac{\partial\varphi}{\partial\xi} + M\frac{\partial^3\varphi}{\partial\xi^3} = 0, \quad (6.42)$$

where $L = \frac{A_1}{A_2}e^{(-A_3/A_2)\phi^{(0)}}$ and $M = \frac{1}{V^2A_2}$. For the sake of simplicity for mathematical development, the variations of the coefficients L and M are assumed insignificant as compared to the scale length or it is supposed that all parameters are locally constant. Therefore, the solitary wave solutions of Eq. (6.42) can be obtained as

$$\varphi = \varphi_{v0}\mathrm{sech}^2\left\{\frac{\chi}{W_{v0}}\right\}, \chi = \xi - U_0X\,, \quad (6.43)$$

where $\varphi_0 = (3U_0/L)$ and $W_{v0} = \sqrt{(4M/U_0)}$ are the amplitudes and widths of KdV solitary waves. It is found that the amplitudes of the KdV solitary waves approach to infinity when $L \to 0$ at the critical density ratio of hot and cold positrons where the validity of the

perturbation technique breaks down. In such case, the structures of positron acoustic solitary waves around the critical densities are studied considering the higher order nonlinear PDE in weakly inhomogeneous multi-components plasmas. To do so, one needs to convert the stretched variables of (6.38) as

$$\xi = \varepsilon\left(\int \frac{dx}{V} - t\right), X = \varepsilon^3 x\,. \tag{6.44}$$

Using Eqs.(6.39) and (6.44) into Eqs. (6.1)-(6.3), one can obtain the same values of $n_{pc}^{(1)}$, $u_{pc}^{(1)}$, and the dispersion relation as mentioned in Eq. (6.40). To the next higher order of ε gives

$$n_{pc}^{(2)} = \frac{3n_{pc}^{(0)}\{\phi^{(1)}\}^2}{2\left(V-u_{pc}^{(0)}\right)^4} + \frac{n_{pc}^{(0)}\phi^{(2)}}{\left(V-u_{pc}^{(0)}\right)^2}, u_{pc}^{(2)} = \frac{\{\phi^{(1)}\}^2}{2\left(V-u_{pc}^{(0)}\right)^3} + \frac{\phi^{(2)}}{\left(V-u_{pc}^{(0)}\right)}, \tag{6.45}$$

$$\left\{\frac{n_{pc}^{(0)}}{\left(V-u_{pc}^{(0)}\right)^2} - R_1 + 2R_2\phi^{(0)} - 3R_3\{\phi^{(0)}\}^2\right\}\phi^{(2)} + \frac{1}{2}\left\{R_2 - 2R_3\phi^{(0)} + \frac{6n_{pc}^{(0)}}{\left(V-u_{pc}^{(0)}\right)^4}\right\}\{\phi^{(1)}\}^2 = 0. \tag{6.46}$$

Finally, combining a set of equations that can be obtained considering the next higher order of ε, one can derive the following PDE with variable coefficients as

$$\frac{\partial\phi^{(1)}}{\partial X} + \frac{A_5}{A_2}\phi^{(1)}\frac{\partial\phi^{(0)}}{\partial X} + \frac{A_4}{A_2}\{\phi^{(1)}\}^2\frac{\partial\phi^{(1)}}{\partial\xi} + \frac{1}{V^2A_2}\frac{\partial^3\phi^{(1)}}{\partial\xi^3} = 0, \tag{6.47}$$

where $A_4 = \frac{3}{2}\left\{\frac{n_{pc}^{(0)}}{\left(V-u_{pc}^{(0)}\right)^2} + \frac{2(1+n_{pc}^{(0)})}{\left(V-u_{pc}^{(0)}\right)^6} + 2R_3\right\}$, $A_5 = \frac{Vn_{pc}^{(0)}(2u_{pc}^{(0)}-V)}{\left(V-u_{pc}^{(0)}\right)^3\{u_{pc}^{(0)}\}^2}$.

To study the electrostatic potential structures, one can reduce Eq. (6.47) considering $\phi^{(1)} = \varphi(\xi, X)e^{(-A_5/A_2)\phi^{(0)}}$ as

$$\frac{\partial\varphi}{\partial X} + L_1\varphi^2\frac{\partial\varphi}{\partial\xi} + M\frac{\partial^3\varphi}{\partial\xi^3} = 0, \tag{6.48}$$

Where $L_1 = \frac{A_4}{A_2} e^{(-A_5/A_2)\phi^{(0)}}$. Equation (6.48) is the well known mKdV equation. Therefore, the solitary wave solutions of Eq. (6.48) can be obtained as

$$\varphi = \varphi_1 \mathrm{sech}\left\{\frac{\chi}{W_4}\right\}, \qquad \chi = \xi - U_0 X\,, \tag{6.49}$$

where $\varphi_1 = (6U_0/L_1)$ and $W_4 = \sqrt{(M/U_0)}$ are the amplitude and width of mKdV PA solitary waves.

6.5 Results and discussion

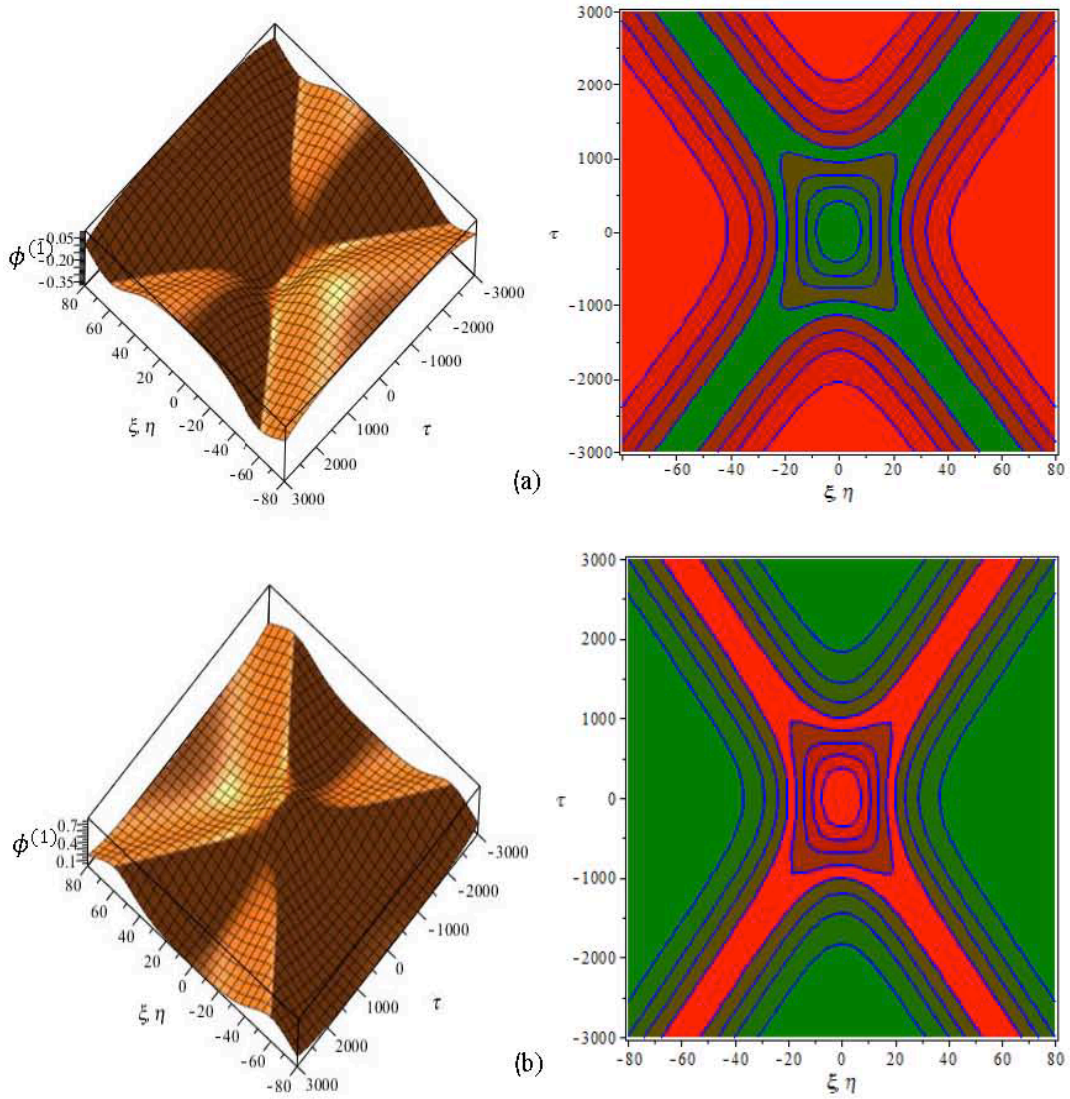

Figure 6.1 Electrostatic potential profiles ($\phi^{(1)}$) after head-on collision between the solitons of equal amplitudes as obtained from the KdV equation receding from each other (a) rarefactive solitons taking $\mu_{ph} = 0.05$, and (b) compressive solitons with surface plot (left column) and contour plot (right column) taking $\mu_{ph} = 0.1$ with regards to space and time. The remaining parameters are considered as $\kappa_e = 3$, $\kappa_p = 10$,$\mu_e = 0.2$, $\sigma_1 = 1$, $\sigma_2 = 0.8$ and $U_0 = 0.02$.

To investigate the unrevealed physical issues concerned in the homogeneous plasma, such as temporal evolution of electrostatic resonances and phase shifts due to the head-on collision of solitons, and modulational instability, two-sided KdV, mKdV, and NLSEs are derived. Besides, the KdV and mKdV equations with variable coefficients are derived to study the propagation characteristics of positron acoustic waves in a weakly inhomogenous collisionless multi-component considered plasmas. The effects of plasma parameters on the structures and propagation characteristics of solitons are considered taking into account the typical ranges $\mu_e = 0.1 - 0.8$, $\sigma_1 = 1 - 6$, $\sigma_2 = 0.1 - 0.9$,

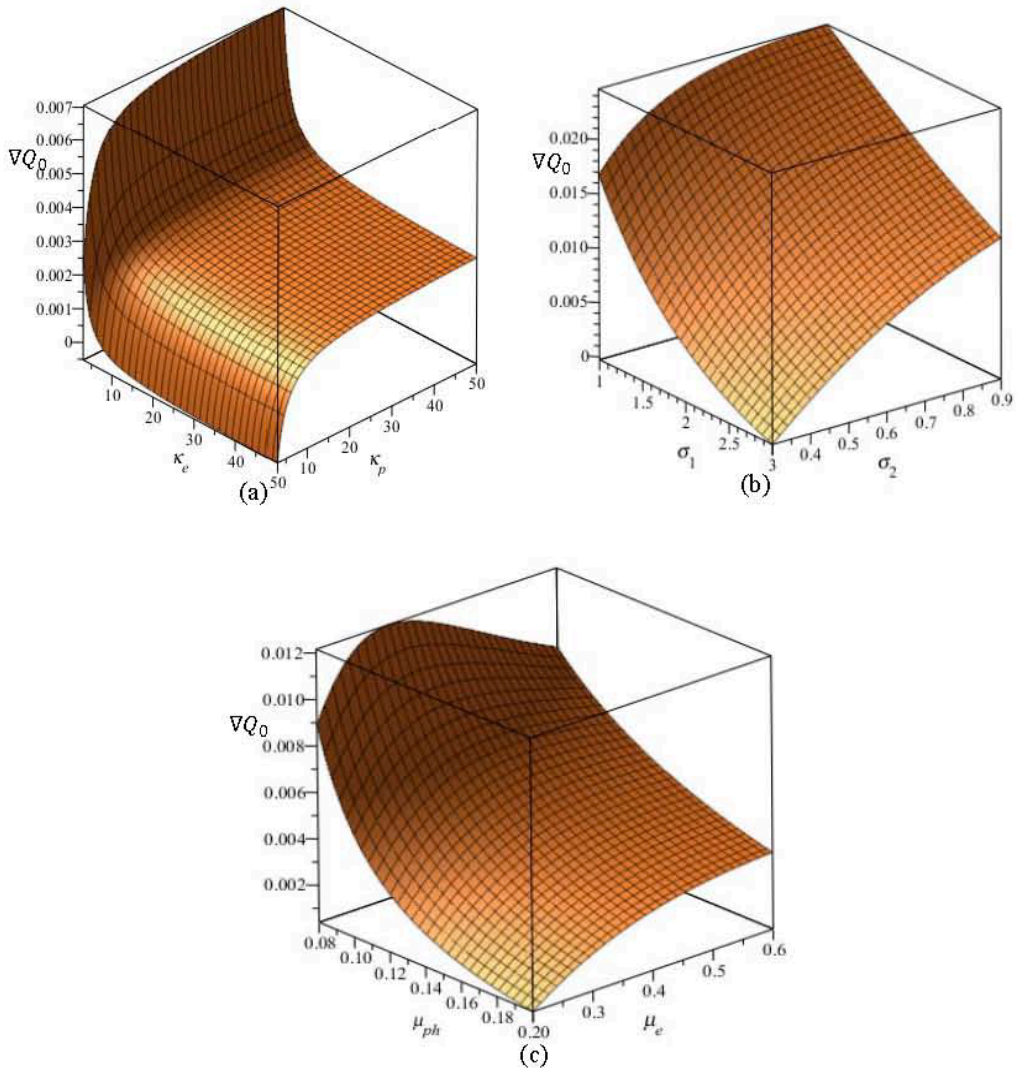

Figure 6.2 Changes of phase shifts ∇Q_0 after head-on collision between the solitons of equal amplitudes as obtained from the KdV equation receding from each other with regards to (a) κ_e and κ_p ($\mu_{ph} = 0.14$, $\mu_e = 0.6$, $\sigma_1 = 1$, $\sigma_2 = 0.5$, $U_0 = 0.02$, and $\varepsilon = 0.1$), (b) σ_1 and σ_2 ($\kappa_e = \kappa_p = 3$, $\mu_{ph} = 0.01$, $\mu_e = 0.6$, $U_0 = 0.02$, and $\varepsilon = 0.1$), (c) μ_{ph} and μ_e ($\sigma_1 = 1$, $\sigma_2 = 0.8$, $U_0 = 0.02$, $\kappa_e = \kappa_p = 3$ and $\varepsilon = 0.1$).

and $\kappa_{e,p} = 3 - 100$ which are consistent with space and laboratory plasmas [1-3,7-8] and are described below: Initially, the solitons S_R is at $\xi = 0, \eta \to -\infty$ and S_L is at $\eta = 0, \xi \to +\infty$ are asymptotically far away from each other. After collision ($t \to \infty$), the soliton S_R is far to the right of S_L, that is, S_R is at $\xi = 0, \eta \to +\infty$, while S_L is at $\eta = 0, \xi \to -\infty$, such collisional phenomena between the solitons are displayed in Figs.6.1. It is clearly seen from Figs.6.1 that the negative (Fig.6. 1(a)) and positive (Fig. 6.1(b)) electrostatic positron acoustic KdV solitary waves are propagating from each other and asymptotically divided away. During the whole processes of collision, one can obtain the motionless composite structure within $-\infty <$

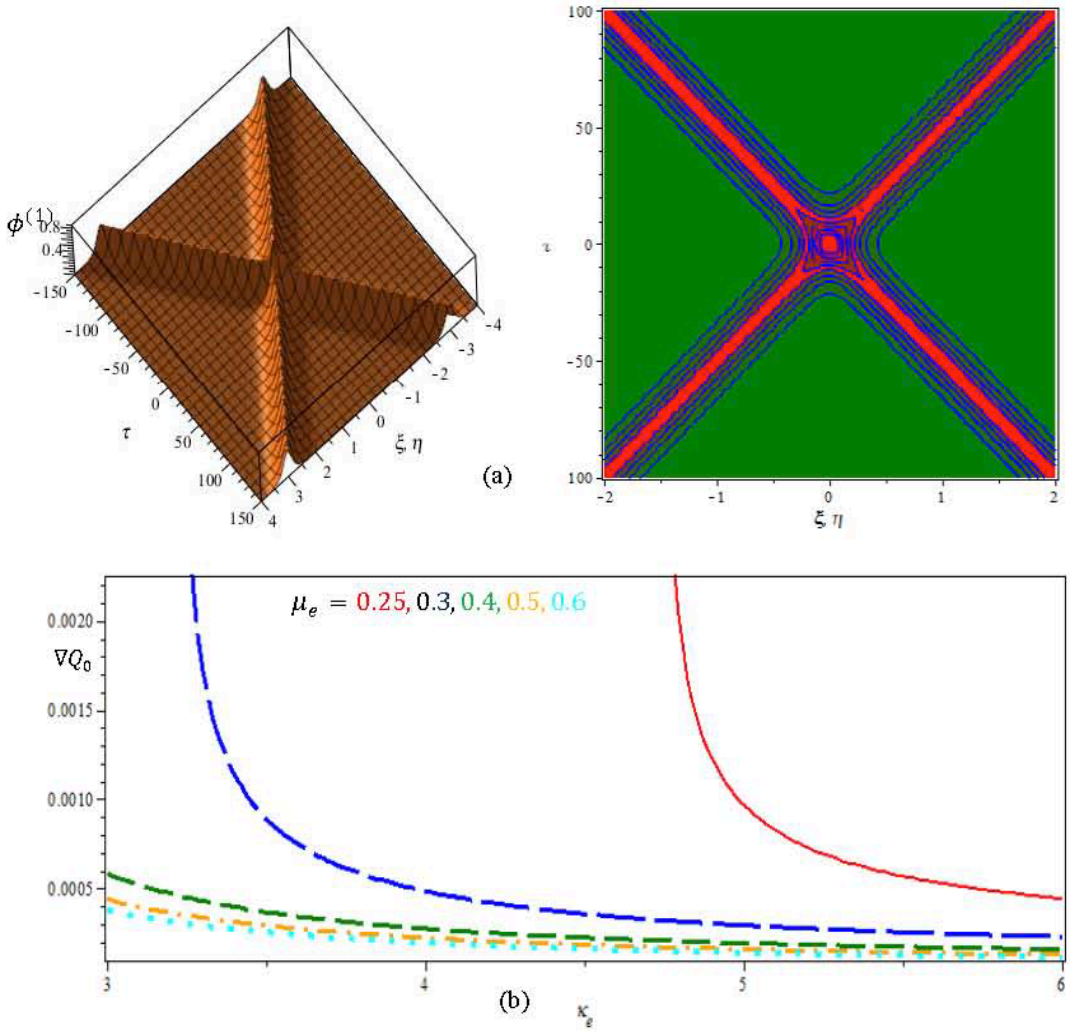

Figure 6.3 (a) Electrostatic potential profiles ($\phi^{(1)}$) after head-on collision between the solitons as obtained from the mKdV equation around the critical value μ_c ($\mu_{ph} = 0.09$, $\mu_e = 0.4$, $\kappa_e = 3$) with surface plot (left) and contour plot (right) with regards to space and time. (b) Changes of phase shift ∇Q_0 after head-on collision around the critical value with regards to κ_e for different values of μ_e. The remaining parameters are considered as $\kappa_p = 10$, $\sigma_1 = 1$, $\sigma_2 = 0.8$, $U_0 = 0.02$. and $\varepsilon = 0.1$.

$t < +\infty$. It is found from these figures that two solitons are propagating along the trajectories that are deviated from their initial position; such deviations are due to the phase shifts for two colliding solitons. It is seen from Eq. (6.26) that each soliton has phase shifts in its direction of propagation due to collision, which means that the velocities of positron acoustic solitary waves are reduced during their collision stages. Figures 6.2(a), (b), and (c) show the effects on phase shifts ∇Q_0 with regards to κ_e and κ_p, σ_1,and σ_2, and μ_{hp} and μ_e after head-on collision between the KdV solitons with equal amplitudes propagating in the

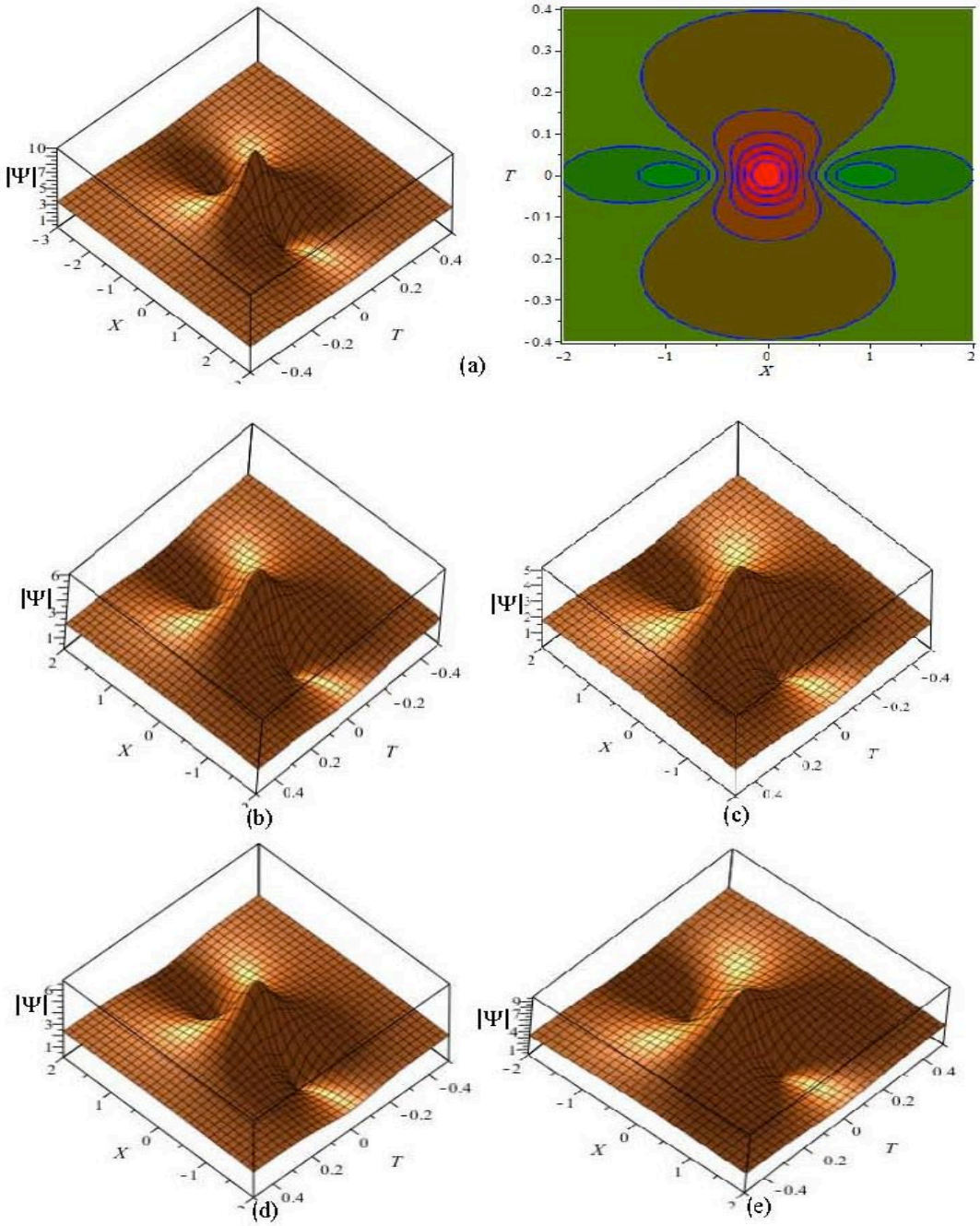

Figure 6.4 Effects of plasma parameters on the rogue waves considering (a) $\mu_{ph} = 0.05, \kappa_e = \kappa_p = 4$, $\mu_e = 0.6$, $\sigma_1 = 1$ and $\sigma_2 = 0.5$ with surface plot (left) and contour plot (right), (b) $\mu_e = 0.5$ with the same value of (a), (c) $\mu_{ph} = 0.1$ with the same value of (b), (d) $\kappa_e = 10$ with the same value of (c) and (e) $\sigma_1 = 2$, with the same value of (d).

opposite directions. It is seen from Figs.6. 2 that the phase shifts are increasing with the increase of κ_p, σ_2, and μ_e, but decreasing with the increase of κ_e, σ_1, and μ_{hp}. This phenomenon indicates that the hot positrons and hot electrons interact more actively with the cold positrons with the decrease of hot electron temperature and cold positron density. Thus,

the restoring force, as produced by hot positrons and electron pressure, reduce with increasing hot electron temperature and cold positron density, and hence the magnitude of phase shift is decreasing. Besides, with the increase in ion density can be interpreted as depopulation of ions from the plasma system as a result of the driving force (provided by cold positrons inertia) of positron acoustic solitary waves decreases.

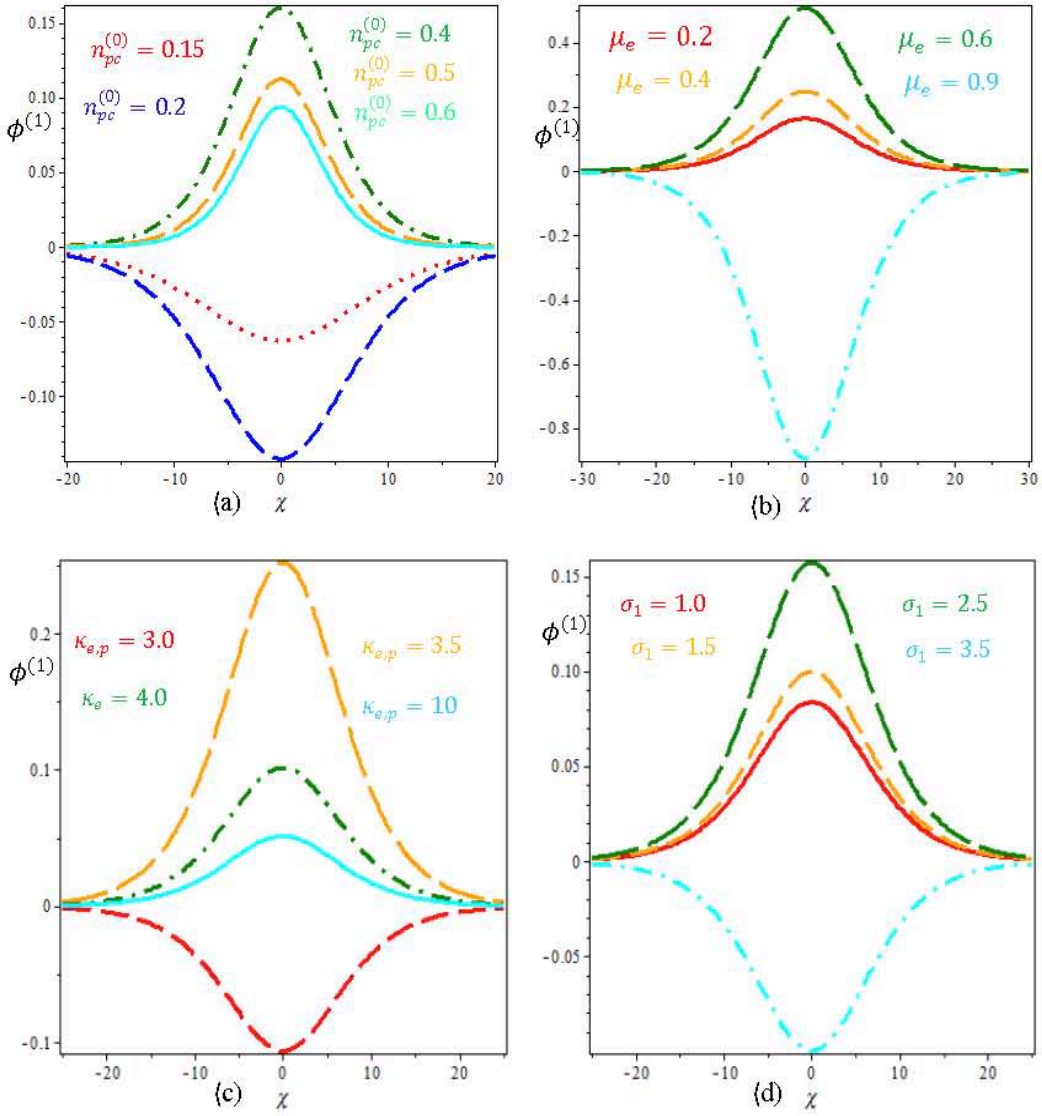

Figure 6.5 Effects of (a) $n_{pc}^{(0)}$ taking $\mu_{ph} = 0.05$, $\kappa_{e,p} = 3$, $\mu_e = 0.6$, $\sigma_1 = 3$, $\sigma_2 = 0.5$, $\phi^{(0)} = 0.4$, and $u_{pc}^{(0)} = 0.6$, (b) μ_e taking the typical values of (a) except $n_{pc}^{(0)} = 0.2$ and $\phi^{(0)} = 0.3$, (c) $\kappa_{e,p}$ taking the typical values of (a) except $\mu_{ph} = 0.1$, $n_{pc}^{(0)} = 0.2$, and $\phi^{(0)} = 0.3$, and (d) σ_1 taking the typical values of (b) except $\mu_e = 0.8$ on the electrostatic potential of positron acoustic KdV solitary waves in weakly inhomogeneous plasmas.

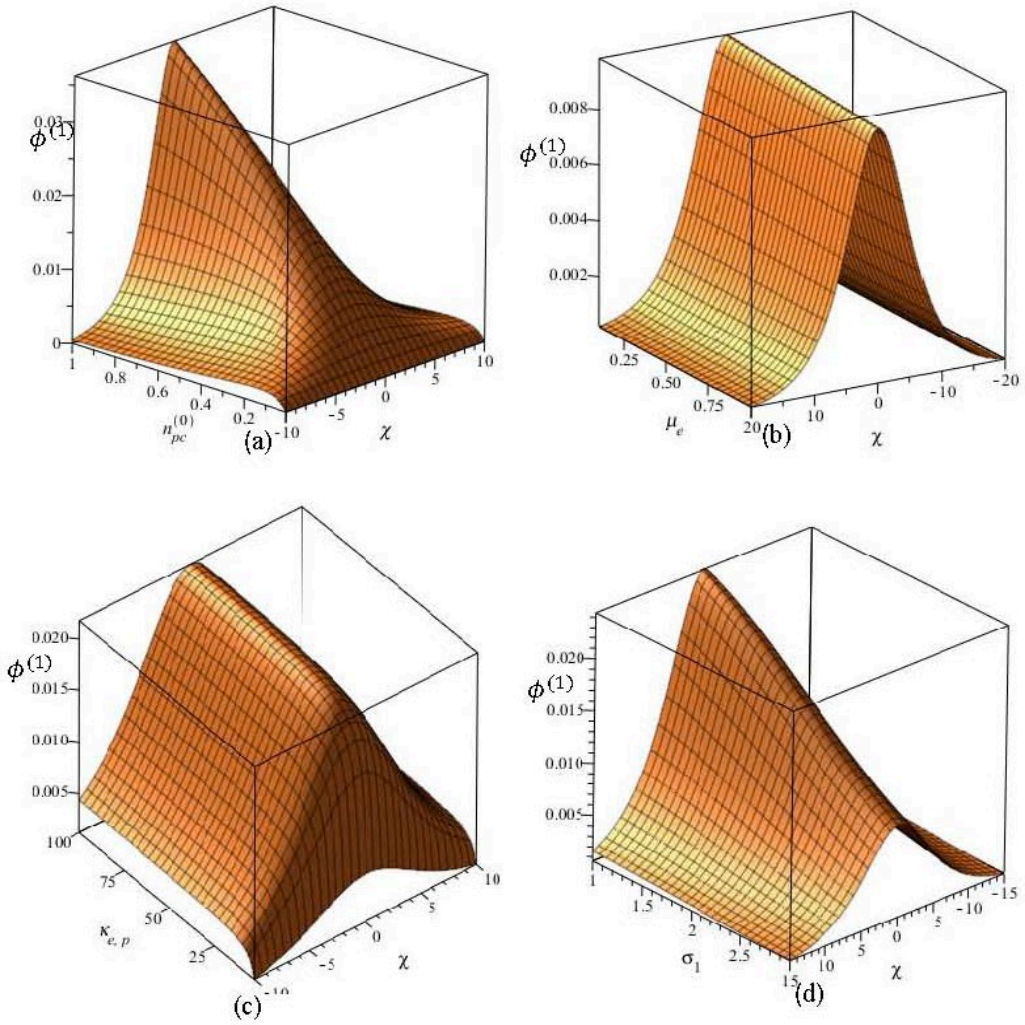

Figure 6.6 Effects of (a) $n_{pc}^{(0)}$, (b) μ_e, (c) $\kappa_{e,p}$, and (d) σ_1 along with χ on the electrostatic mKdV positron acoustic solitary waves in weakly inhogogeneous plasmas considering the typical values as in Fig. 6.5.

On the other hand, the amplitude of the two-sided KdV solitons and their corresponding phase shifts approach to infinity at the critical value $\mu_{hp} = \mu_c$, where the validity of the reductive perturbation technique breaks down. To avoid such difficulty, the two-sided mKdV Eqs. (6.30) and (6.31), and their corresponding phase shifts as in Eq. (6.34) are obtained considering the higher order nonlinearity. Another salient feature of mKdV solitons (Eq. (6.32)) is that if the head-on collision takes place at around the critical value which divulges a combination of only positive solitons with their changing phases as depicted in Figs.6.3.

Figure 6.3(a) reveals that the electrostatic mKdV positron acoustic solitary waves are propagating away from each other and asymptotically divided. The changes of phase shift are enhanced with the increase of μ_e and decreased with the increase of κ_e.This phenomenon can be ascribed as the solitons absorb energy due to collision without changing the shape and velocity. Thus the absorption of energy increases (suppesses) smoothly with the enhancement of plasma parameters for the rarefactive (compressive) positron acoustic solitary waves. Besides, the solitons change their polarities near the critical value, where they absorb maximum energy due to the change of maximum phase shifts. It is found that the phase velocity is slower after collision due to the positive phase shift. It is observed that the NLSE obtained from the KdV equation does not support rogue waves due to modulational stability of the quasi-monochromatic wave packets. But, the NLSE obtained from the mKdV equation supports the rogue wave for the considered plasma parameters. The solution Eq. (6.37) of the NLS equation (6.36) provides the profiles of rogue waves within the modulationally unstable region $\alpha > 0$, where a significant amount of energy accumulated within a relatively small area and therefore the rogue waves produce in the considered plasmas. Figures 6.4 show the effect of plasma parameters on the characteristics of rogue waves. The amplitudes of rogue waves are decreasing with increasing μ_e and μ_{hp} due to the reduction of nonlinearity, which indicates that the rogue wave does not absorb energy and make the envelope shorter. On the other hand, the amplitudes of the rogue waves are increasing with the increase of κ_e and σ_1 due to the absorption of energy in the plasmas.

Further, the electrostatic positron acoustic solitary waves are studied by deriving the KdV equation with variable coefficients in the considered weakly inhomogeneous plasmas using the reductive perturbation method. Figures 6.5 show the electrostatic positron acoustic KdV solitary waves for different values of n_{pc}^0, μ_e, κ_e, and σ_1 considering the remaining parameters constant. It is seen from Figs. 6.5 that the amplitude of positron acoustic solitary waves are decreasing with the increase of n_{pc}^0, μ_e, κ_e and σ_1. The nonlinear term (L_1) of mKdV equation increases due to the enhancement of electron kappa parameters as a result the amplitudes of the positron acoustic solitary waves decrease. The driving force, due to the inertia of the cold positron, also decreases with increasing positron density, consequently the solitary waves are generated as well as the amplitudes of the positron acoustic solitary waves decrease. It is also found that the KdV equation supports both compressive for $A_1 < 0$ and

rarefactive for $A_1 > 0$ solitons depending on the plasma parameters in the inhomogeneous plasmas. Besides, the KdV equation does not support the positron acoustic solitary waves in the weakly inhomogeneous plasmas at the critical unperturbed densities $n_{pc}^{(0)} = \left(V - u_{pc}^{(0)}\right)^4 \left(R_2 - 2R_3\phi^{(0)}\right)/6$. In such case, the mKdV equation with variable coefficients is derived considering further higher order nonlinearity terms to investigate the positron acoustic solitary waves around the critical densities. Figures 6.6 display the effect of n_{pc}^0, κ_e, κ_p, and σ_1 along with χ on the electrostatic positron mKdV solitary waves considering the remaining parameters constant. It is seen from Figs. 6.6 that the amplitudes of mKdV positron acoustic solitary waves are increasing with the increase of n_{pc}^0, κ_e, and κ_p, and decreasing with the increase of σ_1. It is interesting to note that the mKdV equation supports only the compressive solitons depending on the inhomogeneous plasma conditions. This result is in good agreement with the findings of [37] in homogeneous plasmas. From the above discussions, having in mind that an increase in n_{hp0} would lead to a decrease in n_{i0} by virtue of the charge neutrality, one can conclude that ion depletion favors the propagation of solitary positron acoustic waves. Thus, the obtained results in the considered plasmas may be useful for understanding the unraveled physical properties of nonlinear positron acoustic waves in space plasmas [1-8].

6.6 Conclusions

The interaction between the positron acoustic solitary waves, subsequently generation of their phase shifts, and production of rogue waves are investigated deriving the KdV, mKdV and NLSEs in homogeneous, collisionless, unmagnetized plasmas composing immobile positive ions, mobile cold positron, and kappa distributed hot positrons and hot electrons. Besides, the KdV and mKdV equations with variable coefficients are derived to investigate the nonlinear positron acoustic waves in a weakly inhomogeneous plasmas. It is found that the plasma parameters significantly affect the phase shifts after head-on collision and rouge wave in homogeneous, and nonlinear positron acoustic solitary waves in inhomogeneous plasma systems. The rogue waves are found within the modulational unstable region ($\alpha > 0$) that supports only the mKdV equation. It is remarkable to note that the KdV equation admits both compressive and rarefactive solitons, but only compressive solitons are found from the mKdV equations both in homogeneous and inhomogeneous plasmas. Further, it is observed that the

maximum amplitude of solitons are obtained around the critical value in both cases. In conclusion, the results obtained in this study might be useful for understanding the qualitative changes in the dynamics of the positron acoustic waves of various astrophysical and space plasmas like in auroral acceleration regions [40], solar wind [3], naturally doped superthermal astrophysical plasmas [41], cosmic rays [45] etc. as well as in laboratory plasmas [62].

References

1. J. Bremer, P. Hoffmann, A. H. Manson, C. E. Meek, R. Ruster, and W. Singer, Ann. Geophys. **14**, 1317 (1996).
2. J. Franz, P. Kintner, and J. Pickett, Geophys. Res. Lett. **25**, 1277 (1998).
3. V. Pierrard and J. Lemaire, J. Geophys. Res. **101**, 7923 (1996).
4. F. C. Michel, Rev. Mod. Phys. **54**, 1 (1982).
5. H. Ikezi, R. Taylor, and D. Baker, Phys. Rev. Lett. **25,** 11 (1970).
6. H. R. Miller, and P. J. Wiita, Active Galactic Nuclei (Berlin: Springer) pp 202, (1987).
7. P. K. Shukla, N. N. Rao, M. Y. Yu, and N. L. Tsintsadze, Phys. Rep. **138,** 1 (1986).
8. V. Berezhiani, D. D. Tskhakaya, and P. K. Shukla, Phys. Rev. A **46,** 6608 (1992).
9. R.G. Greaves, M.D. Tinkle, C.M. Surko, Phys. Plasmas **1,** 1439 (1994).
10. P. Helander, D.J. Ward, Phys. Rev. Lett. **90,** 135004 (2003).
11. S.I. Popel, S.V. Vladimirov, P.K. Shukla, Phys. Plasmas **2**, 716 (1995).
12. H. Hasegawa, S. Irie, S. Usami, Y. Ohsawa, Phys. Plasmas **9**, 2549 (2002).
13. M. Salahuddin, H. Saleem, M. Saddiq, Phys. Rev. E **66**, 036407 (2002).
14. M. G. Hafez, M. R. Talukder, Astrophys. Space Sci. **359**, 27 (2015).
15. S. Ghosh, R. Bharuthram, Astrophys. Space Sci. **314**, 121 (2008).
16. M. G. Hafez, M. R. Talukder, M.H. Ali, Indian J. Phys. **90**, 631 (2016a)
17. M. G. Hafez, M. R. Talukder, M. H. Ali, Astrophys. Space Sci. **361**,131 (2016b).
18. M. G. Hafez, M. R. Talukder, M. H. Ali, Phys. Plasmas **23**, 012902 (2016c).
19. M. H. Hafez, N.C. Roy, M.R. Talukder, M. H. Ali,: Plasma Sci. Technol. **19**, 015002 (2017a).
20. M. G. Hafez, M. R. Talukder, M. H. Ali, Plasma Phys. Rep. **43**, 499 (2017b).
21. T. K. Baluku, M. A. Hellberg, Plasma Phys. Control. Fusion **53**, 095007 (2011).
22. H. Alinejad, Astrophys. Space Sci. **345**, 85 (2013).
23. O. Adriani, G. C. Barbarino, G. A. Bazilevskaya, Nature **458**, 607 (2009).
24. C. M. Surko, M. Leventhal, A. Passner, Phys. Rev. Lett. **62**, 901 (1989).
25. C. M. Surko, T. J. Murphy, Phys. Fluids B **2**, 1372 (1990).
26. E. F. El-Shamy, W. F. El-Taibany, E. K. El-Shewy, K. H. El-Shorbagy, Astrophys. Space Sci. **338**, 279 (2012).
27. M. Y. Yu, H. Luo, Phys. Plasmas **15**, 024504 (2008).
28. K. Jilani, A. M. Mirza, T. A. Khan, Astrophys. Space Sci. **349**, 255 (2014).

29. V. M. Vasyliunas, J. Geophys. Res. **73**, 2839 (1968).
30. T. K. Baluku, M. A. Hellberg, Phys. Plasmas **15**, 123705 (2008).
31. T. K. Baluku, M. A. Hellberg, I. Kourakis, N.S. Saini, Phys. Plasmas **17**, 053702 (2010)
32. B. Basu, Phys. Plasmas **15**, 042108 (2008).
33. S. A. El-Tantawy, N. A. El-Bedwehy, W.M. Moslem, Phys. Plasmas **18**, 052113 (2011).
34. M. Tribeche, K. Aoutou, S. Younsi, R. Amour, Phys. Plasmas **16**, 072103 (2009).
35. M. Tribeche, Phys. Plasmas **17**, 042110 (2010).
36. B. Sahu, Phys. Scr. **82**, 065504 (2010).
37. M. S. Alam, M. J. Uddin, M. M. Masud, A. A. Mamun, Chaos **24**, 033130 (2014).
38. M. Temerin, K. Cerny, W. Lotko, F. S. Mozer, Phys. Rev. Lett. **48**, 1175 (1982).
39. R. Bostrom, G. Gustafsson, B. Holback, G. Holmgren, H. Koskinen, P. Kintner, Phys. Rev. Lett. **61**, 82 (1988).
40. A. Saha, R. Ali, P. Chatterjee, Adv. Space Res. **60**, 1220 (2017).
41. A. Shah, A. Rakha, Astrophys. Space Sci. **344**, 113 (2013).
42. M. G. Shah, M. R. Hossen, A. A. Mamun, Braz. J. Phys. **45**, 219 (2015).
43. F.C Michel, Theory of Neutron Star Magnetosphere. Chicago University Press, Chicago (1991).
44. A. Saha, Phys. Plasmas **24**, 034502 (2017).
45. A. Saha, J. Tamang, Phys. Plasmas **24**, 082101 (2017).
46. N. J. Zabusky, M. D. Kruskal, Phys. Rev. Lett. **15**, 240 (1965).
47. G. Mandal, K. Roy, A. Paul, A. Saha, P. Chatterjee, Z. Naturforsch. A **70**, 703 (2015).
48. C. H. Su, R.M. Miura, J. Fluid Mech. **98**, 509 (1980).
49. P. Chatterjee, U. N. Ghosh, K. Roy, S.V. Muniandy, C.S. Wong, B. Sahu, Phys. Plasmas **17**, 122314 (2010).
50. P. Chatterjee, U. N. Ghosh, K. Roy, S.V. Muniandy, C.S. Wong, B. Sahu, Astrophys. Space Sci. **353**, 169 (2014).
51. F. Verheest, M. A. Hellber, W.A. Hereman, Phys. Rev. E **86**, 036402 (2012).
52. K. E. Lonngren, Opt. Quantum Electron. **30**, 615 (1998).
53. S. A. Shan, S. A. El-Tantawy, Phys. Plasmas **23**, 072112 (2016).
54. S. A. El-Tantawy, A. M. Wazwaz, R. Schlickeiser, Plasma Phys. Control. Fusion **57**, 125012 (2015a).
55. H. Bailung, Y. Nakamura, J. Plasma Phys. **50**, 231 (1993).

56. S. A. El-Tantawy, E.I. El-Awady, M. Tribeche, Phys. Plasmas **22**, 113705 (2015b).
57. S. A. El-Tantawy, E. I. El-Awady, R. Schlickeiser, Astrophys. Space Sci. **360**, 49 (2015c).
58. S. A. El-Tantawy, Astrophys. Space Sci. **361**, 164 (2016).
59. M. S. Alam, M. G. Hafez, M. R. Talukder, M. H. Ali, Chin. Phys. B **26**, 095203 (2017).
60. S. A. El-Tantawy, W. M. Moslem, Phys. Plasmas **21**, 052112 (2014).
61. N. Asano, Prog. Theor. Phys. Suppl. **55**, 52 (1974).
62. R.G. Greaves, S. J. Gilbert, C.M. Surko, Appl. Surf. Sci. **194**, 56 (2002).

Abbreviation and Nomenclature:

KdV= Korteweg-de Vries

mKdV = modified Korteweg-de Vries

ePLK = extended Poincaré-Lighthill-Kuo

NLS = nonlinear Schrödinger

NLSE = nonlinear Schrödinger equation

RWs = rogue waves

PAMELA= Payload for Antimatter Matter Exploration and Light-nuclei Astrophysics

n_{i0} = density of unperturbed immobile positive ion

n_{e0} = density of unperturbed hot electron

n_{pc0} = density of unperturbed mobile cold positron

n_{ph0} = density of unperturbed kappa distributed hot positron

n_{pc} = cold positron number density

u_{pc} = cold positron fluid speed

C_{pc} = positron acoustic speed

ϕ = electrostatic potential

T_{eh} = hot electron temperature

T_{ph} = hot positron temperature

σ_1 = temperature ratio of effective temperature to hot positron temperature

σ_2 = temperature ratio of effective temperature to electron temperature

T_{ef} = effective temperature $= T_e T_{ph}/(\mu_e T_{ph} + \mu_{ph} T_e)$

μ_{ph} = density ratio of unperturbed density of hot to cold positron

μ_e = density ratio of unperturbed density of electron to cold positron

μ_i = density ratio of unperturbed density of ion to cold positron

v_{ph} = thermal speed of hot positrons

v_e = thermal speed of electrons

v_{pc} = thermal speed of cold positrons

ω = angular frequency

k = wave number

k_B= Boltzmann constant

v_g = group velocity of nonlinear IA waves

e = electronic charge

$\kappa_{e(p)}$= superthermal parameter of hot electrons (positron)

ω_{pc} = period of cold positron plasma

λ_{Dm} = positron Debye length

ϕ_o = amplitude of KdV solitary waves in homogeneous plasma

W_o = width of KdV solitary waves in homogeneous plasma

U_o = constant velocity of the reference frame

ξ, η, τ = stretched coordinates

$\nabla Q_0 (\nabla P_0)$ = phase shift of right (left) moving soliton

ϕ_1 = amplitude of mKdV PA solitary waves in homogeneous plasma

W_1 = width of mKdV PA solitary waves in homogeneous plasma

φ_{v0} = amplitude of KdVPA solitary waves in inhomogeneous plasma

W_{v0} = width of KdV PA solitary waves in inhomogeneous plasma

V = speed of wave propagation

φ_1= amplitude of mKdV PA solitary waves in inhomogeneous plasma

W_4 = width of mKdV PA solitary waves in inhomogeneous plasma

A = coefficient of nonlinearity of KdVE in homogeneous plasma

B = coefficient of dispersion of KdVE in homogeneous plasma

L = coefficient of nonlinearity of KdVE in inhomogeneous plasma

M = coefficient of dispersion of KdVE/mKdVE in homogeneous /inhomogeneous plasma

L_1 = coefficient of nonlinearity of mKdVE in inhomogeneous plasma

P = coefficient of dispersion of NLSE in homogeneous plasma

Q = coefficient of nonlinearity of NLSE in homogeneous plasma

Chapter 7

Conclusions and Recommendation

The collisionless unmagnetized multi-species plasmas are considered to study the salient features of electrostatic solitary wave or solitons and shock wave due to interactions in different plasma conditions. The considered plasma system is homogeneous and/or inhomogeneous, relativistic and/or non-relativistic. To do so, the nonlinear evolution equations are derived employing extended Poincaré-Lighthill-Kue (ePLK) method. The production of rogue waves is also studied in different plasma environment. The results found in this works are summarized below.

The interactions between the ion acoustic solitons, their phase shifts, and the production of rogue waves are investigated by considering the soliton solution of the two-sided KdV equations and the rational function solution of the NLSE, respectively. It is found that the quantum parameters become prominent due to the Bohm potential, which significantly modifies the propagation characteristics, due to the interactions of the small amplitude long-lived solitons as well as large amplitude short-lived rogue waves in the plasmas. The results obtained in this study might be useful for the understanding of the effects of electrostatic resonance and phase shifts after weak interaction between multi-solitons and rogue waves for astrophysical compact objects, e.g., white dwarfs, neutron stars, etc., and for laboratory plasmas like intense laser–solid matter interaction experiments.

The electrostatic nonlinear propagation and head-on collision of ion acoustic solitary waves are investigated taking different plasma parameters into account both for the weakly and highly relativistic regimes by deriving the two-sided KdV equations employing the ePLK method. The phase shift is observed in terms of plasma parameters considering the stationary solutions of the KdV equations. It is found that the change in phase shift, magnitude of amplitude and width of collision of ion acoustic solitary waves are decreasing with the increase of positron concentration, ion-electron temperature ratio, electron-positron temperature ratio, but increasing with the increase of relativistic streaming factor. On the other hand, the nonlinear propagation characteristics of electrostatic collision of ion acoustic solitary waves are almost same for $\beta \leq 0.1$ and slightly larger for $\beta > 0.1$ in HRR rather

than WRR. It is concluded that the collision of ion acoustic solitary waves are propagating faster in highly relativistic rather than weakly relativistic plasmas. The results revel that the propagation characteristics including electrostatic resonances of ion acoustic solitary waves are useful for understanding the physical issues of highly energetic nonthermal particles with relativistic warm ions in astrophysical and laboratory plasmas, especially in pulsar magnetosphere, laser produced, inertial confinement plasmas, pulsar relativistic winds with supernova ejecta, etc. This work is done to study the interaction of collision of ion acoustic solitary waves and their corresponding phase shift derived from two-sided KdV equations. It is to be noted that there can be a possibility of producing instabilities due to higher order nonlinearity that may require further investigation.

To study the propagation characteristics due to the interactions among the dust acoustic solitons composed of negatively charged mobile dust, Boltzmann-distributed electrons, and two-temperature nonthermal cold and hot ions, occupying two different regions of velocity phase space are considered. The KdV equations are derived using the ePLK method. The analytical solutions for solitons are constructed using the well established Hirota bilinear method. The phase shifts due to head-on collisions among the dust acoustic single-, double-, and triple-solitons are determined analytically from the solutions of the two-sided KdV equations. The effects of plasma parameters on the head-on collisions among the electrostatic dust acoustic single-and multi-solitons and their corresponding phase shifts are discussed. The compressive and rarefactive scattered two-,four-, and six- dust acoustic waves are obtained for $A > 0$ and $A < 0$, respectively. The phase shifts due to head-on collision of dust acoustic single- and multi-solitons are strongly dependent on the plasma parameters and the wave numbers, are increasing with increasing μ_{i1}, μ_{i2}, σ_1, and q and are decreasing with the increase of σ_2, and β . One may conclude that the results obtained in this investigation might be useful for understanding electrostatic resonance disturbances and phase shifts after weak head-on collision among the solitons in space and laboratory plasma systems, such as Saturn's E-ring, Saturn's F-ring, noctilucent clouds, Halley's comet, interstellar molecular clouds in cosmic dust-laden plasma, laboratory dusty plasmas, etc., where major plasma species are negatively charged massive mobile dust, Boltzmann distributed electrons, and two-temperature ions following the nonthermal distributions. This work is done to study the interaction of dust acoustic solitons and their corresponding phase shift (time delay) through the two-sided KdV equations. The quadratic nonlinearity of the KdV equations may disappear for a certain critical value; in such case, one may study the interactions among solitons using modified KdV equations.

The plasma system consisting of relativistic warm ions, nonextensive electrons and positions are considered to investigate the head-on collision between ion acoustic shock waves, the change of phase shifts and amplitudes taking into account the effects of nonlinearity and dispersion. To do so, two-sided KdV Burger equations are derived with help of ePLK method. Two shock waves, one is at $\xi = 0, \eta \to -\infty$ and the other at $\eta = 0, \xi \to +\infty$ are traveling toward each other and collide at $t = 0$ and then depart from each other. It is observed that T_{ep}, T_{ip}, η_1, p, β, and q significantly modify the structures of the shock waves. The phase shifts are found to change due to the effects of T_{ep}, β, η_1, and p. The results reveal that the electrostatic ion acoustic shock waves become rarefactive for the temperature ratios, kinematic viscosity and superthermality in both WRR and HRR. The amplitudes of ion acoustic shock waves are increasing for WRR but decreasing for HRR due to increasing ion thermal velocities. Besides, the amplitudes of the solitons are detaining due to the increase of positron concentration for the depopulation of ions. The results obtained may be useful for the clarifications of interactions between ion acoustic shock waves in astrophysical, especially in pulsar magnetosphere and laser produced plasmas in laboratory where nonextensive electrons, positrons and relativistic ions exist.

The interaction between the positron acoustic solitary waves, subsequently generation of their phase shifts, and production of rogue waves are investigated deriving the KdV, mKdV and NLSEs in homogeneous, collisionless, unmagnetized plasmas composing immobile positive ions, mobile cold positron, and kappa distributed hot positrons and hot electrons. Besides, the KdV and mKdV equations with variable coefficients are derived to investigate the nonlinear positron acoustic waves in a weakly inhomogeneous plasmas. It is found that the plasma parameters significantly affect the phase shifts after head-on collision and rouge wave in homogeneous, and nonlinear positron acoustic solitary waves in inhomogeneous plasma systems. The rogue waves are found within the modulational unstable region ($\alpha > 0$) that supports only the mKdV equation. It is remarkable to note that the KdV equation admits both compressive and rarefactive solitons, but only compressive solitons are found from the mKdV equations both in homogeneous and inhomogeneous plasmas. Further, it is observed that the maximum amplitude of solitons is obtained around the critical values in both cases. In conclusion, the results obtained in this study might be useful for understanding the qualitative changes in the dynamics of the positron acoustic waves of various astrophysical and space plasmas like in auroral acceleration regions, solar wind, naturally doped superthermal astrophysical plasmas, cosmic rays etc. as well as in laboratory plasmas.

The finite but small amplitude ion acoustic solitary-, ion acoustic shock-, and dust acoustic- waves are considered to investigate the interaction phenomena of unmagnetized plasmas. In each case the solitons preserved their original identities due to collisions. But the sufficiently large amplitude ion acoustic solitary-, ion acoustic shock-, and dust acoustic -waves do not retain their original size and shape after collisions. Thus, it is suggested to study the interaction phenomena in such cases using particle-in cell simulation method. Finally, laboratory experiments can be carried out to test the presented theory in this work.

List of publications

1. **M. S. Alam** and M. R. Talukder, Head-on collision of ion acoustic solitary waves with two-negative ions in electron-positron-ion plasmas and production of rogue waves, Plasma Phys. Report 45, 9 (2019).
2. **M. S. Alam** and M. R. Talukder, Interaction phenomena of ion acoustic solitary waves with singly charged cold ions and Boltzmann electrons, Waves in Random and Complex Media (2019); DOI: 10.1080/17455030.2019.1626027.
3. **M. S. Alam** and M. R. Talukder, Head-on collision between single- and multi-solitons heavy ion acoustic waves in multi-ion plasmas, Plasma Sci. Techno(2019); doi.org/10.1088/2058-6272/ab20dc
4. **M. S. Alam** and M. R. Talukder, Interaction phenomena of ion-acoustic Quasi-solitons and classical-solitons in three component plasma, Contrib. Plasma Phys. e201800163 (2019); DOI: 10.1002/ctpp.201800163.
5. **M. S. Alam** and M. R. Talukder, Head-on collision of ion acoustic shock and solitary waves in collisionless plasma with pair ions and electrons, Braz. J. Phys. **49**,198(2019).
6. **M. S. Alam**, M. G. Hafez, M. R. Talukder, and M. Hossain Ali, Head-on collision of ion acoustic shock waves in electron-positron-ion nonextensive plasmas for weakly and highly relativistic regimes, Phys. Plasmas **25**, 072904 (2018).
7. **M. S. Alam**, M. G. Hafez, M. R. Talukder, and M. Hossain Ali, Head-on collision between positron acoustic waves in homogeneous and inhomogeneous plasmas, Astrophys. Space Sci. **363**,102 (2018).
8. **M. S. Alam**, M. G. Hafez, M. R. Talukder, and M. Hossain Ali, Head-on collision of ion acoustic solitary waves in electron-positron-ion nonthermal plasmas for weakly and highly relativistic regimes**,** Phys. Plasmas **24**, 072901 (2017).
9. **M. S. Alam**, M. G. Hafez, M. R. Talukder, and M. Hossain Ali, Effects of two-temperature ions on head-on collision and phase shifts of dust acoustic single- and multi-solitons in dusty plasma, Phys. Plasmas **24**, 103705 (2017).
10. **M. S. Alam**, M. G. Hafez, M. R. Talukder, and M. Hossain Ali, Interactions of ion acoustic multi-soliton and rogue wave with Bohm quantum potential in degenerate plasma, Chin. Phys. B **26,** 095203 (2017).

11. **M. S. Alam,** M. G. Hafez, N. C. Roy, M. R. Talukder and M. H. Ali**,** Positron acoustic solitary waves in an inhomogeneous multicomponent plasma, IOP Conf. Series: J. Phys.: Conf. Series 1086, 012001 (2018); doi:10.1088/1742-6596/1086/1/012001.
12. **M. S. Alam** , M. G. Hafez, N. C. Roy, M. R. Talukder and M. Hossain Ali, Proceedings of Int. Conf. on Systems and Processes in Physics, Chemistry and Biology, (**ICSPPCB2018**) at Assam University Silchar, India,(2018).
13. **M. S. Alam** and M. R. Talukder, Interaction phenomena and effect of higher order dispersion on electron acoustic solitary waves in weakly relativistic regimes, Contrib. Plasma Phys. (Communicated).
14. **M. S. Alam**, M R Talukder, Consequences of oblique interactions of dust acoustic waves in dusty plasmas, Astrophys. Space Sci. (Communicated).
15. A.S.M. Moinuddin, **M. S. Alam**, M. R. Talukder,and M. Hossain Ali, Collisional effects of dust acoustic solitary and shock waves in dusty plasma, Phys. Plasmas (Communicated).
16. **M. S. Alam**, M R Talukder, Head-on interactional effects of ion acoustic waves with pair ions and non-Maxwellian electrons in collisional plasmas, Zeitschrift für Naturforschung A (A Journal of Physical Sciences) (Communicated).